Primary T cell immunodeficiencies associated with disturbed proximal T cell receptor signalling caused by human autosomal recessive LCK, ZAP-70 and ITK-mutations

Fabian Hauck

DOCTORAL THESIS

UNIVERSITY PARIS RENÉ DESCARTES

DOCTORAL SCHOOL GC2IDG

GENETICS, CELLS, IMMUNOLOGY, INFECTIOLOGY, DEVELOPMENT

SPECIALITY: IMMUNOLOGY

Presented by **FABIAN HAUCK**

To obtain the PhD degree from the University Paris René Descartes

PRIMARY T CELL IMMUNODEFICIENCIES ASSOCIATED WITH DISTURBED PROXIMAL T CELL RECEPTOR SIGNALLING CAUSED BY HUMAN AUTOSOMAL RECESSIVE LCK, ZAP-70 AND ITK-MUTATIONS

Thesis defended on 12.11.2013

DR	ALAIN	TRAUTMANN	PRÉSIDENT
DR	SYLVAIN	LATOUR	DIRECTEUR DE THÈSE
PR	ORESTE	ACUTO	RAPPORTEUR
DR	NAOMI	TAYLOR	RAPPORTEUR
DR	ROMAIN	RONCAGALLI	EXAMINATEUR
PR	ALAIN	FISCHER	EXAMINATEUR

Preface

Was ist das Schwerste von allem? Was dir das Leichteste dünket: Mit den Augen zu sehn, was vor den Augen dir lieget.

Johann Wolfgang von Goethe
Deutscher Dichter (1749 - 1832)

What is hardest of all? That which seems most simple: to see with your eyes what is before your eyes.

Johann Wolfgang von Goethe
German poet (1749 - 1832)

L'acte le plus difficile est celui que l'on croit le plus simple: percevoir, d'un regard en éveil, les choses qui se présentent à nos yeux.

Johann Wolfgang von Goethe
Poète allemand (1749 - 1832)

Summary

T lymphocytes express either a preTCR, or a clonotypic γδ TCR or αβ TCR together with the CD3-complex and the associated ζ-chain. TCR:CD3:ζ-signalling is crucial for T cell development and antigen-specific activation including proliferation, differentiation, effector functions and apoptosis of mature T cells. Protein tyrosine kinase (PTK) cascades lie at the heart of proximal TCR:CD3:ζ-signalling. The CSK-, SRC-, SYK- and TEC-family members C-terminal SRC kinase (CSK), lymphocyte-specific protein tyrosine kinase (LCK), ζ-chain associated protein tyrosine kinase of 70 kDa (ZAP-70) and interleukin-2-inducible T cell kinase (ITK), respectively, are the major T cell players. After TCR:CD3:ζ-complex triggering, activation of PTKs results in tyrosine phosphorylation signals. These include phosphorylation of immunoreceptor tyrosine-based activation motifs (ITAMs) of the CD3 and ζ-chains, and adaptor proteins that nucleate the proximal LAT:SLP-76-signalosome controlling almost all TCR:CD3:ζ-induced signalling events. These events initiate Ca^{2+}-flux, activation of mitogen-activated protein kinases (MAPKs), activation of nuclear factor of kappa light polypeptide gene enhancer in B-cells (NF-κB), activation of nuclear factor of activated T cells (NFAT) and activator protein 1 (AP-1) as well as actin reorganization, cell-adhesion and motility.

Throughout the last five decades, the immune system has been extensively investigated *in vitro* and in animal models such as the murine system. Additionally, studying and taking care of human primary immunodeficiency diseases (PIDs) has been seminal for our understanding of the human immune system as animal models not always recapitulate the subtleties found in men.

In my doctoral thesis I report the first case of autosomal recessive human LCK-deficiency, a novel autosomal recessive mutation leading to human ZAP-70-deficiency and a novel autosomal recessive mutation leading to human ITK-deficiency. I provide detailed clinical, immunological and biochemical analyses especially of TCR:CD3:ζ-signalling and compare my findings to the well-established *Lck*$^{-/-}$, *Zap-70*$^{-/-}$ and *Itk*$^{-/-}$ murine models.

Keywords: PID, SCID, CID, TCR, T cell, LCK, ZAP-70, ITK

Résumé

Les lymphocytes T sont caractérisés par l'expression d'un récepteur à l'antigène des cellules T (TCR), soit le preTCR, soit le γδ TCR et le αβ TCR clonotypique, associé à un complexe de transduction formé du CD3 et de la chaîne ζ. La signalisation du complexe TCR:CD3:ζ est cruciale pour le développement des cellules T et pour leur activation spécifique par l'antigène. Ces signaux déclenchent la prolifération, la différentation, les fonctions effectrices et l'apoptose des cellules T. Les évènements proximaux de la signalisation du TCR:CD3:ζ impliquent des protéines tyrosine kinases (PTK) des familles CSK, SRC, SYK et TEC dont les acteurs principaux sont CSK (C-terminal SRC kinase), LCK (lymphocyte-specific protein tyrosine kinase), ZAP-70 (ζ chain-associated protein tyrosine kinase of 70 kDa) et ITK (interleukin-2-inducible T cell kinase). Après stimulation du complexe TCR:CD3:ζ, les PTKs sont activées et déclenchent une cascade de phosphorylation sur tyrosine dont la phosphorylation des motifs activateurs ITAM (immunoreceptor tyrosine-based activation motif) du CD3 et de la chaîne ζ, et la phosphorylation des protéines adaptrices. Celles-ci conduisent à l'assemblage du signalosome LAT:SLP-76, lequel contrôle en grande partie la diversité des signaux associés au complex TCR:CD3:ζ, dont le flux calcique, l'activation de la cascade des MAP kinases, l'activation des facteurs de transcription NF-κB, NFAT et AP-1 ainsi que la réorganisation du cytosquellette d'actine, l'adhésion cellulaire et la motilité.

Pendant les cinq dernières décennies, le système immunitaire a été analysé extensivement *in vitro* et à l'aide de modèles animaux comme la souris. Par ailleurs, l'étude des déficits immunitaires héréditaires chez l'homme a permis aussi des avancées importantes et novatrices dans la compréhension du système immunitaire humain que les modèles animaux ne permettaient pas d'appréhender.

Dans ma thèse de doctorat je rapporte le premier cas de déficit humain en LCK de transmission autosomique récessive et l'identification de nouvelles mutations autosomiques récessives provoquant un défaut humain de ZAP-70 et un défaut humain d'ITK. Je rends compte des phénotypes cliniques et immunologiques associés à ces immunodéficiences et je caractérise les défauts biochimiques de la signalisation TCR:CD3:ζ associés à ces déficits. Enfin, je compare mes observations avec les modèles murins déficients *Lck*$^{-/-}$, *Zap-70*$^{-/-}$ et *Itk*$^{-/-}$ déjà bien établis.

Mots clés: PID, SCID, CID, TCR, T cell, LCK, ZAP-70, ITK

Ce travail de thèse a été effectué dans le laboratoire suivant :

INSERM U768

Développement Normal et Pathologique du Système Immunitaire

Hôpital Necker-Enfants Malades

149 rue de Sèvres 75015 Paris

France

Europe

Les illustrations de l'introduction et de la discussion ont été en partie réalisées par Jean-Pierre Laigneau, IRNEM IFR 94.

Table of contents

Table of figures

Table of tables

Abbreviations

ADAP:	Adhesion and degranulation-promoting adaptor protein
AICD:	Activation-induced cell death
AIRE:	Autoimmune regulator
A-loop:	Activation loop
AP-1:	Activator protein 1
APC:	Antigen presenting cell
ARP-2/3:	Actin related protein 2/3
ATF-2:	Activating transcription factor 2
BCL-2/6/10:	B cell lymphoma 2, 6 and 10
BCR:	B cell antigen receptor
BH:	BTK homology
BM:	Bone marrow
C:	Constant
$[Ca^{2+}]_e$:	Extracellular calcium-ion concentration
$[Ca^{2+}]_{er}$:	Endoplasmic reticulum calcium-ion concentration
$[Ca^{2+}]_i$:	Intracellular calcium-ion concentration
CARD:	Caspase recruitment domain
CARMA-1:	CARD-containing MAGUK protein 1
CBL:	Casitas B-lineage lymphoma
CCR-7:	Chemokine C-C motif receptor 7
CD:	Cluster of differentiation
CDC-37:	Cell division cycle 37
CD62L:	CD62 ligand
CDC-42:	Cell division cycle 42
cDNA:	Complementary DNA
CDK:	Cyclin-dependent kinase
CDR:	Complementarity determining region
CGH:	Comparative genomic hybridization
CIP:	Cytokine-induced proliferation
CK-1:	Casein kinase 1
CLP:	Common lymphoïd precursor

CMP:	Common myeloïd precursor
CRAC:	Ca^{2+}-release-activated Ca^{2+}-channel
CRKII:	CT10 regulator of kinase II
CsA:	Cyclosporin A
CSK:	C-terminal SRC kinase
cSMAC:	Central supramolecular activation cluster
CTLA-4:	Cytotoxic T lymphocyte antigen 4
CVID:	Common variable immunodeficiency
CWID:	Cytokine withdrawal-induced cell death
CXCR-5:	Chemokine (C-X-C motif) receptor 5
D:	Diversity
DAG:	Diacylglycerol
DAMP-R:	Danger-associated molecular pattern-receptor
DN:	Double-negative
DNA:	Deoxyribonucleic acid
DOK-1/2:	Docking protein 1 and 2
DP:	Double-positive
DPC:	Distal pole complex
DYRK-2:	Dual-specificity tyrosine-phosphorylation regulated kinase 2
dSMAC:	Distal supramolecular activation cluster
EBER-1:	EBV-encoded small RNA 1
EBV:	Epstein-Barr virus
EDP:	Early double positive
ER:	Endoplasmic reticulum
ERCA:	Endoplasmic reticulum Ca^{2+}-ATPase
ERK-1/2:	Extracellular signal-regulated kinase 1 and 2
ETP:	Early thymic progenitor
FACS:	Fluorescence-activated cell sorting
F-actin:	Filamentous-actin
FAS-L:	FAS ligand
FOX-P3:	Forkhead box P3
FRC:	Fibroblastic reticular cell
FYN:	FYN oncogene related to SRC, FGR, YES
GADS:	GRB-2-related adaptor protein downstream of SHC

GATA-3:	GATA binding protein 3
γ_c:	Common γ-chain
GEF:	Guanine nucleotide exchange factor
GFP:	Green fluorescent protein
GRB-2:	Growth factor receptor-bound protein 2
GSK-3:	Glycogen synthase kinase 3
HLA:	Human leukocyte antigen
HPK-1:	Haematopoïetic progenitor kinase 1
HSCGT:	Haematopoïetic stem cell gene therapy
HSCTx:	Haematopoïetic stem cell transplantation
HSP-90:	Heat shock protein of 90 kDa
ICAM-1:	Intercellular adhesion molecule 1
ICOS:	Inducible T-cell co-stimulator
iDC:	Immature dendritic cell
IFN-γ:	Interferon gamma
Ig:	Immunoglobuline
Igβ:	Immunoglobulin-associated beta chain
IgC:	Immunoglobuline constant
IgV:	Immunoglobuline variable
IκB:	Inhibitor of NF-κB
IKK:	IκB kinase
IL:	Interleukin
IL-R:	Interleukin-receptor
IMGT:	ImMunoGeneTics
iNKT cell:	Invariant natural killer T cell
IP_3:	Inositol 1,4,5-trisphosphate
IP_3-R:	Inositol 1,4,5-trisphosphate-receptor
IPEX:	Immune dysregulation, polyendocrinopathy, enteropathy, X-linked
iSP:	Immature single positive
ITAM:	Immunoreceptor tyrosine-based activation motif
ITK:	Interleukin-2-inducible T cell kinase
iT_{Reg}:	Inducible T_{Reg}
J:	Joining
JAK-1/3:	Janus kinase 1 and 3

JNK:	JUN N-terminal kinase
KREC:	Kappa-deleting recombination excision circle
LAT:	Linker for activation of T cells
LCK:	Lymphocyte-specific protein tyrosine kinase
LFA-1:	Leukocyte function-associated antigen 1
LIP:	Lymphopenia-induced proliferation
LPS:	Lipopolysaccharide
LT-β:	Lymphotoxin β
LTRC:	Long-term repopulating cell
mAb:	Monoclonal antibody
MAGT-1:	Magnesium transporter 1
MAGUK:	Membrane-associated guanylate kinase
MAIT cell:	Mucosa-associated invariant T cell
MALT-1:	Mucosa-associated lymphoïd tissue 1
MAPK:	Mitogen-activated protein kinase
MAP3K:	MAPK kinase kinase
MAP2K:	MAPK kinase
MCU:	Mitochondrial Ca^{2+}-uniporter
$[Mg^{2+}]_e$:	Extracellular magnesium-ion concentration
$[Mg^{2+}]_i$:	Intracellular magnesium-ion concentration
MHC:	Major histocompatibility complex
mDC:	Myeloïd dendritic cell
mDC:	Mature dendritic cell
MEK-1/2:	Mitogen-activated protein kinase 1 and 2
MEP:	Megakaryocyte/erythrocyte precursor
MR1:	Major histocompatibility complex class I-related
MTOC:	Microtubule-organizing center
mTOR:	Mammalian target of rapamycin
NCK:	Non-catalytic region of tyrosine kinase
NFAT:	Nuclear factor of activated T cells
NF-κB:	Nuclear factor of kappa light polypeptide gene enhancer in B cells
NHEJ:	Non-homologous end joining
NHR:	NFAT-homology region
NK cell:	Natural killer cell

NES: Nuclear export signal

NLR: Nucleotide-binding oligomerization domain (NOD)-like receptor

NLS: Nuclear localization signal

nT_{Reg}: Natural T_{Reg}

ORAI-1: ORAI calcium release-activated calcium modulator 1

pAB: Polyclonal antibody

PAG-1: Phosphoprotein associated with glycosphingolipid microdomains 1

PAMP-R: Pathogen-associated molecular pattern-receptor

PAX-5: Paired box protein 5

PBMC: Peripheral blood mononuclear cell

PCR: Polymerase chain reaction

PD: Programmed cell death

pDC: Plasmacytoïd dendritic cell

PDPK-1: PI3K-dependent protein kinase 1

PEP: PEST-domain phosphatase

PH: Pleckstrin homology

PHA: Phytohaemagglutinin

PI3K: Phosphatidylinositol-4,5-bisphosphate 3-kinase

PID: Primary immunodeficiency disease

PIP_2: Phosphatidylinositol 4,5-bisphosphate

PIP_3: Phosphatidylinositol 3,4,5-trisphosphate

PKCθ: Protein kinase Cθ

PLCγ-1: Phospholipase Cγ 1

PMA: Phorbol 12-myristate 13-acetate

PMCA: Plasma membrane Ca^{2+}-ATPase

pMHC: Peptide:major histocompatibility complex

PRR: Proline rich region

pSMAC: Peripheral supramolecular activation cluster

pTα: Pre T cell antigen receptor α

PTEN: Phosphatase and tensin homolog

PTK: Protein tyrosine kinase

PTP: Protein tyrosine phosphatase

PTPRC: Protein tyrosine phosphatase receptor type C

PTPRJ: Protein tyrosine phosphatase receptor type J

qPCR:	Quantitative real-time PCR
RAC-1:	RAS-related C3 botulinum toxin substrate 1
RACK:	Receptor for avtivated C kinase
RAG-1/2:	Recombination activating gene 1 and 2
RASGRP:	RAS guanyl releasing protein
RHO:	RAS-homolog
RHR:	REL-homology region
RICD:	Restimulation-induced cell death
RLK:	Resting lymphocyte kinase
RNA:	Ribonucleic acid
RORγt:	Retinoic acid receptor-related orphan receptor γt
RSS:	Recombination signal sequence
RSV:	Respiratory syncytial virus
RT-PCR:	Reverse transcription polymerase chain reaction
RUNX-3:	Runt-related transcription factor 3
SAP:	Signalling lymphocyte activation molecule-associated protein
SCID	Severe combined immunodeficiency
SDF-1:	Stromal cell-derived factor 1
SDS:	Standard deviation score
SDS-PAGE:	Sodium dodecyl sulfate polyacrylamide gel electrophoresis
SHC:	Src homology 2 domain containing protein
SHIP-1:	SH2 domain-containing 5'-inositol phosphatase 1
SHP-1:	SH2 domain-containing phosphatase 1
SLAM:	Signalling lymphocytic activation molecule
SLP-76:	SH2 domain-containing leukocyte protein of 76 kDa
SMAC:	Supramolecular activation cluster
SNP:	Single nucleotide polymorphism
SOCE:	Store-operated Ca^{2+}-entry
SOCS-1:	Suppressor of cytokine signalling 1
SOS-1:	Son of sevenless homolog 1
SP:	Single-positive
SP:	Ser-Pro-X-X repeat
SRR:	Serine rich region
STAT-5A/B:	Signal transducer and activator of transcription 5A and 5B

STK39:	Serine threonine kinase 39
STIM-1/2:	Stromal interaction molecule 1 and 2
SWAP-70:	Switch-associated protein 70 kDa
SYK:	Spleen tyrosine kinase
TAD:	Transcription activation domain
T_{CM}	Central memory T cell
TCR:	T cell antigen receptor
TCS:	T cell synapse
T_{Cyt}:	Cytotoxic T cell
TEA:	T-early α
TEC:	Thymic epithelial cell
T_{EM}	Effector memory T cell
TGF-β:	Transforming growth factor β
T_{FH}:	Follicular helper T cell
$T_{H1/2/17}$:	Helper T cell type 1, 2 and 17
TH-POK:	T-helper-inducing POZ/Kruppel-like factor
TLR:	Toll-like receptor
T_{Mem}:	Memory T cell
TNF-α:	Tumour necrosis factor alpha
TOX:	Thymus high-mobility group box protein
TRA/B/G/D@:	T cell receptor alpha/beta/gamma/delta locus
TRAF-2/6:	TNF receptor-associated factor 2 and 6
TRA/B/C/DC:	TRA@/TRB@/TRG@/TRD@ constant segment
TRA/B/C/DV:	TRA@/TRB@/TRG@/TRD@ variable segment
TREC:	T cell receptor excision circle
T_{Reg}:	Regulatory T cell
TSAD:	T cell specific adaptor protein
TSLP:	Thymic stromal lymphopoietin
TSP:	Thymus seeding progenitor
V:	Variable
WASP:	Wiskott-Aldrich syndrome protein
XIAP:	X-linked inhibitor of apoptosis
XLP-1:	X-linked lymphoproliferative syndrome type 1
ZAP-70:	ζ-chain associated protein tyrosine kinase of 70 kDa

$[Zn^{2+}]_e$: Extracellular zinc-ion concentration

$[Zn^{2+}]_i$: Intracellular zinc-ion concentration

1 Introduction

1.1 The immune system

Human beings are confronted with physical, chemical and (micro-) biological insults throughout their entire lifespan. To preserve their structural and functional integrity, they have evolved a specialized system, the immune system. The main function of the immune system is to recognize self, altered-self and non-self antigens and to decide whether to reject them by initiating a immune response or to accept them by inducing immune tolerance.[1]

Historically, the immune system has been divided into an innate and adaptive branche, even thought there is important cross-talk at their interface. The primary lymphoïd organs, i.e. bone marrow, thymus and spleen, and the secondary lymphoïd organs, i.e. lymph nodes, tonsils and organ-associated lymphoïd tissues, constitute its principal anatomical compartments.[1] Furthermore, in the context of chronic inflammation, the immune system is able to establish tertiary lymphoïd tissues at almost every site of the body.[2]

Besides an array of secreted molecules, i.e. lipid mediators, interferons, cytokines and chemokines, and their cognate receptors, that are partially shared by both branches, the innate and adaptive immune system comprise particular receptor families, cell populations and their individual effector molecules.[1]

Briefly, the innate immune system is build up by epithelial barriers, antimicrobial peptides, danger-associated molecular pattern- and pathogen-associated molecular pattern-recognizing molecules and receptors (DAMP-Rs and PAMP-Rs), i.e. pentraxins, complement, innate antibodies, nucleotide-binding oligomerization domain (NOD)-like (NLRs) and Toll-like receptors (TLRs), mast cells, monocyte-macrophages, neutrophil/eosinophil/basophil granulocytes, natural killer (NK) cells and antigen presenting cells (APCs), i.e. plasmacytoïd and myeloïd dendritic cells (pDCs and mDCs) and Langerhans cells.[1]

Innate immune responses are triggered by the sensing of DAMPs and PAMPs and initially lead to inflammation, increased effector function and consequently antigen clearance. Thereafter, the innate immune system downmodulates its inflammatory response and initiates tissue repair.[3] Importantly, the innate immune system triggers and finetunes the adaptive immune response by establishing particular cytokine microenvironments and by processing and presenting antigens.[4]

The adaptive immune system comprises T cells, B cells and specific antibodies.[1] A central feature of T cells and B cells is the expression of the T cell antigen receptor (TCR) and the B cell antigen receptor (BCR), respectively, that theoretically endow them with the ability to recognize all possible antigens. While the TCR and the BCR are membrane bound, specific antibodies corespond to secreted forms of the BCR.[1]

T cells are pivotal to the adaptive immune system as they co-ordinate immune tolerance and efficient adaptive immune responses, aquire antigen-specific effector functions and build up antigen-specific memory. A variety of T cell subpopulations exist, i.e. natural killer T cells (NKTs), mucosa-associated invariant T cells (MAITs), innate-like γδ T cells, and conventional αβ T cells. The latter can be further subdivided into $CD4^+$ helper T cells (T_H), $CD4^+CD25^+$ forkhead box $P3^+$ ($FOX\text{-}P3^+$) regulatory T cells (T_{Reg}) and $CD8^+$ cytotoxic T cells (T_{Cyt}).

B cells contribute to the adaptive immune response by acquiring APC function and by differentiating into specific antibody-secreting plasma cells.[1]

To obtain the ability of antigen-specific immune recognition and response, T and B cells pass through unique maturation programms that take place in the thymus and the bone marrow, respectively.[5]

The DAMP-Rs and PAMP-Rs of the innate immune system are encoded by entire genes and can be directly expressed in a non-clonal manner. As they have been evolutionarily selected, they recognize a limited array of conserved molecular patterns, e.g. lipopolysaccharide (LPS), single-strand or double-strand ribonucleic acid (RNA) and deoxyribonucleic acid (DNA), and efficiently discriminate self, altered-self and non-self. Consequently, they can rapidyl initiate immune responses to a narrow antigenic spectrum.[6]

The TCRs and BCRs, however, are encoded in huge genetic loci by particular gene segments and their somatic rearrangement is necessary to express a clonally restricted but highly variable receptor repertoire. As the individual TCRs and BCRs have been selected in somatic cells, they recognize particular epitopes of protein and carbohydrate antigens and their ability to discriminate self, altered-self and non-self is imperfect. Consequently, they can initiate a delayed immune response and immunological memory to virtually all possible antigenic structures.[6]

Throughout the last five decades, the immune system has been extensively investigated *in vitro* and in animal models such as the murine system. Additionally, studying and taking care of human primary immunodeficiency diseases (PIDs) has been seminal for our understanding of the human immune system's developement, homeostasis, and function

(see chapter 1.5.1).[7] Currently, more than 150 PIDs have been classified by the International Union of Immunological Societies Expert Committee for Primary Immunodeficiency.[8]

This immunobiological thesis is aimed to contribute to our knowledge of the human immune system by analyzing disturbed proximal TCR:CD3:ζ-signalling caused by autosomal recessive lymphocyte-specific protein tyrosine kinase (LCK)-, ζ-chain associated protein tyrosine kinase of 70 kDa (ZAP-70)- and interleukin-2-inducible T cell kinase (ITK)-deficiency.

1.2 TCR:CD3:ζ-signalling

On their cell surface T cells express either a preTCR, or an (invariant) γδ TCR or a clonotypic αβ TCR together with the cluster of differentiation (CD) 3-complex and the associated ζ-chain.[9-12] TCR:CD3:ζ-signalling is crucial for T cell development and antigen-specific activation, proliferation, differentiation, effector function and apoptosis of mature T cells.[5, 13, 14] Basically, APCs assimilate and process protein antigens and present antigenic peptide fragments bound to major histocompatibility complex (MHC) molecules to T cells. T cells recognize and bind peptide:MHCs (pMHC) with their TCR and signal with their CD3:ζ-complex at a molecular interface termed T cell synapse (TCS).[15]

The TCS can be devided into different anatomical and functional layers, i.e. the receptor layer, the signalling layer, the ion channel and transporter system, and the cytoskeletal layer.[16]

The nature of the presented antigenic fragment and the spatiotemporal and molecular composition of the TCS are pivotal for the functional outcome of TCR:CD3:ζ-signalling.[17]

1.2.1 The TCR:CD3:ζ-complex

The mature TCR is build up by a disulfide-linked heterodimer of either one TCRα- and one TCRβ- or one TCRγ- and one TCRδ-glycoprotein. The TCRα- has sequence homology to the TCRδ- and the TCRβ- to the TCRγ-chain, respectively.[18, 19] Additionally, during T cell development thymocytes transiently express the preTCR consisting of a TCRβ-chain and the invariant pre T cell antigen receptor α (pTα) -chain, that serves as a surrogate for the TCRα-chain (Fig. 1A).[5, 20, 21]

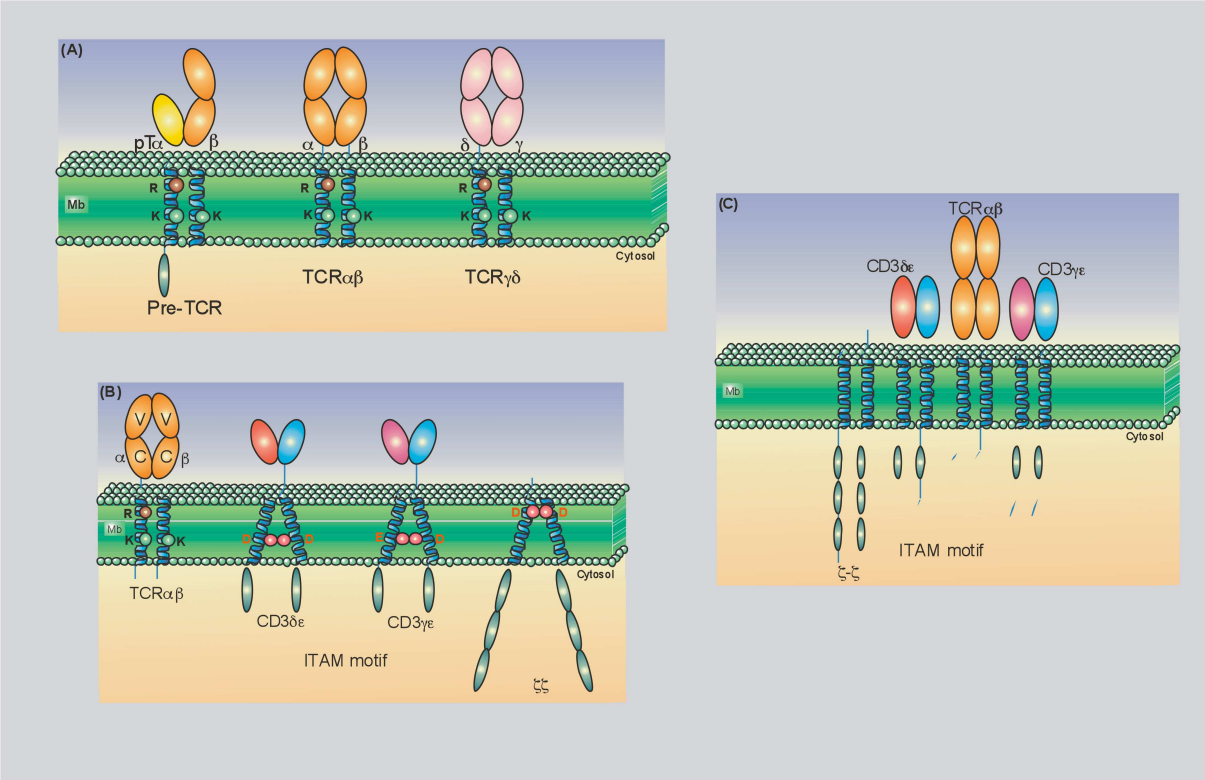

Figure 1. TCR:CD3:ζ-complex.

(A) Schematic representation of the preTCR-, the αβ TCR- and the γδ TCR-heterodimer with the extracellular variable (V) and constant (C) immunoglobulin-like domains, the transmembrane domains containing the basic amino acid residues arginine (R) and lysine (L) and the signalling or non-signalling intracellular domains of the pTα- and the TCR α-, β-, γ- and δ-glycoproteins, respectively.

(B) Schematic representation of the αβ TCR-heterodimer as in (A) and the CD3δε-, CD3γε- and ζζ-heterodimers with the extracellular domains, the transmembrane domains containing the acidic amino acid residues aspartic acid (D) and glutamic acid (E) and/or the signalling intracellular immunoreceptor tyrosine-based activation motif (ITAM)-encompassing domains.

(C) Schematic representation of the canonical TCRαβ:CD3γε:CD3δε:ζζ-complex composed of the heterodimers indicated in (A) and (B).

Figure adapted from Call ME, Wucherpfennig KW, Annu Rev Immunol, 2005.[22]

Each TCR-chain contains an extracellular domain, a transmembrane region and a short intracellular domain. The extracellular domain comprises a variable (V) and constant (C) immunoglobuline (Ig)-like domain, the transmembrane region contains three conserved basic amino acid residues, i.e. one arginine (R) and two lysines (K), and the short intracellular domain lacks intrinsic signalling activity.[10] The pTα-chain comprises a single extracellular Ig-like domain and a transmembrane region, both of which resemble that of the TCRα-chain, and an intracellular domain. In contrast to the TCRα-chain, the intracellular domain of the pTα-

chain possesses two phosphorylation sites, suggesting a CD3:ζ-complex independent signalling capacity of the preTCR.[23, 24]

The prototypical and clonotypic αβ TCR is expressed by conventional T cells, such as $CD4^+$ T_H, $CD4^+CD25^+FOX\text{-}P3^+$ T_{Reg} and $CD8^+$ T_{Cyt}, and recognizes antigenic peptides, that are presented by classical and polymorphic MHC class I or class II molecules.[25] The αβ TCR IgV-like domain binds diagonally over the entire pMHC.[26] Each αβ TCR IgV-like domain consists of three hypervariable complementarity determining regions (CDRs). CDR1 and CDR2 are determined by germline V gene segments while CDR3 is determined by germline diversity (D) and joining (J) gene segments and junctional diversity (see chapter 1.3.3).[27] The CDR3α and CDR3β loops interact with the central part and the CDR1α and CDR1β with the amino-terminal and carboxy-terminal part of the presented peptide, respectively. The MHC molecule principally is bound by CDR1αβ and CDR2αβ loops but CDR3αβ loops as well can form minor contacts.[28]

Semi-invariant αβ TCRs are expressed by invariant NKT (iNKT) cells and bind lipid antigens presented by MHC class I like CD1 molecules by only partially contacting the binding groove and parallel to its long axis. The NKT cell TCR Vα24Jα18 binds the glycosyl head group of α-galactosylceramide with CDR1α and CDR3α that are germline-encoded by Vα24 and Jα18, respectively.[29, 30]

Mucosa-associated invariant T cells (MAITs) express a semi-invariant TCR Vα7.2Jα33 that is restricted by the evolutionarily conserved major histocompatibility complex class I-related (MR1) molecule and recognize bacterially infected cells in a MR1-dependent manner.[31, 32] The lipid antigen α-mannosylceramide has been proposed as the specific MR1-ligand but *in silico* modelling favours a hydrophilic compound.[33, 34]

Invariant γδ TCRs are expressed by γδ T cells with an innate-like phenotype and bind as yet poorly defined bacterial phosphoantigens presented by non-polymorphic MHC-like molecules. This interaction differs strongly from that of TCRαβ:pHMC as the γδ TCR binds sideways to the nonclassical MHC-like molecule and only one CDR, namely the CDR3δ, contacts the binding groove.[35, 36]

Thus, polymorphic αβ TCRs, semi-invariant αβ TCRs and (invariant) γδ TCRs are MHC or MHC-like restricted and this is due to germline encoded sequence and structure homologies that have co-evolved between the MHC molecules and the particular TCR V Ig-like domains.[37, 38]

One monovalent heterodimeric TCR is noncovalently associated with the monomorphic CD3γ-, CD3δ-, CD3ε- and ζ-chain that are not involved in antigen recognition

but responsible for signal transduction. The stoichiometry of the TCRαβ:CD3:ζ-complex is TCRαβ:CD3γε:CD3δε:ζζ while that of the TCRγδ:CD3:ζ-complex is TCRγδ:CD3γε:CD3δε:ζζ.[39-43] The definitive stoichiometry of the human preTCR has not yet been resolved (Fig. 1 B and C).[44]

For correct assembly and surface expression the TCRαβ-, the CD3γε-, CD3δε- and the ζζ-chains are necessary and sufficient.[41, 42] The TM regions of the TCRαβ-heterodimer contain three conserved basic amino acid residues and the TM regions of the CD3γε-,CD3δε- and ζζ-dimers two conserved acidic amino acid residues, i.e. aspartic and glutamic acid. Probably by forming pairwise ionic interactions, these putatively charged residues are crucial for correct TCR:CD3:ζ-complex association.[45]

The CD3- and ζ-chains have cytoplasmic tails containing immunoreceptor tyrosine-based activation motifs (ITAMs) that are phosphorylated upon receptor triggering and that recruit further signalling molecules.[46-49] The entire TCRαβ:CD3:ζ-complex contains ten ITAMs and each ITAM contains two conserved tyrosine, one acidic and two aliphatic amino acid residues. The ITAM consensus sequence is $D/Ex_{0-2}YXXL/Ix_{6-8}YXXL/I$ (with D denominating aspartic acid, E glutamic acid, Y tyrosine and X any amino acid residue with the lower case number indicating their variable frequencies) and the CD3γ-, CD3δ- and CD3ε-chains each contain one ITAM while the ζ-chain contains three tandem ITAMs (Fig. 2).[46]

The cytoplasmic tails of the CD3ε- and the ζ-chain interact with acidic phospholipids of the inner plasma membrane leaflet and it has been proposed that in an untriggered TCRαβ:CD3:ζ-complex the ITAMs might remain in a lipid-bound stage being inaccesible for activating protein tyrosine phosphorylation.[50, 51]

Even though there are different models of how initial TCR triggering is transduced into intracellular signalling, the TCR might be a mechanotransductor and TCR:CD3:ζ-complex interaction with pMHC might induce conformational changes that render the ITAMs accessible for protein tyrosine phosphorylation.[52]

Once the TCR:CD3:ζ-complex has been triggered by pMHC, possible mechanisms of signal termination are dephosphorylation, internalisation and ubiquitin-mediated degradation in the lysosomal compartment.[52, 53]

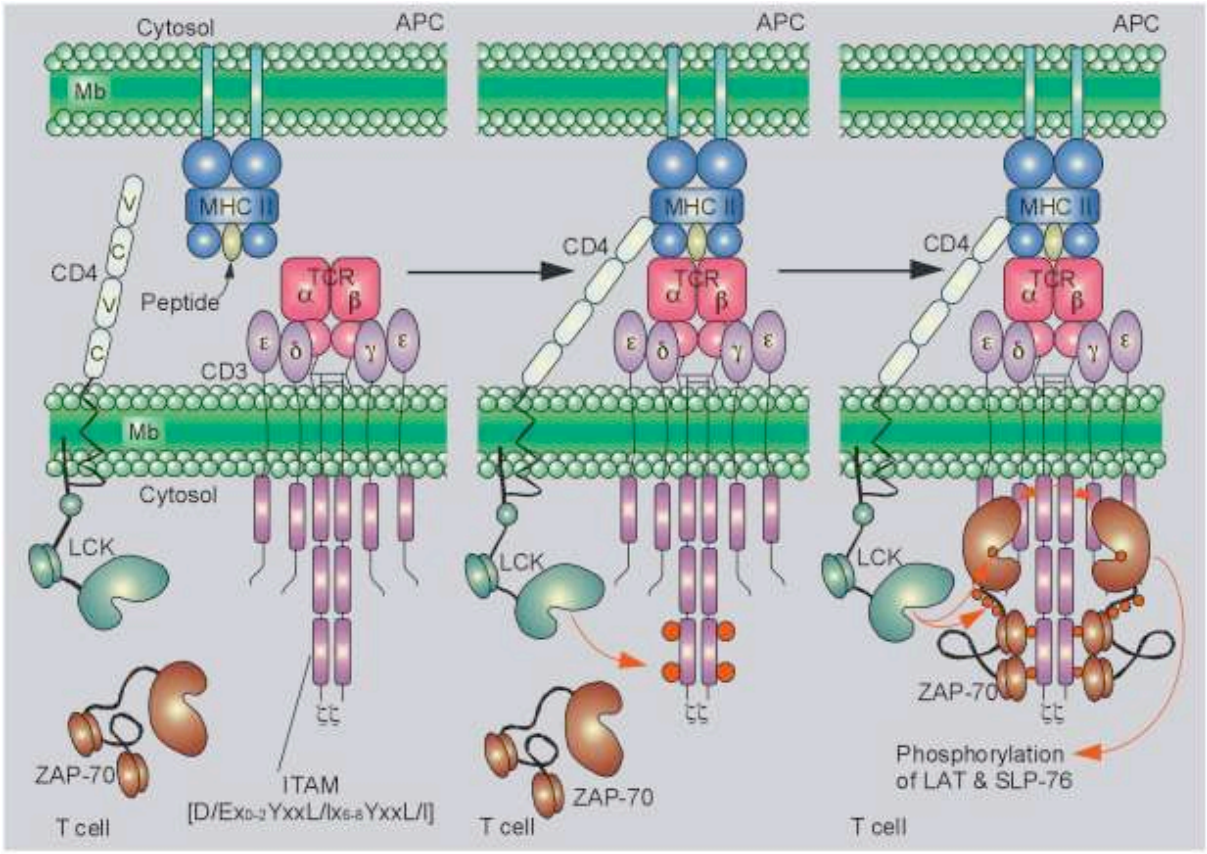

Figure 2. T cell synapse and proximal TCR:CD3:ζ-signalling.

Schematic representation of the membrane interface of an antigen presenting cell (APC) and a T cell forming the T cell synapse (TCS) and initiating proximal TCR:CD3:ζ-signalling. Initially, the peptide:major histocompatibility complex class II (pMHC II) is recognized by its cognate αβ TCR. This enables the co-receptor CD4 to bind the pMHC II and recruits and activates the membrane-anchored and CD4-bound protein tyrosine kinase (PTK) lymphocyte-specific protein tyrosine kinase (LCK). Next, LCK phosphorylates the ITAMs - the ITAM consensus sequence is indicated in parentheses - of the ζζ-heterodimer and creates the docking site for the PTK ζ-chain associated protein tyrosine kinase of 70 kDa (ZAP-70). ZAP-70 binds to the phosphorylated ITAMs, in turn is phosphorylated and activated by LCK and amplifies and diversifies the TCR:CD3:ζ-signalling by phosphorylating downstream adaptor proteins including the linker for activation of T cells (LAT) and the SH2 domain-containing leukocyte protein of 76 kDa (SLP-76).

Figure adapted from Wang H, et al, Cold Spring Harb Perspect Biol, 2010.[54]

1.2.2 The receptor layer

The receptor layer is the cell membrane compartment where antigen:receptor- and receptor:receptor-interactions take place. It contains the TCR:CD3:ζ-complex and co-receptors as well as co-stimulatory, co-inhibitory and adhesions molecules.[16] Additionally, TCR:CD3:ζ-signalling is mediated by a network of ion channels and transporters partially located in the receptor layer (Fig. 3).[55]

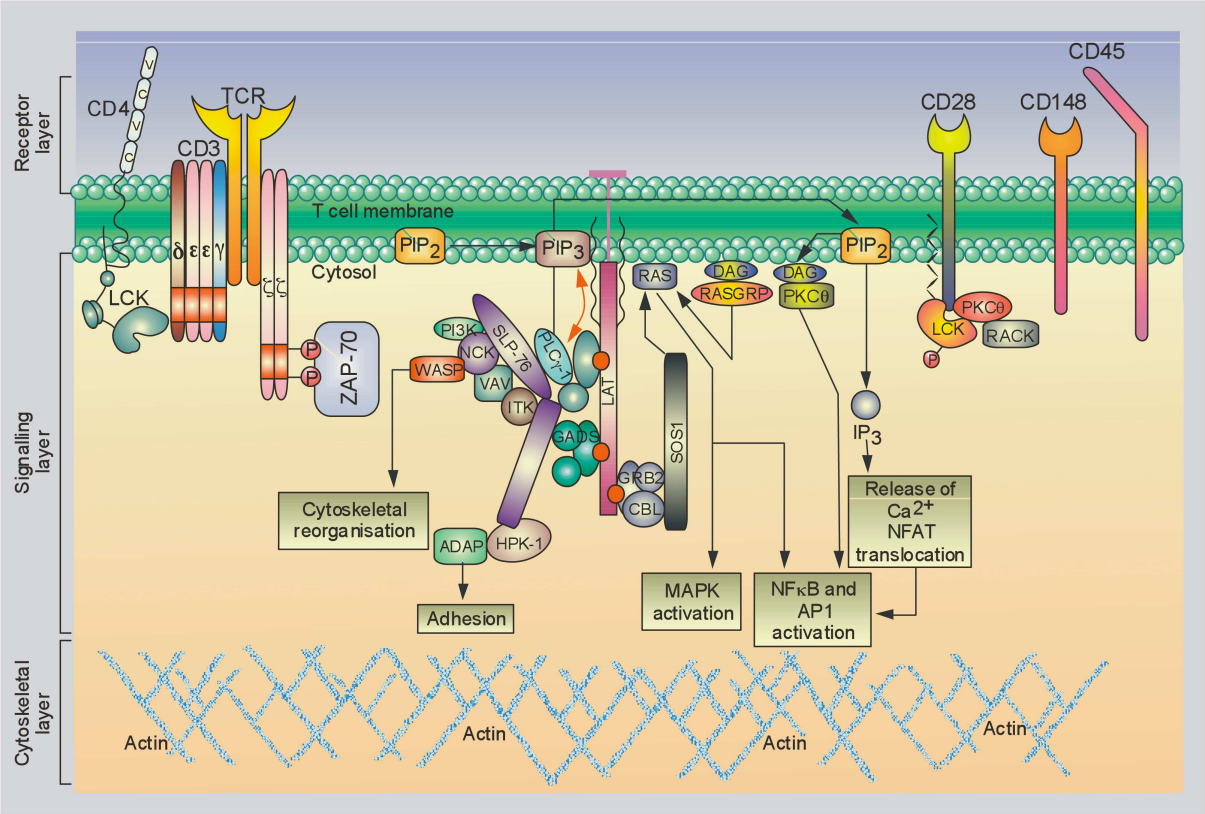

Figure 3. T cell receptor, signalling and cytoskeletal layers.

Once the T cell synapse (TCS) has formed, T cell signalling takes place in three major cellular compartments, i.e. the receptor, signalling and cytoskeletal layer. The receptor layer is comprised of the TCR:CD3:ζ-complex itself, activating co-receptors such as CD4 and CD28 and inhibitory co-receptors such as CD45 and CD148. Furthermore, membrane-bound and -derived phospholipids such as phosphatidylinositol 4,5-bisphosphate (PIP_2), phosphatidylinositol 3,4,5-trisphosphate (PIP_3), inositol 1,4,5-trisphosphate (IP_3) and diacylglycerol (DAG) are important anchor molecules and second messengers, respectively. Ion-channels such as the Mg^{2+}- and the Ca^{2+}-prevalent magnesium transporter 1 (MAGT1) and Ca^{2+}-release-activated Ca^{2+}-channel (CRAC) are also located in the cell membrane. The signalling layer contains a vast array of signalling molecules and intermediates that either are attached directly to the recptor layer or are nucleated basically by the adaptor proteins linker for activation of T cells (LAT) and SH2 domain-containing leukocyte protein of 76 kDa (SLP-76). The so-called proximal TCR-signalosome amplifies and couples the initial TCR:CD3:ζ-signal to various downstream singalling pathways, such as the mitogen-activated protein kinase (MAPK)-, nuclear factor of kappa light polypeptide gene enhancer in B cells (NF-κB)-, nuclear factor of activated T cells (NFAT)- and activator protein 1 (AP-1)-pathway. Additionally, the TCR-signalosome governs cellular processes such as adhesion and cytoskeletal reorganisation predominantly mediated by the cytoskeletal layer.

Figure adapted from Dustin ML, Depoil D, Nat Rev Immunol, 2012, and Balagopalan L, et al, Cold Spring Harb Perspect Biol, 2010.[16, 56]

1.2.2.1 The T cell synapse

The TCS, also termed immunological synapse, lies at the heart of the receptor layer and anatomically is organized in concentric supramolecular activation clusters (SMACs), i.e.

the inner central SMAC (cSMAC), the intermediate peripheral SMAC (pSMAC) and the outer distal SMAC (dSMAC). Basically, SMAC formation is due to lateral segregation of particular molecules.[57] Upon pMHC-recognition, 11-17-valent TCR:CD3:ζ-microclusters form in the pSMAC and move centripetally towards the cSMAC.[58] Additionally, the cSMAC contains microclusters of the co-recptors CD4 and CD8 and of co-stimulators such as CD28.[58, 59] Adhesion molecules, such as the integrin leukocyte function-associated antigen 1 (LFA-1), form microclusters as well but localize to the pSMAC.[60] Inhibitory proteins, such as the protein tyrosine phosphatase (PTP) receptor type C (PTPRC, CD45) and the PTP receptor type J (PTPRJ, CD148), are excluded from the cSMAC and the pSMAC and locate to the dSMAC.[57]

How precisely lateral segregation is achieved, remains a matter of debate. The size of the separated molecules seems to be important as the intercellular APC:T cell-distance spanned by a pMHC:TCR:CD3:ζ-complex is about 15 nm while that of a LFA-1:intercellular adhesion molecule 1 (ICAM-1)-complex is about 40 nm.[61] Moreover, once the TCR:CD3:ζ-microclusters have reached the cSMAC, they loose their interactions with the actin cytoskeleton while the integrin-microclusters of the pSMAC maintain these interactions, that are necessary for their stabilization. It has therefore been proposed, that the cSMAC functions as a drop-off basin that includes microclusters with the right size that rest assembled without stabilizing contacts to the cytoskeleton.[60, 62]

The classical view of TCR:CD3:ζ-signalling being located to the cSMAC has recently been challenged by the observations that TCR:CD3:ζ-micorclusters already signal in the pSMAC and that the cSMAC might instead be the place of signal termination via receptor internalisation.[63, 64]

1.2.2.2 CD4 and CD8

The most important TCR:CD3:ζ-co-receptors are the single-pass type I membrane proteins CD4 and CD8 that phenotypically define $CD4^+$ T_H and $CD8^+$ T_{Cyt} cells, respectively.[65] CD4 is composed of two extracellular IgV-like domains, two IgC-like domains, one TM region and one intracellular domain.[66] The first IgV-like domain interacts with the β_2-domain of MHC class II.[67]

CD8 is a heterodimer generally composed of CD8α and CD8β that are linked by two disulfide bonds. Each CD8 molecule consists of an extracellular IgV-like domain, a TM region and one intracellular domain. The IgV-like domain of CD8α interacts with the α_3-

domain of MHC class I.[68, 69] Thus, CD4 and CD8 stabilize the interaction of the TCR:CD3:ζ-complex with either MHC class II or MHC class I molecules, respectively.

Moreover, the intracellular domains of CD4 and CD8 bind the protein tyrosine kinase (PTK) LCK and recruit it to the TCR:CD3:ζ-complex, thus crucially contributing to the initiation of TCR:CD3:ζ-signalling (Fig. 2).[70]

1.2.2.3 CD45

The PTPRC CD45 is a single-pass type I membrane protein that is expressed in all nucleated haematopoïetic cells.[71] CD45 contains an extracellular portion that is composed of a N-terminal region and two fibronectin-type III repeats, a TM region and an intracellular portion that contains a wedge-like region and two tandem protein tyrosine phosphatase domains (PTPs).[72] The first PTP domain (D1) is catalytically active while the second one (D2) appears inactive and might endow substrate specificity to CD45.[73] The wedge-like region has been found to inhibit D1 of homodimerized CD45 *in trans* and contributes to negative regulation.[74]

Up to eight CD45 isoforms exist and in T cells the most prominent ones are CD45RA, CD45RB and CD45R0. The extracellular N-terminal regions of the CD45 isoforms vary in size and glycosylation pattern as a consequence of alternative splicing and post-translational modification. CD45RA is the longest isoform and is predominantly expressed by naïve T cells while CD45R0 is the shortest isoform and is expressed by activated and memory T cells.[75] CD45 can inhibit TCR:CD3:ζ-complex activation but upon TCR triggering is excluded rapidly from the cSMAC as a function of its size.[76] Importantly, CD45 dephosphorylates the SRC kinase LCK at its inhibitory tyrosine Y505 and therefore is a positive regulator of TCR:CD3:ζ-signalling.[77] Additionally, CD45 dephophorylates the activating tyrosine Y394 at the activation loop (A-loop) of LCK with a lower affinity than that for Y505 and this might again be a negative feedback mechanism.[78] CD45 spontaneously homodimerizes and this inhibits its catalytic activity. The autoinhibitory efficacy of homodimerization is inversely correlated with the size of the N-terminal regions, thus the smallest isoform CD45R0 is less efficient in catalyzing TCR:CD3:ζ-signalling than the longest isoform CD45RA.[74]

1.2.2.4 Co-stimulation

Co-stimulatory and co-inhibitory molecules modulate TCR signalling strenght or duration and importantly fine-tune activation, proliferation, differentiation and effector function.[16] The co-stimulatory CD28 and inducible T-cell co-stimulator (ICOS, CD278) and

the co-inhibitory cytotoxic T lymphocyte antigen 4 (CTLA-4) interact with CD80 and CD86 expressed by APCs and are the best studied examples (Fig. 3).[79] Numerous other co-stimulatory and co-inhibitory receptor families, such as the signalling lymphocytic activation molecule (SLAM)- or the programmed cell death (PD)-receptors exist.[80, 81] Co-stimulation, as illustrated by pMHC:TCR- and CD80/CD86:CD28-interactions, is important for productive T cell activation, as T cells lacking proper co-stimulation enter a state of unresponsiveness designated anergy, an important means of peripheral tolerance.[82, 83]

1.2.2.5 Adhesion molecules

Adhesion molecules function in an antigen-independent manner and predominantly intensify the interaction of APCs with T cells as illustrated by the CD2:CD58- and the LFA-1:ICAM-1-interaction.[61] Adhesion receptors further stabilize and couple the TCS to the cytoskeleton and are involved in cell motility.[84]

1.2.3 The signalling layer

Protein tyrosine kinase (PTK) cascades lie at the heart of TCR:CD3:ζ-signalling. In T cells, the PTKs of the CSK-, SRC-, SYK- and TEC-family are the major players and the most important family members are CSK, LCK, ZAP-70 and ITK, respectively.[54, 85, 86] Globally, these four classes of PTKs act sequentially to propagate protein tyrosine phosphorylation signals. The first class CSK inhibits, the second class LCK initiates, the third class ZAP-70 amplifies and the fourth class ITK diversifies protein tyrosine phosphorylation signals. T cells express a variety of additional PTKs of the SRC-, SYK- and TEC-family, such as the FYN oncogene related to SRC, FGR, YES (FYN), the spleen tyrosine kinase (SYK) related to ZAP-70 and the resting lymphocyte kinase (RLK) related to ITK, respectively.[54, 85, 86]

1.2.3.1 LCK

The PTK LCK comprises 509 amino acid residues, has a molecular weight of 56 kDa and is expressed almost exclusively in T cells. LCK consists of a N-terminal unique SRC homology 3 (SH3) domain, followed by a SH2 and a C-terminal SH1 or kinase domain (Fig. 4). The SH3 and SH2 domains infere intra- and inter-protein interactions by binding to polyproline and phosphotyrosine motifs, respectively.[87] The LCK N-terminus is myristoylated and palmitoylated and is mediating constitutive membrane anchoring.[88] The N-terminus contains a di-cysteine motif that together with a di-cysteine motif in the intracellular tails of the co-receptors CD4 and CD8α, respectively, chelates a Zn^{2+}-ion and mediates co-receptor anchorage (Fig. 2 and 3).[70, 89, 90] Of note, LCK binds to CD4 with higher affinity than to

CD8α and TCR:CD4-co-stimulation generates stronger LCK-mediated signals than TCR:CD8-co-stimulation does.[91] The kinase domain contains the ATP binding lysine residue K273 and the catalytic proton acceptor aspartic acid residue D364 that conduct protein tyrosine phosphorylation of the ITAMs of the TCR:CD3:ζ-complex.[92] Furthermore, LCK functions as an adaptor protein via its SH2 and SH3 domains.[93, 94]

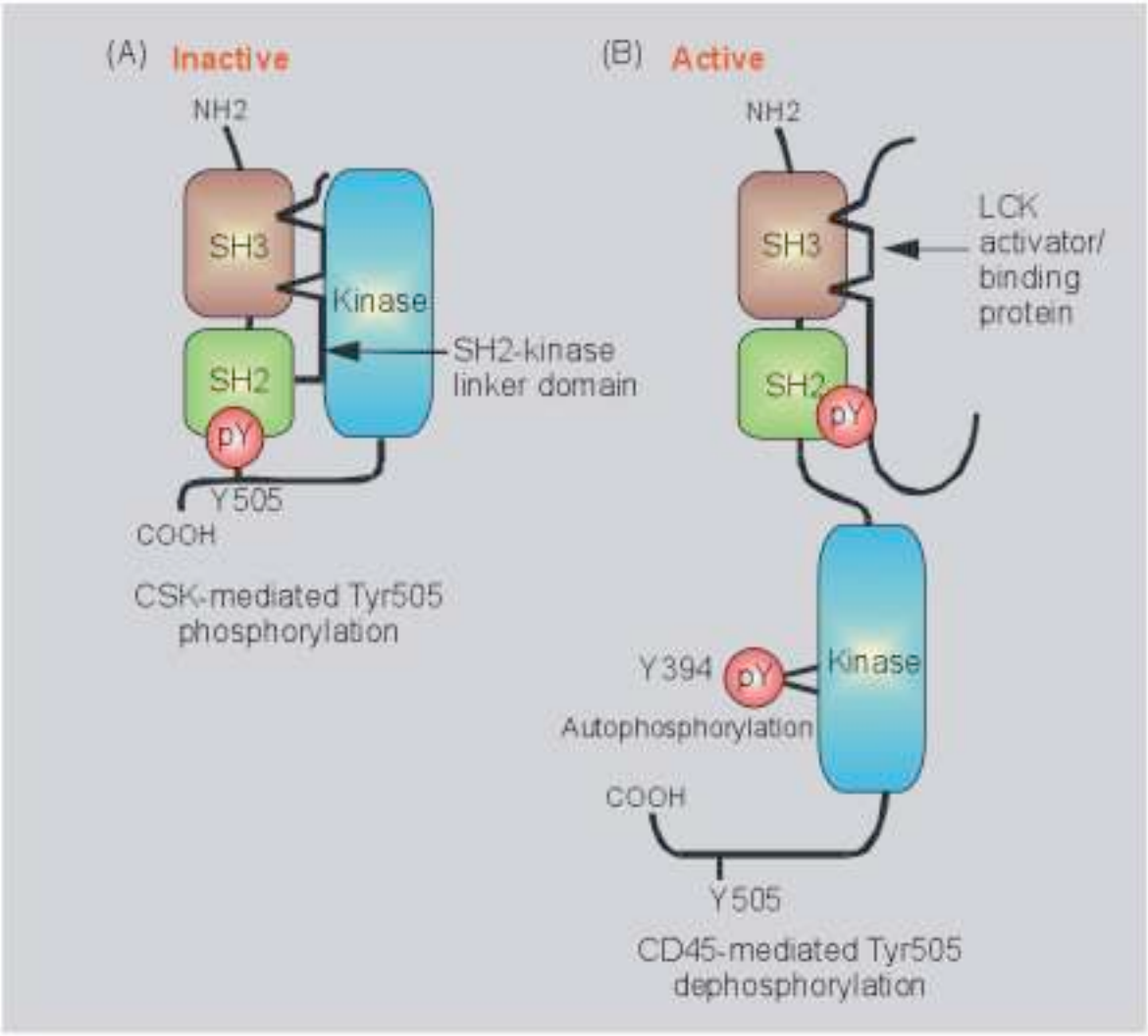

Figure 4. Inactive and active lymphocyte-specific protein tyrosine kinase (LCK).

(A) The inactive conformation of LCK is induced by C-terminal SRC kinase (CSK)-mediated phosphorylation of the inhibitory tyrosine 505 (pY505) that binds to the LCK SH2 domain. The restrained conformation is further stabilized by the interaction of a polyproline motif located in the SH2-kinase linker domain with the SH3 domain.

(B) The active conformation of LCK is induced by CD45-mediated dephosphorylation of the inhibitory Y505. As a consequence the A-loop opens up and the activating Y394 is phosphorylated by LCK auto-/transphosphorylation endowing LCK with full catalytic activity. The active conformation is further stabilized by protein:protein interactions mediated by the SH3 and SH2 domains of LCK.

Figure adapted from Salmond RJ, et al, Immunol Rev, 2009.[85]

The kinase function of LCK is tightly regulated by conformational changes caused by ligand binding of the SH3 and the SH2 domains and by phosphorylation and dephosphorylation of pivotal tyrosine residues.[85] When the inhibitory C-terminal tyrosine Y505 is phosphorylated by CSK, that is recruited by the adaptor phosphoprotein associated with glycosphingolipid microdomains 1 (PAG-1), it binds to the LCK SH2 domain and induces a closed conformation.[95-97] The restrained conformation is further stabilized by the interaction of a polyproline motif located in the SH2-kinase linker domain with the SH3 domain (Fig. 4A).[98] The PTPRC CD45 can dephosphorylate the inhibitory tyrosine Y505 and induces an open and basally active LCK conformation.[77] The activating tyrosine Y394 is located in the A-loop of the kinase and when dephosphorylated the A-loop aquires an α-helical conformation blocking the catalytic center. When tyrosine Y505 is dephosphorylated and LCK opens up, the A-loop is displaced from the catalytic center.[99] LCK then performs auto-/transphosphorylation of tyrosine Y394 and aquires full catalytic activity.[100] Additionally, LCK becomes phosphorylated at the serine residue S59 by the extracellular signal-regulated kinase 1/2 (ERK-1/2) and this and further protein:protein-interactions stabilize the active conformation (Fig 4B).[101]

The overall activating modifications lead to an increase of the molecular weight of LCK from 56 to 60 kDa.[102]

By dephosphorylation events LCK activity is kept in check and several PTPs such as CD45, SH2 domain-containing phosphatase 1 (SHP-1) and PEST-domain phosphatase (PEP) rapidyl dephosphorylate the activating tyrosine Y394.[103-105]

1.2.3.2 ZAP-70

The PTK ZAP-70 comprises 619 amino acid residues, has a molecular weight of 70 kDa and is mainly expressed in T cells. On its N-terminus, ZAP-70 consists of two tandem SH2-domains denominated N-terminal and C-terminal SH2-domain, respectively, that are separated by an interdomain A and followed by an interdomain B and one C-terminal SH1 or kinase domain (Fig. 5A).[106]

In resting T cells ZAP-70 is located in the cytoplasm, but upon TCR:CD3:ζ-signalling rapidly is recruited to the cSMAC plasma membrane.[107, 108] The tandem SH2-domains bind with high affinity and specificity to double phosphorylated ITAMs of the ζ-chain.[109] While the C-terminal phosphotyrosine binding pocket is formed by the C-terminal SH2-domain, the N-terminal one is formed cooperatively by the N-terminal and the C-terminal SH2-domain. The precise positioning of the tandem SH2-domains and the overall conformational changes

of ZAP-70 necessary for ITAM-binding are stabilized by a coiled-coil domain of the interdomain A (Fig. 5B).[110, 111]

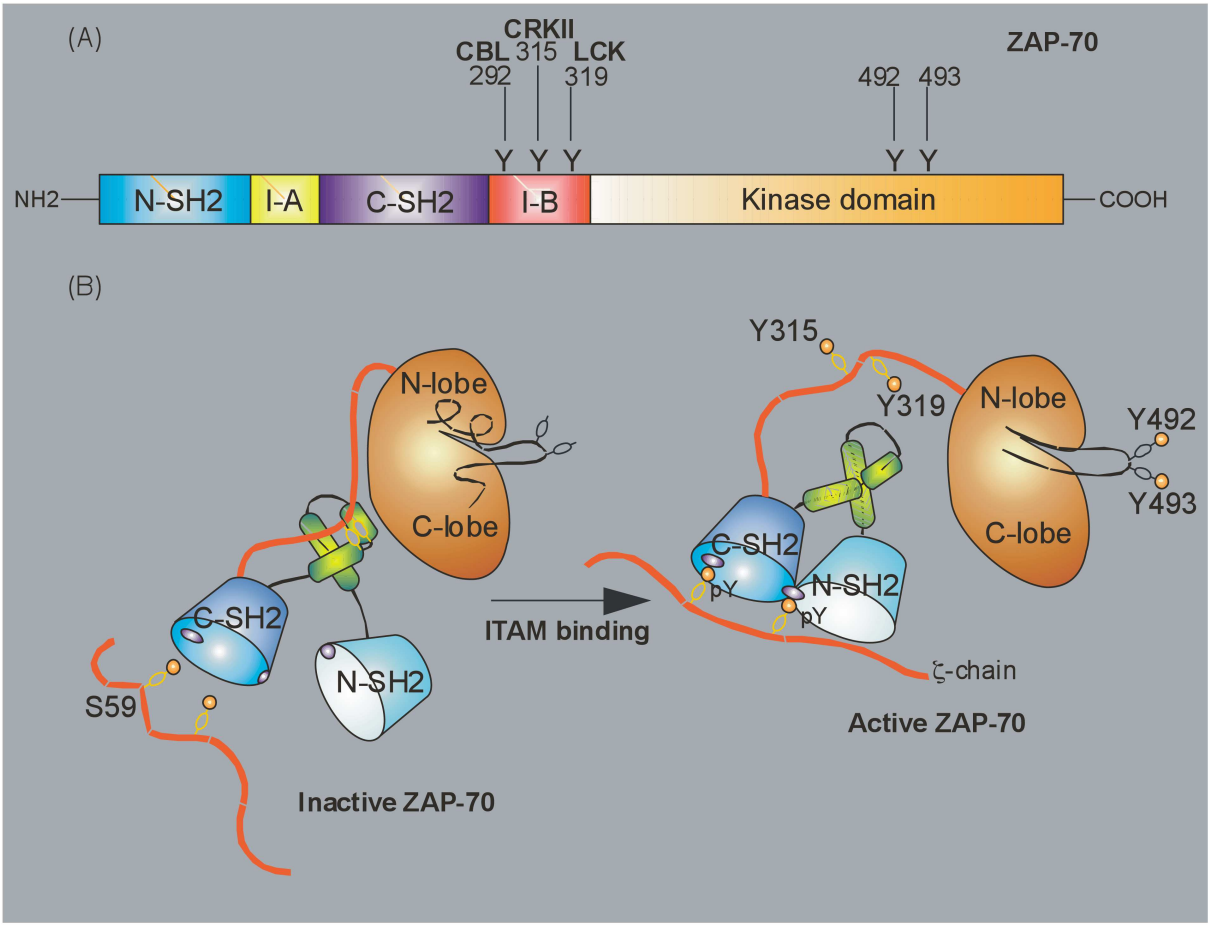

Figure 5. Domain structure and scheme of inactive and active ζ-chain associated protein tyrosine kinase of 70 kDa (ZAP-70).

(A) The domain structure of ZAP-70 is shown with the N-terminal and C-terminal tandem SH2-domains, the interdomains A and B and the kinase domain. The tyrosine residues Y292, Y315 and Y319 of the interdomain B that are targeted by CBL, CRKII and LCK, respectively, and Y492 and Y493 of the A-loop that are trans/autophosphorylated by LCK and ZAP-70 are indicated.

(B) On the left the inactive conformation of ZAP-70 is shown with Y315 and Y319 masked by the coiled-coil domain of the interdomain A and the A-loop bound to the catalytic cleft of the kinase domain. On the right the active conformation of ZAP-70 is shown with the tandem SH2-domains bound to the phosphorylated ITAMs of the ζ-chain. The active confirmation is further stabilized by the coiled-coil domain and the phosphorylated Y315 and Y319 that are now available for protein:protein-interactions. Due to activating phosphorylation of Y492 and Y493 the A-loop has opend up and is endowing ZAP-70 with full catalytic activity.

Figure adapted from Wang H, et al, Cold Spring Harb Perspect Biol, 2010.[54]

Similar to LCK, the A-loop of the ZAP-70 kinase domain becomes phosphorylated predominantly by LCK and to some extend is autophosphorylated by ZAP-70 at tyrosine residues Y492 and Y493.[112, 113] This removes the A-loop from the catalytic center and leads to

full kinase activity.[112] The interdomain B contains the regulatory tyrosine residues Y292, Y315 and Y319. Upon ZAP-70 activation they are bound and phosphorylated by LCK and this further stabilizes the activated conformation by impeeding autoinhibition (Fig. 5B).[114] Furthermore, the regulatory tyrosine residues serve as docking sites for upstream and downstream adaptor and signalling molecules and e.g. in the case of the adaptor protein CT10 regulator of kinase II (CRKII) this links ZAP-70 to the actin cytoskeleton.[115-117]

The negative regulation of activated ZAP-70 is not well established. However, the E3 ubiquitin protein ligase Casitas B-lineage lymphoma (CBL) has been implicated in negative regulation of TCR:CD3:ζ- and ZAP-70-signalling. It has been proposed that by binding phosphorylated tyrosine Y292, CBL uses ZAP-70 as an adaptor to ubiquitinate and target the ζ-chain and ZAP-70 itself for proteosomal degradation.[118, 119] Additionally, the SH2 domain-containing 5'-inositol phosphatase 1 (SHIP-1)-associated docking proteins 1 and 2 (DOK-1/2) are considered negative regulators of ZAP-70.[120]

ZAP-70 phosphorylates the adaptor proteins linker for activation of T cells (LAT) and SH2 domain-containing leukocyte protein of 76 kDa (SLP-76) and thus amplifies and diversifies the initial TCR:CD3:ζ-complex signalling.[121, 122]

1.2.3.3 LAT:SLP-76-signalosome

The adaptor proteins LAT and SLP-76 lack enzymatic activity but are central in TCR:CD3:ζ-signalling as they assemble or exclude important signalling intermediates in a spatial and temporal manner. It is important to understand that the LAT:SLP-76-signalosome is composed of a variety of proteins that undergo reversible post-translational modifications and that the complex is stabilized, modulated and dissolved by cooperative multiprotein-interactions (Fig. 3).[56, 123]

After TCR:CD3:ζ-complex triggering, ITAM phosphorylation and PTK activation, adaptor proteins nucleate the proximal LAT:SLP-76-signalosome controlling almost all TCR:CD3:ζ-induced signalling events such as Mg^{2+}- and Ca^{2+}-flux, activation of mitogen-activated protein kinases (MAPKs), activation of nuclear factor of kappa light polypeptide gene enhancer in B-cells (NF-κB), activation of nuclear factor of activated T cells (NFAT) and activator protein 1 (AP-1, i.e. FOS:JUN-heterodimer) as well as actin reorganization, cell-adhesion and motility (Fig. 3).[56, 123]

The longest LAT isoform comprises 262 amino acids and has a calculated molecular weight of 28 kDa.[122, 124] However, on sodium dodecyl sulfate polyacrylamide gel electrophoresis (SDS-PAGE) LAT migrates at 36 and 38 kDa due to multiple acidic residues

and to post-translational modifications, respectively.[56] Lacking a signal sequence, LAT is a single-pass type III membrane protein with a small N-terminal extracellular region, a transmembrane region and a C-terminal large intracellular region with no apparent classical protein:protein-interaction domains (Fig. 3).[125]

LAT contains nine conserved tyrosine residues, Y36, Y45, Y64, Y110, Y127, Y132, Y171, Y191 and Y226, two conserved cysteine residues, C26 and C29, and two conserved lysine residues, K52 and K204, that are phosphorylated, palmitoylated and ubiquitylated, respectively. Phosphorylation is central for the binding of a variety of SH2 domains, palmitoylation is required for membrane targeting and localization to lipid rafts and ubiquitylation might modulate internalization and protein turnover.[126-128]

Upon TCR:CD3:ζ-signalling, LAT is primarily phosphorylated by ZAP-70 and to a lesser extend by LCK and ITK.[129-131] LAT is constitutively anchored in glycolipid-enriched membrane microdomains and after TCR:CD3:ζ-signalling recruits its binding partners, such as SLP-76, from the cytosol to the membrane anchored LAT:SLP-76-signalosome.[132, 133] For signal termination, LAT is dephosphorylated by the PTPRJ CD148 and by a variety of not clearly defined PTPs.[134]

LAT binds the N-terminal SH2 domain of the phospholipase Cγ 1 (PLCγ-1) with high affinity via the phosphorylated tyrosine residue Y132 and the phosphorylated tyrosine residues Y171, Y191 and Y226 contribute with lower binding affinities.[129, 135, 136] For full catalytic activity of PLCγ-1, cooperative assembly of the entire LAT:SLP-76-signalosome is necessary as additional binding partners such as SLP-76, the adaptor protein GRB2-related adaptor protein downstream of SHC (GADS), the PTK ITK, the guanine nucleotide exchange factor (GEF) VAV, and all three SH domains of PLCγ-1 are required (Fig. 3).[56, 136-138]

The adaptor protein GADS contains a N-terminal SH3 domain, a central SH2 domain followed by a unique glutamine and proline riche domain and a C-terminal SH3 domain. GADS binds the PRR of SLP-76 via high-affinity Arg-X-X-Lys-motifs of its SH3 domains and phosphorylated LAT (pY191) via its SH2 domain and thus stabilizes the LAT:SLP-76-signalosome.[56, 139, 140]

The adaptor protein growth factor receptor-bound protein 2 (GRB-2) comprises a N-terminal and a C-terminal SH3 domain enclosing a central SH2 domain.[141] Via its SH2 domain GRB-2 binds pairs of phosphorylated tyrosine residues of LAT, such as Y171/Y191, Y171/Y226 and Y191/Y226, and recruits the GEF son of sevenless homolog 1 (SOS-1).[136, 142] This interaction couples the LAT:SLP-76-signalosome via the MAPKs RAS and RAF to the MAPK-pathway, finally resulting in activation of the extracellular signal-regulated kinase 1

and 2 (ERK-1/2) (Fig. 3).[143] Furthermore, the GRB-2:SOS-1-intraction can mediate LAT-clustering contributing to higher order complex formation.[144]

CBL constitutively binds to GRB-2 and after TCR:CD3:ζ-signalling is recruited to LAT.[145] However, CBL also interacts with other proteins of the LAT:SLP-76-signalosome such as non-catalytic region of tyrosine kinase (NCK), the regulatory p85 subunit of the phosphatidylinositol-4,5-bisphosphate 3-kinase (PI3K) and PLCγ-1, that are associated with SLP-76.[145-147] Thus, CBL appears to have a dual function by stabilizing the LAT:SLP-76-signalosome and by targeting CD3δ, the ζ-chain and ZAP-70 for proteosomal degradation.[148]

SLP-76 comprises 533 amino acids, has a molecular weight of 76 kDa and consists of a N-terminal acidic region, followed by a central proline rich region (PRR) and a C-terminal SH2 domain.[149] The acidic region contains three tyrosines, Y113, Y128 and Y145, that are phosphorylated by ZAP-70 and bind to VAV, NCK, PI3K and ITK.[150-152] The PRR contains a SH3 domain binding motif mediating the constitutive binding to the SH3 domain of GADS and of PLCγ-1. Via its SH2 domain GADS binds to phosphorylated LAT and the LAT:SLP76-interaction is further stabilized by PLCγ-1.[136, 139, 153]

The C-terminal SH2 domain of SLP-76 can bind the adaptor protein adhesion and degranulation-promoting adaptor protein (ADAP) that is associated with the haematopoïetic progenitor kinase 1 (HPK-1).[154, 155] ADAP links the LAT:SLP-76-signalosome to the integrin inside-out signalling pathway and mediates firm cell adhesion (Fig. 3).[156] However, HPK-1 appears to be a negative regulator of SLP-76.[157]

VAV binding to SLP-76 stabilizes the VAV:NCK:ITK-complex and activates RAS-homolog (RHO)-family GTPases such as cell division cycle 42 (CDC-42) (Fig. 3).[158] NCK recruits the Wiskott-Aldrich syndrome protein (WASP) and VAV-activated CDC-42 activates WASP.[159] WASP triggers actin related protein 2/3 (ARP-2/3) mediated actin polymerization and links the LAT:SLP-76-signalosome to the cytoskeletal layer.[160]

The inositol-kinase PI3K is composed of a regulatory 85 kDa and a catalytic 110 kDa subunit and phosphorylates phosphatidylinositol 4,5-bisphosphate (PIP_2) to produce membrane bound phosphatidylinositol 3,4,5-trisphosphate (PIP_3).[161, 162] The membrane recruitment of proteins of the LAT:SLP-76-signalosome containing pleckstrin homology (PH) domains such as PLCγ-1, ITK, VAV and SOS-1 is dependent on PIP_3 and thus enhanced by PI3K.[161]

1.2.3.4 ITK

The PTK ITK comprises 620 amino acid residues, has a molecular weight of 72 kDa and is predominantly expressed in T cells.[163, 164] ITK contains a N-terminal PH domain, followed by a Zn^{2+}-binding BTK homology (BH) motif, a PRR, a SH3 domain, a SH2 domain, a SH2-kinase linker region and a C-terminal SH1 or kinase domain (Fig. 6).[86, 165] Following TCR:CD3:ζ-induced and LAT:SLP-76-mediated activation of PI3K and consecutive accumulation of PIP_3 in the plasma membrane, cytosolic ITK is recruited to the LAT:SLP-76-signalosome.[166] Via its SH3 and SH2 domains, ITK cooperatively interacts with a PRR (amino acid residues 184-195) and the phophorylated tyrosine residue Y145 of SLP-76, respectively, and via its PH domain additionally anchors to membrane bound PIP_3.[152, 167]

Figure 6. Domain structure of interleukin-2-inducible T cell kinase (ITK).

The domain structure of ITK is shown with the N-terminal PH-domain containing the BH-motif, the PRR, the SH3-domain, the SH2-domain, the SH2-kinase linker and the C-terminal kinase domain.

Figure adapted from Andreotti AH, et al, Cold Spring Harb Perspect Biol, 2010.[86]

Only SLP-76-bound ITK is activated by LCK-mediated phosphorylation of the tyrosine residue Y511 of its A-loop and consequently performs autophosphorylation of the tyrosines residue Y180 of its SH3 domain that is thought to further stabilize ITK binding to the LAT:SLP-76-signalosome.[168, 169] The main target of ITK is PLCγ-1 that binds to ITK via its second SH2 domain and that is directly activated by ITK via phosphorylation of its tyrosine residue Y783. Thus, ITK is important for the generation of the second messengers inositol 1,4,5-trisphosphate (IP_3) and diacylglycerol (DAG).[170, 171]

Additionally, ITK functions as an adaptor stabilizing the SLP-76:VAV:NCK-complex and thus is involved in actin reorganization (Fig. 3).[172, 173]

The ITK PRR has been proposed to interact with PLCγ-1, VAV, GRB-2 and FYN.[152, 171] How precisely the structure of ITK is involved in protein:protein-interactions and kinase-dependent or kinase-independent functions is not definitively established as ITK has proven resistent to crystalization up to now[86] While the isolated kinase-domain of SRC kinases retain their function, the isolated ITK-kinase domain shows only residual activity indicating that the

additonal domains and cooperative interactions with the LAT:SLP-76-signalosome are essential for ITK-kinase-activity.[174, 175] In that context, the tryptophan residue W335 in the SH2-kinase linker region appears to be an important activating residue of ITK, while the comparable tryptophan residue in SRC kinases behaves as an inhibitory one.[174, 175]

ITK is negatively regulated by the lipid phosphatase and tensin homolog (PTEN) that cleaves PIP_3 and thus interferes with ITK membrane recruitment.[176] Taking into account available comparative structural data, it has been proposed that an extended ITK configuration with reduced interdomain contacts might lead to ITK-homodimerization thus impeeding association with the LAT:SLP-76-signalosome and infering further negative regulation of adaptor- and kinase-function.[177-179]

1.2.3.5 PLCγ-1

PLCγ-1 is composed of a N-terminal PH domain that binds to membrane bound PIP_3, a Ca^{2+}-binding EF-hand, two SH2 domains, one SH3 domain for protein:protein-interactions and one C-terminal catalytic PI-PLC X-box. PLCγ-1 hydrolyzes PIP_2 to liberate the second messengers IP_3 and DAG.[180] DAG activates the serine/threonine protein kinase Cθ (PKCθ) and the GEF RAS guanyl releasing protein (RASGRP).[181] IP_3 binds to IP_3-receptors (IP_3-Rs) expressed on the endoplasmic reticulum.[55] Thus, ITK-mediated PLCγ-1 activation contributes to Ca^{2+}-, MAPK- and NF-κB-signalling (Fig. 3).[182]

1.2.3.6 PKCθ

PKCs are serine/threonine protein kinases that can be devided into conventional (cPKC), novel (nPKC) and atypical (aPKC) subfamilies activated by Ca^{2+} and DAG, DAG alone or neither Ca^{2+} nor DAG, respectively.[183] The nPKC PKCθ comprises 706 amino acid residues, has a molecular weight of 82 kDa and is mainly expressed in T cells where it has non-redundant functions in TCR:CD3:ζ- and CD28-(co-)signalling.[183, 184]

PKCθ consists of a N-terminal C2-like domain, followed by a pseudosubstrate, a C1, a V3 and a C-terminal kinase domain.[183] Unlike conventional C2 domains, the regulatory C2-like domain is not able to bind Ca^{2+} but instead mediates phospholipid- and protein:protein-interactions. Furthermore, it contains the regulatory tyrosine residue Y90 that is phosphorylated by LCK.[185] The structure of the pseudosubstrate domain resembles that of PKC substrates, but the serine residue targeted by the kinase domain is replaced by an alanine residue. Thus, the pseudosubstrate domain binds to the kinase domain *in cis* and induces a closed and inactive conformation of PKCθ. The cysteine-rich C1 domain is the DAG binding domain and is involved in membrane recruitment of PKCθ and subsequent activation of its

kinase function. The C3-domain contains a PRR motif necessary for association with CD28.[186] Upon TCR:CD3:ζ-triggering, PKCθ is recruited from the cytoplasm to the cSMAC where it persists in DAG-enriched lipid rafts in a catalytically active conformation.[187, 188]

As PKCθ has no membrane anchor moieties, its subcellular translocation to the cSMAC depends on protein:protein-interactions. Membrane anchored LCK, CD28 and the receptor for activated C kinase (RACK) are proposed to perform this adaptor function (Fig. 3).[189]

Importantly, PKCθ translocation to the cSMAC strongly depends on CD28 co-stimulation with the CD28:PKCθ-microclusters being spatially separated from the TCR:CD3:ζ-microclusters and takes place in the absence of ZAP-70.[59, 187, 190] The A-loop of the PKCθ kinase domain is phosphorylated by PI3K-dependent protein kinase 1 (PDPK-1) at the threonine residue T538 and in combination with autophosphorylation at the threonine residue T219 and the serine residues S676 and S695 contributes to membrane localization and kinase activity.[191-193]

Once activated, PKCθ phosphorylates several serine residues of the caspase recruitment domain (CARD)-containing membrane-associated guanylate kinase (MAGUK) protein 1 (CARMA1) and thus couples TCR:CD3:ζ- and CD28-signaling to the canonical NF-κB1 pathway (Fig. 3).[194, 195] The alternative NF-κB2 pathway is in part controlled by the canonical NF-κB1 pathway and thus is indirectly depending on PKCθ.[181]

Furthermore, PKCθ phosphorylates the serine threonine kinase 39 (STK39), a MAPK, that mediates the activation of ERK1/2 and JUN N-terminal kinase (JNK), thereby contributing to MAPK-signalling and AP-1 activation (Fig. 3).[196]

1.2.3.7 NF-κB

NF-κB transcription factor signalling is devided into canonical NF-κB1 (p50 and its precursor p105) and alternative NF-κB2 (p52 and its precursor p100) pathways. Both pathways can be activated by a variety of receptors expressed in the immune system. NF-κB1 and NF-κB2 themselves are devoid of transcription activation domains (TADs) and therefore heterodimerize with TAD-containing RelA, RelB and cRel transcription factors in variable combinations.[197]

In T cells, TCR:CD3:ζ-signalling and especially CD28 co-stimulation activate and localize PKCθ to the TCS.[59, 187, 190] PKCθ than recruits and phosphorylates CARMA1 that in turn assembles with B cell lymphoma 10 (BCL-10) and mucosa-associated lymphoïd tissue 1 (MALT-1) to form the CBM-complex.[198] The CBM-complex than recruits the inhibitor of

IκB kinase (IKK) complex and together with TNF receptor-associated factor 2 (TRAF-2) and TRAF-6 activates the regulatory IKKγ via lysine residue K63-linked polyubiquitination.[199] The catalytic components of the IKK-complex, IKKα and IKKβ, next target the inhibitors of NF-κB (IκBs). Especially, IκBα bound to NF-κB1:RelA retains the transcription factor in the cytoplams by blocking nuclear localization signals (NLSs). Once IκBα is phosphorylated by IKKα on its serine residues S32 and S36 it becomes ubiquitinylated and degraded by the proteasome.[200] The transcription factor gets liberated and translocates to the nucleus where it regulates T cell gene expression.[201] Importantly, a classical target of NF-κB1:RelA is IκBα and this constitutes an important negative feedback-loop of NF-κB1 signalling.[202]

Little is known about the alternative NF-κB2 pathway in TCR:CD3:ζ-signalling.[197]

1.2.3.8 NFAT

TCR:CD3:ζ-signalling via PLCγ-1 activates store-operated Ca^{2+}-entry (SOCE) and increases the intracellular concentration of the second messenger Ca^{2+} $[Ca^{2+}]_i$.[55] In T cells, this activates the $[Ca^{2+}]_i$-sensitive NFAT transcription factor family that controls T cell development, activation, proliferation, differentiation and function.[203]

Besides the $[Ca^{2+}]_i$-insensitive primordial NFAT5, T cells express four classical NFAT family members, i.e. NFAT1 (or NFATc2), NFAT2 (or NFATc1), NFAT3 (or NFATc4) and NFAT4 (or NFATc3).[204-207] NFATs contain a N-terminal TAD, followed by the regulatory NFAT-homology region (NHR), the highly conserved DNA-binding REL-homology region (RHR) and a variable C-terminal domain.[203] The regulatory NHR contains two serine rich regions (SRRs), three Ser-Pro-X-X repeats (SPs), one NLS, one nuclear export signal (NES) and docking sites for kinases and phosphatases.

In resting T cells, the SRRs and the SPs of NFATs are hyperphosphorylated, the NLS is masked and the transcription factors resides in the cytoplams.[203] However, upon TCR:CD3:ζ-induced and PLCγ-1-mediated SOCE, the $[Ca^{2+}]_i$-sensor calmodulin binds the NFAT phosphatase calcineurin that in turn becomes activated and bind to its NFAT docking motif SPRIEIT.[208] Calcineurin than dephosphorylates all but one of the 14 phosphosites in the SRRs and SPs of the NFATs leading to a conformational change and unmasking of the NLS.[209] NFATs translocate to the nucleus, bind NFAT consensus sites in various promoter regions and critically alter T cell gene expression.[203, 210]

In non-stimulated cells, NFAT is actively keept in a hyperphosphorylated state by the cytoplasmic maintenance kinases casein kinase 1 (CK-1) and dual-specificity tyrosine-phosphorylation regulated kinase 2 (DYRK-2).[211, 212]

In activated cells, dephosphorylated NFAT is rephosphorylated by nuclear export kinases such as glycogen synthase kinase 3 (GSK-3) and DYRK-2.[212, 213] Additonal mechanisms of regulation such as cytoplasmic scaffolding proteins and sumoylation exist.[214, 215]

Importantly, dephosphorylation leads to a change in molecular weight that can be illustrated by SDS-PAGE. Experimentally, the calcineurin inhibitors cyclosporin A (CsA) and tacrolimus (FK506) and the ionophore ionomycine are used to impede or induce dephosphorylation and nuclear translocation, respectively.[216]

NFATs are central transcription factors in T cells, as they directly regulate a variety of promoters, e.g. the interleukine 2 (IL-2)-promoter. Additionally, NFATs function as transcriptional scaffolders interacting with JUN homodimers or JUN:FOS-heterodimers (AP-1) via their RHD and thus integrate the MAPK-pathway into the Ca^{2+}-signalling pathway (Fig. 3).[203, 217, 218]

1.2.3.9 MAPKs

In T cells, MAPK-signalling controls development, activation, proliferation, differentiation, homeostasis and effector function.[219-223] The most important MAPK-cascades are the ERK1/2-, the JNK- and the p38 kinase-cascades. They are induced by TCR:CD3-ζ-signalling and a plethora of other stimuli such as mitogens, cytokines, PAMPs and DAMPs.[223]

Initially, membrane receptor signalling is transduced via GEFs and in T cells especially SOS, RASGRP and RAS-related C3 botulinum toxin substrate 1 (RAC-1) are operational.[224-226] GEFs activate GTPases such as RAS and CDC-42 and these initiate the MAPK cascade.[226, 227] The first MAPK enzyme that is activated in the classical cascade is a serine/threonine kinase designated MAPK kinase kinase (MAP3K).[228] The second enzyme, phosphorylated and activated by MAP3Ks, is a dual-specificity kinase termed MAPK kinase (MAP2K).[229] The third MAPK (MAP1K), i.e. ERK1/2, JNK and p38, is activated by double phosphorylation of conserved threonine-X-tyrosine motifs in their A-loops and this leads to conformationl changes, increased substrate specificity and activation of their downstream transcription factors FOS, JUN and activating transcription factor 2 (ATF-2), respectively (Fig. 3).[223, 230]

In T cells, the prototypical MAPK-cascade downstream of TCR:CD3:ζ-signalling is the ERK1/2-pathway. This cascade consists of the GEF RASGRP, the GTPase RAS, the

MAP3K RAF, the MAP2K mitogen-activated protein kinase 1 and 2 (MEK-1/2) and the MAP1K ERK-1/2 targeting the transcription factor FOS.[231]

It is becoming apparent, that besides acting as a simple GTPase, RAS compartmentalizes MAPK-signalling by acting as a shuttle between different membraneous compartments such as the cell membrane, the endoplasmic reticulum (ER) and the Golgi apparatus.[231]

1.2.4 Ion and lipid second messengers

The positively charged ions calcium (Ca^{2+}), magnesium (Mg^{2+}) and zinc (Zn^{2+}) are important second messengers of TCR:CD3:ζ-signalling. As these ions can not passively diffuse across hydrophobic cell membranes, a network of ion channels and transporters is regulating their concentrations in a spatial and temporal manner.[55]

Basically, ATP-dependent sodium (Na^{2+}), potassium (K^{+}) and chloride (Cl^{-}) transporters actively build up a constitutive electrochemical membrane gradient termed the resting membrane potential. In T cells, this negative membrane potential is about -60 mV and together with extra- and intracellular concentration gradients is the driving force of second messenger ion-flux.[232]

The extracellular Ca^{2+}-concentration $[Ca^{2+}]_e$ is ~$1x10^{-3}$ M, the intracellular Ca^{2+}-concentration $[Ca^{2+}]_i$ is ~$1x10^{-7}$ M and the ER Ca^{2+}-concentration $[Ca^{2+}]_{er}$ is ~0.5-$1.0x10^{-3}$ M. The extracellular Mg^{2+}-concentration $[Mg^{2+}]_e$ is ~$0.8x10^{-3}$ M and the intracellular Mg^{2+}-concentration $[Mg^{2+}]_i$ is ~0.5-$1x10^{-3}$ M. The extracellular Zn^{2+}-concentration $[Zn^{2+}]_e$ is ~$16x10^{-6}$ M and the intracellular Zn^{2+}-concentration $[Zn^{2+}]_i$ is ~0.35-$1x10^{-9}$ M. Thus, in addition to the resting membrane potential, there are important concentration gradients for $[Ca^{2+}]$ of ~$1x10^{4}$ M and for $[Zn^{2+}]$ of ~$5x10^{5}$ M while the concentration gradient for $[Mg^{2+}]$ is quite small.[55, 233]

Ion channels are pore forming transmembrane proteins that allow passive ion-flux exploiting the electrochemical gradients actively established by ion transporters. Physicochemically, they are characterized by their selectivity, i.e. their specificity for a particular ion, and their conductance, i.e. their ability to carry a certain electrical charge at a given potential difference.[234]

In T cells, the best studied second messenger system is the Ca^{2+}-signalling system.[235] After TCR:CD3:ζ-triggering by pMHC, proximal TCR-signalling results in the activation of PLCγ-1.[180] PLCγ-1 hydrolyzes PIP_2 to liberate the second messengers IP_3 and DAG.[180] DAG activates the serine/threonine protein kinase Cθ (PKCθ) and the GEF RAS guanyl releasing

protein (RASGRP).[181] IP_3 binds to the Ca^{2+}-permeable IP_3-receptor (IP_3-R) located in the ER membrane and this triggers the efflux of Ca^{2+} out of the ER into the cytoplasm (Fig. 7).[55,236] The $[Ca^{2+}]_{er}$-sensing molecules stromal interaction molecule 1 (STIM-1) and STIM-2 are single-pass type I transmembrane proteins located in the ER.[237] STIMs comprise a N-terminal intraendoplasmic Ca^{2+}-sensing EF-hand, followed by a sterile alpha motif involved in STIM-self association, a TM region, and three intracytoplasmic coiled-coil domains. When $[Ca^{2+}]_{er}$ is diminished by IP_3:IP_3-R-mediated store-depletion, the inactive STIM-conformation, that is maintained by Ca^{2+} bound to the EF-hand, folds up into an activated conformation.[238] The activated STIMs oligomerize, form microclusters, and redistribute to junctional sites of the ER that are in close proximity to the plasma membrane.[239] Via their coiled-coil domains STIMs than interact with the Ca^{2+}-release-activated Ca^{2+}-channel (CRAC) and induce a process called SOCE.[240] STIM1 and STIM2 differ in their ER-depletion sensitivity and oligomerization and CRAC-binding kinetics with STIM2 being more sensitive but slower (Fig. 7).[241]

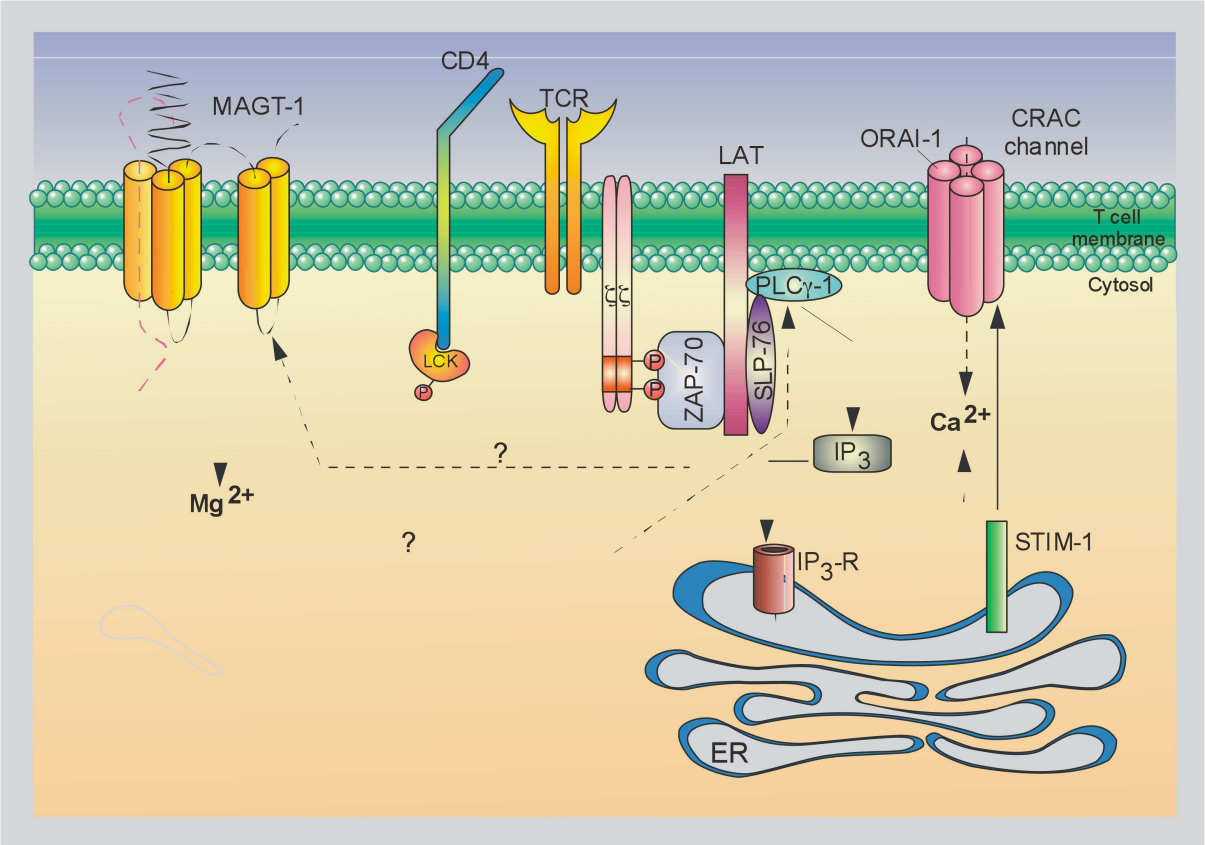

Figure 7. Ca^{2+}- and Mg^{2+}-signalling in T cells.

TCR:CD3:ζ-signalling and LCK-mediated ITAM-phosphorylation via ZAP-70 probably lead to the activation of the highly Mg^{2+}-selective magnesium transporter 1 (MAGT-1) that is predicted to contain five transmembrane (TM) regions. This leads to a spatiotemporal increase in the intracellular Mg^{2+}-concentration $[Mg^{2+}]_i$ and Mg^{2+} might acts as an allosteric activator of PLCγ-1. Activated PLCγ-1 in turn provides the lipid mediator IP_3 that

binds to the Ca^{2+}-permeable IP_3-receptor (IP_3-R) located in the endoplasmic reticulum (ER) membrane. This triggers the efflux of Ca^{2+} out of the ER into the cytoplasm and the reduction of the ER Ca^{2+}-concentration $[Ca^{2+}]_{er}$ induces the activating interaction of stromal interaction molecule 1 (STIM-1) with the Ca^{2+}-release-activated Ca^{2+}-channel (CRAC) composed of four ORAI-1 molecules and located in the cell membrane. The highly Ca^{2+}-selective and low-conductance CRAC generates an Ca^{2+}-influx and the overall process is called store-operated Ca^{2+}-entry (SOCE).
Figure adapted from Feske S, et al, Nat Rev Immunol, 2012.[55]

In T cells, the most abundant CRAC is a highly Ca^{2+}-selective low-conductance ion channel build up by four ORAI-1 transmembrane glycoproteins.[242] Each ORAI-1 subunit is composed of four TM regions with an intracellular N-terminus and an intracellular C-terminus, respectively. The four ORAI-1 glycoproteins build up the pore forming unit with four glutamic acid residues E106 infering Ca^{2+}-binding and selectivity. The overall small pore diameter of CRAC determines its low-conductancy.[243, 244] The intracellular C-termini contain CC-domains that interact with the STIM CC-domains opening up the Ca^{2+}-pore and allowing for Ca^{2+}-influx.[245]

Finally, Ca^{2+}-homeostasis is achieved by clearing Ca^{2+} from the cytoplasm into the mitochondria or the ER by the mitochondrial Ca^{2+}-uniporter (MCU) and the endoplasmic reticulum Ca^{2+}-ATPase (ERCA), respectively, and by export into the extracellular compartment by plasma membrane Ca^{2+}-ATPases (PMCAs).[55, 246]

Overall, SOCE is coupling TCR:CD3:ζ-signalling to various transcription factor pathways such as NFAT and NF-κB1 (Fig. 3).

Although more than 90% of $[Mg^{2+}]_i$ is bound to ATP, about 5% of $[Mg^{2+}]_i$ is free and functions as a second messenger in T cells following TCR:CD3:ζ-signalling.[247] Little is known about Mg^{2+}-homeostasis and -signalling in T cells. Noteworthy, magnesium transporter 1 (MAGT-1) has been found to mediate a transient Mg^{2+}-flux after TCR:CD3:ζ-triggering, ITAM-, ZAP-70- and LAT-phosphorylation.[247] MAGT-1 is a highly selective Mg^{2+}-transporter that is predicted to contain five TM regions and a short N-terminal intracellular tail (Fig. 7).[248] MAGT-1-deficiency abrogates Mg^{2+}-flux, delays the activation of PLCγ-1 and impeeds consecutive SOCE. Therefore, it has been proposed that Mg^{2+} acts as an allosteric activator of PLCγ-1 downstream of PTPs in T cells, although the precise molecular requirements and mechanisms remain elusive (Fig 7).[247]

The trace ion Zn^{2+} is an essential co-factor of various metalloproteins and in the immune system especially zinc finger containing transcription factors are operational. Moreover, it is becoming evident that Zn^{2+} directly is involved in lymphocyte signalling as a

second messenger.[249] TCR:CD3:ζ-signalling leads to a localized and transient Zn^{2+}-flux at the TCS and increased $[Zn^{2+}]_i$ sustains Ca^{2+}-flux by enhancing LCK and PKCθ kinase activity and ZAP-70 phosphorylation.[250, 251] However, higher $[Zn^{2+}]_i$ exerts inhibitory effects as illustrated by the impeded activation of the phosphatase calcineurin.[252] Therefore, as a function of its intracellular concentration, Zn^{2+} seems to play a dual role in T cell signalling.[55]

1.2.5 The cytoskeletal layer

The cytoskeletal layer is regulating T cell motility, adhesion, polarity, TCS formation, T cell development, differentiation and effector function. The principal molecules controlling these processes are actin, myosin II and tubulin (Fig. 3).[253]

T cells travers the secondary lymphoïd organs at an average speed of 10 µm/min and slow down to establish extensive contacts with APCs when they encounter their cognate pMHC (Fig. 2).[254] These two basical motility modes are largely dependent on chemokine receptors and integrins, such as LFA-1, that are coupled to the cytoskeletal proteins filamentous-actin (F-actin) and myosin II especially by the molecules talin and vinculin.[255, 256] Upon pMHC induced TCR:CD3:ζ-signalling, the T cell becomes polarized and the microtubule-organizing center (MTOC) positions between the APC:T cell-contact site and the nucleus.[257] This MTOC translocation is essential for the formation of a mature TCS and the TCR:CD3:ζ-induced cytoskeleton rearrangements depend on the adaptor adhesion and degranulation-promoting adaptor protein (ADAP). ADAP is coupled to the LAT:SLP-76-signalosome and recruits the microtubule motor protein dynein.[258] Furthermore, the LAT:SLP-76-signalosome is connected to the cytoskeleton via the adaptor proteins WASP and ARP-2/3 (Fig. 3).[160, 256, 259]

To establish a functional TCS TCR:CD3:ζ-microclusters and integrin-microclusters form and are leterally segregated into the cSMAC and pSMAC, respectively. Furthermore, F-actin generated protrusions might contribute in bridging the intercellular space bringing pMHC and TCR:CD3:ζ in close contact.[260] Again both processes critically depend on F-actin dynamics.[15, 57]

At the opposite of the TCS and the MTOC, another polarity region named distal pole complex (DPC) or the anti-synapse, is formed by cytoskeletal rearrangements. The DPC has been implicated in sequestration of negative TCR:CD3:ζ-signalling regulators and finetuning of T cell differentiation.[261]

1.3 T cell development

Most of the current knowledge of thymopoïesis originates from mouse studies as this model system allows *in vivo* experimental setups that are not feasible in humans for obvious reasons.[262] Human thymopoïesis predominantly has been analysed *in vitro* and only partially *in vivo* taking advantage of certain PIDs characterized by disturbed thymocyte development.[5, 8, 263] Even thought the principles of murine and human thymopoïesis seem to be identical, there are phenotypical differences of the initiating haematopoïetic stem cells (HSCs), the distinct transitional thymocyte populations and the naïve T cell subsets that finally egress from the thymus.[264] Thus, the definitive human phenotypes have not yet been established.

However, murine and human thymopoïesis are both characterized by the gradual maturation of distinct thymocyte populations under the influence of the thymic microenvironement.[5, 262]

A central feature of thymocyte development into mature γδ T cells and αβ T cells is a process called V(D)J-recombination.[265, 266] During V(D)J-recombination gene segments encoded in the germline TCR loci are assembled by a mechanism termed non-homologous end joining (NHEJ).[27] These somatic recombination events govern γδ T cell and αβ T cell lineage commitment and account for the highly variable preimmune TCR repertoire.[267, 268]

Immature thymocytes further pass quality checkpoints called positive and negative selection and especially αβ T cells take their $CD4^+$ versus $CD8^+$ single-positive (SP) lineage choice, before entering the immunological periphery as mature but naïve T cells.[269]

1.3.1 Haematopoïetic stem cells and precursors

Human adult HSCs are long-term repopulating cells located in specialized bone marrow (BM) niches.[270, 271] Phenotypically, they are characterized as $CD34^+CD38^-Lineage^-$ (Lin^-) cells. Functionally, by a process called asymmetric cell division, they continously self-renew and give rise to short-term repopulating HSCs, that are $CD34^+CD38^+Lin^-$ (Fig. 8).[272] Following the traditional model of haematopoïesis, these HSCs further differentiate into megakaryocyte/erythrocyte precursors (MEPs), common myeloïd precursors (CMPs) and common lymphoïd precursors (CLPs), all of which lose self-renewal but retain multilineage differentation capacity.[5] MEPs terminally differentiate into magakaryocytes, that generate platelets, and erythrocytes. CMPs are $CD34^+CD45RA^-$ precursors that via $CD34^+CD45RA^+CD123^+$ granulocyte/monocyte precursors develop into granulocytes, monocytes, pDCs and mDCs.[273]

CLPs are $CD34^+CD45RA^+CD7^+CD10^+$ precursors that via $CD34^+CD45RA^+CD7^+CD10^-IL7\text{-}R\alpha^-$ precursors develop into NK cells and T cells and via $CD34^+CD45RA^+CD7^-CD10^+IL\text{-}7R\alpha^+$ precursors into B cells while pDCS and mDCs additionally seem to stem from both precursors.[274, 275]

This phenotypical classification of the individual precursors currently is supported by incomplete expression analysis of lineage specific transcripts such as the transcription factor paired box protein 5 (PAX-5) and the BCR co-receptor immunoglobulin-associated beta chain (Igβ, CD79B) for B cells or the transcription factor GATA binding protein 3 (GATA-3) and pTα for T cell precursors.[273, 276]

1.3.2 Thymopoïesis

Especially, the $CD34^+CD45RA^+CD7^+CD10^-IL7\text{-}R\alpha^-$ precursors leave the BM, migrate to the thymus and on their way further differentiate into thymic seeding progenitors (TSPs). Quantitatively, this process is most important in early life but seems to continue througout life until advanced age.[5]

The thymus can be divided into four major anatomical and functional compartments, the corticomedullary junction, the cortex, the subcapsular zone and the medulla. The corticomedullary junction is build by a framework of endothelial cells that enables thymic entry and egress of TSPs or mature naïve T cells, respectively. The cortex harbours cortical thymic epithelial cells (TECs), fibroblasts and macrophages, the subcapsular zone mainly contains cortical TECs and the medulla is build by a stromal network of DCs and medullary TECs.

Once TSPs enter the thymus, they encounter the thymic microenvironement necessary to establish their T cell identity and become early thymic progenitors (ETPs).[277] ETPs are best characterized as $CD34^+CD38^-CD7^+CD45RA^+IL7\text{-}R\alpha^+$ thymocytes that are still $CD1a^-$. Paralleling the murine system and using the TCR co-receptors CD4 and CD8, developping human thymocytes principally can be divided into $CD4^-CD8^-$ double-negative (DN), immature $CD4^+$ single-positive (iSP), $CD4^+CD8^+$ double-positive (DP) and $CD4^+$ or $CD8^+$ SP cells. Furthermore, DN thymocytes can be subdivided into the most immature $CD34^+CD38^-CD1a^-$, the consecutive $CD34^+CD38^+CD1a^-$ and the $CD34^+CD38^+CD1a^+$ stages. Immature SP thymocytes further differentiate into $CD3^-$ and $CD3^+$ DP thymocytes and finally mature into naïve $CD4^+$ and $CD8^+$ SP T cells[278] (Fig. 8).

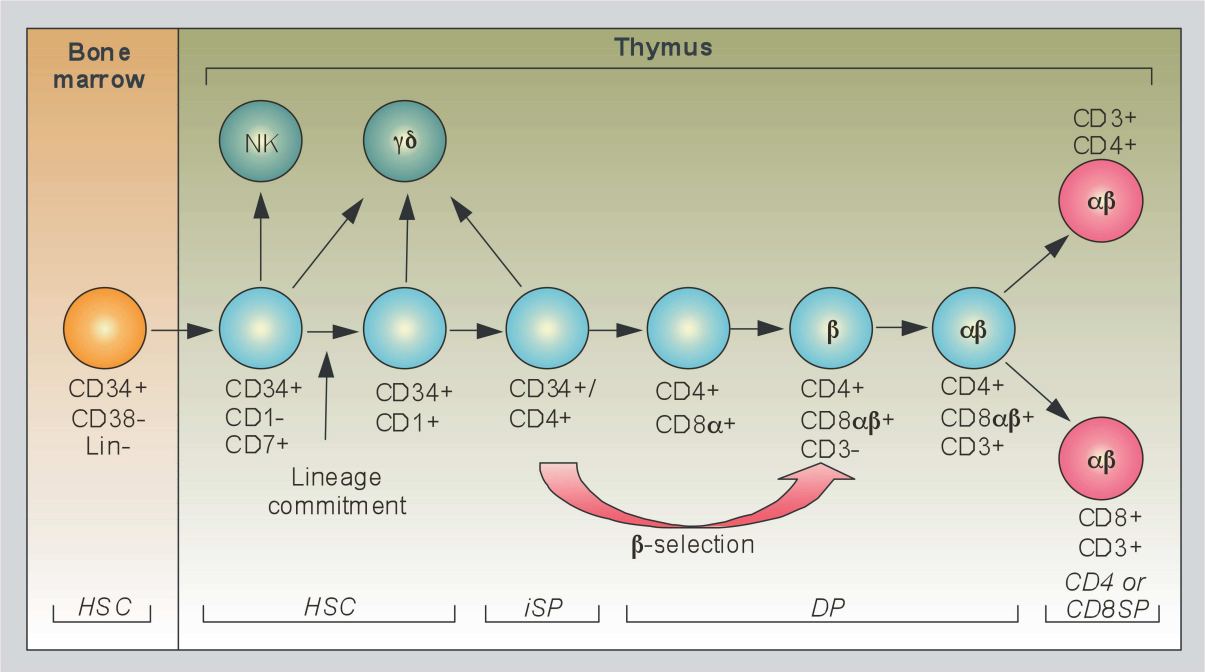

Figure 8. Human thymopoïesis.

Long-term repopulating human haematopoïetic stem cells (HSCs) are $CD34^+CD38^-Lin^-$ cells that reside in the bone marrow and continuously give rise to a progeny that migrates into the thymus where it differentiates into $CD34^+CD1^-CD7^+$ short-term repopulating HSCs. The interaction of these HSCs with the particular thymic microenvironement induces their lineage commitment and via $CD34^+CD1^+$ intermediates they differentiate into $CD34^{+/-}CD4^+$ immature single-positive (iSP) thymocytes. They further develop into $CD4^+CD8\alpha^+$ double-positive (DP) thymocytes and pass β-selection to become $CD4^+CD8\alpha\beta^+CD3^-$ DP thymocytes that express a preTCR with a TCRβ-chain. Finally and having passed the state of $CD4^+CD8\alpha\beta^+CD3^+$ DP thymocytes with an αβ TCR, they become $CD3^+CD4^+$ or $CD3^+CD8^+$ single-positive (SP) mature but naïve T cells. Natural killer (NK) cell and γδ T cells branch off as well from HSCs and/or iSPs.

Figure adapted from Koch U, Radtke F, Annu Rev Cell Dev Biol, 2011, and Holland AM, et al, Semin Immunopathol, 2008.[262, 264]

1.3.3 V(D)J-recombination

The generation and expression of a functional TCR is a central feature of thymocyte development and the consecutive steps serving as developmental checkpoints can be assigned to particular thymocyte populations.[278] A functional TCR is either composed of a TCRαβ- or a TCRγδ-heterodimer[22]. In stark contrast to other receptor proteins, TCRα-, TCRβ-, TCRγ- and TCRδ-chains are not encoded by unique genes in the germline, but by various gene segments that are located in the diploïd T cell receptor α, β, γ and δ loci (TRA@ 14q11.2, TRB@ 7q34, TRG@ 7p14 and TRD@ 14q11.2), respectively (Fig. 9 and 10).

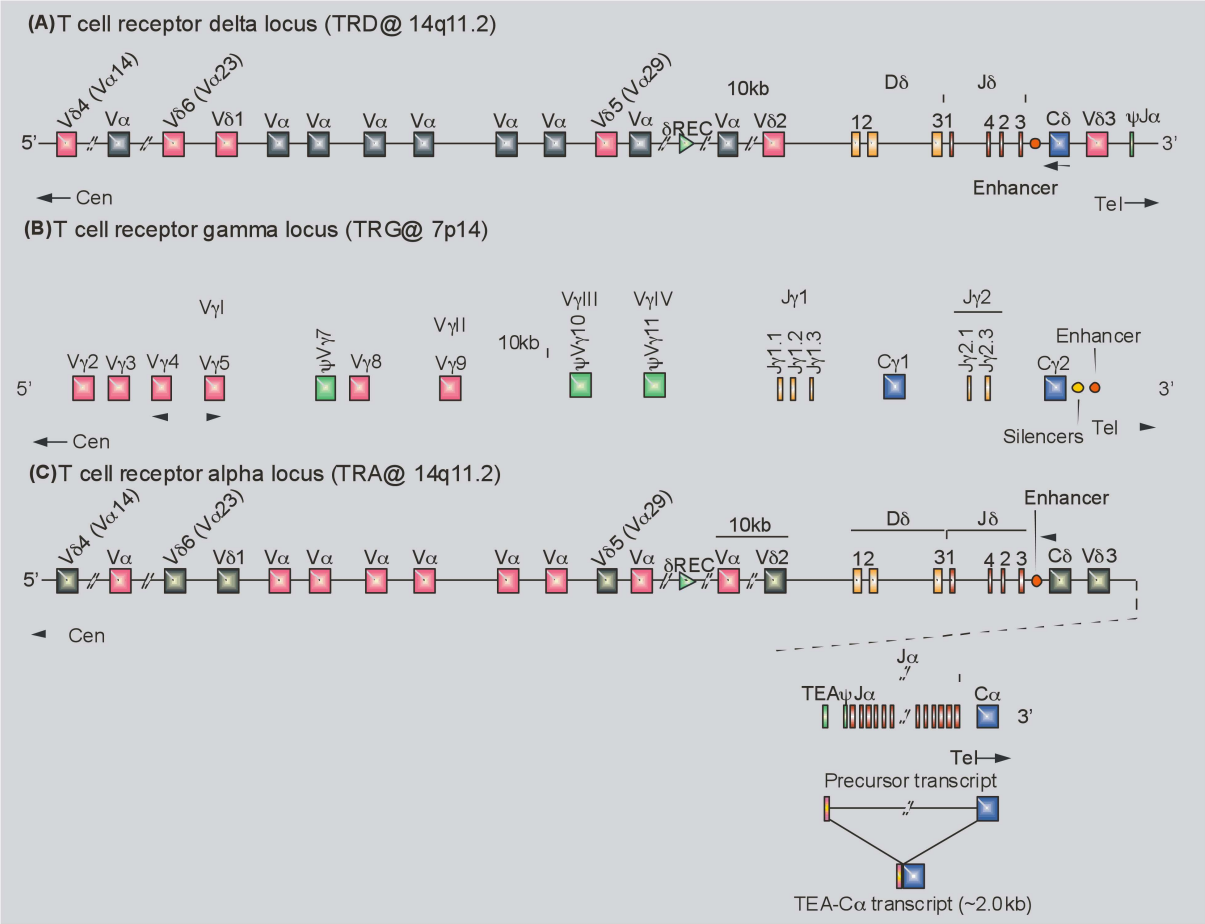

Figure 9. Human T cell receptor delta, gamma and alpha loci (TRD/G/A@s).

(A) The human TRD@ locus on chromosome 14q11.2 is shown with rearrangable variable (V) δ gene segments that are scattered between Vα gene segments and depicted in red and black, respectively. Since Vδ4, Vδ5, and Vδ6 are also recognized as Vα gene segments, their Vα gene code is given in parentheses. Diversity (D) δ, joining (J) δ and the constant (C) δ gene segments are depicted in orange, brown and blue, respectively. Additionally, the localization of the TRD@-deleting δREC and ψJα gene segments and the 3'enhancer are shown in green and billiant red, respectively.

(B) The human TRG@ locus on chromosome 7p14 is shown with rearrangeable Vγ gene segments, non-rearrangeable Vγ pseudogen segments, Jγ and Cγ gene segments depicted in red, green, brown and blue, respectively. Additionally, the 3' silencer and enhancer are shown in yellow and brilliant red.

(C) The human TRA@ locus on chromosome 14q11.2 is shown with rearrangable Vα gene segments that are scattered between Vδ gene segments and depicted in red and black, respectively. Since Vδ4, Vδ5, and Vδ6 are also recognized as Vα gene segments, their Vα gene code is given in parentheses. Jα and Cα gene segments that are scattered inbetween Dδ, Jδ and Cδ are depicted in brown and blue, respectively. Additionally, the localization of the TRD@-deleting δREC and ψJα gene segments and the TRA@-initiating T-early α (TEA)-Cα transcript are shown in green and in the lower right corner, respectively.

In (A), (B) and (C) the ImMunoGeneTics (IMGT) nomenclatures according to Lefranc is used with the exception of Vα segments that are not numbered due to their abundance (~45 Vα).[279, 280]

Figure adapted from van Dongen JJ, et al, Leukemia, 2003.[281]

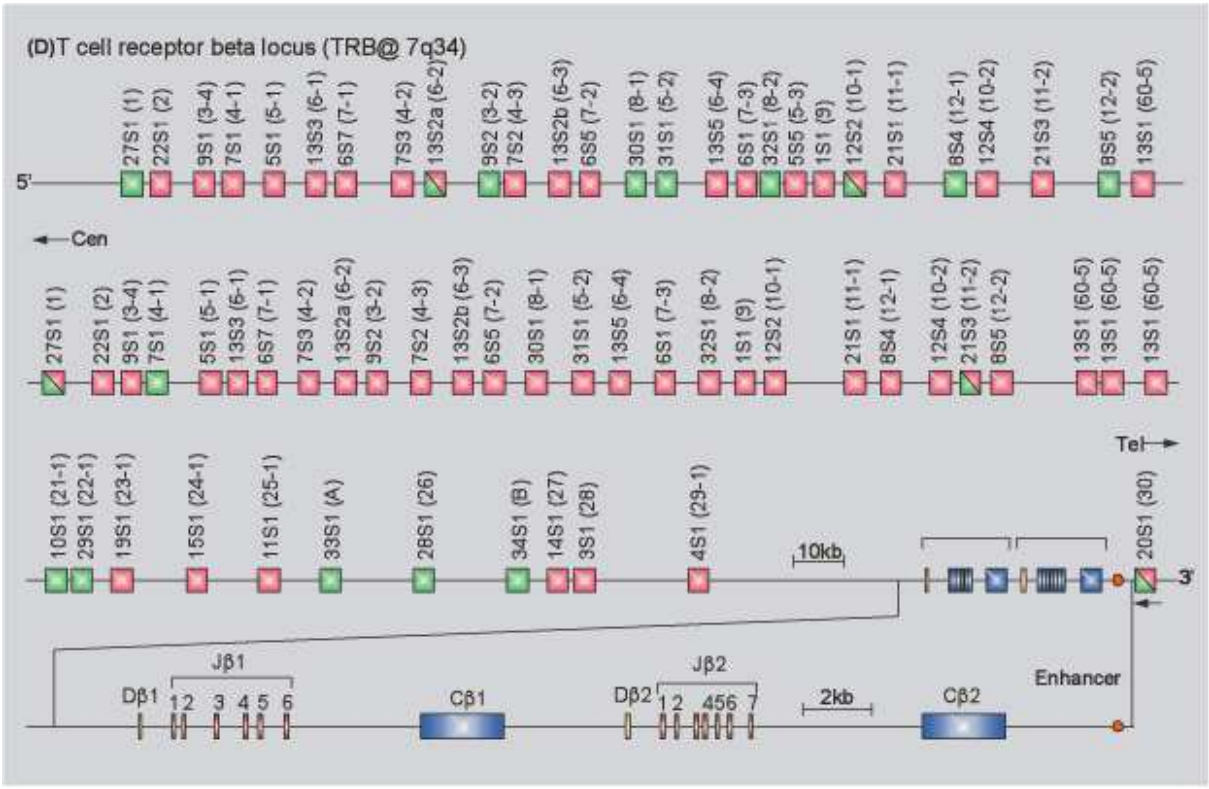

Figure 10. Human T cell receptor beta locus (TRB@).

The human TRB@ locus on chromosome 7q34 is shown with rearrangable Vβ gene segments, Vβ pseudogene segments and potential Vβ pseudogene segments in red, green and half red/green, respectively. Dβ, Jβ and Cβ gene segemnts are depicted in orange, brown and blue, respectively. Additionally, the 3' enhancer is indicated in brilliant red. The gene segment designation is according to Arden with the designation according to Lefranc in parentheses.[279, 280, 282]

Figure adapted from van Dongen JJ, et al, Leukemia, 2003.[281]

During thymopoïesis these loci are activated and become accessible following a strict order at precisely defined developmental phases, i.e. TRG@ > TRD@ > TRB@ > TRA@ (Fig. 11).[267] This specificity is orchestrated by the co-ordinated expression of enzymes, transcription factors, and chromatin structure-modifying enzymes.[27]

In a somatic rearrangement process called V(D)J-recombination, the variable (V), diversity (D) and joining (J) germline segments are assembled into a large variety of functional TCR genes. While TCRδ- and TCRβ-chains a created by rearranging V, D and J segements, TCRγ- and TCRα-chains are build up only by V and J segments. Finally, the rearranged V(D)J segments are joined to TCRγ, δ, α or β constant regions (C) through messanger RNA (mRNA) splicing (Fig. 11 and 12).[27]

Furthermore, inside the individual loci the segments are assembled following a particular hierarchy as illustrated by the TRD@ where V(D)J-recombination starts with the Dδ2-Dδ3 rearrangement, followed by Dδ2-Jδ1 and Vδ-Jδ1 rearrangements (Fig. 11).[283]

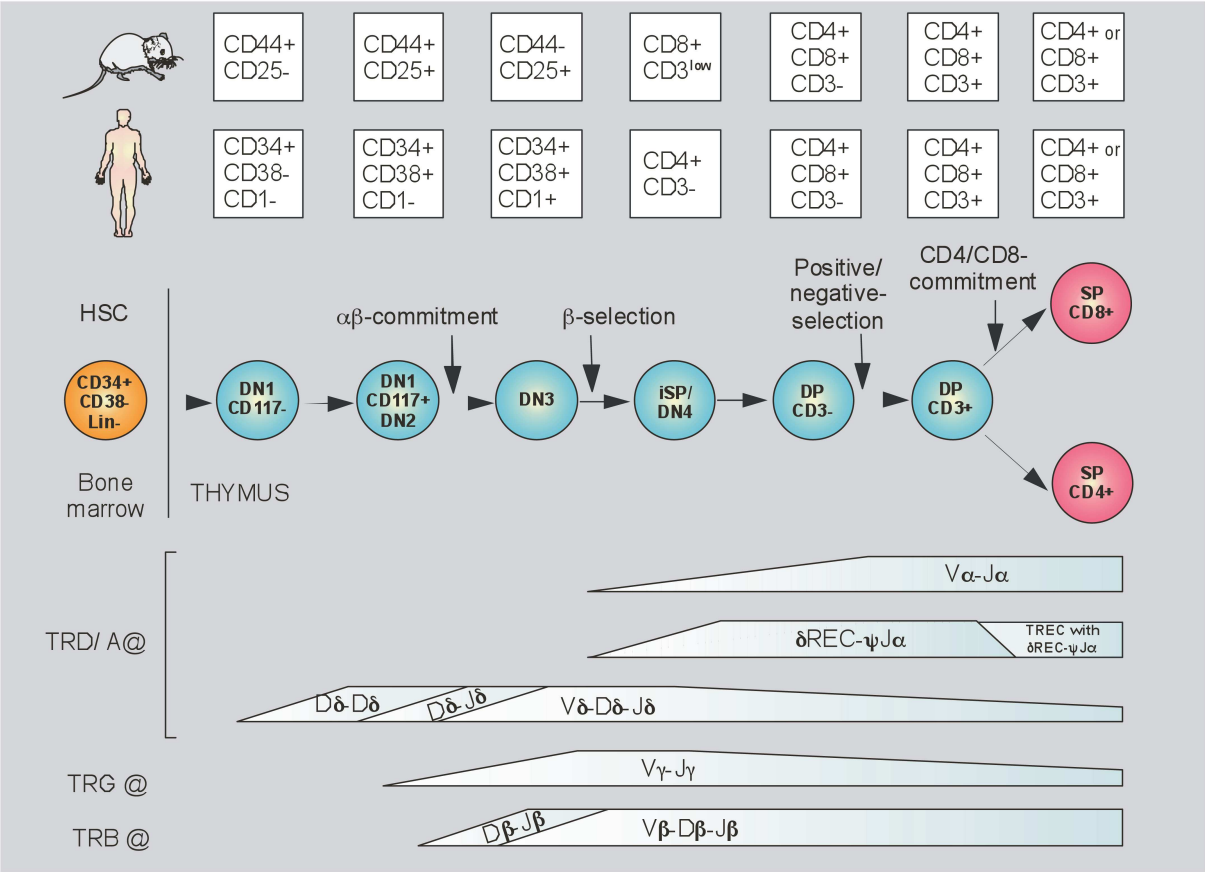

Figure 11. Thymocyte developmental sequence of V(D)J-recombination.

Murine thymocyte development is indicated from the HSC (yellow) throught the particular DN, iSP and DP thymocyte (blue) to the SP naïve T cell. The appropriate murine cellular phenotype is indicated above and, even thought human thymopoïesis differs slightly (Fig. 8), the corresponding human cellular phenotype is given as well. The developmental timing of V(D)J-recombination is indicated by particular beams for each T cell receptor locus, i.e. TRD@, TRA@, TRG@ and TRB@, as compared to the corresponding thymocyte population and the particular V(D)J-rearrangements taking place in an ordered fashion are marked inside the beams, respectively. Figure adapted from Dik WA, et al, J Exp Med, 2005.[278]

Even though there is variability inbetween individual humans, and there are variable numbers of pseudogenes due to missense indel mutations, the average human TRA@ comprises 45 V, 61 J and 1 C, the TRB@ 42 V, 2 D, 14 J and 2 C, the TRG@ 6 V, 5 J and 2 C and the TRD@ 5 V, 3 D, 4 J and 1 C functional gene segments (http://www.imgt.org/IMGTrepertoire/), respectively (Fig. 9 and 10).

During V(D)J-recombination P- or N-nucleotide additions and deletions at the junctions add to TCR repertoire diversity and this is called junctional diversity.[282] A further

source of diversity is the pairing of particular TCRα- to TCRβ- or TCRγ- to TCRδ-chains, respectively. The theoretical TCR repertoire has thus been calculated to be ~10^{15} for TCRαβ and ~10^{18} for TCRγδ.[284] However, the effective TCR repertoire is much more restricted as only a minor fraction of rearranged TCR is able to correctly bind to pMHC.[285] The vast majority of rearranged TCR will be deleted by positive and negative selection, as discussed below (paragraphe 1.3.4).

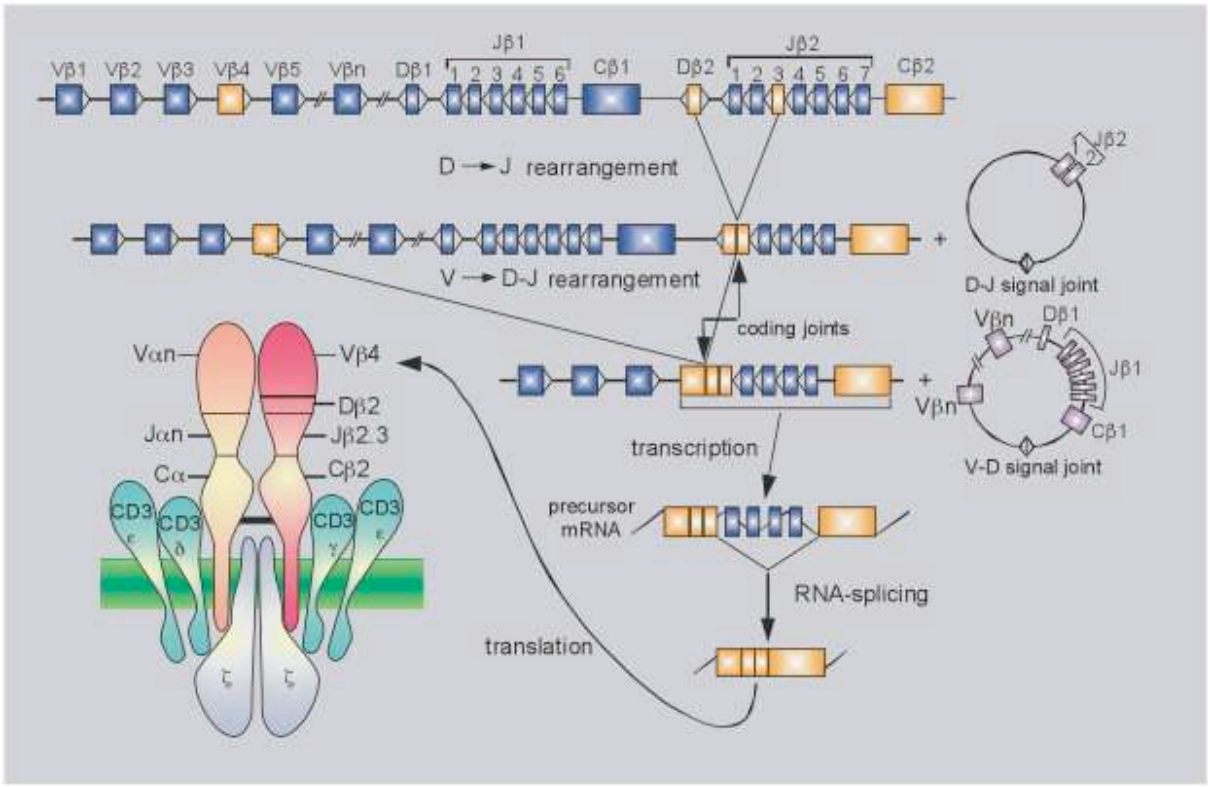

Figure 12. V(D)J-recombination mechanism.

In the first line the germline TRB@ with its Vβ, Dβ, Jβ and Cβ gene segements is shown and these that will be somatically recombined are depicted in yellow while those that will be deleted are shown in blue, respectively. In the second line D-J rearrangement has taken place generating a Dβ2-Jβ2.3 coding joint and a T cell receptor excision circle (TREC) encompassing the deleted Jβ2.1 and Jβ2.2 gene segments and the D-J signal joint. In the third line V-DJ rearrangement has occured creating a Vβ4-Dβ2Jβ2.3 coding joint and a TREC comprising the deleted Cβ1, Jβ1.1-6, Dβ1 and Vβn and the V-D signal joint. In the fourth line transcription of the precursor messanger ribonucleic acid (mRNA) has taken place and in the fifth line RNA splicing has given rise to the final transcript deleting the remaining Jβ2.4-7 gene segment transcripts. Finally, RNA translation has taken place and the TCRβ-chain build up by Vβ4Dβ2Jβ2.3Cβ2 is shown already integrated into a functionl TCRαβ:CD3:ζ-complex.

Figure adapted from van Dongen JJ, et al, Leukemia, 2003.[281]

Mechanistically, V(D)J-recombination is conducted by the V(D)J-recombinase consisting essentially of the enzymes recombination activating gene 1 (RAG-1) and RAG-2

that are exclusively expressed in particular thymocyte populations. The multiprotein-complex V(D)J-recombinase targets recombination signal sequences (RSSs). RSSs are flanking the individual V, D and J gene segments and comprise a conserved palindromic seven basepair (bp) sequence (CACAGTG) that is followed by an AT-rich nine bp motif (ACAAAAACC). These two conserved motifs are separated either by 12 or 23 bp variable motifs that correspond to one or two turns of the DNA double-helix, repectively, and guarantee that the heptamer and nonamere motifs are positioned at the same side of the DNA double-helix and can be accessed by the V(D)J-recombinase simultaneously.[286] V(D)J-recombination only takes place between RSSs with one 12 bp and one 23 bp spacer. V segments are flanked by one 3' 23 bp spacer, D segments are flanked by one 5' 12 bp spacer and one 3' 12 bp spacer and J segments are flanked by one 5' 23 bp spacer. This is known as the „12/23" rule and it guarantees that V, D and J segments are arranged in the correct order. However, in special cases the „12/23 rule" is broken in a process called „beyond the 12/23 rule" that allows for D-D rearrangements resulting in longer CDR3s than usual.[27]

V(D)J-recombination starts by positioning two individual gene segments in the correct orientation by creating a loop of the intermediate DNA. Next, the V(D)J-recombinase induces a pair of DNA double strand breaks at the border of the heptamer motif.[287] The DNA double strand of the coding sequence forms a covalent hairpin structure by trans-esterification and is conserved. The intermediate loop forms the covalent signal joint and is deleted as a so called T cell receptor excision circle (TREC) (Fig. 11 and 12).[288, 289] TRECs are found in naïve T cells, i.e. $CD4^+CD45RA^+CD31^+$ recent thymic emigrants, and are diluted by every further cell division. Next, the coding hairpin structure is opened asymetrically by the nuclease Artemis and the resulting overhang is filled in with palindromic (P) nucleotides.[290, 291] Additionally, the terminal deoxynucleotidyl transferase (TdT) modifies coding ends by adding random N (nucleotides).[292] The modified DNA ends are finally ligated by a multiprotein complex in a mechanism called non-homologous end joining (NHEJ).[27, 293, 294]

As T cells are diploïd, they can rearrange each locus twice and thus augment the probability of a productive rearrangement, a fact that is referred to as receptor editing. Once a productive in-frame rearrangement has taken place, a process termed allelic exclusion guarantees that each T lymphocyte finally only expresses one unique TCR.[27]

1.3.3.1 TRD@

The TRD@ is the first locus to undergo VDJ-recombination and the initiating but yet incomplete Dδ2-Jδ1 rearrangement can be observed as early as in DN $CD34^+CD38^-CD1^-$,

increases in DN $CD34^+CD38^+CD1^-$ and peaks in DN $CD34^+CD38^+CD1^+$ thymocytes. The first complete Vδ1-Dδ2Jδ1 or Vδ2-Dδ2Jδ1 rearrangement can be observed in DN $CD34^+CD38^+CD1^-$, peaks in $CD4^+$ iSP and decreases when the majority of DN thymocytes becomes commited to $TCR\alpha\beta^+$ thymocytes (Fig. 11).[278] As the TRD@ is embedded in the TRA@, it becomes deleted once the TRA@ locus starts to be rearranged (Fig. 9 and 11). This results in a T cell receptor excision circle (TREC) that is not replicated during further cell devisions and therefore declines throughout thymocyte development.[295] While the Vδ1 gene segement is essentially used in postnatal $TCR\gamma\delta^+$ thymocytes, the Vδ2 gene segment dominates the peripheral blood $TCR\gamma\delta^+$ T cell pool later on in life.[12]

1.3.3.2 TRG@

The initiating TRG@ rearrangements Vγ-Jγ1.1/2.1 can be found in DN $CD34^+CD38^+CD1^-$ thymocytes one developmental step after the initiating TRD@ rearrangement, peak in DN $CD34^+CD38^+CD1^+$ and decrease in consecutive thymocyte populations. TRG@ rearrangements Vγ-Jγ1.3/2.3 start in DN $CD34^+CD38^+CD1^-$ and outcompete Vγ-Jγ1.1/2.1 rearrangements from the $CD4^+$ iSP stage on (Fig. 9 and 11). While the Jγ1.2 gene segment is underrepresented in thymocytes, peripheral expansion of $TCR\gamma\delta^+$ cells epressing Jγ1.2 gene segment occurs.[278, 296]

1.3.3.3 TRB@

The initiating Dβ1-Jβ1 rearrangement can be found in DN $CD34^+CD38^+CD1^-$ and is followed by the Dβ2-Jβ2 rearrangement one step later in DN $CD34^+CD38^+CD1^+$ thymocytes. The first in frame Vβ-Dβ2Jβ2 rearrangement can be detected in iSP and remains stable thereafter while the Vβ-Dβ1Jβ1 rearrangement starts at the DP $CD3^-$ stage and is less common. Thus, β-selection takes place in the transition from $CD34^+CD38^+CD1^+$ to iSP thymocytes (Fig. 10 and 11).

1.3.3.4 TRA@

TRA@ recombination is initiated by the T-early α (TEA)-Cα rearrangement that can be first detected at the $CD34^+CD38^+CD1^+$ stage and peaks at the iSP and DP thymocyte stages.[297] As TRD@ is located inside TRA@, next the δREC-ψJα rearrangement deletes the TRD@ and generates δREC-ψJα containing TRECs at the iSP stage that peak in SP thymocytes (Fig. 9 and 11).[295] Thereafter, multiple Vα-Jα rearrangements occur as demonstrated by the loss of germline ψJα starting at the $CD34^+CD38^+CD1^+$ thymocyte stage.[278]

1.3.4 Kinetic signalling model

Once $CD4^+CD8^+$ DP thymocytes have somatically rearranged their TRB@ and TRA@ by V(D)J-recombination, they express a plethora of different αβ TCRs on their cell surface. However, the majority, i.e. >95 %, of these αβ TCRs does not recognize self-pMHC-molecules presented predominantly by TECs and therefore is of no further interest for a functional immune system. As these DP thymocytes can not be signalled by their TCR:CD3:ζ-complex to receive survival signals, they succumb to apoptosis, a process referred to as death-by-neglect (Fig. 13).[83, 269]

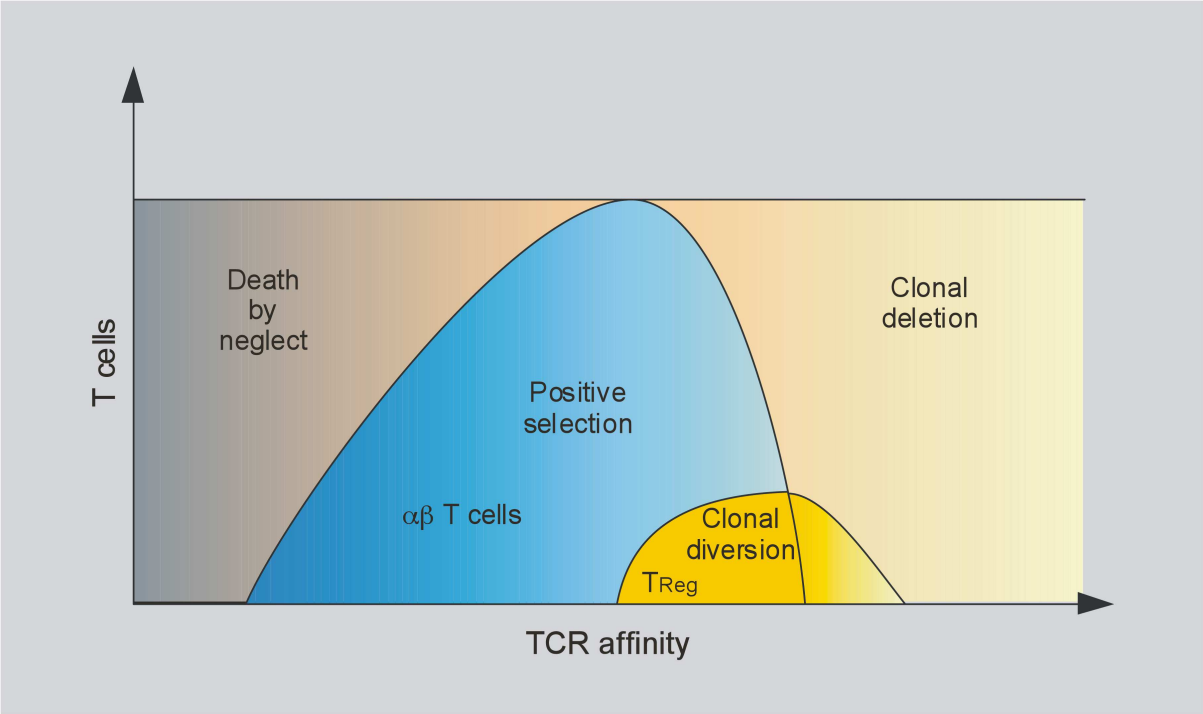

Figure 13. Thymocyte selection processes.

The major thymocyte selection processes depending on the individual TCR affinity for its cognate self-pMHC are shown. $CD4^+CD8^+$ DP thymocytes that do not recognize self-pMHCs are eliminated by death-by-neglect. DP thymocytes that bind to self-pMHCs with low or boarderline high binding affinity are signalled to develop into conventional $CD4^+$ or $CD8^+$ SP αβ T cells by positive selection or $CD4^+CD25^+FOX\text{-}P3^+$ regulatory T cells (T_{Reg}) by clonal diversion. DP thymocytes that display high affinity towards self-pMHCs succumb to clonal deletion or negative selection.

Figure adapted from Xing Y, Hogquist KA, Cold Spring Harb Perspect Biol, 2012.[83]

Only a small fraction of the generated αβ TCRs is capable of binding self-pMHC molecules with low affinity and consequently receives survival signals by their TCR:CD3:ζ-complex, a process called positive selection (Fig. 13).[298] To ensure efficient TCR:CD3:ζ-complex-mediated positive selection, DP thymocytes become virtually independent of

common γ-chain (γ_c, CD132) cytokine growth signalling, as they transiently do not express the IL-7-receptor (IL-7-R) but instead the suppressor of cytokine signalling 1 (SOCS-1).[299]

DP thymocytes that bind self-pMHC with high affinity and are thus potentially self-reactive receive death signals and execute apoptosis, a process referred to as clonal deletion or negative selection (Fig. 13).[300] A small fraction of borderline high affinity αβ TCR thymocytes escapes from clonal deletion and under the influence of particular cytokines such as IL-2 and transforming growth factor β (TGF-β), develops into $CD4^+CD25^+FOX\text{-}P3^+$ T_{Reg}, a process called clonal diversion (Fig. 13).[301-303]

Taken as a whole, positive selection, clonal diversion and clonal deletion/negative selection form central tolerance mechanisms as they take place in the thymus and importantly reduce autoreactive αβ TCRs in the pre-immune repertoire or render them towards immunoregulatory T_{Reg}.[83]

In a mutually exclusive manner, positively selected DP thymocytes further develop into $CD4^+$ or $CD8^+$ SP thymocytes and this process is termed CD4/CD8-lineage commitment. Importantly, DP thymocytes that express αβ TCRs restricted to MHC class I finally develop into $CD8^+$ T_{Cyt} while thymocytes that express αβ TCRs restricted to MHC class II develop into $CD4^+$ T_H or $CD4^+CD25^+FOX\text{-}P3^+$ T_{Reg}.[304] As the signalling intensity of the CD4 co-receptor is stronger than that of the CD8 co-receptor partially due to stronger LCK binding affinity, more $CD4^+$ SP thymocytes than $CD8^+$ SP thymocytes develop.[91, 305, 306]

On a molecular level CD4/CD8-lineage commitment is not completely understood but at present the kinetic signalling model is best integrating available experimental data (Fig. 14).[269]

Positively signalled DP thymocytes transcriptionally silence the expression of the CD8 co-receptor, independently of whether their αβ TCR is MHC I or MHC II restricted. Phenotypically, this results in $CD4^+CD8^{low}$ or $CD4^+CD8^-$ thymocytes that are not yet lineage-committed and that retain the capacity to develop into $CD4^+$ or $CD8^+$ SP thymocytes.[307, 308] After having downregulated CD8, MHC II restricted $CD4^+CD8^{low/-}$ thymocytes continue to receive TCR:CD3:ζ-complex signalling that keeps them independent of γ_c-cytokine signalling and progressively establishes their $CD4^+$ SP lineage identity (Fig. 14).

However, MHC I restricted $CD4^+CD8^{low/-}$ thymocytes loose TCR:CD3:ζ-complex signalling and this restores γ_c-cytokine signalling.[309] As a consequence, they transcriptionally silence CD4 expression and reinitiate CD8 expression in a process termed co-receptor reversal.[307] This re-establishes TCR:CD3:ζ-signalling and determines their $CD8^+$ SP lineage identity.[310] Of note, as a function of αβ TCR affinity for self-pMHC I, in thymocytes

expressing high-affinity αβ TCRs, CD8 lineage commitment takes place in $CD4^+CD8^-$ thymocytes, whereas in low-affinity αβ TCR thymocytes it takes place already in $CD4^+CD8^{low}$ or $CD4^+CD8^+$ thymocytes (Fig. 14).[269]

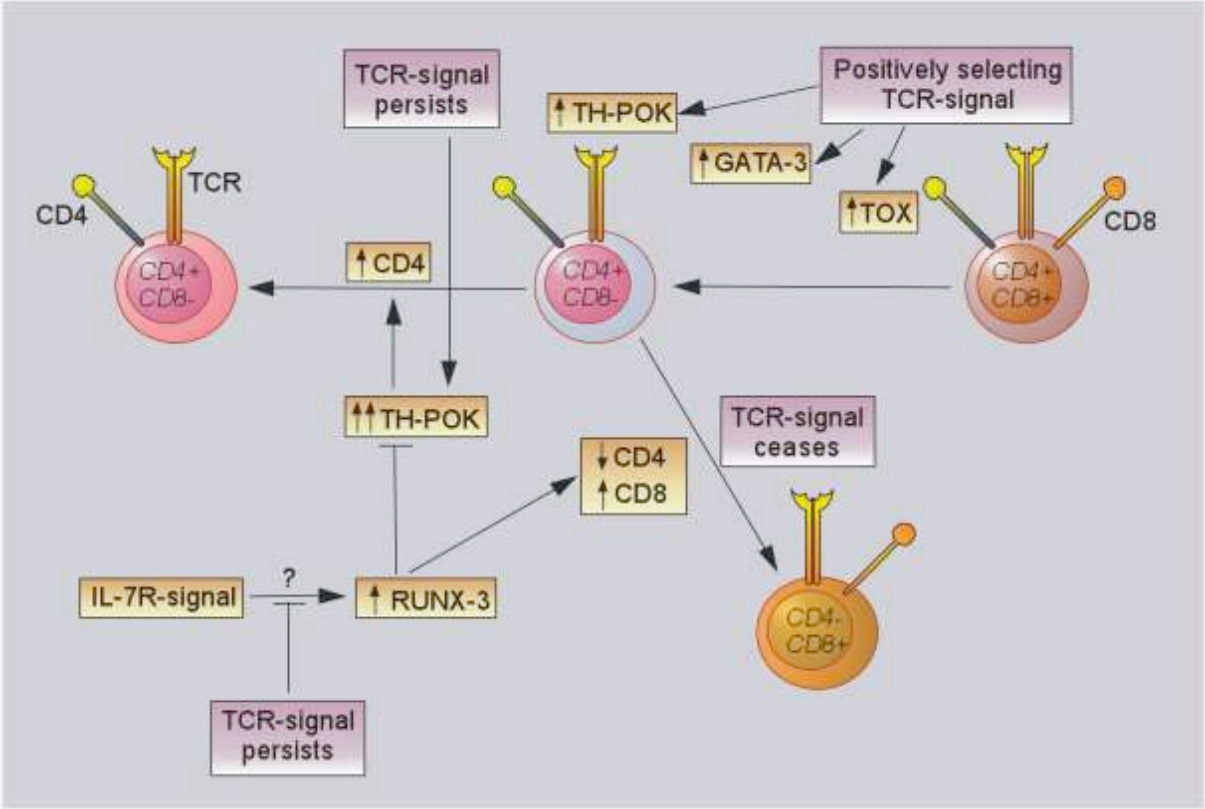

Figure 14. Kinetic signalling model.

Positive selection of $CD4^+CD8^+$ DP thymocytes induces the transcription factors thymus high-mobility group box protein (TOX), GATA binding protein 3 (GATA-3) and T-helper-inducing POZ/Kruppel-like factor (TH-POK) and independently of the particular TCR:MHC-restriction thymocytes stop expressing CD8. In the case of MHC class II-restriction, persisting TCR:CD3:ζ-signalling promotes sustained TH-POK expression that maintains CD4 expression, suppresses IL-7R-signalling and governs CD4-lineage commitment. In the case of MHC class I-restriction, ceasing TCR:CD3:ζ-signalling allows for IL-7R-signalling that induces the transcription factor runt-related transcription factor 3 (RUNX-3). RUNX-3 governs co-receptor reversal, i.e. downregulation of CD4 and re-expression of CD8, and together with re-established TCR:CD3:ζ-signalling promotes CD8-lineage commitment.

Figure adapted from Singer A, et al, Nat Rev Immunol, 2008.[269]

Transcriptionally, co-receptor reversal is governed by a silencer of *CD4* and by two principal enhancers of *CD8* and CD4/CD8-lineage commitment is orchestrated especially by the transcription factors T-helper-inducing POZ/Kruppel-like factor (TH-POK) and runt-related transcription factor 3 (RUNX-3), respectively.[311-314] The expression of TH-POK is dependent on persistent TCR:CD3:ζ-signalling. On the one hand, it maintains CD4 expression

by inhibiting RUNX-3-mediated silencing and on the other hand suppresses CD8 expression by silencing the CD8 enhancer I.[315-317] RUNX-3 expression is dependent on γ_c-cytokine signalling. It acts to silence TH-POK and CD4 expression while it re-initiates CD8 expression by activating the CD8 enhancer I (Fig. 14).[309, 315, 318, 319]

In summary, the kinetic signalling model posits a crosstalk between TCR:CD3:ζ- and γ_c-cytokine-signalling, with $CD4^+$ lineage choice controlled by persisting TCR:CD3:ζ-signalling and $CD8^+$ lineage choice controlled by reinforced γ_c-cytokine-signalling respectively.[269]

1.4 The T cell immune response

1.4.1 Naïve αβ T cell homeostasis

αβ T cells that have passed thymic selection processes and have further developed into $CD4^+$ T_H, $CD4^+CD25^+FOX\text{-}P3^+$ T_{Reg} and $CD8^+$ T_{Cyt} leave the thymus to form the peripheral mature T cell pool.[298] As they have not yet encountered foreign antigens, they are designated (antigen-) naïve T cells and consequently express the so called pre-immune TCR-repertoire that is composed of TCRs with low affinity for self-pMHC class II or class I, respectively.[268]

In order to survive in secondary lymphoïd tissues, they are dependent on tonic TCR:CD3:ζ-signalling and on intermittent IL-7-R-signalling.[320, 321] These signals are delivered by APCs via self-pMHC molecules, for which the T cells have been positively selected in the thymus, and by fibroblastic reticular cells (FRCs) that express the membrane bound cytokine IL-7.[320, 321] The IL-7-R is composed of IL-7-Rα (CD127) and γ_c (CD132) and binding of IL-7 to IL-7-Rα induces its downmodulation thus preventing the consumption of IL-7 and repetitive stimulation. [322] IL-7 is the rate limiting factor in naïve T cell homeostasis as it is critically influencing the size of the peripheral T cell pool.[323]

As APCs and FRCs reside in secondary lymphoïd tissues, especially in the lymph nodes, naïve T cells have to recirculate this compartment, a process called homing. To that end, they express the lymph node homing molecules CD62 ligand (CD62L) and chemokine C-C motif receptor 7 (CCR-7).[324] Tonic TCR:CD3:ζ- and intermittent IL-7-R-signalling via Janus kinase 1 (JAK-1) and JAK-3 and signal transducer and activator of transcription 5A (STAT-5A) and STAT-5B keep them in interphase and preclude apoptosis by inducing anti-apoptotic molecules such as BCL-2.[325, 326] Of note, these signals are too weak to induce T cell activation and proliferation and do not lead to autoreactivity under physiological conditions.[323]

When peripheral naïve T cell numbers decrease as a consequence of acute insults, the former subliminal effects of self-pMHC and IL-7 are converted into the driving force of homeostatic proliferation, a process called lymphopenia-induced proliferation (LIP, Fig. 15).[327]

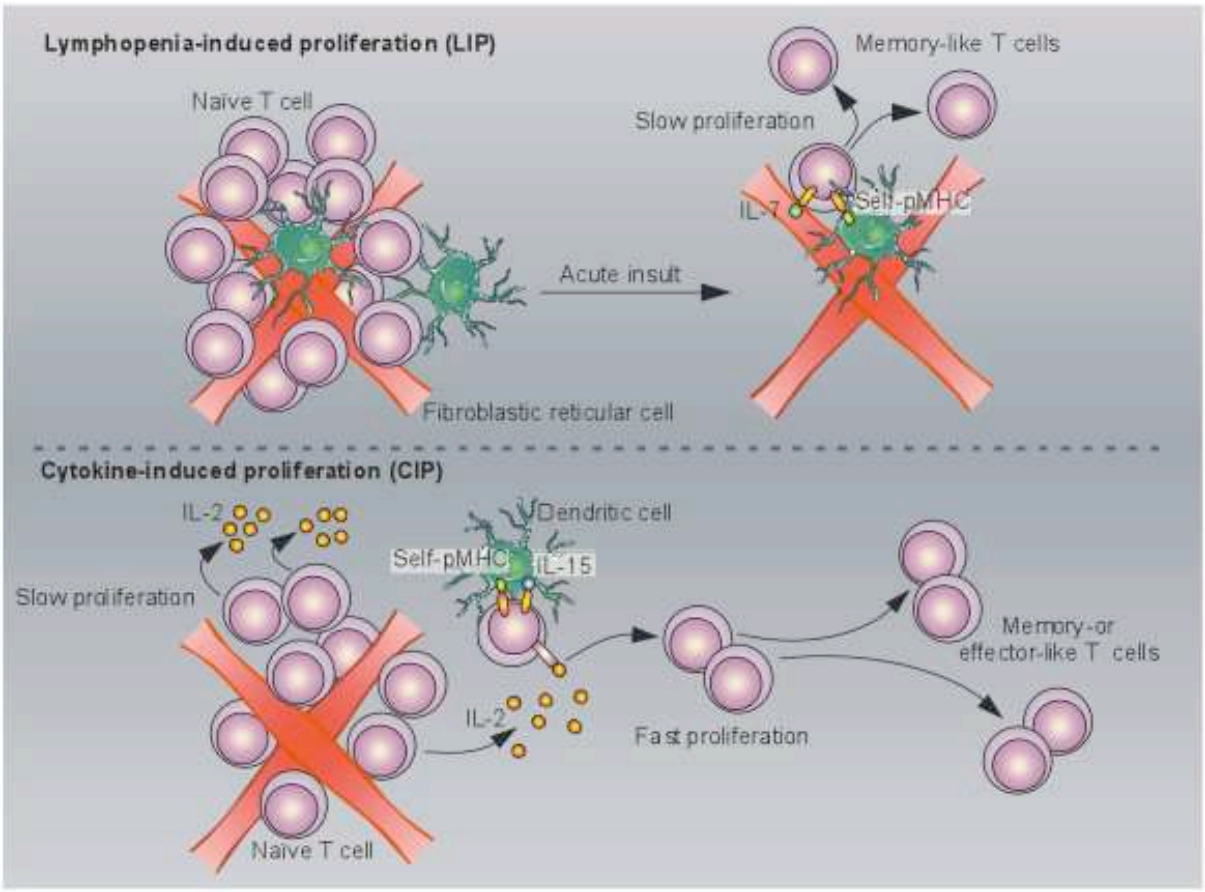

Figure 15. Naïve αβ T cell homeostasis.

In the context of acute lymphopenia, homeostatic TCR:CD3:ζ-signalling induced by self-pMHC is amplified by increased IL-7:IL-7-R-signalling and naïve T cells slowly proliferate in a process designated lymphopenia-induced proliferation (LIP) to become memory-like T cells. Additionally, high concentrations of the γ_c-cytokines IL-2 and IL-15 in combination with self-pMHC trigger cytokine-induced proliferation (CIP) leading to the fast expansion of central memory-like T cells and effector memory-like T cells, repectively.

Figure adapted from Surh CD, Sprent J, Immunity, 2008.[323]

It is assumed that in the context of acute lymphopenia, below-threshold TCR:CD3:ζ-signalling induced by self-pMHC is amplified by increased IL-7-R-signalling, resulting in a proliferation signal.[328, 329] Probably, sustained IL-7-R-signalling induces degradation of the cyclin-dependent kinase (CDK) inhibitor $P27^{KIP1}$ and consequently T cells progess from interphase to S phase of the cell cycle.[330] Besides the co-receptors CD4 and CD8, LIP is independent of co-stimulatory receptors such as CD28 and LFA-1.[323] LIP proceeds at a

relatively slow rate for both $CD4^+$ T_H and $CD8^+$ T_{Cyt} with the latter being more susceptible to it. Naïve polyclonal T cells expanding by LIP gradually acquire phenotypic characteristics of T_{Mem} but as LIP is independent of foreign antigen they are designated memory-like T cells (Fig. 15).[323, 327]

Additionally, very high amounts of the γ_c-cytokines IL-2 and IL-15 in combination with self-pMHC can induce homeostatic proliferation, a process referred to as cytokine-induced proliferation (CIP) (Fig. 15). In contrast to LIP, CIP favours the relatively fast expansion of $CD8^+$ T_{Cyt} memory-like T cells, with IL-2 inducing $CD45R0^+CD62L^-CCR\text{-}7^-$ effector memory-like T cells (T_{EM}) and IL-15 inducing $CD45R0^+CD62L^+CCR\text{-}7^+$ central memory-like T cells (T_{CM}).[331, 332] Importantly, $CD8^+$ T_{Cyt} deficient for SOCS-1 display inceased IL-15-induced CIP, while there is no such effect found for $CD4^+$ T_H.[333]

1.4.2 Immune expansion and effector αβ T cells

Naïve $CD4^+$ and $CD8^+$ αβ T cells recirculate the secondary lymphoïd organs, receive homeostatic signals and remain quiescent in the interphase of the cell cycle.[323] When the host becomes infected, macrophages residing in the subcapsular region of the draining lymph nodes phagocytose the infectious agent and cross-present it to immature DCs (iDCs). The iDCs assimilate the corresponding antigens, process them and differentiate into mature DCs (mDCs) presenting the antigenic fragments on pMHC class I or pMHC class II together with co-stimulatory molecules such as CD80 and CD86.[334] The interaction of mDCs and naïve $CD4^+$ and $CD8^+$ T cells takes place at the border of the subcapsular sinus and in the interfollicular regions of the draining lymph nodes.[335, 336]

Naïve $CD4^+$ and $CD8^+$ T cells consequently receive two activating signals, the first one by the interaction of pMHC class I or class II with the TCR:CD3:ζ-complex and the second one by the interaction of CD80 or CD86 with CD28.[337, 338] This is refered to as T cell priming and leads to antigen specific T cell activation and massive clonal expansion. As a consequence of the cytokine microenvironment established by the innate immune system, specific master transcription factors are expressed that govern differentiation into particular T cell effector populations.[339, 340]

The theoretical clonal expansion rate for naïve $CD8^+$ T cells has been estimated to be one division in 4-6 h, thus leading to ~19 cell divisions in the first week resulting in a 500.000-fold expansion.[341] The profound metabolic changes underlying this expansion are essentially controlled by the serine/threonine protein kinase mammalian target of rapamycin (mTOR).[342]

In the presence of IFN-γ and IL-12 naïve $CD4^+$ T cells upregulate the transcription factor T-box expressed in T cells (T-BET) and STAT-4 and differentiate into IFN-γ-, TGF-β- and lymphotoxin β (LT-β)-secreting T_H type 1 (T_H1) cells that are important for eliminating intracellular pathogens by delivering help to T_{Cyt}.[339, 343-346]

In the presence of IL-2, IL-4, IL-7 and thymic stromal lymphopoietin (TSLP) naïve $CD4^+$ T cells upregulate the transcription factors GATA-3 and STAT-5 and differentiate into IL-4-, IL-5- and IL-13-secreting T_H type 2 (T_H2) cells that are important for eliminating parasites by delivering help to B cells.[339, 347-349]

In the presence of IL-6, IL-21, IL-23 and TGF-β, naïve $CD4^+$ T cells upregulate the transcription factors retinoic acid receptor-related orphan receptor γt (RORγt) and STAT-3 and differentiate into IL-17A-, IL-17F- and IL-21-secreting T_H type 17 (T_H17) cells. T_H17 are important for eliminating extracellular bacteria and fungi by mediating the cross-talk between the innate and adaptive immune system.[339, 350-353]

In the presence of IL-2 and TGF-β naïve $CD4^+$ T cells upregulate the transcription factors FOXP-3 and STAT-5 and differentiate into inducible T_{Reg} (iT_{Reg}) that together with natural, i.e. thymus derived, T_{Reg} (nT_{Reg}) modulate immune responses and maintain self-tolerance partially by secreting TGF-β and IL-10.[339, 354-356]

Additionally, naïve $CD4^+$ T cells can specialize into a distinct population that is found in the lymph node B cell follicle where they home to via chemokine C-X-C motif receptor 5 (CXCR-5).[357] They are termed follicular helper T cells (T_{FH}) because of their capacity to interact with B cells via PD-1 and IL-21 and contribute to class-switch recombination and somatic hypermutation. T_{FH} cells depend on the transcriptional repressor BCL-6, but currently it is not clear whether they constitute a particular population or subspecialized members of the T_H1, T_H2 and/or T_H17 compartments.[358, 359]

In the presence of IL-2, IL-12, IL-21 and IL-27 naïve $CD8^+$ T cells upregulate the transcription factors BLIMP-1, T-BET and EOMES and differentiate into T_{Cyt} that express tumour necrosis factor alpha (TNF-α), IFN-γ, perforin and granzymes and conduct immune responses directed against intracellular pathogens.[360-363]

Initially, naïve T cell differentiation and expansion is antigen-dependent and relies on combined TCR:CD3:ζ- and cytokine-receptor-signalling. IL-2 is central to clonal expansion and naïve T cells that have received proper stimulation and co-stimulation upregulate the high affinity IL-2Rα-chain (CD25) and establish an autocrine IL-2 loop.[364] However, T cell clones not specific for the presented antigen can undergo discrete phenotypic changes without clonal expansion due to the activating cytokine milieu, a process called bystander-activation.[365]

Furthermore, effector cytokine production in differentiated T cells can become independent of TCR:CD3:ζ-signalling and can be triggered by combined cytokine-receptor-signalling, i.e. by a STAT-inducing cytokine and an IL-1-family cytokine.[340, 366, 367]

Once primed and expanded in the secondary lymphoïd organs, effector T cells change their migratory patterns and invade the infected target tissue. This allows for on-site expansion to further acquire effector functions and to perform the antigen-specific immune response spatially restricted to the infected tissue. In that way, collateral damage of bystander tissues is minimized. Besides classical effector cytokines, on-site differentiated T cells can acquire the capacity to secrete immunomodulatory cytokines such as IL-10 to restrain immunopathology.[368, 369]

1.4.3 Immune contraction and memory αβ T cells

Once clonally expanded and differentiated, the majority, i.e. >90%, of $CD4^+$ T_H and $CD8^+$ T_{Cyt} effector cells, that have succesfully eliminated their cognate antigen, will die off in a two-week lasting homeostatic process called immune contraction.[370] Immune contraction is necessary to prevent non-essential end-organ damage and autoimmunity, as well as lymphoïd malignancies.[14]

This programmed T cell death is essentially mediated by the pro-apoptotic molecules FAS and BIM that are central to the extrinsic and intrinsic apoptotic pathways, respectively. Repetitive TCR-stimulation of proliferating effector T cells in the presence of IL-2 signalling induces restimulation-induced cell death (RICD) - also termed activation-induced cell death (AICD) - via upregulation of FAS and FAS ligand (FAS-L) and thus restrains on-site expansion in the presence of antigen.[14, 371-373] Once antigen has been cleared, cytokine-signalling shuts down and induces cytokine withdrawal-induced cell death (CWID) via upregulation of BIM, by this way eliminating the majority of effector T cells at the end of the immune response in the absence of antigen (Fig. 16).[14, 374, 375]

In parallel, the immune response leads to the generation of long-lived antigen-specific $CD4^+$ and $CD8^+$ memory T cells (T_{Mem}).[370] Homeostasis and survival of $CD4^+$ and $CD8^+$ T_{Mem} is virtually independent of TCR:CD3:ζ-signalling and largely dependent on IL-7-R- and IL-15-R-signalling.[376-380]

However, $CD4^+$ T_{Mem} seem to be less stable than $CD8^+$ T_{Mem}.[381] T_{Mem} can be discriminated into two classes, i.e. central memory T cells (T_{CM}) and effector memory T cells (T_{EM}). T_{CM} home to secondary lymphoïd tissues by virtue of the expression of L-selectin CD62L and the chemokine receptor CCR7. When they are re-challenged with their cognate

antigens, they rapidly proliferate and terminally differentiate into effector T cells, thus initiating a secondary immune response. T_{EM} home to non-lymphoïd tissues and do not express CD62L and CCR7. However, they exhibit a capacity to rapidly exert effector functions at the site of inflammation, when they re-encounter their cognate antigens.[382-384]

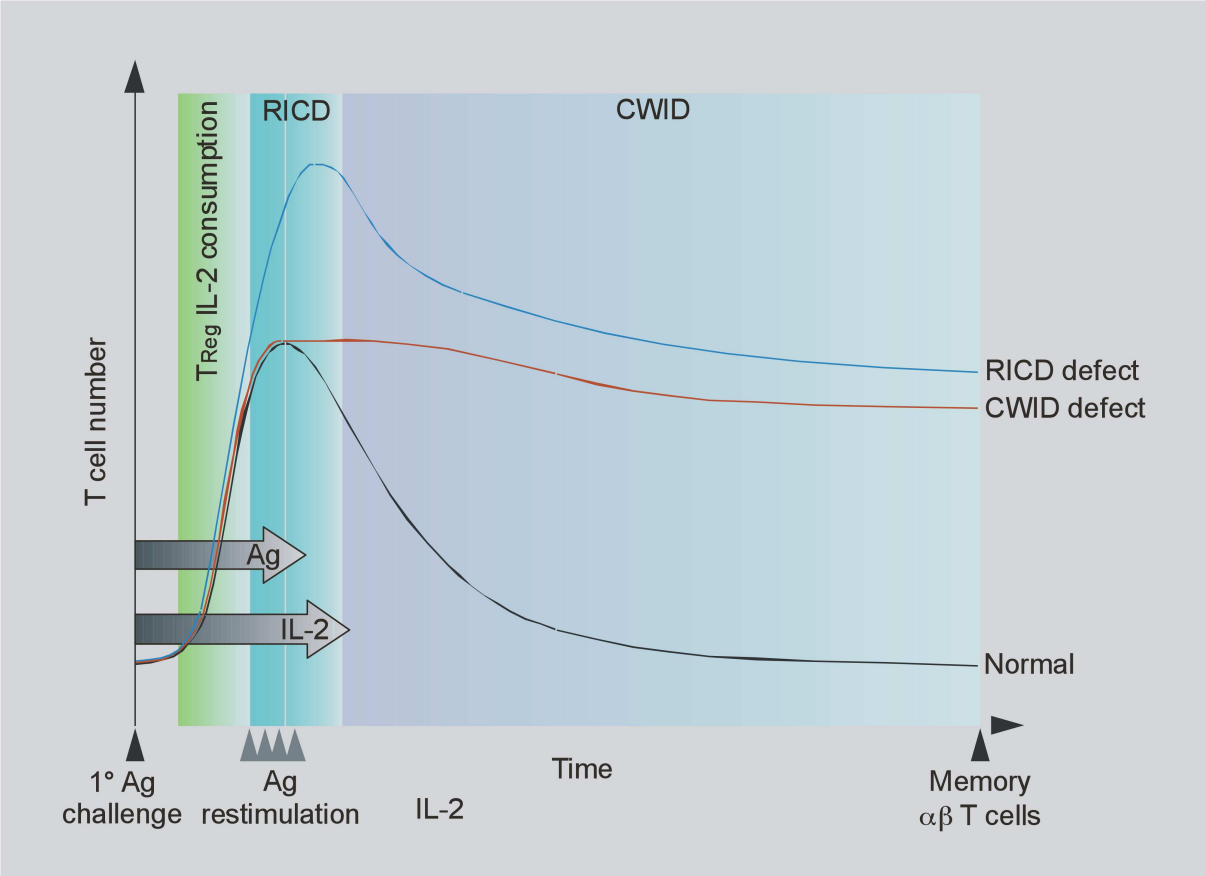

Figure 16. Immune contraction and memory αβ T cells.

Quiescent naive T cells that have encountered their cognate antigen (Ag) establish an autocrine IL-2:IL-2R-loop and clonally expand. The initial proliferative burst is kept in check by T_{Reg} that consume IL-2 and by repetitive antigenic TCR-stimulation that induces apoptotic restimulation-induced cell death (RICD). After antigen has been cleared, IL-2 cytokine-signalling shuts down and induces cytokine withdrawal-induced cell death (CWID). RICD and CWID thus govern immune contraction and are involved in T cell memory (Black line). Additionally, the population kinetics for RICD- and CWID-defects are shown in blue and red, respectively.

Figure adapted from Snow AL, et al, Immunol Rev, 2010.[14]

1.4.4 Innate-like γδ T cells

γδ T cells make up a minor fraction of the total T cell compartment and, although expressing a TCR, they are termed innate-like cells as they share several features with cells of the innate immune system.[12] During thymopoïesis, development of γδ T cells preceeds that of conventional αβ T cells, even though in humans the exact branching point currently is not defined (Fig. 8).[5, 278] The γδ TCR is generated by V(D)J-recombination and, while the

theoretical repertoire has been calculated to be 10^{18}, peripheral γδ T cells display a narrow repertoire with an important contribution of invariant receptors due to programmed V(D)J-recombination that e.g. is not generating junctional diversity.[27, 284, 385, 386]

These γδ T cells seem to be derived from early thymic waves and populate different epithelial surfaces such as skin, gut, respiratory tract and urogenital tract, with a particular invariant γδ TCR being specific for a particular niche.[12] However, peripheral blood γδ T cells exist having a broader repertoire due to more classical V(D)J-recombination including generation of junctional diversity.[12]

Binding properties of the γδ TCR differ from that of the αβ TCR and the former recognizes phosphoantigens that are rapidly presented by stressed or infected cells via non-polymorphic MHC-like molecules.[387-389] During their development, γδ T cells aquire a pre-activated, i.e. memory-like phenotype, and they can rapidly execute their effector functions as, in additon to the γδ TCR, they express an array of TLRs and NK-receptors.[390-392] Of note, these receptors predominantly act in synergy with γδ TCR:CD3:ζ-signalling but under the influence of proinflammatory cytokines can activate γδ T cells independently of the latter.[393, 394]

Innate-like γδ T cells are involved in multiple processes such as immune defense against extra- and intracellular pathogens, modulation of innate and adaptive immune responses, tumour surveillance and epithelial tissue homeostasis.[390] [395]The combination of DAMP-Rs, PAMP-Rs, invariant γδ TCR-expression, subset specific tissue homing and rapid antigen specific effector functions adds up to the particular role of innate-like γδ T cells.[12]

1.4.5 Innate-like natural killer T cells

During thymocyte development, iNKT cells branche from DP thymocytes and in contrast to conventional αβ T cells are not selected by pMHC-complexes presented on TECs, but by the non-classical MHC molecule CD1d expressed on DP thymocytes.[396] iNKT cells express the invariant TCRVα24Jα18Vβ11 that binds the glycosyl-headgroup of α-galactosylceramide and that generates a relatively strong TCR:CD3:ζ-signal necessary for positive agonist-selection.[29, 30] Additionally, co-stimulation mediated by homotypic interactions of the signalling lymphocytic activation molecule (SLAM)-family members SLAMF1 (CD150) and SLAMF6 (CD352) are necessary to pass the positive selection step.[397, 398] iNKT cells leave the thymus as immature precursors and complete their maturation in the periphery where they home preferentially to the blood, the liver, the spleen and the omentum.[399] Mature iNKT cells display an effector-memory phenotype and upon antigenic

encounter rapidly produce proinflammatory cytokines such as IL-4, IFN-γ and IL-17, thus contributing to the initiation of a protective innate immune response.[400] Furthermore, they activate the adaptive immmune system and even downmodulate overt inflammation with immunomodulatory cytokines such as IL-10, thus bridging the innate and adaptive immune system.[401] Recently, iNKT cell have been found to interact with a variety of particular innate and adaptive immune cells, confirming their multiple roles in balancing immune responses and homeostasis.[402]

1.4.6 Innate-like mucosa-associated invariant T cells

Innate-like mucosa-associated invariant T (MAIT) cell thymopoïesis follows a particular pathway characterized by agonist-selection as described for iNKT cells. MAIT cells express a semi-invariant TCRVα7.2Jα33 that is restricted by the evolutionarily conserved non-classical major histocompatibility complex class I-related (MR1) molecule and recognizes bacterially infected cells in a MR1-dependent manner.[31, 32, 403] Recently, it has been shown that MR1 binds and presents microbial vitamin B2 metabolites to MAIT cells.[404] MAIT cells leave the thymus with a naïve phenotype and depending on interactions with B cells and commensal bacteria acquire an effector phenotype.[405, 406] They are present in the blood stream and home to peripheral tissues such as the liver and the gastrointestinal tract. It has been proposed that in the case of bacterial infection, MAIT cells rapidly become activated and secrete effector cytokines such as IL-17-family members and IFN-γ thereby contributing to protective immunity.[32, 33]

1.5 (Severe) combined immunodeficiency

1.5.1 The human experience

Severe combined immunodeficiency (SCID) commonly is regarded as a developmental disorder of NK, T and B cells that manifests with lymphopenia and life-threatening opportunistic infections in early infancy (Fig. 17).[7, 407] SCID is an inherited PID and due to pioneering scientific and medical work performed throughout the last 30 years, nowadays SCID can be assumed by screening dried blood spots for T cell receptor excision circles (TRECs) and kappa-deleting recombination excision circles (KRECs).[408, 409] TRECs and KRECs are found in naïve T cells, i.e. recent thymic emigrants, and naïve B cells, i.e. transitional B cells, respectively, as products of effective V(D)J-recombination and are diluted by every further cell division thereafter. TRECs and KRECs can easily be detected by qPCR and indicate whether the T and B cell pools are present and predominantly naïve, as expected

in a healthy individual, or absent and memory-like/exhausted, as expected in a SCID individual.[408]

Once the diagnosis is established by mutational analysis, SCID frequently is cured by haematopoïetic stem cell transplantation (HSCTx) and haematopoïetic stem cell gene therapy (HSCGT), thus showing how basic science can make its way to become successful medical treatment.[410, 411]

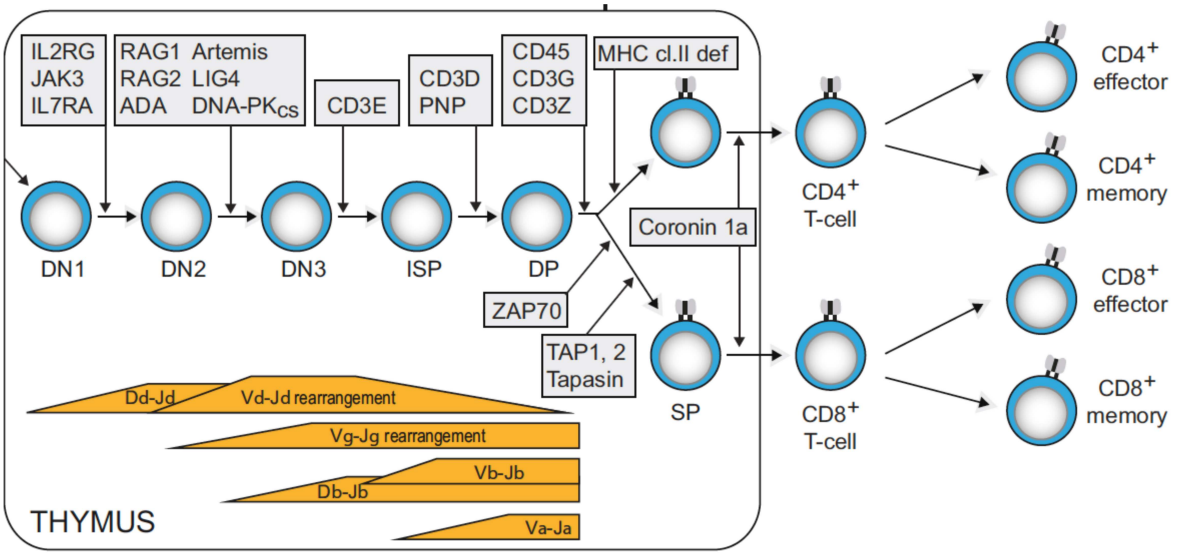

Figure 17. Severe combined immunodeficiency (SCID).

A scheme of human thymocyte development throught the particular DN1-3, iSP, DP and SP thymocyte stages and peripheral T cell differentiation into $CD4^+$ and $CD8^+$ T effector and memory cells is shown. The developmental timing of V(D)J-recombination is indicated by particular beams for each T cell receptor locus, i.e. TRD@, TRG@, TRB@ and TRA@, as compared to the corresponding thymocyte populations. The most common genetic causes of SCID are given in boxes and the resulting particular blocks in thymopoïesis are indicated by arrows.

Figure adapted from van Zelm MC, et al, Front Immunol, 2011.[407]

Currently, combined immunodeficiency (CID) is emerging as a novel group of PIDs, that is predominantly characterized by functional T cell deficiency, albeit developmental alterations are present to variable degrees. CID might escape TREC- and KREC-screening strategies and even present with normal or elevated lymphocyte counts in children or adolescents. In order to correctly diagnose CID, it is therefore important to be aware of its clinical presentations such as opportunistic infections, immunodysregulation and malignant lymphoma, all of which might aggravate over time as the immune system exhausts.[412-414]

Even though, we have now defined several monogenetic entities that can be classified in different groups based on the clinical phenotypes and/or the structure and function of the gene defects such as the „channelopathies“ (ORAI-1-, STIM-1- and MAGT-1-deficiency)[242,

[247, 415], the „cytoskeletopathies“ (WASP-, WIP- and DOCK-8-deficiency)[416-418], the genetic susceptibilities to EBV infection (SAP, ITK, CD27 and CORO-1A-deficiency)[419-427], we are just beginning to establish a comprehensive concept of diagnosing and curing CID (Tab. 1)

On the other hand, insights gained from diagnosing, analyzing and treating (S)CIDs has been fundamental for our basic understanding of the human immune system and remains a field of intensive translational research.[7] For example the indentification of the Ca^{2+}- and Mg^{2+}-channelopathies ORAI calcium release-activated calcium modulator 1 (ORAI-1)-, stromal interaction molecule 1 (STIM-1)- and magnesium transporter 1 (MAGT-1)-deficiency have disclosed Ca^{2+}- and Mg^{2+}-flux as central TCR:CD3:ζ-mediated second messenger pathways crucial for T cell activation (Tab. 1).[242, 247, 415] Additionally, the description and characterization of the Wiskott-Aldrich syndrome (WAS) and the dedicator of cytokinesis 8 (DOCK-8)-deficiency have illustrated the importance of actin dynamics for the formation of the immunological synapse and signalsome-nucleation in T cell activation (Tab. 1).[417, 418] The finding, that X-linked lymphoproliferative syndrome type 1 (XLP-1) is caused by signalling lymphocyte activation molecule-associated protein (SAP)-deficiency has boosted the description of the signalling lymphocytic activation molecule (SLAM)-co-receptor family and paved the way towards a better understanding of iNKT cell development and biology (Tab. 1).[419, 421, 422] In summary, discoveries first made by analyzing human PIDs have initiated novel fields in basic research that led to the generation of important knowledge far beyond the initial findings.

Table 1. Gene defects associated with combined immunodeficiencies (CIDs) in humans.

Gene	Major consequences	Ref.
TRAC (TCRα constant gene)	Impaired αβ TCR expression	428
CD3G, *CD3D*, *CD3E* (cluster of differentiation γ, δ, ε) and *CD247* (ζ-chain)	Impaired TCR:CD3:ζ-assembly and signalling	429-432
LCK (lymphocyte-specific protein tyrosine kinase)	Impaired CD4 and CD8 expression, ITAM-phosphorylation and Ca^{2+}-flux	433
UNC119 (uncoordinated 119)	Impaired LCK trafficking	434
ZAP70 (ζ-chain associated protein tyrosine kinase of 70 kDa)	Impaired ITAM-phosphorylation and Ca^{2+}-flux	435-437
RHOH (RAS homology family member H)	Impaired LCK and ZAP-70 recruitment to the LAT:SLP-76-signalosome	438
ITK (interleukin-2-inducible T cell kinase)	Impaired Ca^{2+}-flux and chemokinesis	420

STK4 (serine/threonine kinase 4)	Impaired T cell proliferation and increased apoptosis	[439, 440]
MAGT1 (magnesium transporter 1)	Impaired Mg^{2+}- flux and NKG2D expression	[247, 441]
ORAI1 (ORAI calcium release-activated calcium modulator 1)	Impaired Ca^{2+}-flux	[242]
STIM1 (stromal interaction molecule 1)	Impaired Ca^{2+}-flux	[415]
CARD11 (caspase recruitment domain family member 11)	Impaired CBL-formation and cannonical NF-κB-signalling	[442, 443]
MALT1 (mucosa-associated lymphoid tissue 1)	Impaired CBL-formation and cannonical NF-κB-signalling	[444]
NFKBIA (nuclear factor of kappa light polypeptide gene enhancer in B-cells inhibitor alpha)	Impaired NF-κB-signalling	[445]
IL21R (interleukin 21 receptor)	Impaired STAT1/3/5 signalling	[446]
CD27 (cluster of differentiation 27)	Impaired CD70:CD27-co-stimulation	[424, 426]
OX40 (OX40 antigen)	Impaired OX40L:OX40-co-stimulation	[447]
TTC7A (tetratricopeptide repeat domain 7A)	Impaired protein trafficking and scaffolding	[448, 449]
CORO1A (coronin, actin binding protein, 1A)	Impaired actin dynamics and integrin signalling	[423, 425]
DOCK8 (dedicator of cytokinesis 8)	Impaired actin dynamics	[418]
WASP (Wiskott-Aldrich syndrome protein)	Impaired actin dynamics	[417]
WIP (Wiskott-Aldrich syndrome protein-interacting protein)	Impaired actin dynamics	[416]
SAP (signalling lymphocyte activation molecule-associated protein)	Impaired iNKT development and SLAMFR-signalling	[419, 421, 422]
POLE1 (polymerase ε1)	Impaired DNA replication and cell cycle progression	[450]

CID-causing genes described in this doctoral thesis are depicted in red.

2 Objective of the doctoral thesis

This translational immunobiological thesis is aimed to contribute to our knowledge of the human immune system by carefully analyzing the clinical and immunological phenotypes and the proximal TCR:CD3:ζ-signalling alterations in patients presenting with CIDs in order to find the causative gene defects. By this approach, I report three cases of (S)CID caused by autosomal recessive mutations in the lymphocyte-specific protein tyrosine kinase (*LCK*)-, ζ-chain associated protein tyrosine kinase of 70 kDa (*ZAP-70*)- and interleukin-2-inducible T cell kinase (*ITK*)-genes.

Keeping in mind, that biological samples of these extremely rare (S)CIDs are sparse, the precise characterization of these particular human (S)CIDs might not only recapitulate the data generated *in vitro* and in the murine model system, but additionally elucidate differences between mice and men not always predictable by mere extrapolation of the murine data.

Furthermore, the results obtained by this approach might contribute to our knowledge of (S)CIDs, thus facilitate future diagnosis of further LCK-, ZAP-70 and ITK-deficient patients or related TCR:CD3:ζ-signalling disorders and set the stage for more timely and hopefully life-saving therapeutical interventions such as HSCTx and HSCGT.

3 Results

3.1 Identification of the first *LCK* mutation causing CID with immunodysregulation

3.1.1 Clinical phenotype

We examined a child conceived by *in vitro* fertilization and born at term to healthy non-consanguineous parents from France. Her birth weight was normal and she was vaccinated at birth with the live-vaccine *Bacillus Calmette-Guérin* (BCG) with no adverse event. Latter on, she received four 7-valent conjugate vaccines against *Streptococcus pneumoniae* and four 5-valent vaccines against *Haemophilus influenzae type b*, the toxoïd of *Corynebacterium diphtheriae*, *Bordetella pertussis*, the toxoïd of *Clostridium tetani* and *Poliovirus type 1, 2 and 3* at the age of two, four, six and 14 months. She also was vaccinated twice with attenuated *Measles*, *Mumps* and *Rubella* viruses without adverse events at 12 and 16 months.

From the age of 15 months, she presented with undocumented protracted diarrhea and recurrent upper and lower respiratory tract infections, including pneumonia complicated by pneumatocele. Consecutively, a failure to thrive with a weight loss of -2 standard deviation scores (SDSs) and inadequate gain of height of -1 SDS was noted.

Upper airway endoscopy showed congestive and ulcerative inflammation of the airway mucosa resulting from local inflammation and recurrent infections. Ear, nose and throat biopsies could not be carried out because of severe dyspnea. Gastrointestinal endoscopy and biopsies were found to be normal.

From the age of 22 months, she developed daily bouts of fever accompanied by multiple nodular skin lesions and sterile inflammation of the interphalangeal joints (Fig. 18A). A skin biopsy of a representative nodule was taken, embeded in paraffine and stained with haematoxylin and eosin. Histopathological analysis showed a normal epidermis, but the dermis and especially the hypodermis displayed lymphohistiocytic infiltration, predominantly consisting of macrophages and histiocytes with large cytoplasm. Additionally, large foci of neutrophilic necrosis with abscesses and rare gigantocellular cells were seen in the hypodermis without granuloma formation. Lymphohistiocytic bystander vasculitis was found but immunohistochemical staining of lymphocytes and clonality analysis failed due to insufficient sample quantity (Fig. 18B and C). Importantly, no infectious agent could be

identified and thus lobular and septal neutrophilic panniculitis with bystander vasculitis was diagnosed.

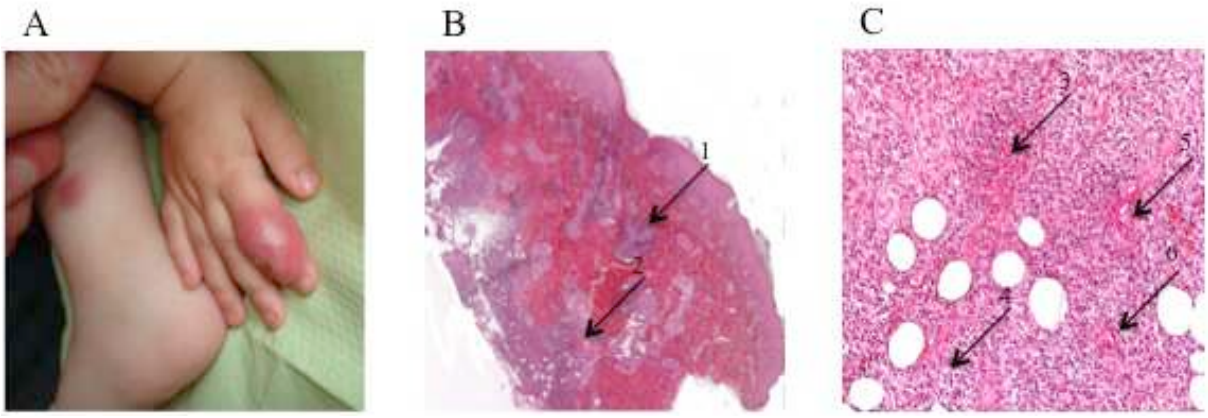

Figure 18. Macroscopic and microscopic aspects of sterile skin and joint inflammation.

(A) The macroscopic aspects of a representative skin nodule and of the interphalangeal joint of the right index finger are shown. (B) A representative skin nodule biopsy stained with haematoxylin and eosin shows dermal (1) and hypodermal (2) lymphohistiocytic and neutrophilic infiltration at low magnification. (C) The same skin nodule specimen at high magnification displays predominant neutrophilic infiltration of the hypodermal connective (3) and fatty tissue (4), i.e. septal and lobular panniculitis, with neutrophilic necrosis and abscesses (5) and lymphohistiocytic bystander vasculitis (6).

Prophylactic immunoglobulin substitution and intensive anti-bacterial, anti-mycobacterial and anti-fungal treatments initiated at the age of 24 months had no major effect neither on skin lesions nor on fever bouts.

From the age of 26 months, the patient developed serositis, i.e. ascites and pericarditis, and thereon a transient systemic capillary leak syndrome. In parallel, ophthalmologic assessment disclosed retinal vasculitis.

Immunosuppressive treatment with glucocorticoids had a transient effect on skin lesions and fever bouts, but both these symptoms subsequently recurred and aggravated. Treatment with neutralizing antibodies against TNF-α led to apyrexia and a partial regression of skin lesions and serositis. However, from the age of 29 months, the patient presented with normocytic aregenerative anaemia and thrombocytopenia and anti-thrombocyte autoantibodies were detected.

At the age of 30 months, the patient was conditioned with busulfane, fludarabine and anti-thymocyte globuline and underwent allogeneïc haematopoïetic stem cell transplantation (HSCTx) from a phenotypically human leukocyte antigen (HLA) matched (10 out of 10) unrelated donor with a non T cell-depleted graft (with a dossage of 7.9 x 10^8 PBMCs, 8.3 x 10^6 $CD34^+$ HSCs and 5.4 x 10^7 $CD3^+$ T cells per kg bodyweight). Unfortunately, the patient

deceased at day seven after transplantation because of pulmonary and hepatic veno-occlusive disease.

Taken as a whole, the patient presented the clinical picture of profound CID characterized by increased susceptibility to respiratory and gastrointestinal tract infections and severe immunodysregulation such as skin and joint autoinflammation and autoimmunity.

3.1.2 Immunological phenotype

Immunological investigations at the age of 23 and 29 months are summarized in Tab. 2.

Table 2. Immunological features of the LCK-deficient patient.

	23 months[1]	**29 months[2]**
Lymphocytes (3,600-8,900/µl)[3]	2,200	1,300
T cells (/µl)		
$CD3^+$ (2,100-6,200)	1,254	520
$CD4^+$ (1,300-3,400)	154	156
$CD8^+$ (620-2,000)	1,012	338
T cells (%)		
$TCR\alpha\beta^+$ cells (90-100)	n.d.	64.3
$TCR\gamma\delta^+$ cells (0-10)	n.d.	33.5
$CD4^+CD45RA^+CD31^+$ (recent thymic emigrants) (57-65)	7	n.d.
$CD4^+CD45R0^+$ (7-20)	84	n.d.
$CD8^+CD45RA^+$ (71-94)	91	n.d.
$CD8^+CD45R0^+$ (6-29)	6	n.d.
T cell proliferation (cpm x 10^3)		
PHA (6.25 µg/ml) (>50)	0.5	1
OKT3 (50 ng/ml) (>30)	4.0	0
PMA (10^{-7} M) + ionomycin (10^{-5} M) (>80)	40	36
PMA (10^{-8} M) + ionomycin (10^{-6} M) (>80)	66	31
Tetanus toxoïd (300 ng/ml) (>10)	2	n.d.
NK cells (/µl)		
$CD16^+CD56^+$ (180-920)	440	n.d.
B cells (/µl)		
$CD19^+$ (720-2,600)	506	559

Serum immunoglobulins (g/l)		
IgG (4.82-8.96)	8.7	n.d.
IgA (0.33-1.22)	1.21	n.d.
IgM (0.5-1.53)	3.06	n.d.
IgE (<2 kIU/l)	<2	n.d.
Specific antibodies[4] (IU/ml)		
Tetanus toxoïd (>0.1)	0.05	n.d.
Diphtheria toxoïd (>0.1)	<0.1	n.d.
Poliovirus type 1, 2, 3 (>40 each)	<10, <10, 20	n.d.
Blood group allohaemagglutinins[5]		
IgM-anti-A (>1:8)	1:128	n.d.
IgM-anti-B (>1:8)	1:8	n.d.
Autoantibodies		
ANA (<1:100)	1:1,600	n.d.
dsDNA (<4 IU/ml)	>50	n.d.
Rheumatoïd factor (<20 IU/ml)	100	n.d.
Anti-thrombocyte (negative)	positive	n.d.

n.d.: not determined. [1]As determined before cytotoxic treatment. [2]As determined after cytotoxic treatment. [3]Age-matched normal values are indicated in parentheses. [4]The patient had received four 7-valent conjugate vaccines against *Streptococcus pneumoniae* and four 5-valent vaccines against *Haemophilus influenzae type b*, the toxoïd of *Corynebacterium diphtheriae*, *Bordetella pertussis*, the toxoïd of *Clostridium tetani* and *Poliovirus type 1, 2 and 3* at the ages of two, four, six and 14 months. [5]The patients had the blood group 0.

Peripheral blood mononuclear cells (PBMCs) of a healthy control and the patient were isolated, stained with fluorochrome-labelled isotype controls or monoclonal antibodies (mAbs) to analyse the different lymphocyte populations by flow cytometry.

The child had profound $CD4^+$ T cell lymphopenia while $CD8^+$ T cells were not altered in terms of numbers. The proportion of $TCR\alpha\beta^+$ cells was reduced while that of $TCR\gamma\delta^+$ cells was augmented. B cell counts were slightly diminished and NK cell counts were normal. Thymic output was reduced as $CD4^+CD45RA^+CD31^+$ recent thymic emigrants were diminished and the majority of $CD4^+$ T cells expressed the memory marker CD45R0 (Tab. 2).[451] Furthermore and in contrast to a healthy control, the majority of $CD4^+CD45RA^-$ T cells expressed CD27 and $CD4^+CD45R0^+$ had lost the lymphoïd homing molecule CD62L and gained the activation marker CD95, thus corresponding to the phenotype of activated T_{EM}-like cells (Fig. 19A, B and C).[452]

In contrast, the majority of $CD8^+$ T cells expressed CD45RA and only a minor fraction expressed the memory marker CD45R0 (Tab. 2). However, only the minority of $CD8^+CD45RA^+$ T cells expressed CD27 and, therefore corresponded to naïve T cells. The majority of the $CD8^+CD45RA^+$ T cells was negative for CD27 and the majority of $CD8^+CD45R0^+$ T cells was negative for CD62L and positve for CD95, thus corresponding to activated but exhausted T_{EMRA}-like cells (Fig. 19A, B and C).[452]

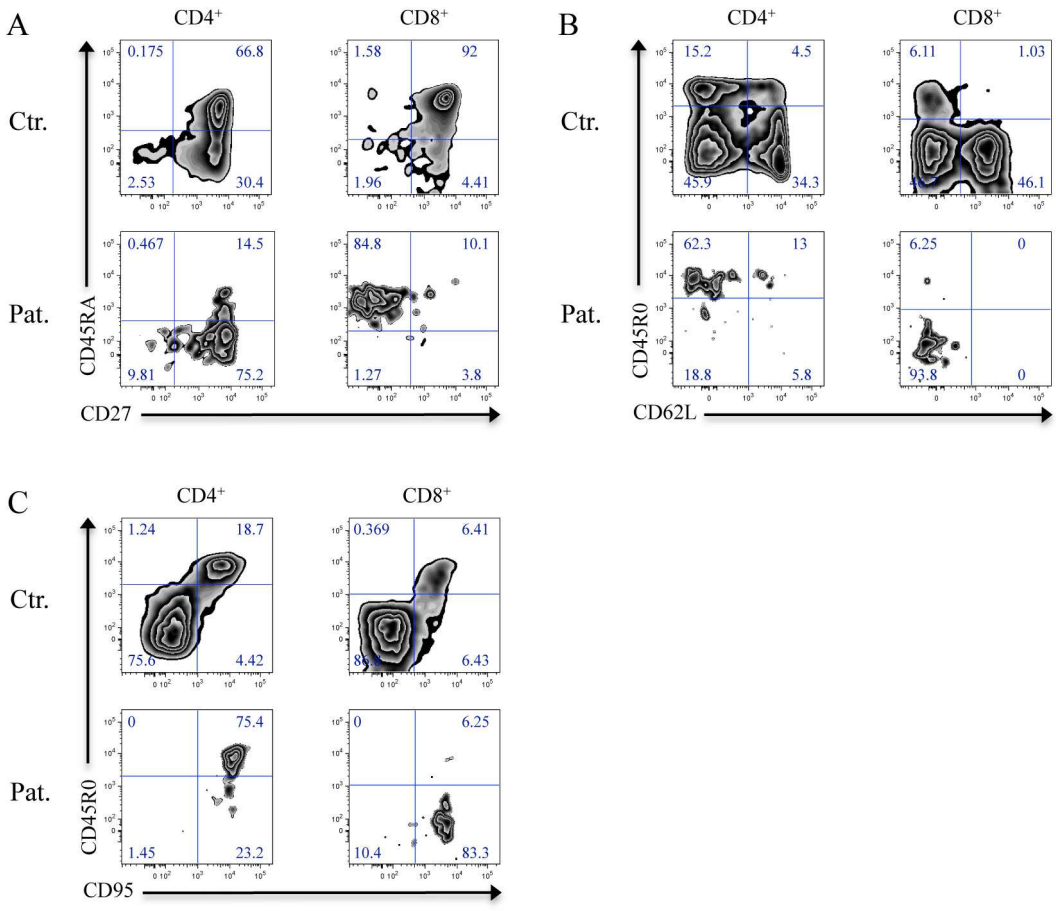

Figure 19. Immunophenotype of LCK-deficient peripheral $CD4^+$ and $CD8^+$ T cells.

Flow cytometric analysis of the expression of (A) CD45RA and CD27, (B) CD45R0 and CD62L and (C) CD45R0 and CD95 on PBMCs from a healthy control (Ctr.) and the LCK-deficient patient (Pat.) are shown after gating on $CD3^+CD4^+$ ($CD4^+$) or $CD3^+CD8^+$ ($CD8^+$) cells. The corresponding percentages are indicated for each square.

The percentages of $CD4^+CD25^+CD127^{low}$ and $CD4^+CD25^+FOX\text{-}P3^+$ T_{Reg} were in normal ranges (3-15%). However, as a consequence of $CD4^+$ T cell lymphopenia, the number of these *bona fide* T_{Reg} was diminished (Fig. 20).

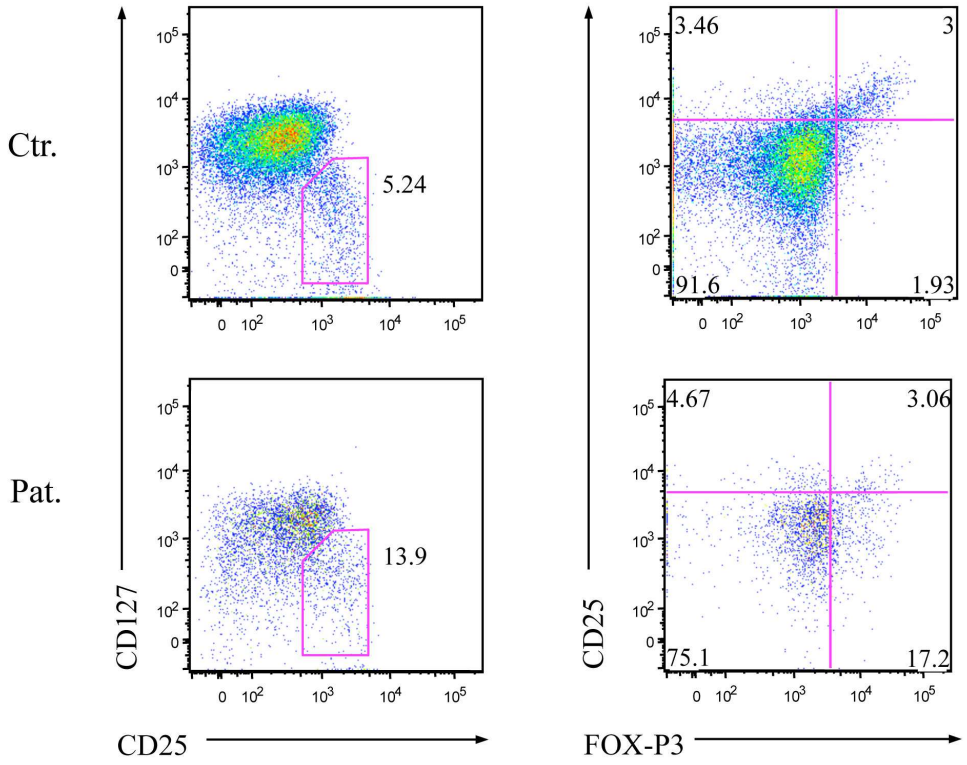

Figure 20. Immunophenotype of LCK-deficient peripheral T_{Reg}.

Flow cytometric analysis of the expression of CD25, CD127 and FOX-P3 on PBMCs from a healthy control (Ctr.) and the LCK-deficient patient (Pat.) are shown after gating on $CD3^+CD4^+$ cells. The corresponding percentages are indicated for each square.

Because of $CD4^+$ T cell lymphopenia and the abnormal phenotype of T cell populations, the proliferation capacity of the patient's T cells was further analysed. PBMCs were either unstimulated or stimulated with the lectin phytohaemagglutinin (PHA), the agonistic anti-CD3ε-antibody OKT3, the PKCθ-activating phorbol 12-myristate 13-acetate (PMA) plus the Ca^{2+}-prevalent ionophore ionomycin or the specific antigen tetanus toxoïd. Proliferation was defective in response to PHA, OKT3 and tetanus toxoïd but incompletely preserved in response to PMA plus ionomycin, suggesting a proximal TCR:CD3:ζ-signalling defect (Tab. 2).

The patient's IgM was elevated whereas IgG, IgA and IgE levels were in the upper normal range. However, specific antibodies against tetanus toxoïd, diphtheria toxoïd and *Poliovirus type 1, 2 and 3* were absent despite repeated vaccinations. The blood group IgM allohaemagglutinins anti-A and anti-B were present and autoantibodies such as anti-nuclear antibodies, anti-double-stranded DNA, rheumatoïd factor, i.e. IgM anti-constant fragment of IgG, and anti-thrombocyte were detected (Tab. 2). Taken as a whole and in combination with

the assumed TCR:CD3:ζ-signalling defect, this was suggesting a reduced or absent function of T_H and T_{Reg} towards B cells.

The αβ and γδ TCR repertoire of the patient's T cells was also examined by quantitative real-time PCR (qPCR). The relative usage of each TRAV, TRBV, TRGV and TRDV was calculated by immunoscope technique and displayed by histograms placing control and patient values side-to-side.[453, 454] The nomenclature used for the TRAV, TRBV, TRGV and TRDV subgroups is that of the international ImMunoGeneTics information system (http://www.imgt.org/IMGTrepertoire/) and the Arden nomenclature is given in brackets.[282] TCR spectratyping suggested an oligoclonal TRAV9 and TRBV6a dominated αβ TCR repertoire (Fig. 21). Oligoclonality was further supported by the loss of the normal Gaussian-like lenght-distribution of the qPCR products, that under normal conditions results from random P- and N-nucleotide insertions (Fig. 22 and data not shown).

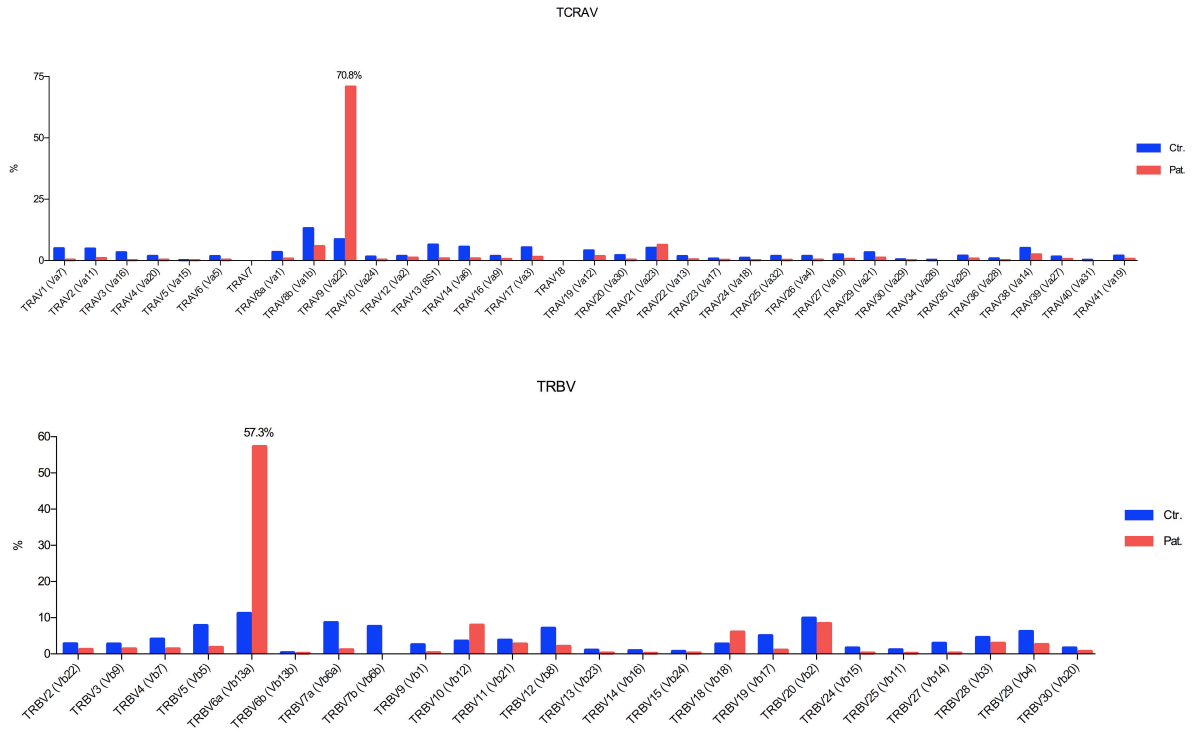

Figure 21. Analysis of LCK-deficient αβ TCR repertoire by spectratyping.

The relative usage of 35 TRAVs (upper panel) and 24 TRBVs (lower panel) was determined by qPCR and is displayed by histograms placing particular variable segments of the control (Ctr. in blue) side-to-side to that of the LCK-deficient patient (Pat. in red). The IMGT nomenclature is used for the particular variable segments and the Arden nomenclature is given in brackets. αβ T cells of the control display a balanced repertoire as exemplified by TRAV9 usage of 8.6% and TRBV6a usage of 11.2%. The repertoire of the patient is restricted to TRAV9 usage of 70.8% and TRBV6a usage 57.3%, thus suggesting oligoclonality.

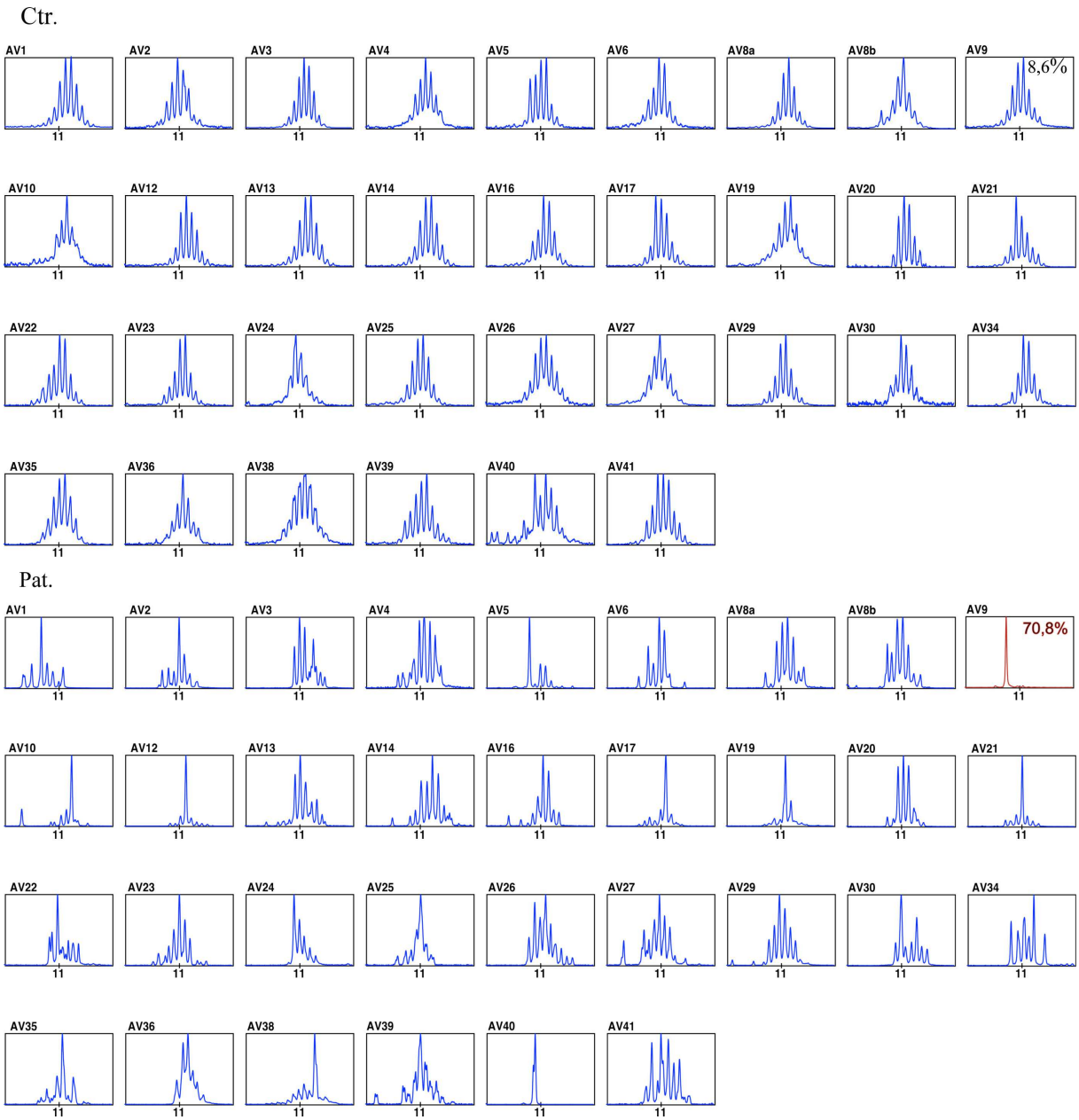

Figure 22. Analysis of LCK-deficient αβ TCR repertoire by electropherogram.

The particular TRAV qPCR products of the control (Ctr., upper pannel) show a normal Gaussian-like lenght-distribution, that is due to random P- and N-nucleotide insertions. The Gaussian-like lenght-distribution for the particular TRAV qPCR products of the LCK-deficient patient (Pat., lower pannel) is lost, thus suggesting oligoclonality.

Furthermore and as opposed to the healthy control, for which the usual dominance of TRGV9 and TRDV2 were found, TCR spectratyping of the patient showed an altered γδ TCR repertoire with TRGV5 and TRDV1 dominating (Fig. 23).

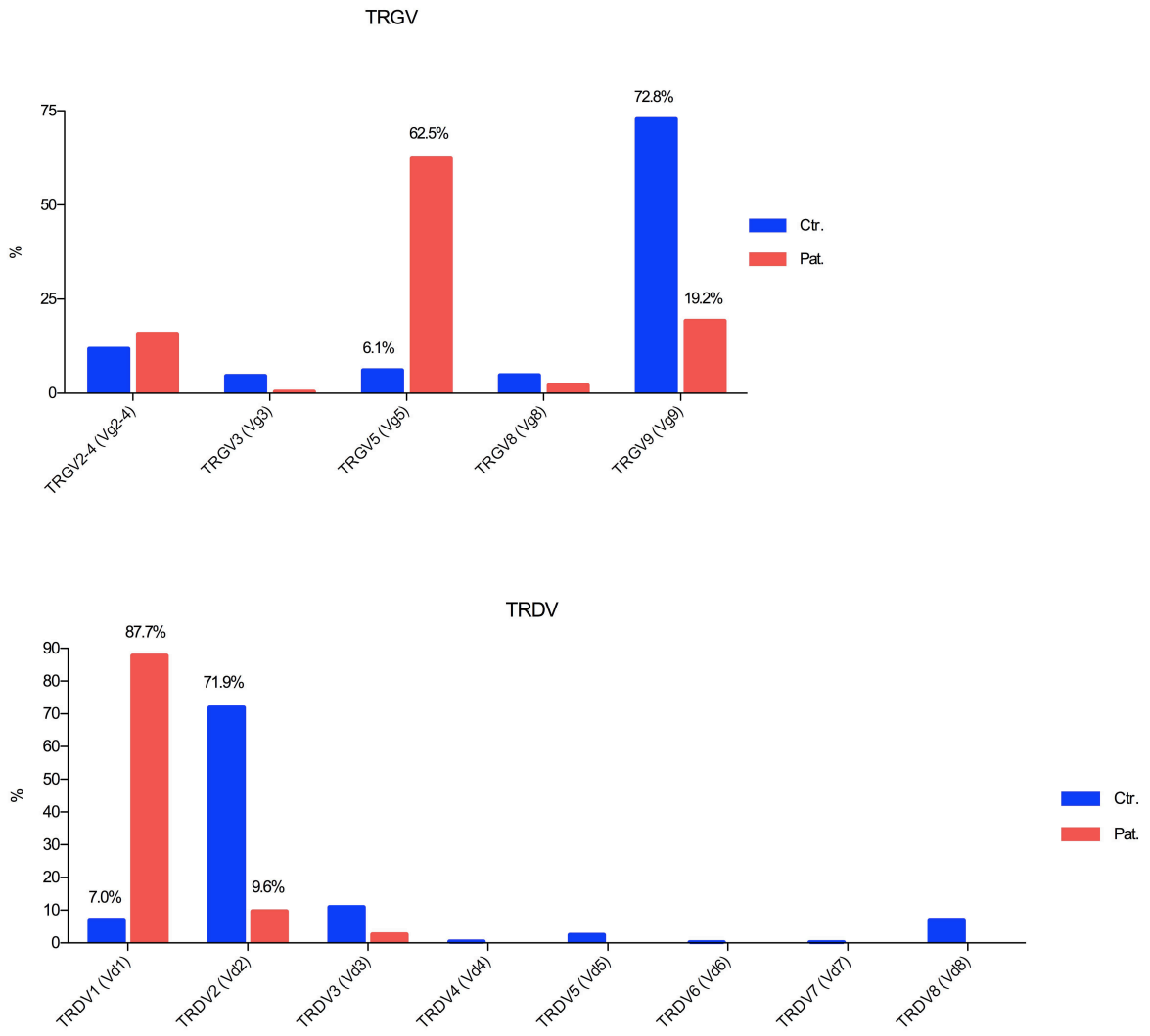

Figure 23. Analysis of LCK-deficient γδ TCR repertoire by spectratyping.

The relative usage of five TRGVs (upper panel) and eight TRDVs (lower panel) was determined by qPCR and is displayed by histograms placing particular variable segments of the control (Ctr. in blue) side-to-side to that of the LCK-deficient patient (Pat. in red). The IMGT nomenclature is used for the particular variable segments and the Arden nomenclature is given in brackets. γδ T cells of the control display an usual repertoire as exemplified by predomiant TRGV9 usage of 72.8% and TRDV2 usage of 71.9%. The repertoire of the patient is unusual with a predomiant TRGV5 usage of 62.5% and TRDV1 usage of 87.7%.

To formaly prove monoclonality of the predominating TRAV9-TRAC and TRBV6a-TRBC rearrangements, the corresponding qPCR products were cloned and the particular CDR3s were Sanger-sequenced.[454] In total, 74 clones of TRAV9-TRAC and 90 clones of TRBV6a-TRBC were analysed with the IMGT/V-Quest algorithm and the assigned V, D and J segments were compiled, respectively.[455] CDR3 sequencing showed a productive rearrangement with ≤ 100% sequence identity for TRAV9-2 J26 and a productive

rearrangement with ≤ 100% sequence identity for TRBV6-6 J2-5 D2 and was thus confirming monoclonality of these predominating clones (Tab. 3 and 4).

Table 3. CDR3 sequencing of 74 clones of TRAV9-TRAC.

Productive rearrangement with ≤100% sequence identity for TRAV9-2 J26		
V-Gene and allele	TRAV9-2*01	Identity = **100.00%** (90/90 nt)
J-Gene and allele	TRAJ26*01	Identity = **96.23%** (51/53 nt)
CDR-IMGT lenght	[9 aa]	ALRNGQNFV

Table 4. CDR3 sequencing of 90 clones of TRBV6a-TRBC.

Productive rearrangement with ≤100% sequence identity for TRBV6-6 J2-5 D2		
V-Gene and allele	TRBV6-6*01	Identity = **100.00%** (229/229 nt)
J-Gene and allele	TRBJ2-5*01	Identity = **93.75%** (45/48 nt)
D-Gene and allele	TRBD2*01	D region is in reading frame 2
CDR-IMGT lenght	[12 aa]	ASSYWGSGETQY

Flow cytometric analysis of the patient's αβ T cells confirmed that $CD4^+$ and $CD8^+$ cells predominantly expressed the monoclonal Vβ2 (TRBV20)- and Vβ13 (TRBV6a)-containing TCRs on their cell surface (compare Fig. 21 to Fig. 24). The majority of the patient`s γδ T cells were found to be $CD8\alpha^+$ and to express Vδ1 (TRDV1) instead of Vδ2 (TRDV2) (compare Fig. 23 to Fig. 24). Of note, Vδ1 expressing γδ T cells are known to represent tissue-resident γδ T cells while Vδ2 expressing γδ T cells are rather circulating cells found in the peripheral blood.[12]

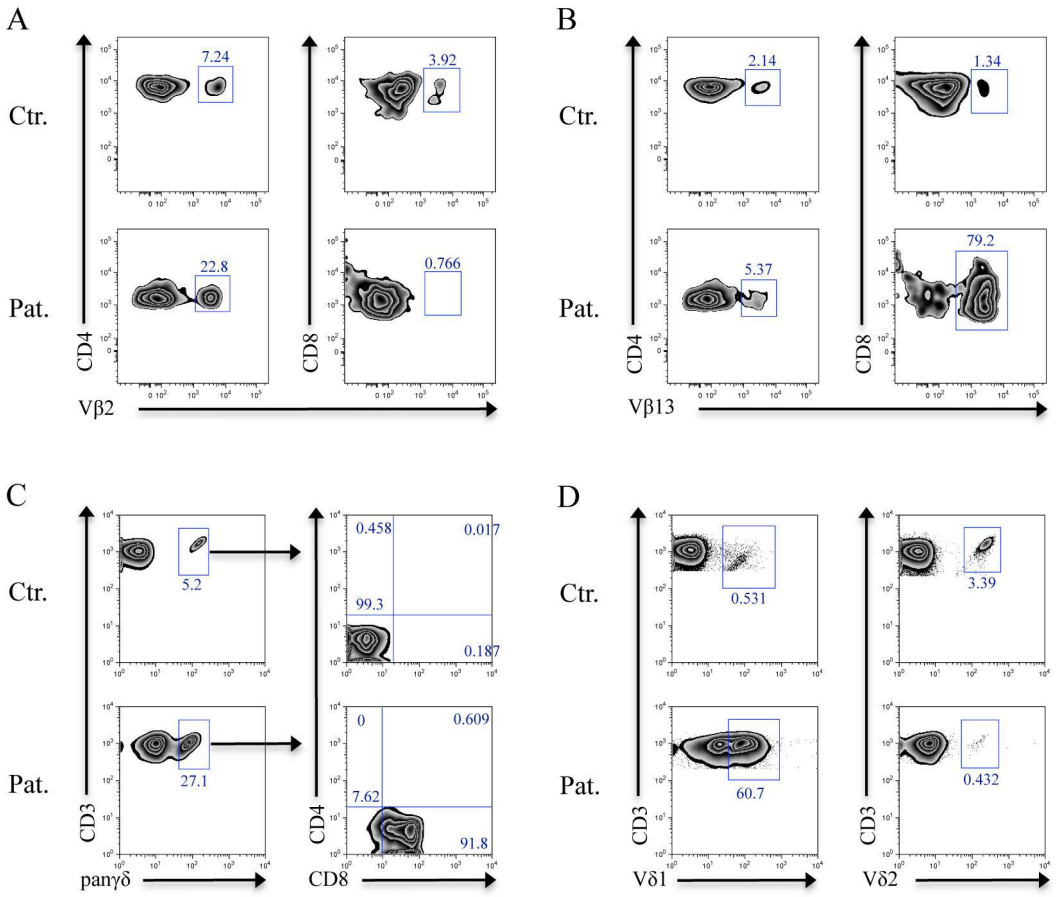

Figure 24. Immunophenotype of Vβ- and Vδ-expressing LCK-deficient PBMCs.

Flow cytometric analysis of the expression of (A) Vβ2 and (B) Vβ13 on $CD4^+$ and $CD8^+$ T cells, of (C) panγδ on $CD3^+$ T cells or CD4 and CD8 on γδ T cells and (D) of Vδ1 and Vδ2 on $CD3^+$ T cells from a healthy control (Ctr.) and the patient (Pat.) are shown. The corresponding percentages are indicated for each square.

Finally and strikingly, it was noticed when compared to cells from a healthy control that $CD3^+CD4^+$ and $CD3^+CD8^+$ primary T cells of the patient displayed reduced surface expression of the TCR co-receptors CD4 and CD8, respectively, while that of CD3 was unchanged (Fig. 25). This diminished expression was also observed in T cell blasts expanded *in vitro* from the patient's PBMCs for further biochemical analysis (Fig. 25).

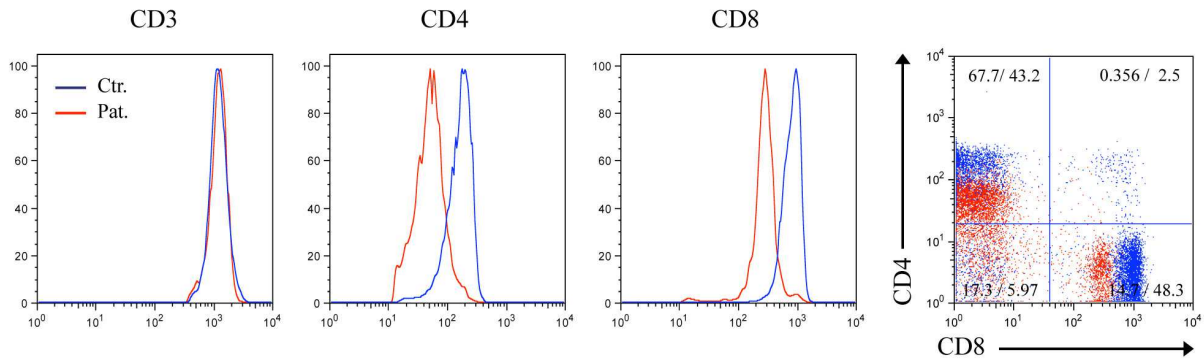

Figure 25. Expression of CD3, CD4 and CD8 on LCK-deficient PBMCs and T cell blasts.

Flow cytometric analyses of the expression of CD3, CD4 and CD8 on PBMCs (histograms) and T cell blasts expanded *in vitro* (dot plots) from a healthy control (Ctr. in blue) and the LCK-deficient patient (Pat. in red) after gating on TCRαβ$^+$CD3$^+$ cells (not shown). Histograms and dot plots for the control and the patient are superimposed and the corresponding percentages are indicated for each square.

In conclusion, the patient showed disturbed V(D)J-recombination and reduced thymic output as judged by oligoclonal αβ and altered γδ TCR repertoires and reduced numbers of CD4$^+$CD45RA$^+$CD31$^+$ recent thymic emigrants. The proportion of innate-like CD8α$^+$ γδ T cells was augmented and that of conventional αβ T cells was decreased, while there was overall CD4$^+$ and CD8$^+$ T cell lymphopenia. The remaining peripheral T cell populations displayed memory-like phenotypes more pronounced for the CD8$^+$ T_{Cyt} compartment, probably as a consequence of LIP and CD4$^+$ T_H were not able to provide adequate help towards B cells as judged by absent vaccination-induced specific antibody production. Most importantly, the αβ T cells had a CD4^{low} and CD8^{low} phenotype, that had been reported in the *Lck*$^{-/-}$ murine model.[456]

3.1.3 Gene defect

The clinical and immunological phenotype was indicative of a profound T cell immunodeficiency. Taking into account the reduced surface expression of CD4 and CD8, that had been reported for *Lck*$^{-/-}$ mice, and the predominat CD4$^+$ T cell lymphopenia, that had been reported in an infant with SCID and disturbed LCK-expression, LCK-deficiency seemed possible.[456, 457]

Genomic DNA was isolated from PBMCs and fibroblasts from the patient and her parents and from amniotic fluid cells from the fetus sibling and the exons 2-14 including the flanking intronic regions of *LCK* (NM_001042771.1) were Sanger-sequenced (for primer information see Tab. 5).

PBMCs and fibroblasts of the patient were found to carry the mono- or homozygous nucleotide transition *LCK* c.1022T>C in thecoding exon 9. The patient's mother was found to be heterozygous while the father and the fetus sibling did not carry the transition (Fig. 26A). As the mono- or heterozygous transition was found in PBMCs and fibroblasts of the patient, an additional somatic mutagenesis confined to the haematopoïetic lineage was excluded.

Table 5. Genomic *LCK* sequencing primers.

Primer name	Primer sequence
Forward primer exons 2, 3, 4	5'-GTTTGCCCATCCCAGGTGGGAGGGTGG-3'
Reverse primer exons 2, 3, 4	5'-CAGGGATCCGCAGGCCTTGTCTTTCAG-3'
Forward primer exons 5, 6	5'-ACTGGTTACCTACGAAGGCTCCAATCC-3'
Reverse primer exons 5, 6	5'-GGAGCTGCCGCTCCGCGTCCTTGCGGC-3'
Forward primer exons 7, 8	5'-AGATCCGACGACAGCCGACGGCCTTCG-3'
Reverse primer exons 7, 8	5'-GGGAGATAGGCTGATAGGGCACGGGGG-3'
Forward primer exons 9, 10	5'-TCGAATCACTTTTCCCGGCCTGCATGA-3'
Reverse primer exons 9, 10	5'-AGCAGGGAGAGCAGTATCCCCTGGTAG-3'
Forward primer exons 11, 12, 13	5'-CTCCCCCTGGGGCAACTTGGGCCAGCA-3'
Reverse primer exons 11, 12, 13	5'-GACTTGCCCTTCCCATCACCCTTTCAG-3'
Forward primer exon 14	5'-GGCTTCCAGTGCCTGACCTTGATGTCC-3'
Reverse primer exon 14	5'-TCAGGCTGGAGAGAAAGGGGGAGAACC-3'

To further investigate the genetic mechanism leading to mono- or homozygosity of *LCK* c.1022T>C in the patient, her chromosome 1 was analysed by single nucleotide polymorphism (SNP)-chip and array-comparative genomic hybridization (array-CGH) with a resolution of 200 bp.[458] The patient was found to have two identical copies of the entire chromosome 1 that were both carrying the *LCK* c.1022T>C transition found in one maternal allele and therefore demonstrating a complete maternal uniparental isodisomy (UPD) (Fig. 26C).

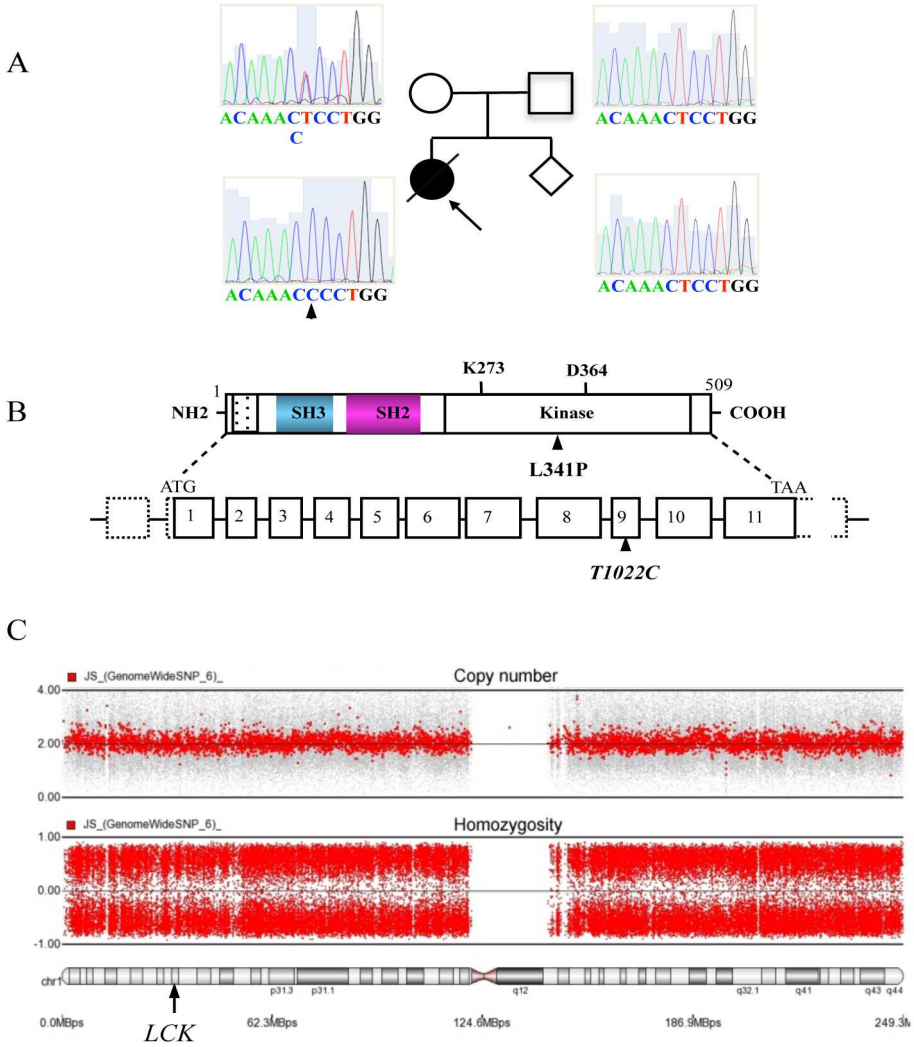

Figure 26. Genetic analysis of the LCK-deficient patient and her family.

(A) The pedigree and the corresponding electropherograms obtained by sequencing of genomic *LCK* of the index patient's (arrow) family are shown The LCK-deficient and deceased patient (black circle dashed with a diagonal line), her mother (white circle), father (white square) and unborn sibling (white diamond) are homozygous (arrowhead) or heterozygous for the *LCK* c.1022T>C transition or homozygous for the *LCK* wildtype, respectively.

(B) The domain structure of the LCK protein and the exon organization of its genomic locus are shown. The N-terminal (NH2) spotted box corresponds to the CD4 and CD8 binding region and the SH2, SH3 and the C-terminal (COOH) kinase domains are indicated by blue, purple or white boxes, respectively. The ATP-binding K273, the proton acceptor D364 and the p.L341P substitution (upper arrowhead) are indicated (not drawn to scale). Protein coding exons (1-11) and non-coding exons are represented by solid or spotted boxes, respectively, and the c.1022T>C transition in coding exon 9 is indicated (lower arrowhead, not drawn to scale).

(C) A scheme of chromosome 1 (lower graph) with the *LCK* locus at 1p34.3 indicated by an arrow is shown in comparison to the data obtained by array-CGH (upper graph) and SNP-chip (middel graph). Array-CGH shows a copy number of two and SNP-chip demonstrates homozygosity througout the entire chromosome 1. Each SNP analysed is represented by a red dot.

The *LCK* c.1022T>C translated into the amino acid substitution LCK p.L341P in the protein kinase domain (NP_001036236). This variation was not found in several databases (NCBI http://www.ncbi.nlm.nih.gov/, UCSC http://genome.ucsc.edu/, 1000 Genomes http://www.1000genomes.org/ and the NHLBI exome project http://www.nhlbi.nih.gov/resources/exome.htm). The LCK p.L341P substitution affected a phylogenetically conserved α-helix (aa 338-357) close to the active site D364 (UniProtKB P06239, Fig. 26B and 28A) and PolyPhen-2 analysis (http://genetics.bwh.harvard.edu/pph2/) predicted it to be probably damaging with a score of 0.995 (data not shown). *In silico* sequence alignment of the catalytic domain of LCK orthologs and additional members of the human tyrosine kinase superfamily showed that L341 occupied a highly conserved position at which hydrophobicity was maintained suggesting a crucial role in stabilizing the structure of the protein (Fig. 27 and 28). The three-dimensional LCK structure analysis confirmed that L341 belonged to a cluster of hydrophobic aa (L328, L336, L341, I433) making critical contacts especially to the lateral chain of I433 in the opposite α-helix and to L328 and L336 in its own α-helix (Fig. 28B). Thus, with the proline introducing a kink, the LCK p.L341P substitution was likely to disturb proper protein folding as it disrupted the three-dimensional secondary structure of its own α-helix and the local hydrogen bond network of the adjacent α-helices, necessary for the correct three-dimensional tertiary structure of LCK.

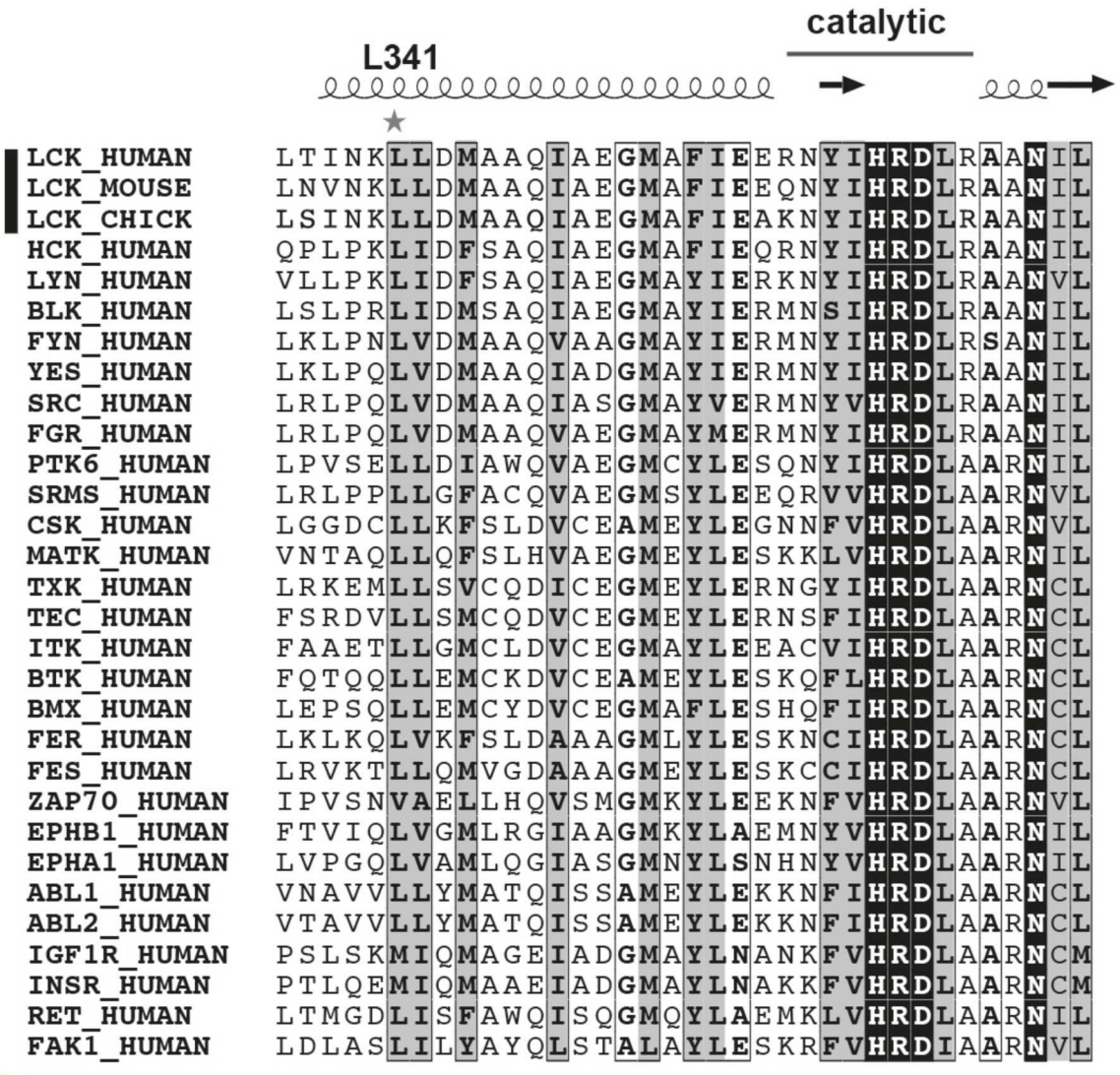

Figure 27. Sequence alignment of LCK orthologs and tyrosine kinase superfamily members.

The partial amino acid sequences of human LCK and its murine and chicken orthologs (black vertical beam) as well as that of additional human tyrosine kinase superfamily members are shown. The corresponding α-helical secondary structures and the catalytic region of the kinase domain are indicated above the alignment (not drawn to scale). The position of the substituted L341 is indicated by an grey asterisk. Conserved hydrophobic positions are shaded in grey and strictly conserved residues are given in white on black background.

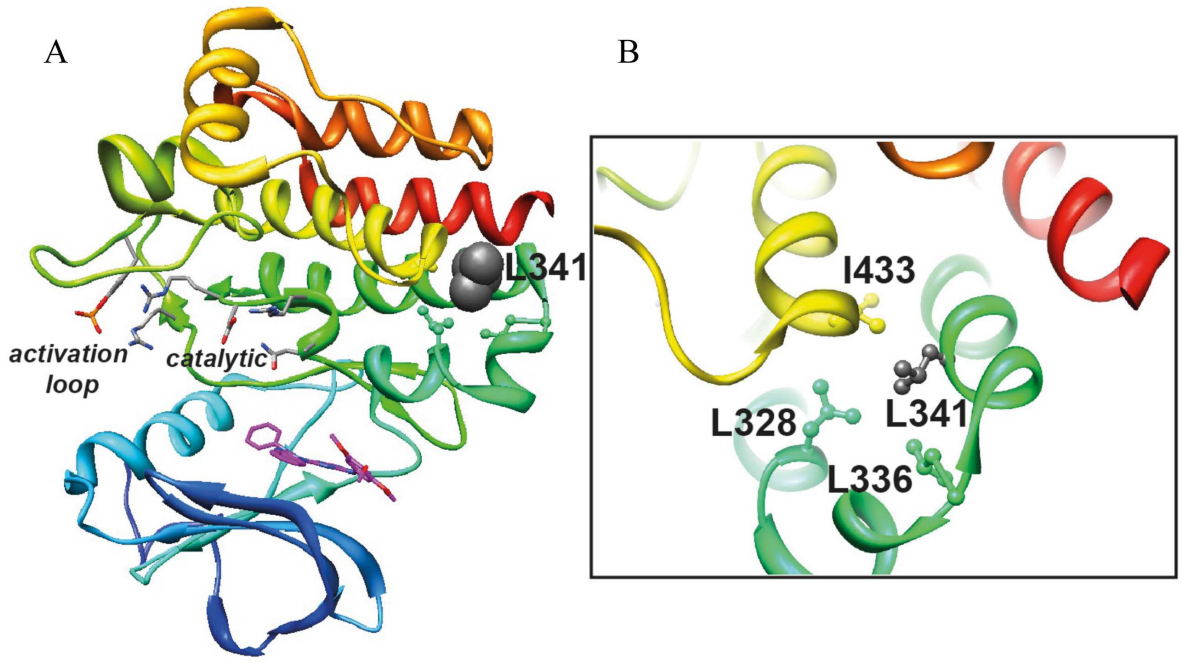

Figure 28. Three-dimensional LCK protein structure.

(A) Ribbon representation of the three-dimensional protein structure of human LCK (pdb identifier 3bym) highlighting the position of the substituted L341 (grey), the catalytic region and the activation loop.

(B) Focus on the cluster of hydrophobic aa (L328, L336, L341, I433) with the substituted L341 (grey) making critical contacts especially to the lateral chain of I433 in the opposite α-helix (yellow) and to L328 and L336 in its own α-helix (green).

To further analyse LCK protein expression and to perform biochemical assays, T cell blasts of the patient were expanded by stimulation with PMA and ionomycin to bypass the defect in TCR:CD3:ζ-mediated proliferation. Blasts were then stimulated with anti-CD3 antibodies cross-linked with rabbit anti-mouse Ig for 0, 5 and 10 minutes, lysed and immunoblots were performed on lysates following standard protocols. While PBMCs and T cell blasts of the control expressed the unmodified and post-translationally modified wildtype LCK protein migrating as a characteristic doublet at 56 and 60 kDa, respectively, PBMCs and T cell blasts of the patient expressed only residual amounts of the unmodified LCK p.L341P (Fig. 29 and for LCK expression in PBMCs Figure 3B in the JACI paper). However, the second SRC family kinase FYN, the SYK family kinase ZAP-70 and PLCγ-1, as well as the loading control actin were expressed in comparable amounts (Fig. 29)

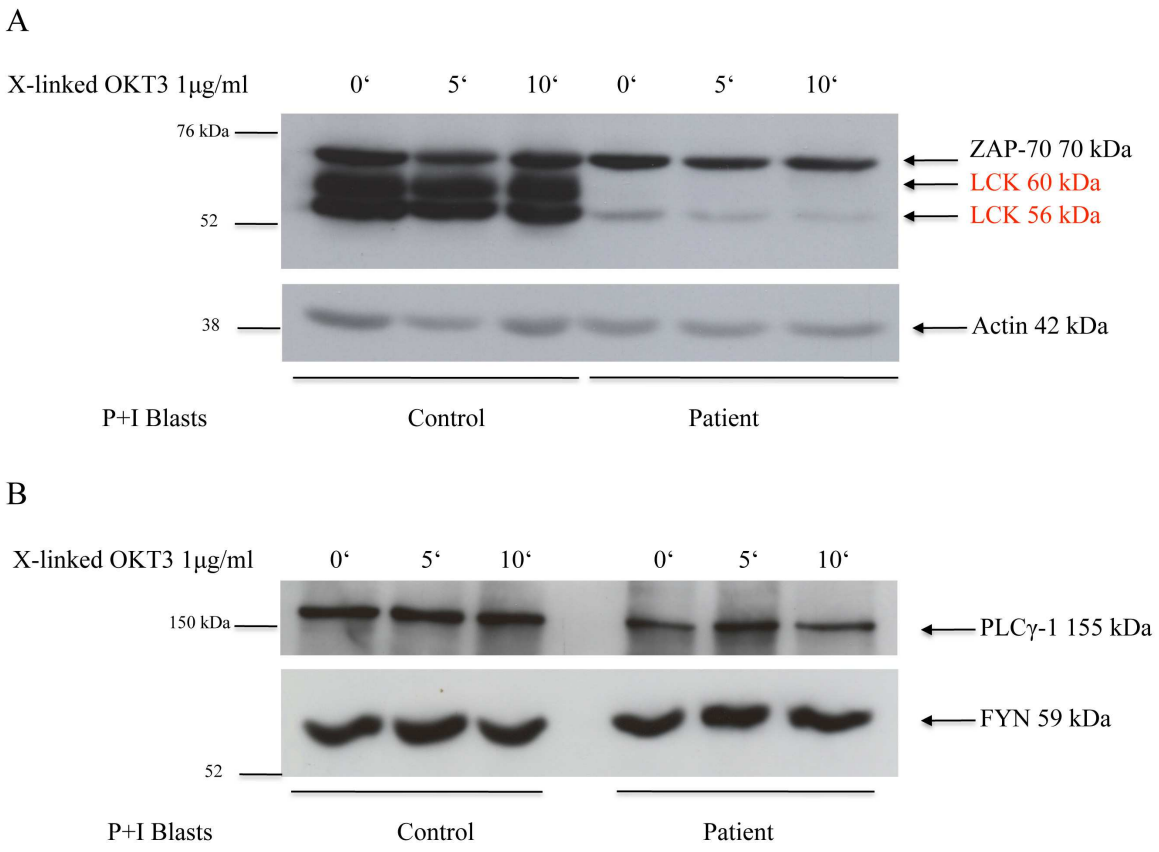

Figure 29. Expression of LCK p.L341P and other kinases in T cell blasts.

PMA and ionomycin-induced T cell blasts (P+I Blasts) of a healthy control and the patient were stimulated with cross-linked OKT3 (X-linked OKT3) for 0, 5, and 10 minutes and the expression of (A) LCK wildtype compared to LCK p.L341P, ZAP-70, the loading control actin, (B) PLCγ-1 and FYN were compared by immunoblotting. Molecular weight markers in kDa are given on the left (black lines) and names and molecular weights of specific bands are indicated on the right (black arrows). LCK 56 kDa and LCK 60 kDa correspond to the unmodified and post-translationally modified forms, respectively.

To further analyse the consequence of the LCK p.L341P substitution, a cDNA coding for LCK wildtype was cloned from a healthy control by RT-PCR and modified by PCR mutagenesis taking advantage of a primer pair designed to introduce the c.1022T>C transition. Additionally, the splice variant LCK ΔEx7 (Δaa 362-387, calculated molecular weight 52 kDA), that is lacking the coding exon 7 of the kinase domain (Fig. 26B) and that has been proposed to code for an unstable LCK protein, was cloned from a healthy control.[457, 459] The three cDNAs were verified by Sanger-sequencing, inserted into an eukaryotic expression vector and expressed in HEK 293T cells in the presence or not of the proteasome inhibitor MG132. Cells were thereafter lysed, and lysates subjected to immunoblotting. The monoclonal or the polyclonal LCK antibodies failed to detect specific material corresponding to LCK from lysates of cells transfected with the empty vector. In contrast, a specific doublet

characteristic for LCK was detected in lysates from cells expressing wild-type LCK, thus validating the experimental system. The upper band of the doublet corresponds to mature LCK protein that has been post-translationally modified.[102] Importantly, in lysates from cells expressing LCK p.L341P, both antibodies detected the lower band corresponding to unmodified LCK while the post-translationally modified band was virtually absent. Additionally, the polyclonal LCK antibody detected a pattern of specific bands in the LCK ΔEx7 protein lysats resembling that of LCK wildtype with the two major bands migrating at 52 and 55 kDa, respectively.

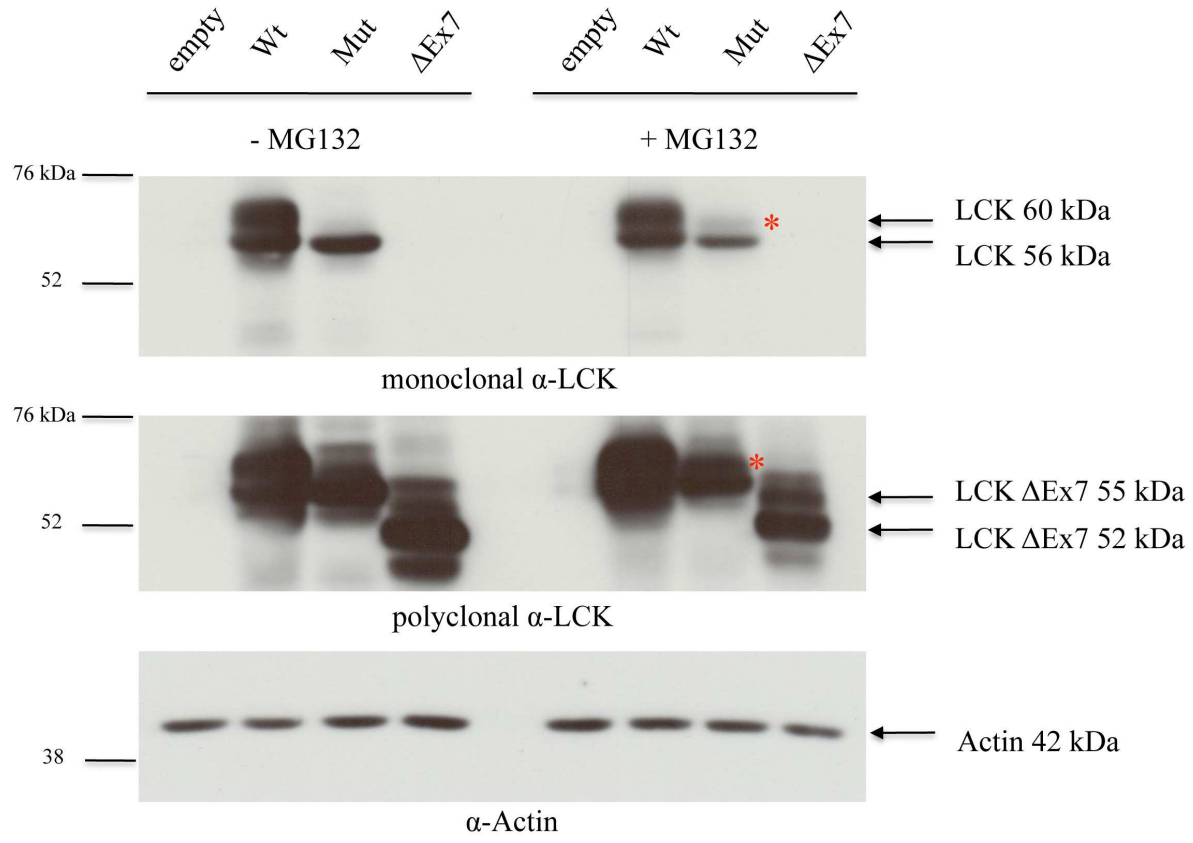

Figure 30. Transient expression of LCK variants in HEK 293T cells.

HEK 293T cells were transiently transfected with the expression plasmid pcDNA3.1 containing no insert (empty), LCK wildtype (Wt), LCK p.L341P (Mut) and LCK ΔEx7 (ΔEx7), respectively. Cells were left untreated (-MG132) or treated with 1 µM of the proteasome inhibitor MG132 (+MG132) for the last four hours of culture. Total protein lysats were subjected to SDS-PAGE and immunoblotting was performed with a monoclonal (monoclonal α-LCK) and a polyclonal (polyclonal α-LCK) antibody directed against LCK and an antibody against the loading control actin (α-Actin). The post-translationally modified LCK p.L341 relatively augmented after inhibiting proteasomal degradation is highlighted by a red asterisk. Molecular weight markers in kDa are given on the left (black lines) and names and molecular weights of specific bands are indicated on the right (black arrows).

However, the monoclonal LCK antibody produced by immunizing mice with a GST-LCK fusion protein containing aa 1-234 (see product information http://www.cellsignal.com/pdf/2657.pdf), did not detect these bands. Interestingly, when blocking proteasomal degradation with MG132 the expression of the post-translationally modified LCK p.L341P was discretely augmented (Fig. 30).This data indicated that *LCK* c.1022T>C could be considered a missense mutation and that LCK p.L341P was instable and likely degraded before post-translational modification, partially by the proteasomal pathway. Additionally, these experiments showed that LCK ΔEx7 could give rise to a stable protein that displayed the same migratory profile than the unmodified and the post-translationally modified wild-type LCK.

In order to analyse whether LCK p.L341P and LCK ΔEx7 were endowed with kinase activity, lysates from cells transfected with empty vector, LCK wildtype, LCK p.L341P and LCK ΔEx7 were immunoprecipitated with the polyclonal LCK antibody Next, input control lysates and immune complexes were incubated at room temperature in kinase assay buffer with or without the kinase substrate ATP. Samples were split in two, and LCK protein and tyrosine phosphorylated products, i.e. autophosphorylated LCK and random substrates phosphorylated *in trans*, were detected by immunoblotting with a polyclonal LCK antibody (expression control, data not shown) and a mAb directed against phosphorylated tyrosine residues. In lysates from cells with empty vector, almost no kinase activity was detectable in the total lysates or in immune complexes with polyclonal LCK antibody. In contrast, lysates and LCK immune complexes from cells expressing LCK wildtype displayed a strong *in cis* and *in trans* kinase activity that could be further augmented by the addition of ATP. However, lysates and LCK immune complexes from cells expressing LCK p.L341P or LCK ΔEx7 did not show kinase activity with or without ATP similarly to lysates from cells expressing the empty vector (Fig. 31). Thus functionally, LCK p.L341P can be considered as a kinase-dead mutation and LCK ΔEx7 a kinase-less protein isoform.

To rule out that the observed kinase-dead feature of the LCK p.L341P protein was an effect of protein misloading, the immune complex kinase assay was repeated with total protein titration series. Before immunoprecipitation all samples were adjusted with empty vector protein lysates to an equal total protein amount and kinase assays and immunoblotting were performed as described before. Even though comparable amounts of LCK wildtype and LCK p.L341P could be precipitated in these conditions, there was no detectable kinase activity in immune complexes of LCK p.L341P independently of the precipitated amount of protein (Fig. 32), thus further proving that LCK p.L341P is kinase-dead.

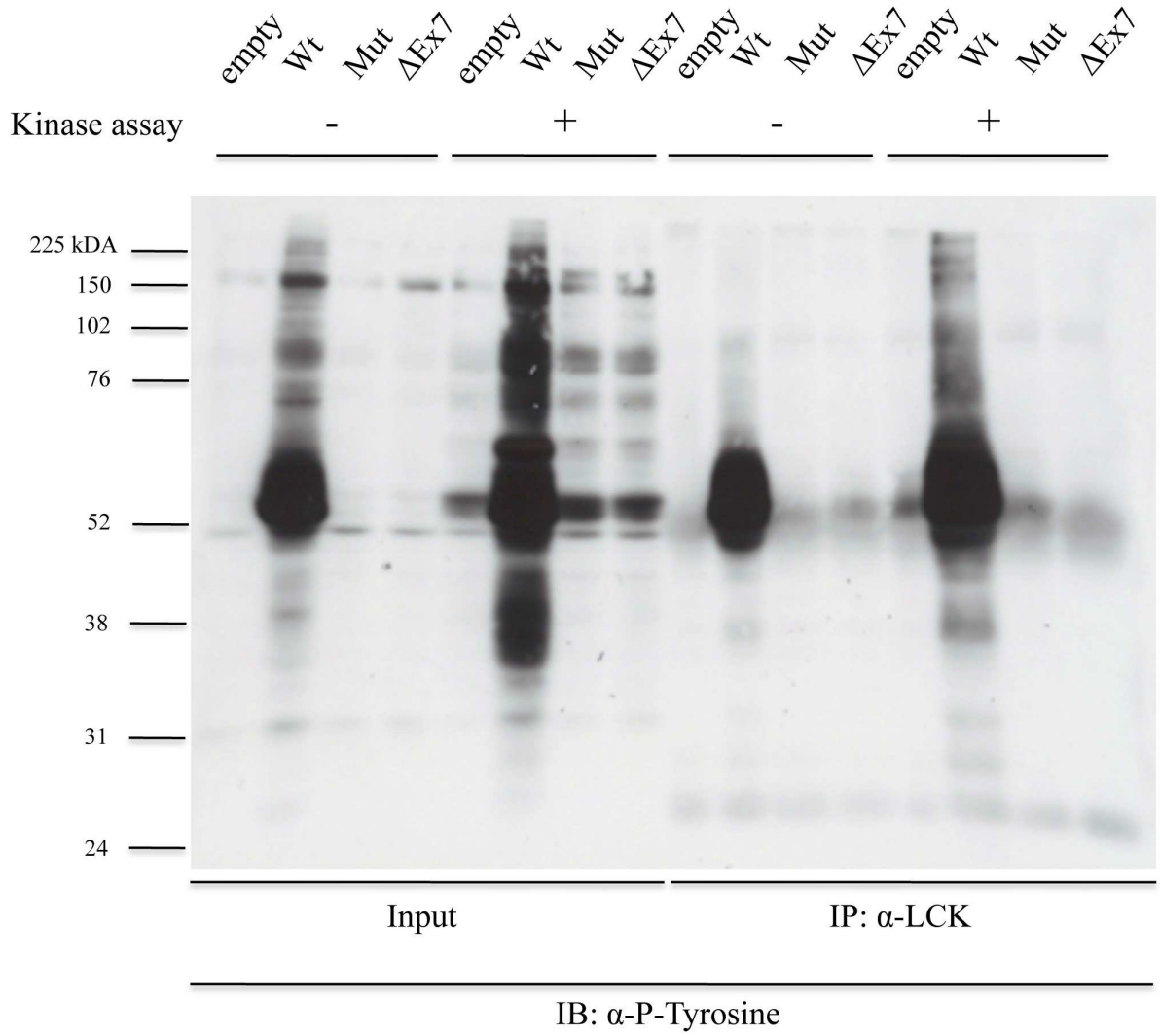

Figure 31. Kinase activity of LCK variants.

HEK 293T cells were transiently transfected with the expression plasmid pcDNA3.1 containing no insert (empty), LCK wildtype (Wt), LCK p.L341P (Mut) and LCK ΔEx7 (ΔEx7), respectively. 1 mg of total protein lysat was subjected to immunoprecipitation with 5 µg of polyclonal LCK antibody and thereafte 100 µg of total protein lysat (input) or LCK immune complexes (IP: α-LCK) were incubated in kinase assay buffer without (Kinase assay -) or with 100 µM ATP (Kinase assay +) for five minutes at room temperature. Samples were analysed by SDS-PAGE and immunoblotting with a mAb directed aginst phosphorylated tyrosine residues (IB: α-P-Tyrosine). Molecular weight markers in kDa are given on the left (black lines).

We also observed a pattern reminiscent of polyubiquitination in the kinase assays that was much more pronounced with LCK p.L341P immune complexes than with LCK wildtype (Fig. 32 upper panel). To prove that LCK p.L341P was preferentially ubiquitinated, the immunoblot was stripped and reprobed with a mAb directed against ubiquitin (#3936, Cell Signaling Technology). Indeed, immunoprecipitated LCK p.L341P was found to be much more ubiquitinated than LCK wildtype (data not shown).

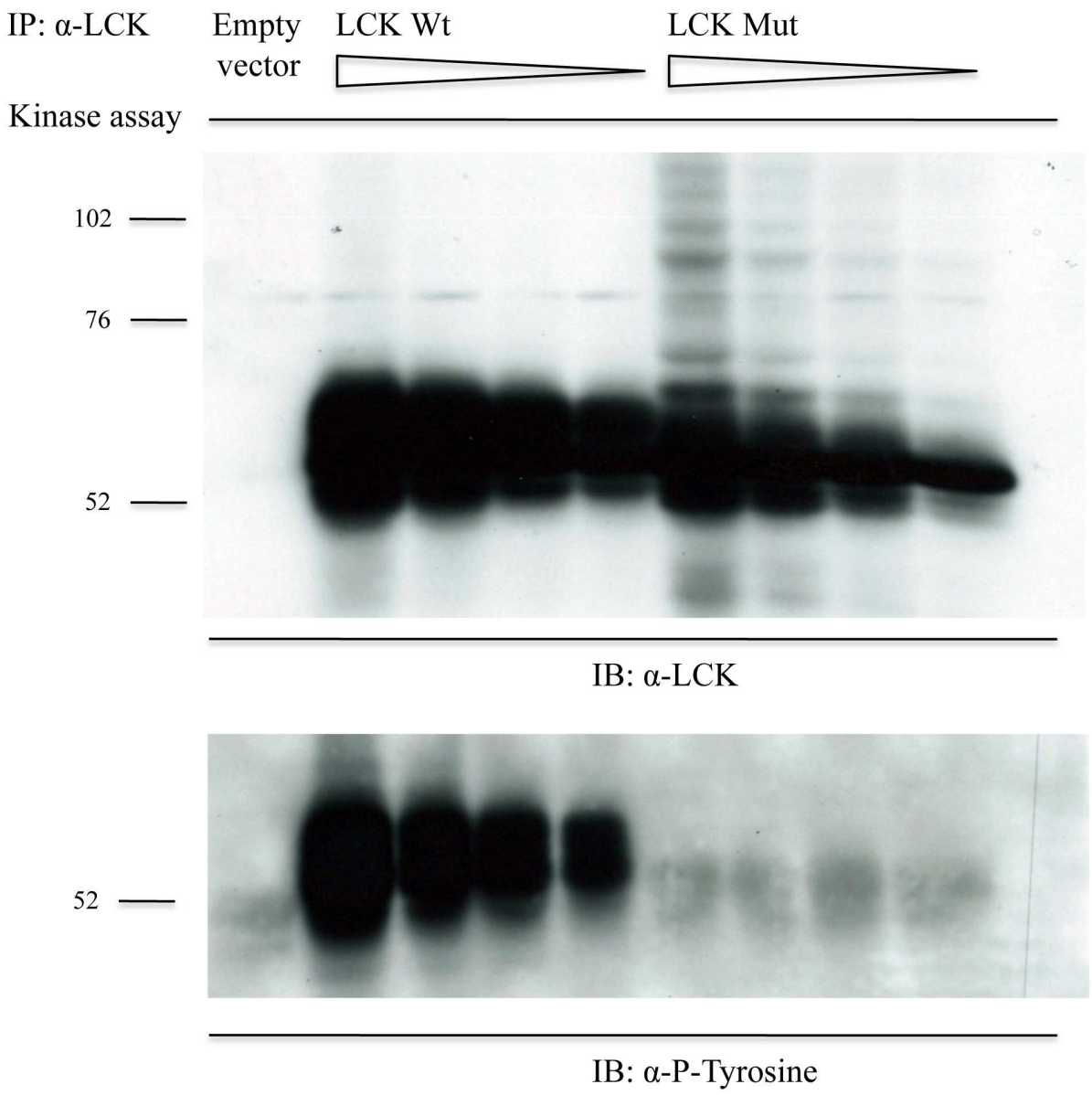

Figure 32. Kinase activity of titrated LCK variants.

HEK 293T cells were transiently transfected with the expression plasmid pcDNA3.1 containing no insert (empty), LCK wildtype (Wt) and LCK p.L341P (Mut), respectively. Different quantities of total protein lysat, i.e. 2.0 mg of empty vector, 1 / 0.5 / 0.25 / 0.125 mg of LCK wildtype and 2.0 / 1.0 / 0.5 / 0.25 mg of LCK p.L341P were adjusted to the final protein concentration of 2 mg with empty vector protein lysats and subjected to immunoprecipitation with 5 µg of polyclonal LCK antibody. LCK immune complexes were incubated in kinase assay buffer with 100 µM ATP (kinase assay) for five minutes at room temperature. Samples were split in two and analysed by SDS-PAGE and immunoblotting with a pAb against LCK (IB: α-LCK) and a mAb against phosphorylated tyrosine residues (IB: α-P-Tyrosine). Molecular weight markers in kDa are given on the left (black lines).

Together these data show that the LCK c.1022T>C mutation leads to the expression of an immature, instable LCK p.L341P protein lacking kinase activity, that is likely targeted to

the proteasome via ubiquitination and subsequently degraded. Furthermore, the LCK ΔEx7 protein is stable and may represent a LCK kinase-less protein isoform with a physiological function, as it is expressed in healthy donors, where it was cloned from.

3.1.4 Analysis of TCR:CD3:ζ-signalling in LCK-deficiency

In order to characterize the consequence of the LCK p.L341P mutation on proximal TCR:CD3:ζ-signalling, protein lysates from PMA and ionomycin induced T cell blasts stimulated with anti-CD3 antibodies for 0, 5 and 10 minutes were analysed for their contents of tyrosine phosphorylated proteins by SDS-PAGE and immunoblotting with a mAb directed against phosphorylated tyrosine residues. While TCR:CD3:ζ-signalling in T cell blasts of a healthy control resulted in a strong protein tyrosine phosphorylation, T cell blasts of the LCK-deficient patient displayed only a residual signal. Especially, the signal intensity of bands corresponding to known TCR:CD3:ζ-signalling substrates such as the ζ-chain itself, ZAP-70, LAT, SLP-76 and PLCγ-1 was reduced while that of the band corresponding to the negative regulator CBL was increased. Total protein load was checked with immunoblotting for actin and found to be comparable (Fig. 33). As shown before, defective tyrosine phosphorylation could not be explained by decreased expression of other kinases or substrates such as FYN, ZAP-70 and PLCγ-1 and was therefore related to the LCK p.L341P expressed in the cells of the LCK-deficient patient (Fig. 29).

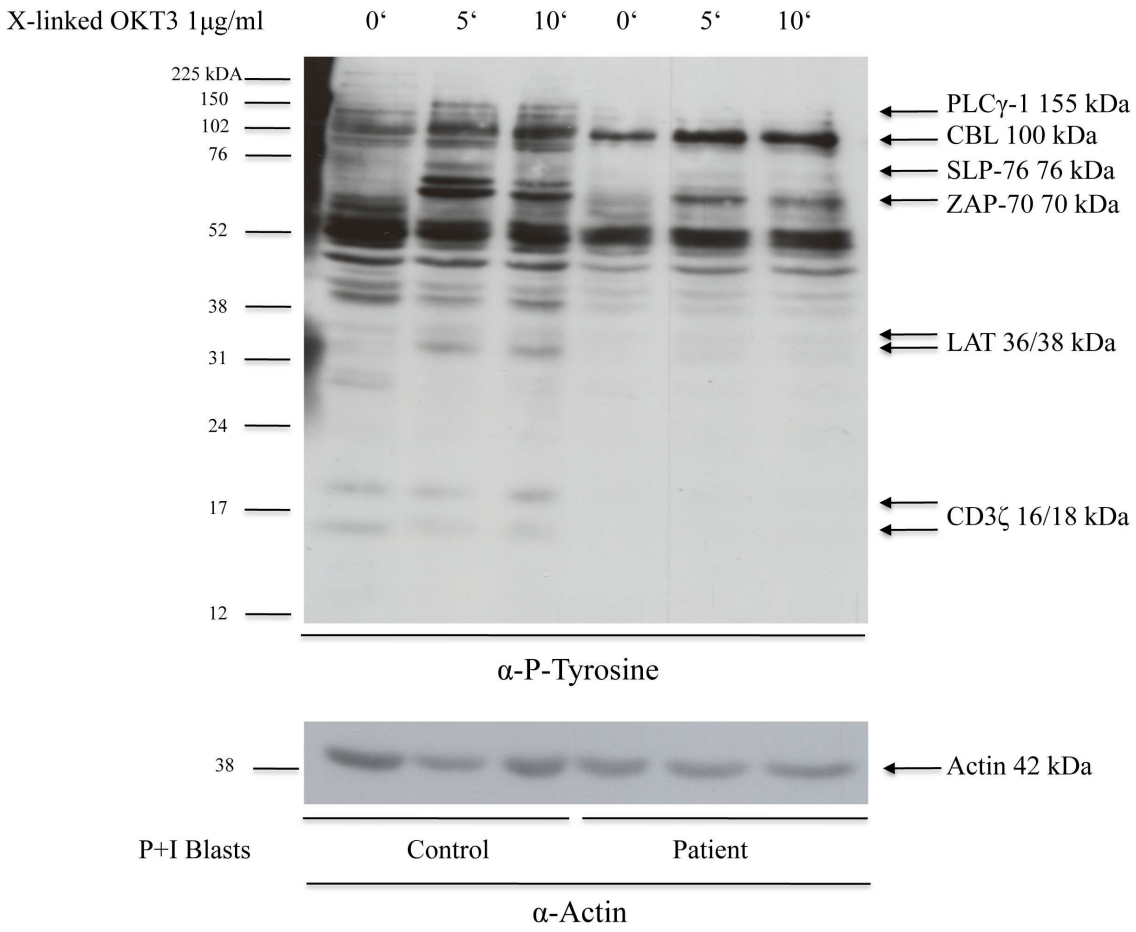

Figure 33. Impaired protein tyrosine phosphorylation in LCK-deficient T cell blasts.

T cell blasts of a control and the LCK-deficient patient induced with PMA 20 ng/ml and ionomycin 1 µM (P+I Blasts) were stimulated with OKT3 1 µg/ml and cross-linked with polyclonal rabbit anti-mouse Ig 2 µg/ml for 0, 5 and 10 minutes. Total protein was extracted by TNE lysis buffer, separated by SDS-PAGE and immunoblotting with a mAb against phosphorylated tyrosine residues (α-P-Tyrosine) and the loading control actin (α-Actin) was performed. Molecular weight markers in kDa are given on the left (black lines) and names and molecular weights of specific bands are indicated on the right (black arrows).

Next TCR:CD3:ζ-induced Ca^{2+}-flux in PBMCs and T cell blasts was analysed by flow cytometry and fluorescence imaging, respectively. Stimulation with anti-CD3 mAbs induced no Ca^{2+}-flux neither in *ex vivo* $CD3^+CD4^+$ T_H and $CD3^+CD8^+$ T_{Cyt} nor in *in vitro* expanded T cell blasts of the LCK-deficient patient, whereas it resulted in Ca^{2+}-flux in the corresponding cell populations of a healthy donor. Stimulation with ionomycin and thapsigargin, respectively, resulted in strong Ca^{2+}-flux in all analysed cell populations, serving as positive control for proper loading of cells with the fluorescent reporter and cell viability (Fig. 34). Thus, LCK p.L341P has lost the capacity to transduce signals required for Ca^{2+}-flux in response to TCR:CD3:ζ stimulation.

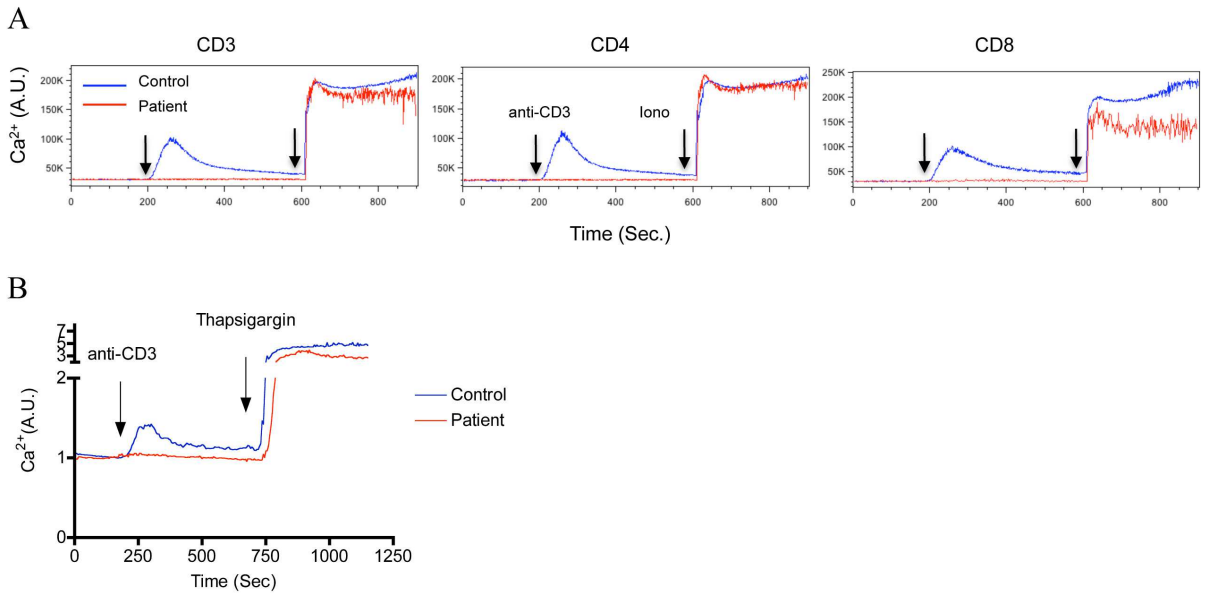

Figure 34. Impaired Ca^{2+}-flux in LCK-deficient primary T cells and T cell blasts.

(A) Primary T cells of a control (blue) and the LCK-deficient patient (red) were stained with anti-CD3, anti-CD4 and anti-CD8 and charged with 5 µM of the Ca^{2+}-sensitive fluorescent dye Indo-1-acetoxymethyl ester. Ca^{2+}-flux was analysed with a FACS Vantage Diva for two minutes, than PBMCs were stimulated with 0.125 µg/ml OKT3 cross-linked with 10 µg/ml rabbit-anti-mouse-IgG (anti-CD3) for eight minutes and finally stimulated with 1 µM ionomycin (iono) (vertical arrowa). Ca^{2+}-flux was calculated and expressed in arbitrary units (A.U.).
(B) T cell blasts of a control (blue) and the LCK-deficient patient (red) were charged with 1 µM of the Ca^{2+}-sensitive fluorescent dye Fura-2-acetoxymethyl ester. Ca^{2+}-flux was analysed with a Nikon Diaphot 300 microscope and an IMSTAR imaging system for four minutes and PBMCs were than stimulated with 10 µg/ml UCHT-1 (anti-CD3) for eight minutes and finally stimulated with 500 nm thapsigargin (vertical arrows). 50 T cell blasts of the control and 23 of the patient were analysed and arbitrary units of Ca^{2+}-flux were plotted against time. Ca^{2+}-flux was calculated and expressed in arbitrary units (A.U.).

To analyse TCR:CD3:ζ-signalling events downstream of ITAM-phosphorylation and Ca^{2+}-flux, the immunoblots for LCK and phosphorylated tyrosine residues were stripped and reprobed with mAbs against phosphorylated ERK-1/2 and against phosphorylated IκBα. While in T cell blasts of a healthy control, phosphorylation of ERK-1/2 and IκBα was strongly increased upon CD3 stimulation, in the cells of the LCK-deficient patient only residual phosphorylation of ERK-1/2 and no phosphorylation of IκBα was detected (Fig. 35). Thus, the LCK p.L341P mutation infereed with TCR:CD3:ζ-downstream signalling events such as MAPK-and NF-κB-signalling.

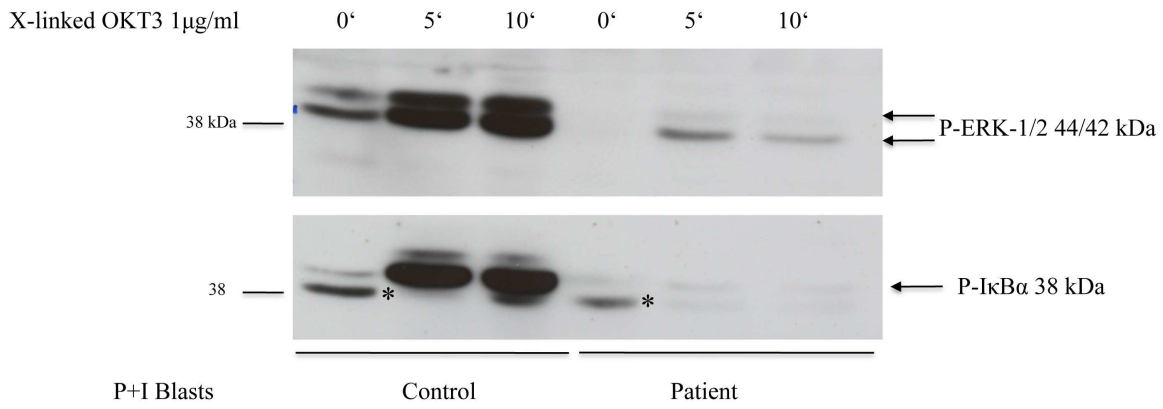

Figure 35. Disturbed downstream signalling in LCK-deficient T cell blasts.

The membranes of the immunoblots for LCK (Fig. 29) and phosphorylated tyrosine residues (Fig. 33) were reprobed with mAbs against phosphorylated ERK-1/2 (P-ERK-1/2) and phosphorylated IκBα (P-IκBα). Molecular weight markers in kDa are given on the left (black lines), names and molecular weights of specific bands are indicated on the right (black arrows) and residual bands that were not completely eliminated by stripping are marked with black asterisks.

Finally, activation-induced cell death (AICD) that is a functional T cell response depending on intact TCR:CD3:ζ-signalling was analysed. While αβ and γδ T cell blasts from a healthy donor performed AICD in response to TCR:CD3:ζ-signalling, cells of the LCK-deficient patient did not (Fig. 36), thus showing that the LCK p.L341P mutation hampered TCR:CD3:ζ-signalling induced functional T cell responses.

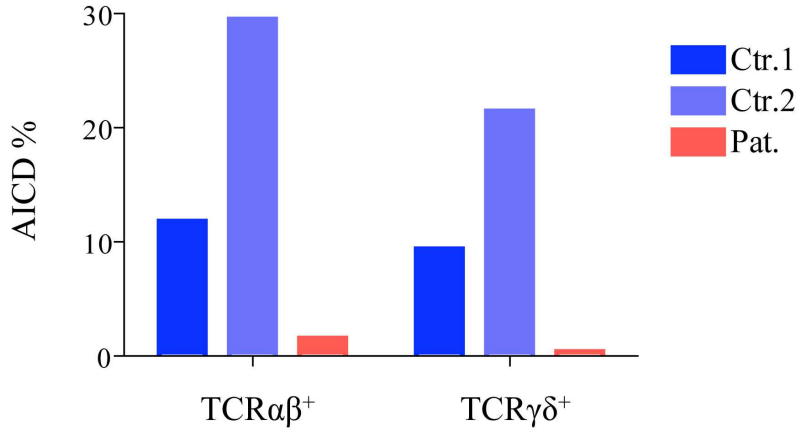

Figure 36. Disturbed AICD in LCK-deficient T cell blasts.

Duplicates of 10^5 T cell blasts of two healthy controls (blue) and the LCK-deficient patient (red) were incubated for 24 h in 48 flat bottom well plates coated with 10 µg/ml OKT3. Cells were recovered, stained with anti-CD3, anti-TCRαβ, anti-TCRγδ, Annexin V and 7-AAD and analysed on a FACSCanto II. Annexin V and 7-AAD positive cells were considered apoptotic and expressed as a percentage of the entire population, i.e. $TCR\alpha\beta^+$ and $TCR\gamma\delta^+$, respectively.

In summary, the LCK p.L341P mutation leads to disturbed TCR:CD3:ζ-signalling affecting protein tyrosine phosphorylation, Ca^{2+}-flux, MAPK- and NF-κB-signalling and overall TCR-dependent functions as illustrated by AICD, even though these results might be biased by the presence and accumulation of T_{EMRA} cells in the T cell blast expansion of the patient.

3.1.5 Complementation

Because no primary T cells of the LCK-deficient patient were available at that time point of the study any longer, indirect complementation experiments were carried out to confirm that LCK p.L341P accounted for the observed TCR:CD3:ζ-signalling defect observed.

To that end, LCK wildtype, LCK p.L341P and LCK ΔEx7 were subcloned into the bicistronic lentiviral expression vector pLenti7.1 (Invitrogen) encoding the green fluorescent protein (GFP) as a reporter and the inserts were verified by Sanger-sequencing. The LCK-deficient JCam1.6 T cell line, a derivative of the Jurkat T cell leukaemia cell line, that does not generate Ca^{2+}-flux after TCR:CD3:ζ-activation, was left untransduced or transduced with lentiviruses containing the empty vector, LCK wildtype, LCK p.L341P and LCK ΔEx7, respectively.[47] Transduction rates of ~ 15% were obtained as measured by GFP expression via flow cytometry and GFP^+ JCam1.6 were enriched by fluorescence-activated cell sorting (FACS) to an initial purity of ≥ 99 % (data not shown). Cells were expanded for further analysis and the percentages of GFP^+ cells in the expansions were determined. GFP^+ cells moderately declined in the cultures of JCam1.6 cells transduced with empty vector (93.5 %) and LCK p.L341P (97.2 %) while in those of LCK wildtype (82.3 %) and LCK ΔEx7 (70.7 %), the decrease was more pronounced probably due to a selective disadvantage (Fig. 37A and B). All cell lines expressed comparable amounts of FYN and actin and the Jurkat cells expressed high amounts of the unmodified and the post-translationally modified LCK and residual amounts of LCK ΔEx7. In contrast, untransduced and empty vector transduced JCam1.6 expressed residual amounts of the unmodified LCK and high amounts of LCK ΔEx7. JCam1.6 transduced with LCK wildtype, LKC p.L341P and LCK ΔEx7 expressed high amounts of LCK ΔEx7, high amounts of unmodified and of post-translationally modified LCK wildtype, high amounts of unmodified and residual amounts of post-translationally modified p.L341P LCK and residual amounts of unmodified LCK, respectively (Fig. 37C). However, JCam1.6 transduced with LCK ΔEx7 did not show overexpression of LCK ΔEx7 when compared to untransduced and empty vector transduced JCam1.6 cells.

Thus, the LCK-deficient JCam1.6 T cell line transduced with various LCK constructs could be used for further TCR:CD3:ζ-signalling studies, although LCK wildtype and LCK ΔEx7 seemingly infereed a selective disadvantage and transduced LCK ΔEx7 did not result in overexpression of LCK ΔEx7.

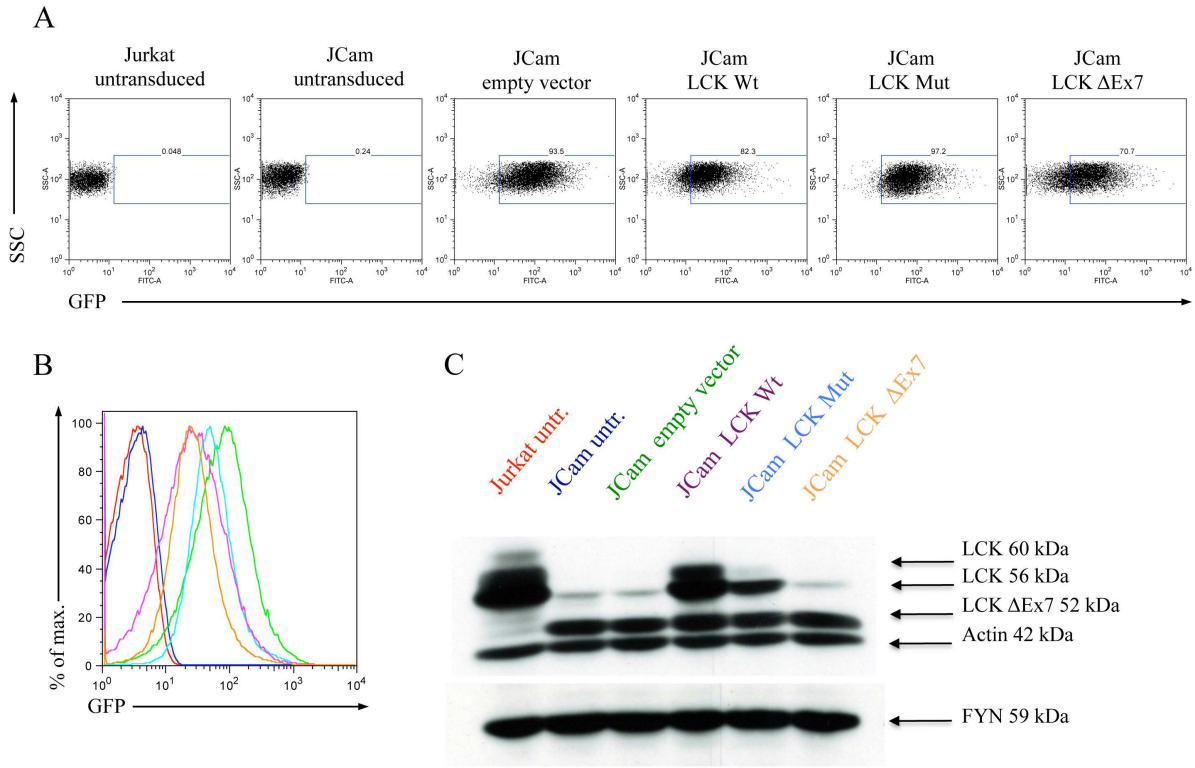

Figure 37. Expression of LCK variants in Jurkat and transduced JCam1.6 cells.

Jurkat (red) or JCam1.6 cells left untransduced (dark blue) or lentivirally transduced with empty vector (green), LCK wildtype (LCK Wt violet), LCK p.L341P (LCK Mut, light blue) and LCK ΔEx7 (orange) were analysed by flow cytometry and immunoblotting. (A) Dot blots of the various cell lines with gating on the GFP^+ fraction indicate the particular percentage (numbers are given above the gate) of transgene expressing cells after lentiviral transduction and FACS. (B) MFI of GFP is shown as a histogram and particular histograms are superimposed. (C) The expression of particular LCK forms in the untransduced or transduced cell lines is compared by immunoblotting with polyclonal antibodies directed against LCK, FYN and the loading control actin. Names and molecular weights of specific bands are indicated on the right (black arrows).

To assess the effect of the particular LCK transgenes, JCam1.6 transduced with the empty vector, LCK wildtype and LCK p.L341, respectively, were stimulated with anti-CD3 for variable time points, lysed and lysates were analysed by immunoblotting with the mAbs anti-phosphorylated tyrosine and anti-actin. Only JCam1.6. expressing LCK wildtype were able to phosphorylate known TCR:CD3:ζ-signalling substrates such as the ζ-chain, LCK itself, ZAP-70, LAT, SLP-76 and PLCγ-1, while JCam1.6 transduced with empty vector or LCK p.L341P were not able to do so (Fig. 38).

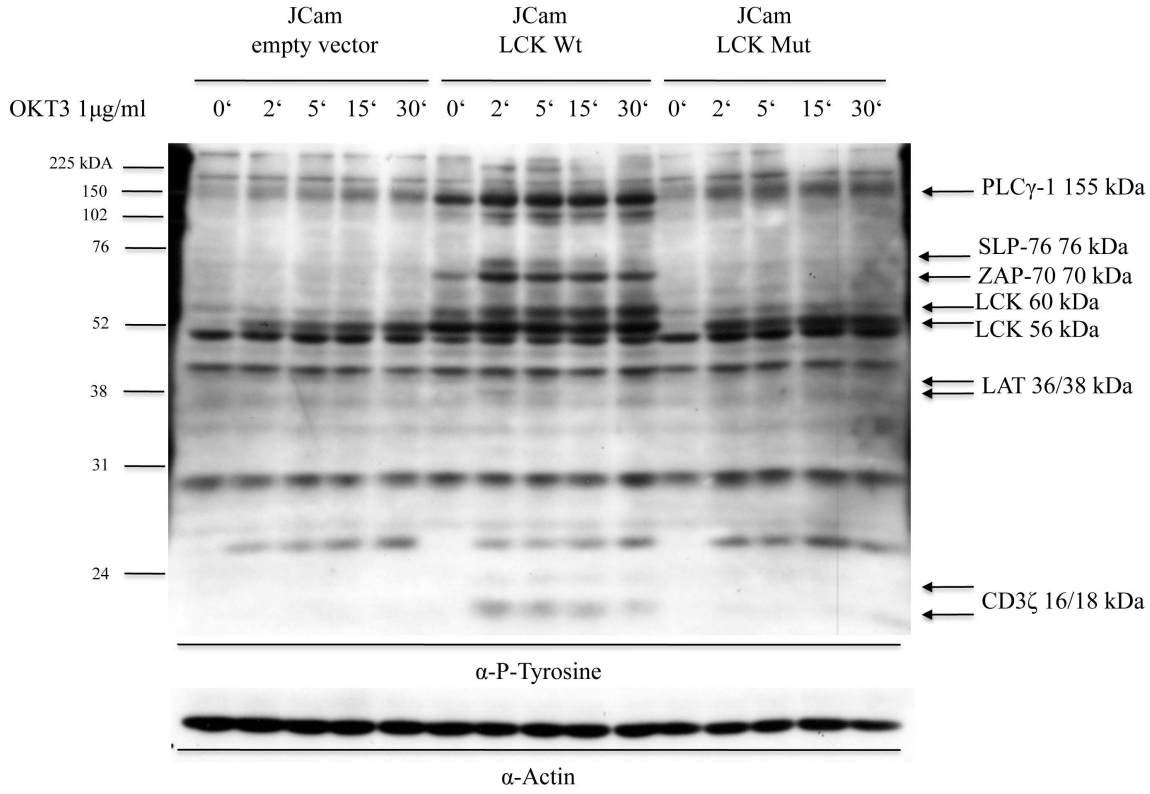

Figure 38. Complementation of protein tyrosine phosphorylation in JCam1.6 cells.

JCam1.6 transduced with empty vector, LCK wildtype (LCK Wt) and LCK p.L341P (LCK Mut) were stimulated with OKT3 1 µg/ml for the indicated time points (minutes). Protein lysats were separated by SDS-PAGE and immunoblotting with mAbs against phosphorylated tyrosine residues (α-P-Tyrosine) and the loading control actin (α-Actin) was performed. Molecular weight markers in kDa are given on the left (black lines) and names and molecular weights of specific bands are indicated on the right (black arrows).

Additionally, the capacity to generate Ca^{2+}-flux in response to TCR:CD3:ζ-signalling was tested in JCam1.6 transduced with empy vector, LCK wildtype, LCK p.L341P and LCK ΔEx7 by spectrofluorimetry. Only JCam1.6 cells transduced with LCK wildtype but not the ones transduced with empty vector, LCK p.L341P and LCK ΔEx7 displayed Ca^{2+}-flux after TCR:CD3:ζ-activation. Stimulation with ionomycin resulted in strong Ca^{2+}-flux in all analysed cell populations, serving as positive control for proper loading with the fluorescent reporter and cell viability (Fig. 39).

We therefore conclude, that the TCR:CD3:ζ-signalling defect observed in the LCK-deficient patient's T cells is indeed caused by LCK p.L341P that has no capacity to transduce signals from the TCR:CD3:ζ-complex. LCK ΔEx7 that is strongly expressed in the JCam1.6 but not in the parental Jurkat cell line is also unable to transduce signals and seems to exert a

selective disadvantage in the retroviral overexpression setting. Thus, LCK ΔEx7 might have a role as a negative regulator of TCR:CD3:ζ-signalling.

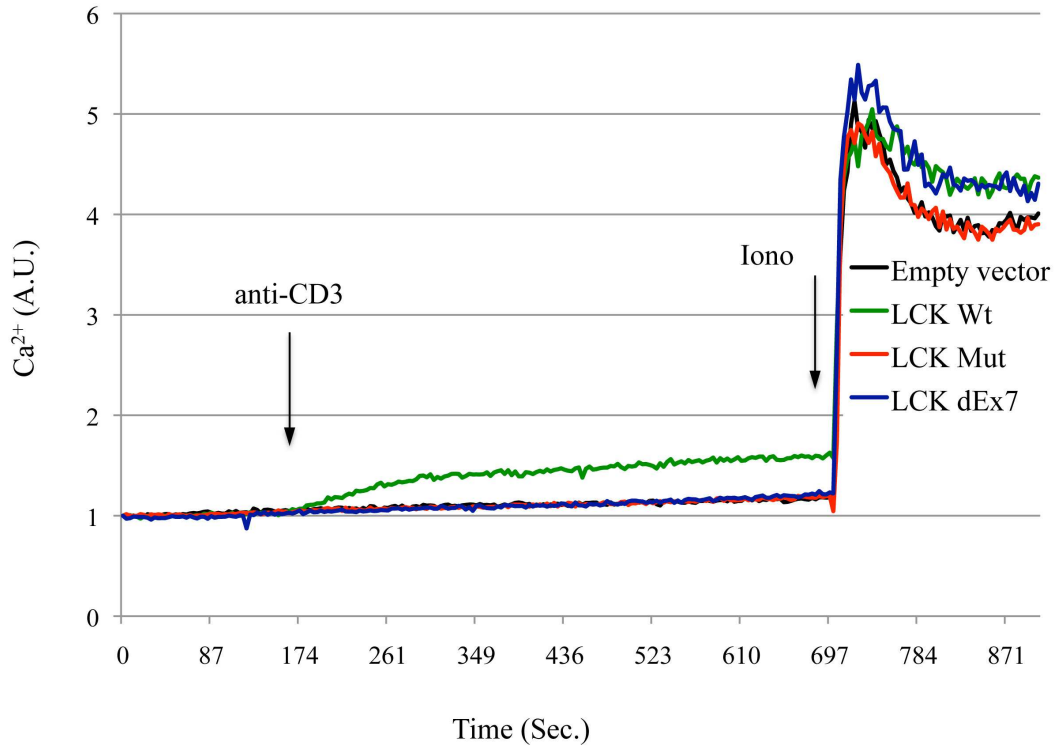

Figure 39. Complementation of Ca^{2+}-flux in JCam1.6 cells.

JCam1.6 transduced with empty vector (black), LCK wildtype (LCK Wt, green), LCK p.L341P (LCK Mut, red) and LCK ΔEx7 (blue) were charged with 1 µM of the Ca^{2+}-sensitive fluorescent dye Fura-2-acetoxymethyl ester and analysed with a Varian Cary Eclipse spectrometer. Cells were left unstimulated for three minutes and than stimulated with 10 µg/ml of the anti-CD3 antibody UCHT-1 (anti-CD3) for eight minutes and finally with 1 µM ionomycin (Iono) (vertical arrows). Ca^{2+}-flux was calculated and expressed in arbitrary units (A.U.).

3.2 Identification of a novel null mutation in *ZAP-70* causing SCID

3.2.1 Clinical phenotype

The patient was born with a moderate intrauterine growth retardation at term to first-degree consanguineous Kurdish cousins that had migrated to France. At the age of eleven days he was hospitalized for five days with a severe bronchiolitis caused by human *respiratory syncytial virus* (RSV). He thereafter received one 7-valent conjugate vaccine against *Streptococcus pneumoniae* and two 5-valent vaccines against *Haemophilus influenzae type b*, the toxoïd of *Corynebacterium diphtheriae*, *Bordetella pertussis*, the toxoïd of *Clostridium tetani* and *Poliovirus type 1, 2 and 3* without adverse events.

At five months of age, he developed diffuse and consecutively superinfected cutaneous *varizella zoster virus* (VZV) infection, accompanied by an undocumented acute gastroenteritis. He was hospitalized for seven days and treated with intravenous anti-viral and anti-bacterial drugs leading to symptom reduction. Five days later, he was hospitalized again as the cutaneous efflorescences reaggravated and a second acute gastroenteritis caused by *rotavirus* took place. During the next two days, he degraded into acute respiratory distress syndrome and had to be ventilated mechanically for 26 days while producing multiple pneumatothoraces. Peripheral blood (VZV DNA > 10^5/ml) and bronchoalveolar lavage were tested positive for VZV, thus establishing the diagnosis of systemic VZV infection with severe VZV pneumonitis. Consecutively and besides intensive anti-viral and anti-bacterial treatment, pulmonary disease was complicated by additional infections with the opportunistic fungus *Pneumocystis jirovecii* and the opportunistic bacterium *Stenotrophomonas maltophilia*. Additionally, VZV skin lesions remained florid for about four weeks and were superinfected with *Staphylococcus aureus*. Peripheral VZV count fluctuated ~ 10^3/ml and became negative at nine months of age under continuous anti-viral treatment.

At seven months, he developed a central line-associated sepsis caused by *Staphylococcus aureus* that could be controlled by catheter-explantation and anti-bacterial treatment.

At nine months, he was conditioned with busulfane, fludarabine and anti-thymocyte globuline and developed a grade IV mucositis. He underwent allogeneïc HSCTx from a phenotypically matched (10 out of 10) unrelated donor with a dosage of 15.5 x 10^6 $CD34^+$ PBMCs per kg bodyweight. From day eight he developed a skin graft-versus-host disease grade III that was controlled with immunosuppressive drugs. Since he gradually recovered and now is fine and well presenting a donor chimerism of 98%.

Taken as a whole, the patient presented the clinical picture of SCID characterized by severe and life-threatening bacterial, viral and fungal infections.

3.2.2 Immunological phenotype

Immunological investigations at the age of seven months are summarized in Tab. 6. PBMCs of a healthy control and the patient were analysed for the different lymphocyte populations by flow cytometry on a FACSCanto II and data was processed with FlowJo software as described in paragraphe 3.1.2.

Table 6. Immunological features of the ZAP-70-deficient patient.

	7 months
Lymphocytes (3,400-9,000/µl)[1]	7,200
T cells (/µl)	
$CD3^+$ (1,900-5,900)	4,464
$CD4^+$ (1,400-4,300)	4,248
$CD8^+$ (500-1,700)	72
T cells (%)	
$TCR\alpha\beta^+$ cells (90-100)	96
$TCR\gamma\delta^+$ cells (0-10)	3
$CD4^+CD45RA^+CD31^+$ (recent thymic emigrants) (60-71)	12
$CD4^+CD45RA^+$ (64-93)	31
$CD4^+CD45R0^+$ (6-25)	68
$CD8^+CD45RA^+CCR7^+$ (52-68)	4
$CD8^+CD45RA^-CCR7^+$ (3-4)	1
$CD8^+CD45RA^-CCR7^-$ (11-22)	53
$CD8^+CD45RA^+CCR7^-$ (16-28)	43
T cell proliferation (cpm x 10^3)	
PHA (6.25 µg/ml) (>50)	0.85
OKT3 (50 ng/ml) (>30)	0.25
Tetanus toxoïd (300 ng/ml) (>10)[2]	0.25
VCV antigen (n.d.) (>10)[3]	0.25
PMA (10^{-7}M) + ionomycin (10^{-5}M) (>80)	39
PMA (10^{-8}M) + ionomycin (10^{-6}M) (>80)	18.5
NK cells (/µl)	
$CD16^+CD56^+$ (160-950)	792
B cells (/µl)	
$CD19^+$ (610-2,600)	1.872
Serum immunoglobulins (g/l)	
IgG (3.5-11.8)	0.61
IgA (0.36-1.65)	0.1
IgM (0.36-1.04)	0.87

n.d.: not determined. [1]Age-matched normal values are indicated in parentheses. [2]The patient had received 5-valent vaccines against *Haemophilus influenzae type b*, the toxoïd of *Corynebacterium diphtheriae*, *Bordetella pertussis*, the toxoïd of *Clostridium tetani* and *Poliovirus type 1, 2 and 3* at the ages of two and four months. [3]After having experienced VCV wildtype infection over two months.

The child had profound $CD8^+$ T cell lymphopenia while $CD4^+$ T cells were not altered in terms of numbers. The proportion of $TCR\alpha\beta^+$ and $TCR\gamma\delta^+$ cells was not affected and B and NK cell counts were normal. Thymic output was reduced as $CD4^+CD45RA^+CD31^+$ recent thymic emigrants were diminished and the majority of $CD4^+$ T cells expressed the memory marker CD45R0 (Tab. 6). Furthermore, only 31.3% of the $CD4^+CD45RA^+$ cells expressed the central lymphoïd homing marker CCR7 corresponding to naïve T cells, while 37.9% of the $CD4^+CD45RA^-$ cells were $CCR7^+$ and 26.2% were $CCR7^-$ corresponding to central memory T cells (T_{CM}) and peripheral effector T cells, respectively (Fig. 40). In the $CD8^+$ compartment, there were hardly any naïve cells (4.1%) and T_{CM} cells (1.35%) and the majority of cells were $CD45RA^-CCR7^-$ peripheral effector cells (49.7%) and $CD45RA^+CCR7^-$ exhausted T_{EMRA} cells (44.8%) (Fig. 40).[452]

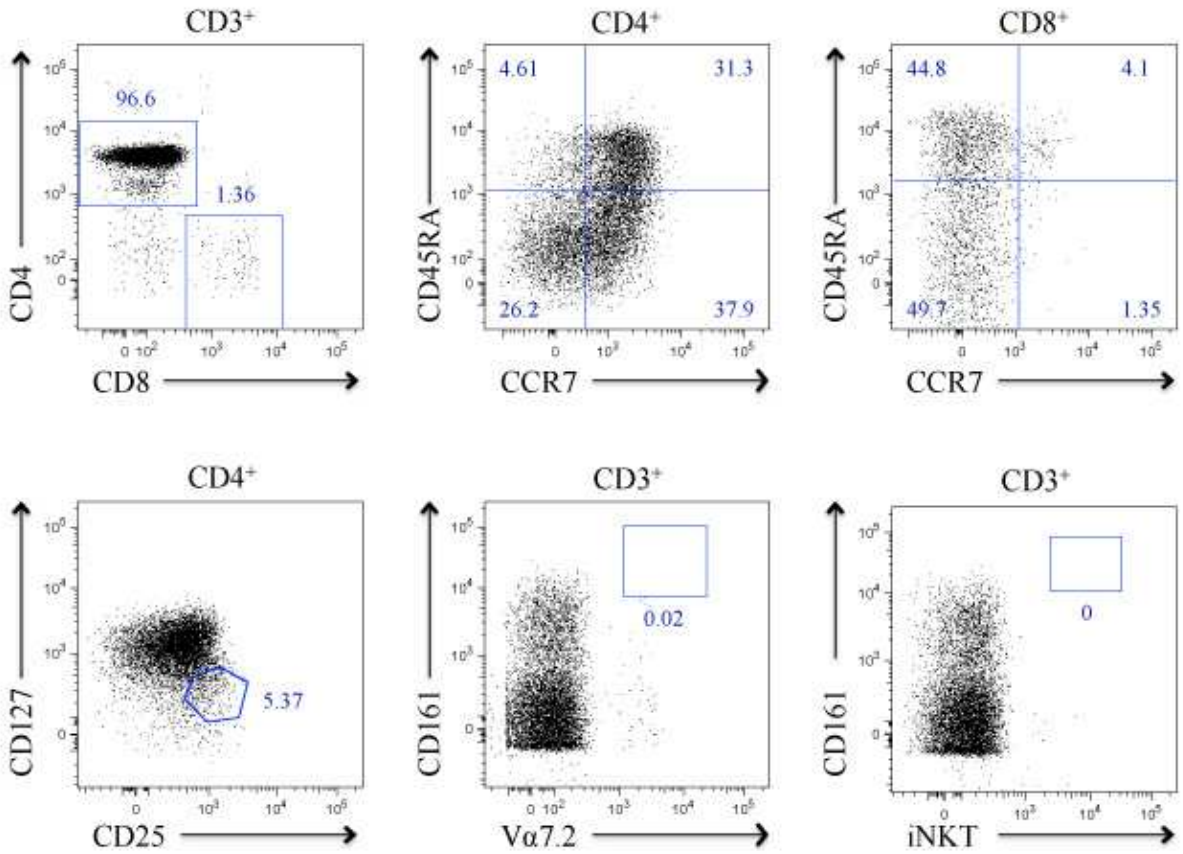

Figure 40. Immunophenotype of ZAP-70-deficient primary T cells.

Flow cytometric analysis of the expression of CD45RA and CCR7 after gating on $CD3^+CD4^+$ T_H and $CD3^+CD8^+$ T_{Cyt} and determination of the percentages of $CD25^+CD127^{low}$ T_{Reg}, $CD161^+V\alpha7.2^+$ MAIT and $CD161^+iNKT^+$ NKT cells after gating on $CD3^+CD4^+$ T_H or total $CD3^+$ T cells, respectively. The corresponding percentages are indicated for each square.

The percentage of T_{Reg} cells ($CD4^+CD25^+CD127^{low}$) was normal (3-15%) but there were no detectable MAIT cells ($CD3^+CD161^+V\alpha7.2^+$) and iNKT cells ($CD161^+$ $iNKT^+$, i.e. $TCRV\alpha24^+V\beta11^+$) (Fig. 40).

The proliferation capacity of the patient's T cells was analysed as indicated in paragraphe 3.1.1. and additionally a VCV specific antigen was used for stimulation. The patient's T cell proliferation was abolished in response to PHA, OKT3, tetanus toxoïd and VCV specific antigen but incompletely preserved in response to PMA plus ionomycin, suggesting a TCR:CD3:ζ-signalling defect (Tab. 6).

The patient's IgM was normal whereas IgG and IgA were diminished (Tab. 6). Specific antibodies and the blood group IgM allohaemagglutinins were not quantified due to the young age of the child.

The αβ and γδ TCR repertoire of the patient's T cells was compared to that of a healthy control as described in paragraphe 3.1.2. TCR spectratyping showed a polyclonal αβ and γδ TCR repertoire (Fig. 41, 42 and data not shown). The usage of the dominant TRGV9 (control, 75.8% ; patient, 45.5%) and TRDV2 (control, 77.3% ; patient, 18%) chains was relatively impaired, but this was most probable due to the young age of the patient.

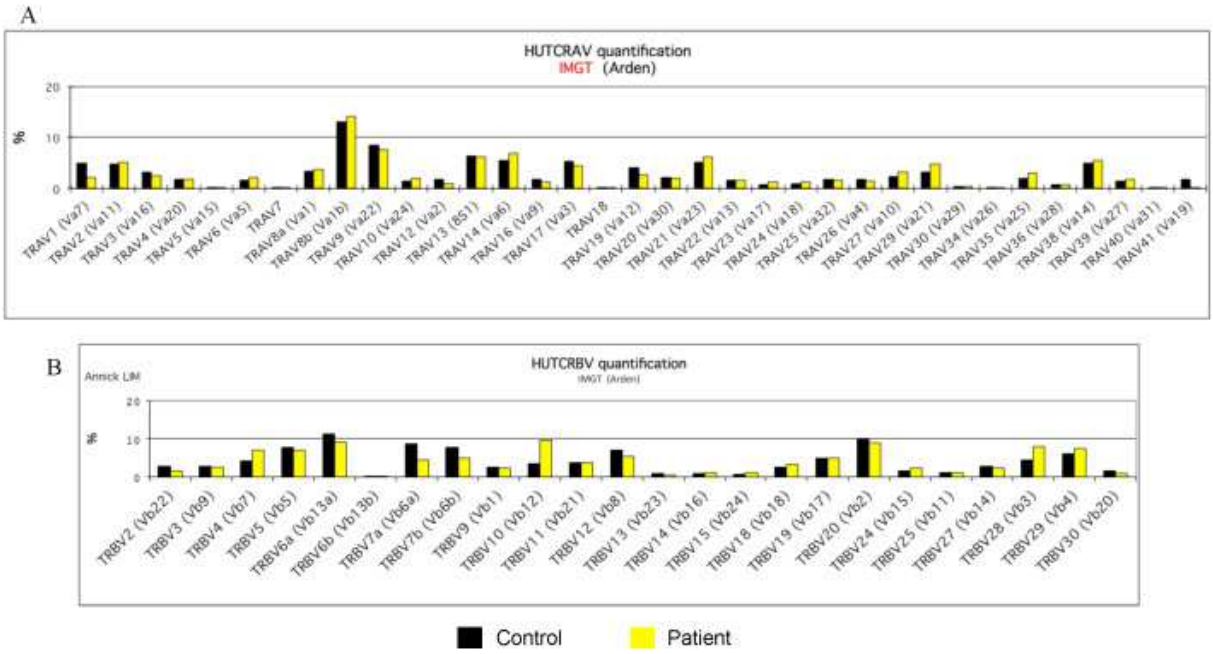

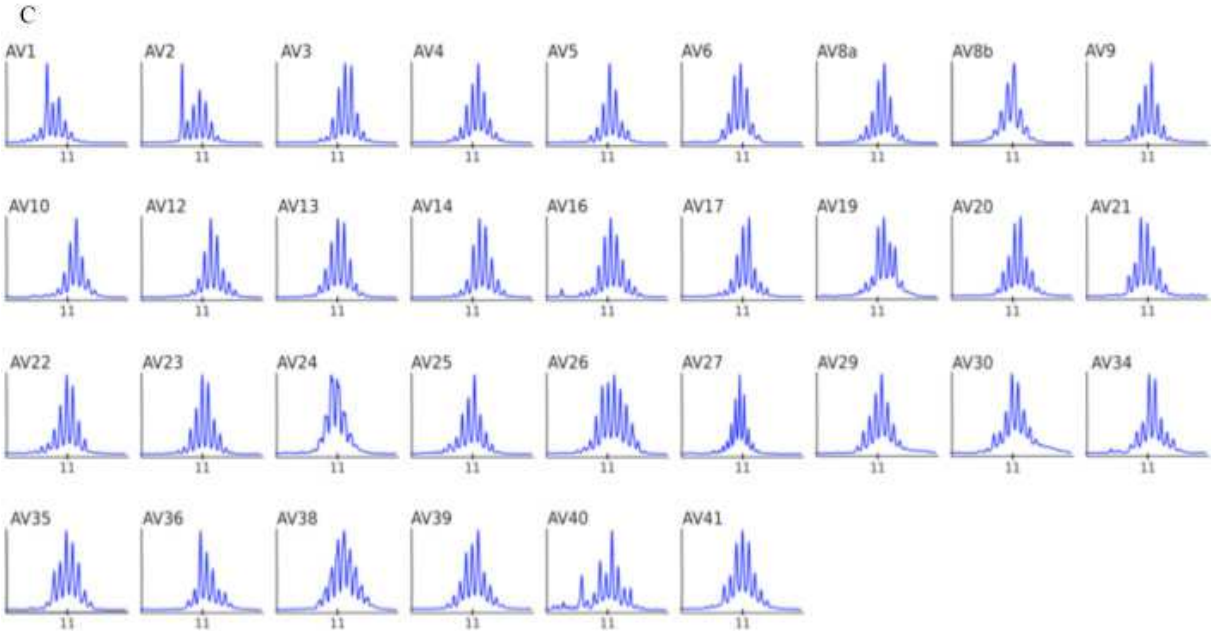

Figure 41. Analysis of the ZAP-70-deficient αβ TCR repertoire by spectratyping and electropherogram.

The relative usage of 35 TRAVs (A) and 24 TRBVs (B) was determined by qPCR and is displayed by histograms placing particular variable segments of the control (Ctr. in black) side-to-side to that of the ZAP-70-deficient patient (Pat. in yellow). The IMGT nomenclature is used for the particular variable segments and the Arden nomenclature is given in brackets. αβ T cells of the control and the patient display a balanced repertoire, thus suggesting polyclonality.

(C) The particular TRAV qPCR products of the ZAP-70-deficient patient show a normal Gaussian-like lenght-distribution that is due to random P- and N-nucleotide insertions, thus indicating polyclonality. Comparable results were obtained for the control and the TRBV qPCR products but are not shown.

Taken as a whole, the patient showed normal V(D)J-recombination as judged by the presence of polyclonal αβ and γδ TCR repertoires. However, the patient exhibited diminished thymic output exemplified by the reduced numbers of $CD4^+CD45RA^+CD31^+$ recent thymic emigrants. While $CD4^+$ T_H were present in normal numbers, $CD8^+$ T_{Cyt} numbers were reduced and innate-like MAIT and NKT cells were virtually absent, arguing for a TCR:CD3:ζ-signalling disorder especially affecting their development and lineage commitment. The remaining peripheral T cell populations displayed memory-like phenotypes more pronounced in the $CD8^+$ T_{Cyt} compartment probably as a consequence of LIP. $CD4^+$ T_H were not able to provide adequate help towards B cells as judged by the hypogammaglobulinaemia. The predominant $CD8^+$ T cell lymphopenia was reminiscent of that reported for ZAP-70-deficient individuals.[435-437]

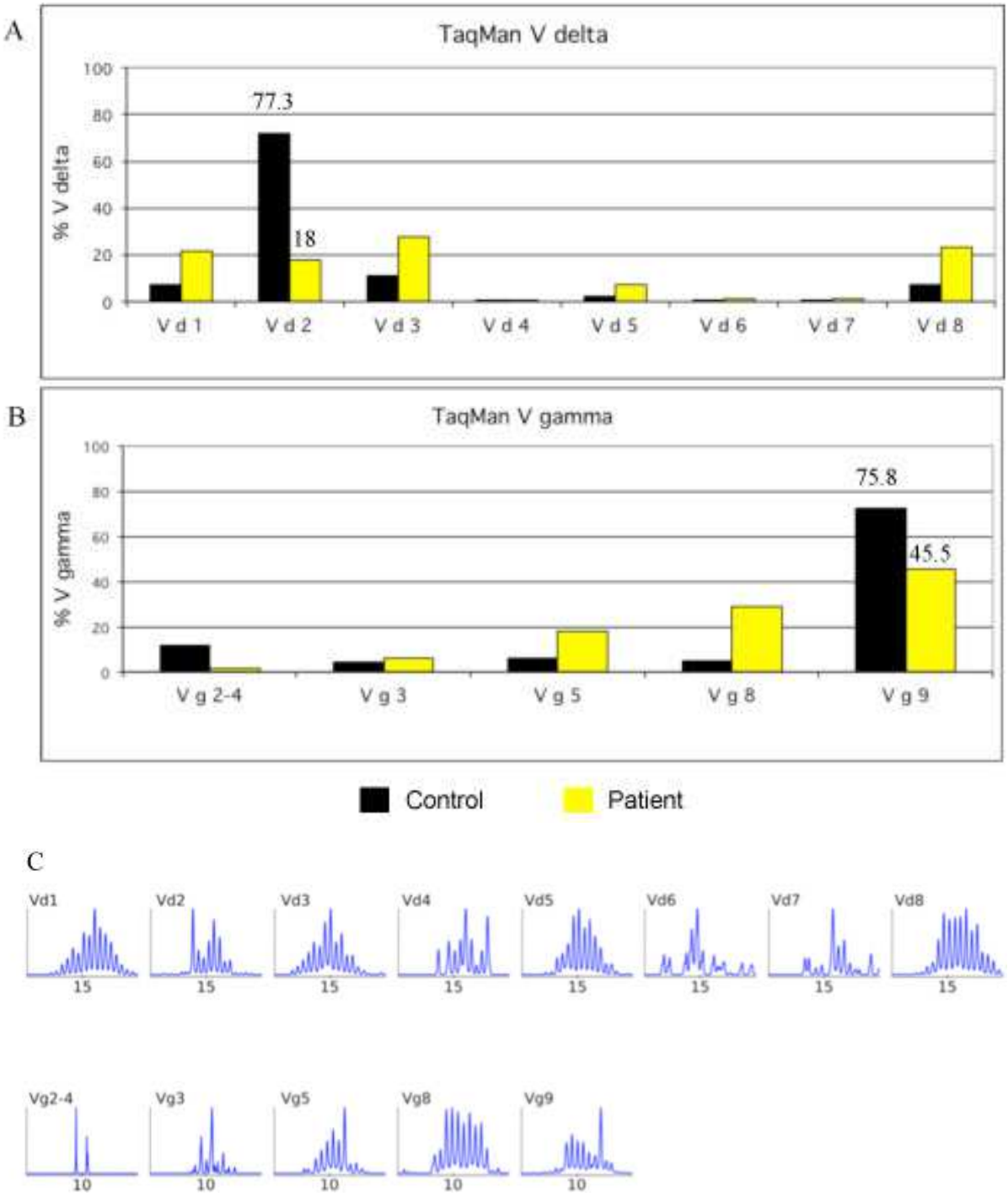

Figure 42. Analysis of the ZAP-70-deficient γδ TCR repertoire by spectratyping and electropherogram.

The relative usage of eight TRDVs (A) and five TRGVs (B) was determined by qPCR and is displayed by histograms placing particular variable segments of the control (Ctr. in black) side-to-side to that of the ZAP-70-deficient patient (Pat. in yellow). The IMGT nomenclature is used for the particular variable segments and the Arden nomenclature is given in brackets. γδ T cells of the control display a usual repertoire as exemplified by predomiant TRGV9 usage of 75.8% and TRDV2 usage of 77.3%. The repertoire of the patient is lacking this predomiant TRGV9 usage of 45.5% and TRDV2 usage of 18% most probably due to his young age.

3.2.3 Gene defect

The clinical and immunological phenotype of the patient was indicative of a profound T cell immunodeficiency. Taking into account the predominant $CD8^+$ T cell lymphopenia, that had been associated with ZAP-70-deficiency, a mutation in *ZAP-70* was plausible and thus examined.[435-437] Total RNA was extracted from PBMCs of the patient and then cDNA coding ZAP-70 was obtained by RT-PCR and sequenced (for primer information see Tab. 7). A deletion of 13 nucleotides, c.1483-1495del13 (NM_001079.3, GCCCGCTCAGCAG) was found (Fig. 43B). At the genomic level, these 13 nucleotides were located in exon 12 of *ZAP-70* (NG_007727.1). To determine the cause of this deletion, genomic DNA was isolated from PBMCs of the patient and his parents and exon 12 including flanking intronic regions were sequenced (for primer information see Tab. 7). PBMCs of the patient were found to carry the homozygous nucleotide transition *ZAP-70* g.24189G>C/IVS11-1G>C changing the splice acceptor AG of intron 11 into AC (Fig. 43A and B). The patient's parents were found to be heterozygous carriers of the transition and the sibling was not analysed. Most probably, the 13 bp deletion in the mRNA was caused by alternative splicing using a cryptic splice acceptor AG in exon 12 located 13 bp downstream of the mutated intronic splice acceptor. On the protein level, this deletion was predicted *in silico* to cause a frame shift leading to a different amino acid sequence of 75 residues with a premature stop codon thereafter corresponding to ZAP-70 p.A495fsX75 (NP_001070.2) (Fig. 43C).

Table 7. Genomic and complementary *ZAP-70* sequencing primers.

Primer name	Primer sequence
Complementary forward (121) primer 1	5'-TTGGCATTGGGACCAGAGAC-3'
Complementary reverse (675) primer 1	5'-CGTCGTAGCAATGAGCTTCT-3'
Complementary forward (656) primer 2	5'-AGAAGCTCATTGCTACGACG-3'
Complementary reverse (1195) primer 2	5'-GCTTCTTGTCCTTGAGCTCC-3'
Complementary forward (1088) primer 3	5'-CTGAGCCAGCACGCATAACG-3'
Complementary reverse (1690) primer 3	5'-CAGTGTAGTAGCTGTCGTCG-3'
Complementary forward (1671) primer 4	5'- CGACGACAGCTACTACACTG-3'
Complementary reverse (2161) primer 4	5'-ACAACCAAGCAGGGCTCAGC-3'
Genomic forward intron 11 / exon 12	5'-TGGGGATGAAGTACCTGGAG-3'
Genomic reverse intron 12 / exon 12	5'-CCCACTGGCACTCACTTGTA-3'

To analyse the consequence of the p.A495fsX75 mutation on ZAP-70 protein expression, T cell blasts of a healthy control and the patient were generated as described in paragraphe 3.1.3. with the exception that PMA 10 ng/ml, ionomycin 1 µM and IL-2 100 U/ml were used. Cells were lysed and protein lysates analysed by immunoblotting with a rabbit polyclonal anti-ZAP-70 antibody that might have the capacity to recognize the p.A495fsX75 ZAP-70 protein as it was directed against aa residues 253-329.[460] While control cells expressed ZAP-70, there was no detectable expression of ZAP-70 in the cells of the patient, strongly suggesting that p.A495fsX75 behaved as an amorphic (or null) mutation (Fig. 43 C).

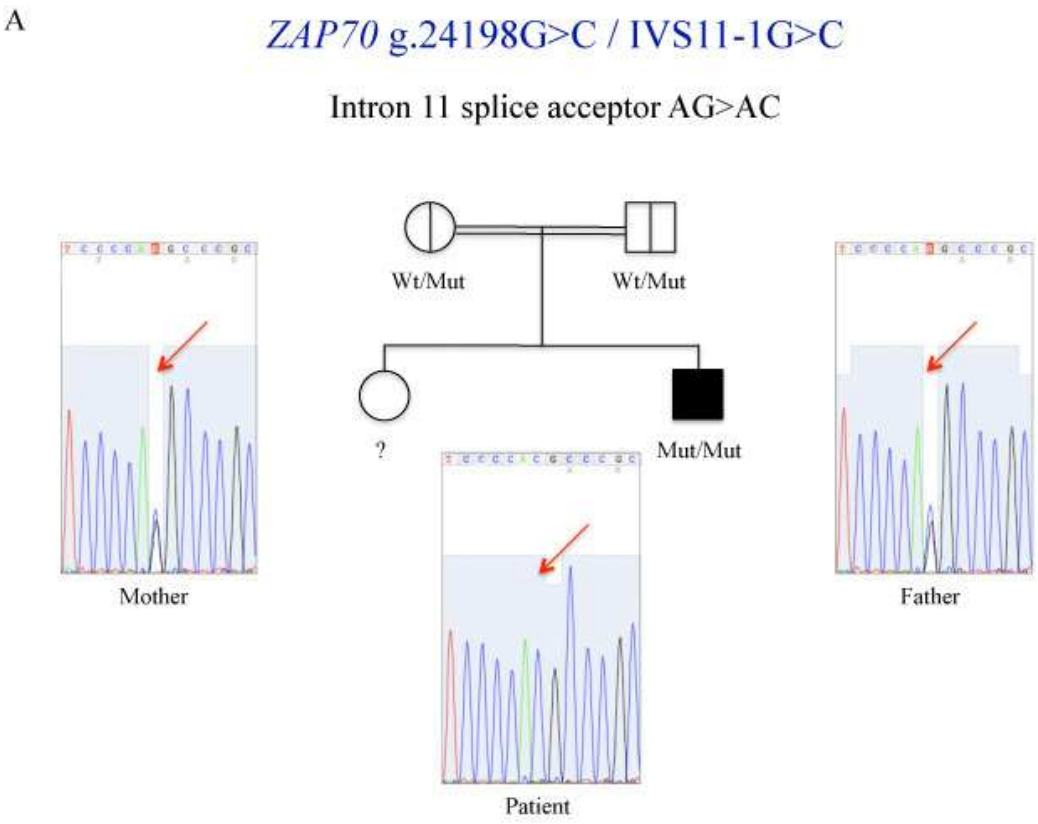

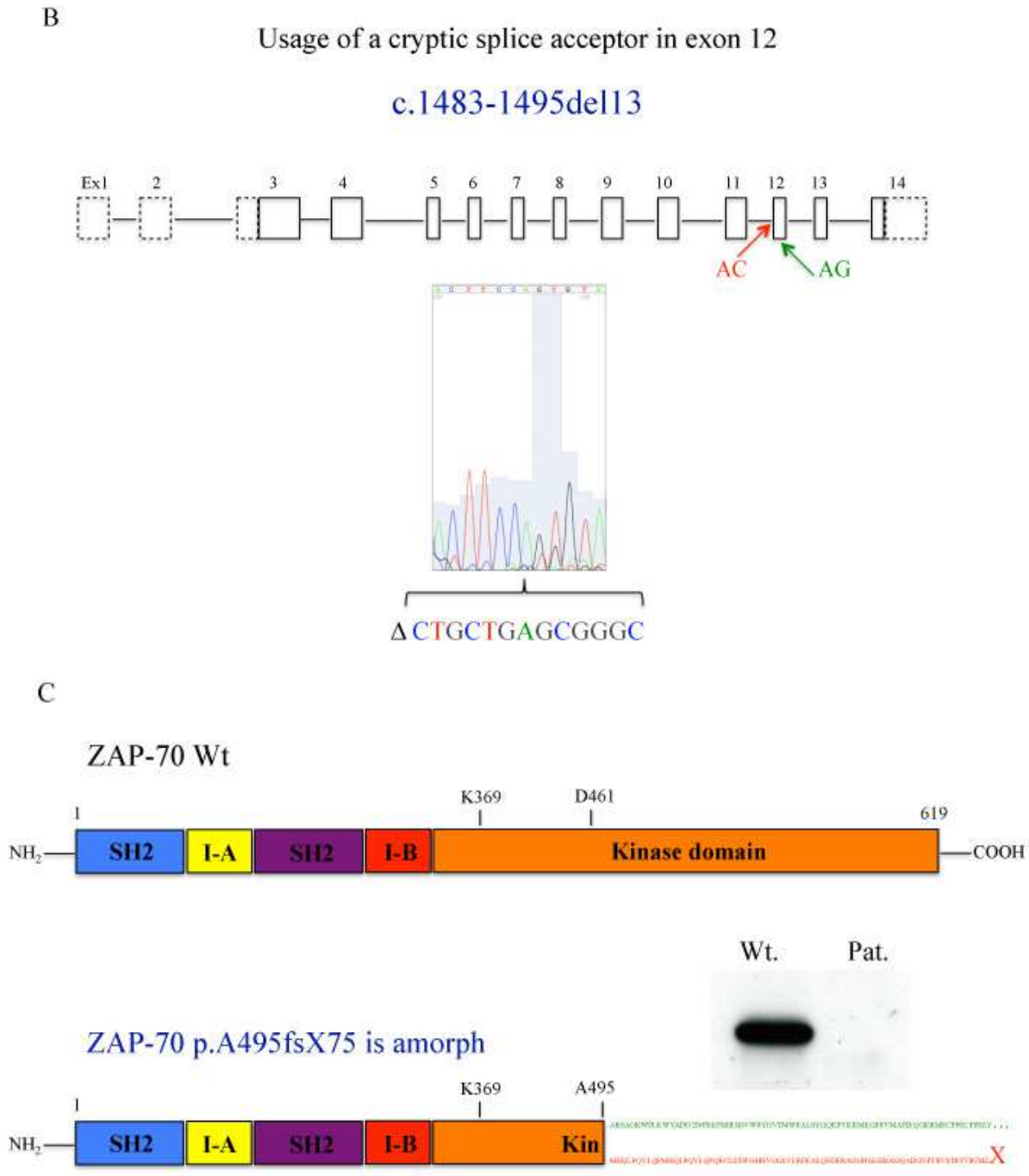

Figure 43. Genetic analysis of the ZAP-70-deficient patient and his family.

(A) The pedigree and the corresponding electropherograms obtained by sequencing exon 12 of *ZAP-70* including its intronic regions of the index patient and his family are shown. The ZAP-70-deficient patient (black square) was found homozygous for the splice acceptor mutation g.24189G>C/IVS11-1G>C (red arrow), while his mother (white circle with vertical line), and his father (white square with vertical line) were heterozygous (red arrows). The female sibling (white circle) was not analysed (question mark).

(B). The exon and intron organization of the genomic *ZAP-70* locus and the electropherogram obtained by sequencing of the patient's *ZAP-70* cDNA are shown. Protein coding and non-coding exons and introns are represented by solid or spotted boxes and solid lines, respectively. The position of the mutated splice acceptor

AC in intron 11 and the cryptic splice acceptor AG in exon 12 used for alternative splicing are indicated by a red and green arrow, respectively (not drawn to scale). The electropherogram shows the missing reverse 13 nucleotides (ΔCTGCTGAGCGGGC) that are indicated by a bracket.
(C) The domain structure of wildtype (Wt) and mutated ZAP-70 p.A495fsX75 are shown. The tandem SH2 domains, the interdomains A and B and the kinase domain are indicated in blue, purple, yellow, red and orange, respectively. The ATP-binding K369, the proton acceptor D461 and the residue A495 followed by the wildtype sequence (green) or the frame-shifted sequence (red) including the premature stop codon (X) are indicated (not drawn to scale). Immunoblotting for ZAP-70 of lysates from T cell blasts from a healthy control (Ctr.) and the patient (Pat.) are shown.

3.2.4 Analysis of TCR:CD3:ζ-signalling in ZAP-70-deficiency

In order to characterize the consequence of the amorphic ZAP-70 p.A495fsX75 mutation on proximal TCR:CD3:ζ-signalling, T cell blasts were stimulated with anti-CD3 antibody for 0, 2, 5, 15, 30 and 60 minutes or with PMA + ionomycin for 30 minutes, lysed and lysates were subjected to immunoblotting with a mAb directed against phosphorylated tyrosine residues (see paragraphe 3.2.3). While TCR:CD3:ζ-signalling in T cell blasts of a healthy control resulted in strong protein tyrosine phosphorylation, T cell blasts of the patient displayed virtually no signal. Phosphorylated proteins corresponding to known TCR:CD3:ζ-signalling substrates such as LCK, ZAP-70, SLP-76 and PLCγ-1 were not detectable, while a phosphorylated band corresponding presumably to the negative regulator CBL was preserved. Protein loading of samples was checked by immunoblotting for actin and found to be comparable (Fig. 44).

Defective protein tyrosine phosphorylation could not be explained by decreased expression of other kinases such as SYK, LCK, FYN and ITK or other signalling molecules such as LAT, PLCγ-1, PKCθ and ERK-1/2. (Fig. 45). On the contrary, the second SYK-family kinase SYK was found to be relatively overexpressed, as well as the signalling molecules LAT, PLCγ-1 and PKCθ, eventhought to lesser extents.

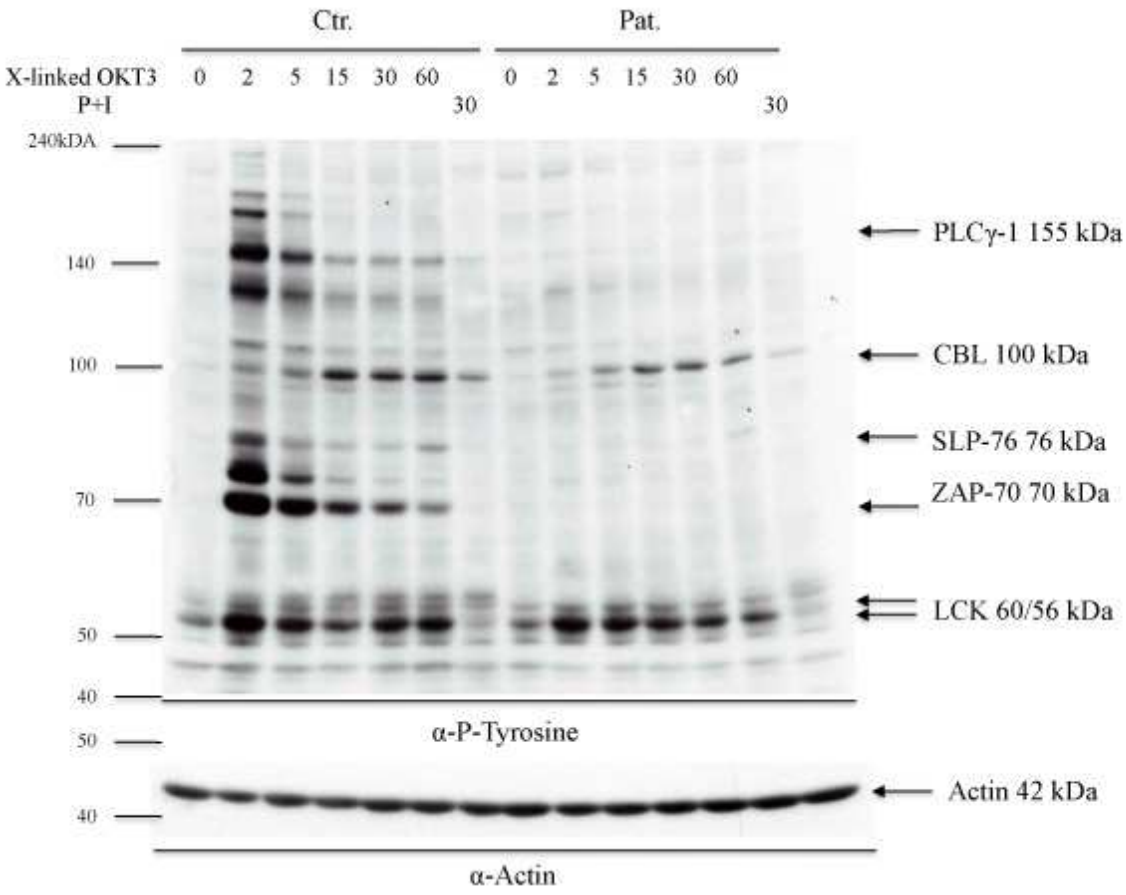

Figure 44. Impaired protein tyrosine phosphorylation in ZAP-70-deficient T cell blasts.

T cell blasts of a healthy control (Ctr.) and the ZAP-70-deficient patient (Pat.) expanded with PMA 10 ng/ml and ionomycin 1 µM were stimulated with OKT3 1 µg/ml cross-linked with polyclonal rabbit anti-mouse IgG 2 µg/ml (x-linked OKT3) for 0, 2, 5, 15, 30 and 60 minutes or with PMA 10 ng/ml and ionomycin 1 µM (P+I) for 30 minutes. Total protein was extracted, separated by SDS-PAGE and immunoblotting with mAbs against phosphorylated tyrosine residues (α-P-Tyrosine) and actin (α-Actin) was performed. Molecular weight markers in kDa are given on the left (black lines) and names and molecular weights of specific bands are indicated on the right (black arrows).

TCR:CD3:ζ-induced activation of signalling molecules of the proximal TCR:CD3:ζ- and the LAT:SLP-76-signalosome were further analysed taking advantage of the protein lysates already obtained. Immunoblotting was performed with mAbs directed against phosphorylated ZAP-70 (phosphotyrosine 493), phosphorylated LAT (phosphotyrosine 171), phosphorylated PLCγ-1 (phosphotyrosine 783), phosphorylated PKCθ (phosphothreonine 538) and actin serving as a loading control. While in control cells, a rapid and strong phosphorylation of all analysed signalling molecules was seen, in the cells of the ZAP-70-deficient patient the phosphorylation of PLCγ-1 and PKCθ was weakened and delayed and virtually no phosphorylation of LAT was detected (Fig. 46).

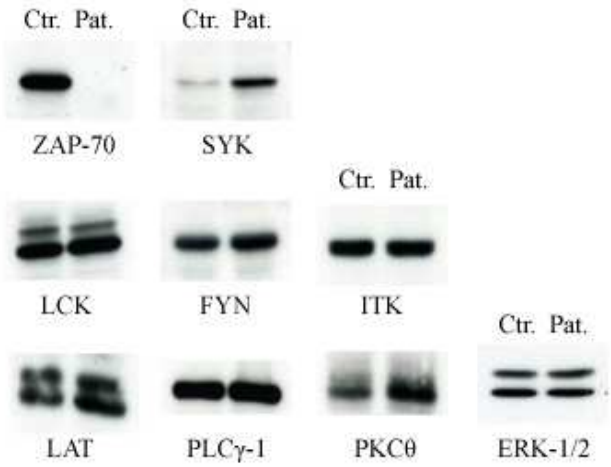

Figure 45. Expression of signalling molecules in ZAP-70-deficient T cell blasts.

The expression of the SYK-family kinases ZAP-70 and SYK, of the SRC-family kinases LCK and FYN, of the TEC-family kinase ITK and of the signalling molecules LAT, PLCγ-1, PKCθ and ERK-1/2 were analysed in T cell blasts of a healthy control (Ctr.) and the ZAP-70-deficient patient (Pat.).

Therefore, these data strongly suggest that defective protein tyrosine phosphorylation and phosphorylation of LAT:SLP-76-signalosome molecules is due to the amorphic ZAP-70 p.A495fsX75 mutation. Interestingly, the second SYK-family kinase SYK was found to be relatively overexpressed, as well as the signalling molecules LAT, PLCγ-1 and PKCθ, eventhought to lesser extents. This might represent a compensatory mechanism for ZAP-70-deficiency (Fig. 45).

TCR:CD3:ζ-induced Ca^{2+}-flux in PBMCs was analysed by flow cytometry as described in paragraphe 3.1.4. Stimulation with 1 µg/ml OKT3 cross-linked with 10 µg/ml rabbit-anti-mouse-IgG induced a clear Ca^{2+}-flux in *ex vivo* $CD4^+$ T_H and $CD8^+$ T_{Cyt} from a healthy control whereas no Ca^{2+}-flux was seen in $CD4^+$ T_H of the ZAP-70-deficient patient. Interestingly and in contrast to $CD4^+$ T_H, $CD8^+$ T_{Cyt} of the ZAP-70-deficient patient showed an intermediate Ca^{2+}-flux. Stimulation with ionomycin resulted in strong Ca^{2+}-flux in all analysed cell populations serving as positive control for cell loading with the fluorescent reporter and cell viability (Fig. 47).

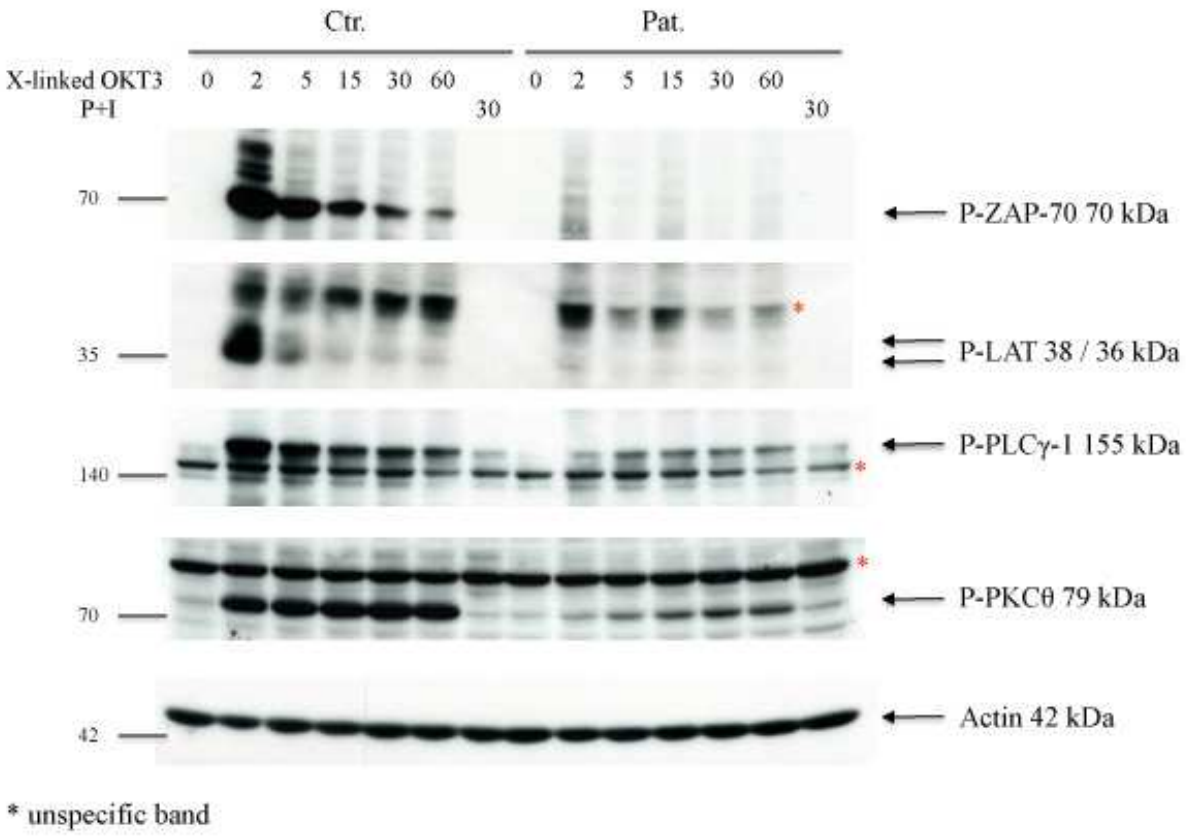

Figure 46. Impaired proximal TCR:CD3:ζ- signalling in ZAP-70-deficient T cell blasts.

T cell blasts of a healthy control (Ctr.) and the ZAP-70-deficient patient (Pat.) expanded with PMA 10 ng/ml and ionomycin 1 µM were stimulated with OKT3 1 µg/ml cross-linked with polyclonal rabbit anti-mouse IgG 2 µg/ml (x-linked OKT3) for 0, 2, 5, 15, 30 and 60 minutes or with PMA 10 ng/ml and ionomycin 1 µM (P+I) for 30 minutes. Total protein was extracted, separated by SDS-PAGE and immunoblotting with mAbs raised against phosphorylated ZAP-70 (P-ZAP-70), phosphorylated LAT (P-LAT), phosphorylated PLCγ-1 (P-PLCγ-1), phosphorylated PKCθ (P-PKCθ) and the loading control actin (Actin) was performed. Molecular weight markers in kDa are given on the left (black lines) and names and molecular weights of specific bands are indicated on the right (black arrows). Unspecific bands are marked with a red asterisk.

Thus, the amorphic ZAP-70 p.A495fsX75 mutation completely abrogated Ca^{2+}-flux in the polyclonal $CD4^+$ T_H population while the residual $CD8^+$ T_{Cyt} population displayed an intermediate Ca^{2+}-flux. In ZAP-70-deficient $CD8^+$ T_{Cyt}, signals required for Ca^{2+}-flux might have been transduced by compensatory SYK, LAT and PLCγ-1 expression.

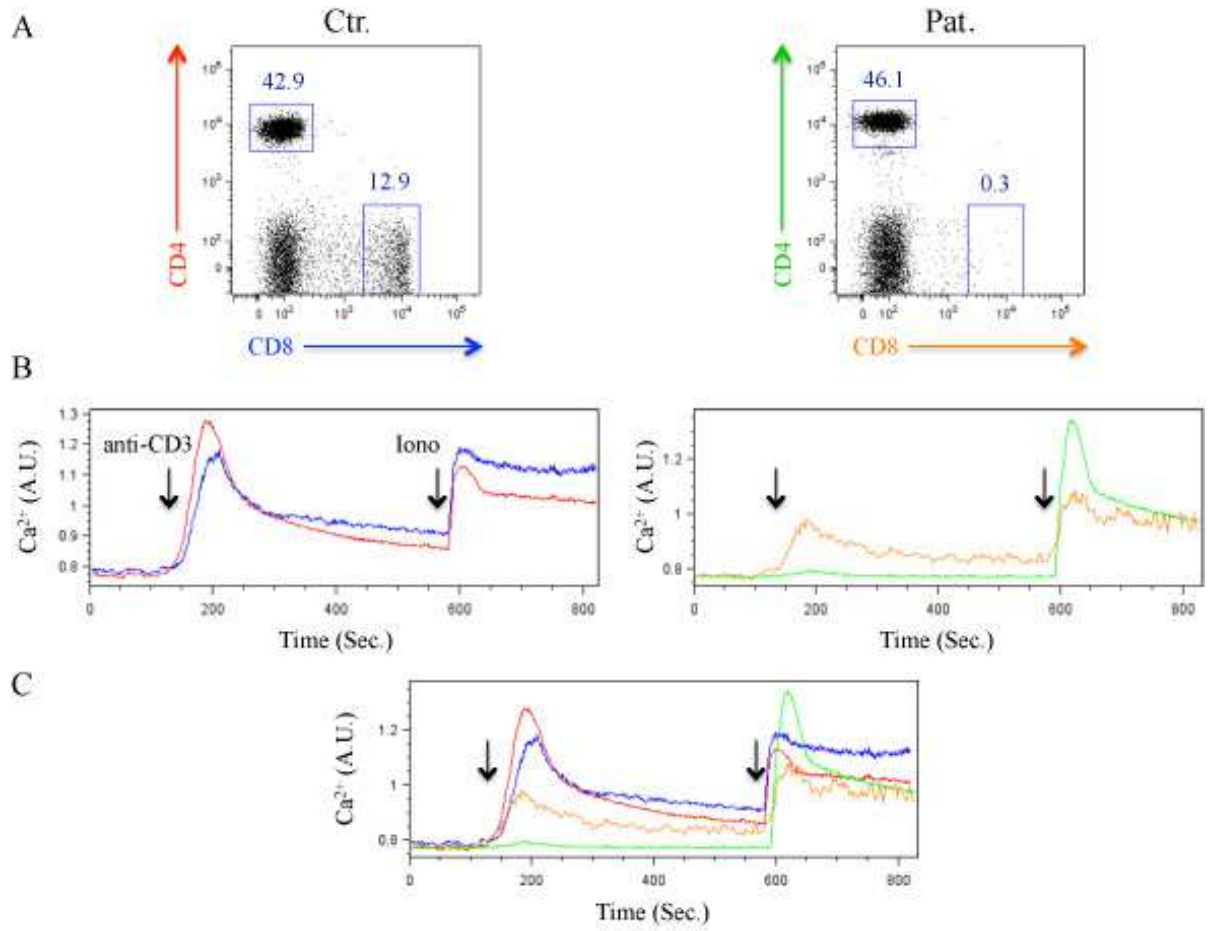

Figure 47. Impaired Ca^{2+}-flux in ZAP-70-deficient primary T cells.

(A) Primary PBMCs were stained with anti-CD4 and anti-CD8 antibodies and charged with 5 µM of the Ca^{2+}-sensitive fluorescent dye Indo-1-acetoxymethyl ester. Dot blots show $CD4^+$ T_H (red) and $CD8^+$ T_{Cyt} (blue) of a healthy control and of the ZAP-70-deficient patient (green and orange), respectively. Percentages corresponding to the particular cell populations are indicated.

(B) Ca^{2+}-flux in the particular cell populations was analysed with a FACS ARIA II after PBMCs were stimulated with 1 µg/ml OKT3 cross-linked with 10 µg/ml rabbit-anti-mouse-IgG (anti-CD3) for eight minutes and thereafter stimulated with 1 µM inomycin (Iono) (vertical arrows). Ca^{2+}-flux was calculated and expressed in arbitrary units (A.U.) and displayed over time (Sec.).

(C) Ca^{2+}-fluxes of the particular cell populations of the healthy control and the ZAP-70-deficient patient are superimposed.

TCR:CD3:ζ-induced distal signalling was analysed with mAbs directed against NFATc2 (phosphotyrosine 493), phosphorylated ERK-1/2 (phosphothreonine 202/phosphotyrosine 204) and actin serving as a loading control. In healthy control T cell blasts, anti-CD3 stimulation triggered a rapid dephosphorylation of NFAT2c and the phosphorylation of ERK1/2. In contrast, in T cell blasts of the ZAP-70-deficient patient, the responses were almost abrogated (Fig. 48). Thus, the amorphic ZAP-70 p.A495fsX75

mutation also leads to defects in TCR:CD3:ζ-downstream signalling events such as MAPK- and NFAT-signalling.

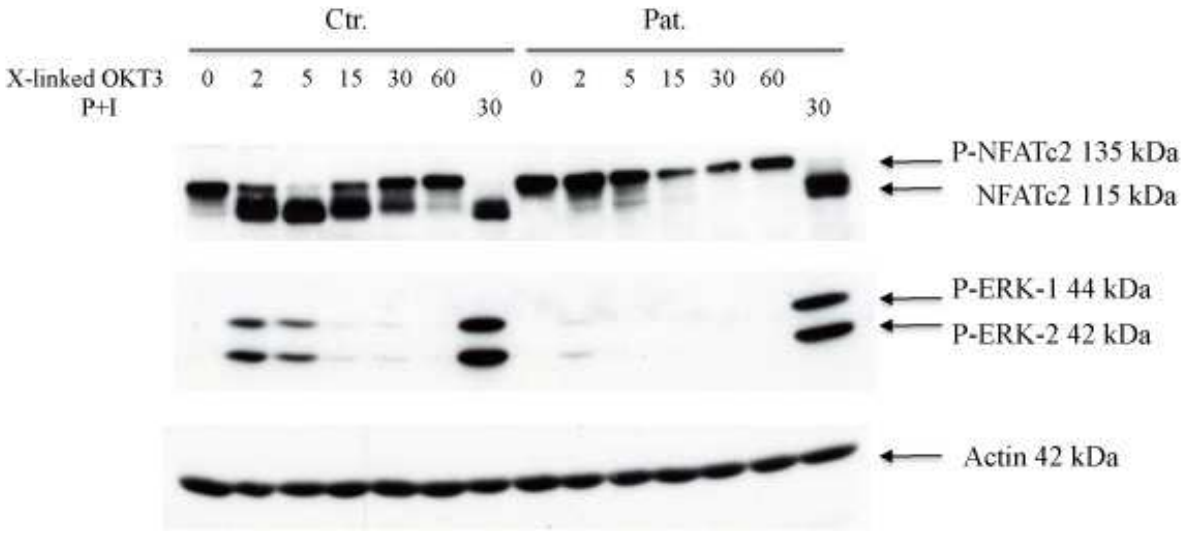

Figure 48. Impaired distal TCR:CD3:ζ- signalling in ZAP-70-deficient T cell blasts.

T cell blasts of a healthy control (Ctr.) and the ZAP-70-deficient patient (Pat.) expanded with PMA 10 ng/ml and ionomycin 1 µM were stimulated with OKT3 1 µg/ml cross-linked with polyclonal rabbit anti-mouse IgG 2 µg/ml (x-linked OKT3) for 0, 2, 5, 15, 30 and 60 minutes or with PMA 10 ng/ml and ionomycin 1 µM (P+I) for 30 minutes. Total protein was extracted, separated by SDS-PAGE and immunbloting with mAbs raised against pan-NFATc2 that detected phosphorylated and dephosphorylated NFATc2 (P-NFATc2 and NFATc2), phosphorylated ERK-1/2 (P-ERK-1 and P-ERK-2) and the loading control actin (Actin) was performed. Names and molecular weights of specific bands are indicated on the right (black arrows).

Finally, AICD of αβ T cells was analysed as described in paragraphe 3.1.4 using increasing concentrations of OKT3, i.e. 0.01 / 0.1 / 1 / 10 µg/ml. While αβ T cell blasts of a healthy control performed AICD in a dose-dependant manner with a saturation at 1.0 µg/ml, αβ T cell blasts of the ZAP-70-deficient patient did not shown AICD (Fig. 49), thus indicating that the amorphic ZAP-70 p.A495fsX75 mutation hampers TCR:CD3:ζ-signalling induced functional T cell responses.

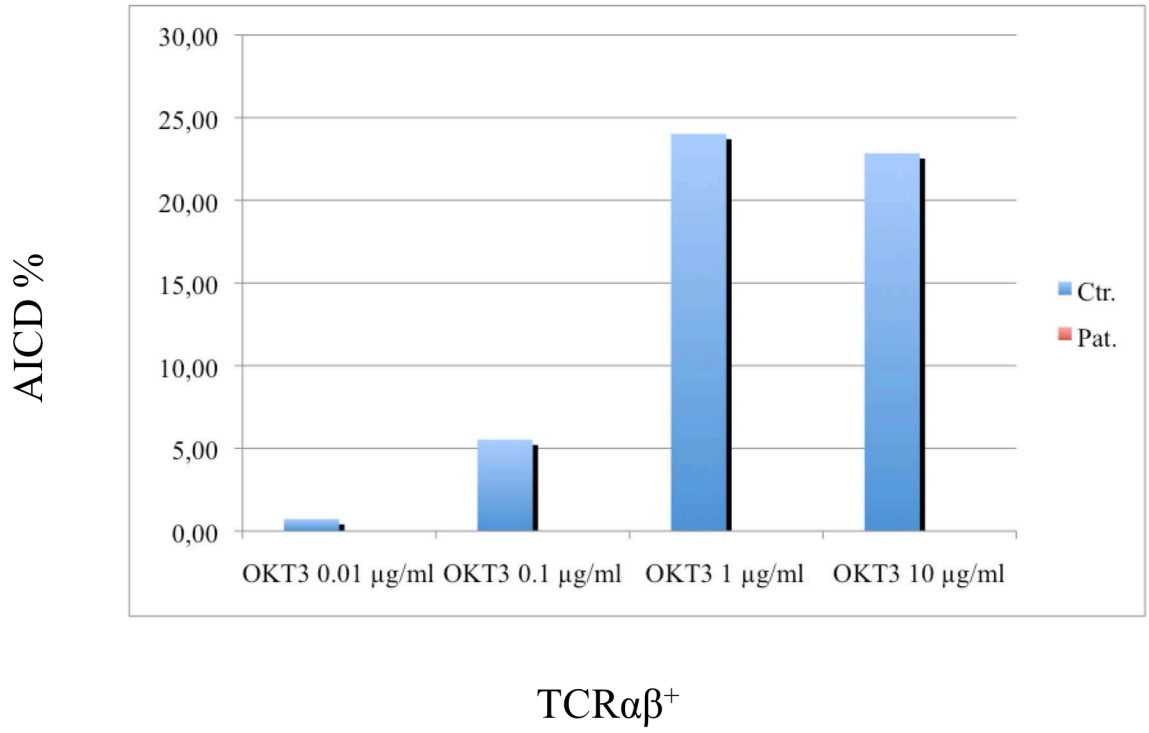

Figure 49. Disturbed AICD in ZAP-70-deficient T cell blasts.

Duplicates of 10^5 T cell blasts of a healthy control (blue) and the ZAP-70-deficient patient (red) were incubated for 24 h in 48 flat bottom well plates coated with increasing concentrations of OKT3, i.e. 0.01 / 0.1 / 1 / 10 µg/ml. Cells were recovered, stained with anti-CD3, anti-TCRαβ, Annexin V and 7-AAD and analysed on a FACSCanto II. Annexin V and 7-AAD positive cells were considered as apoptotic cells and expressed as a percentage of the entire $TCR\alpha\beta^+$ population.

Taken as a whole, this study demonstrates that the amorphic ZAP-70 p.A495fsX75 mutation leads to disturbed TCR:CD3:ζ-signalling affecting protein tyrosine phosphorylation, Ca^{2+}-flux, MAPK- and NFAT-signalling and overall TCR-dependent functions, even though these results might be biased by the presence of T_{EMRA} cells in the T cell blast culture. Relative overexpression of SYK, LAT, PLCγ-1 and PKCθ was observed in ZAP-70-deficient T cells and we speculate that the intermediate Ca^{2+}-flux exclusively detected in the residual $CD8^+$ T_{Cyt} population might depend on the overexpression of these molecules. This might also account for lineage commitment of the residual $CD8^+$ T_{Cyt} in the absence of ZAP-70.

3.3 Identification of a novel null mutation in *ITK* causing CID with susceptibility to EBV-infection

3.3.1 Clinical phenotype

The patient was born at term to first-degree consanguineous Pakistani cousins that had migrated to England. He was healthy in the first year of live and received the live-vaccine

Bacillus Calmette-Guérin (BCG), four 7-valent conjugate vaccines against *Streptococcus pneumoniae*, four 5-valent vaccines against *Haemophilus influenzae type b*, the toxoïd of *Corynebacterium diphtheriae*, *Bordetella pertussis*, the toxoïd of *Clostridium tetani* and *Poliovirus type 1, 2 and 3* and one attenuated live-vaccine against the *Measles*, *Mumps* and *Rubella* viruses without adverse events.

From one year of age, he developed frequent infections of the upper and lower airways and repeatedly received anti-bacterial treatment with moderate success. From two years of age, he established almost monthly bouts of fever and a failure to thrive became evident (weight 11.8 kg / < 0.4 perc., occipito-frontal circumference 49.5 cm / > 2.0 perc.). From three years of age, daily bouts of fever were accompanied by dry cough and vomiting. A chest radiography (Fig. 50) showed miliary shadowing of the entire lung and as a ten-year-old relative recently had been treated for tuberculosis, the patient was met on quadruple anti-mycobacterial treatment, even though the diagnosis of tuberculosis could not be established formally. Treatment was performed for six months with minor improvement of clinical and radiological signs and therefore multi-drug-resistent infection with *Mycobacterium tuberculosis* was suspected. The patient was transfered to the regional peadiatric reference center and an intensive medical work-up disclosed highly elevated *Epstein-Barr virus* (EBV) copy numbers in the peripheral blood (EBV DNA > 10^4/ml) and in the bronchoalveolar lavage. A thoracic computed tomography scan detected multiple pulmonary nodules and an open lung biopsy was performed.

Immunohistochemical work-up of the lung sections showed a pulmonary parenchyma containing nodular masses of abnormal lymphoïd tissue composed of cellular nodules separated and surrounded by fibrosis. The basal lymphohistiocytic infiltrate was composed of $CD2^+CD3^+$ T cells with slightly more $CD4^+$ than $CD8^+$ T cells and some IgD^+ B cells and plasma cells expressing polyclonal Ig light-chains. The infiltrate contained large atypical lymphoïd cells with vesicular nuclei and prominent nucleoli some of them being mononuclear Hodgkin cells and some being multinucleated Reed-Sternberg cells. Hodgkin and Reed-Sternberg cells were positive for the B cell markers CD20 and PAX-5 and the activation marker CD30. The basal lymphohistiocytic infiltrate and the large atypical cells were both highly positive for the proliferation marker Ki-67 and the EBV-encoded small RNA 1 (EBER-1) (Fig. 51). Thus, EBV-associated Hodgkin`s lymphoma-like lymphoproliferative disease was diagnosed.

The patient subsequently underwent an intensity- and duration-reduced chemotherapy with steroids, vinblastin, etoposide and rituximab, a mAb directed against CD20 expressed by

B cells. Thereafter, he successfully underwent allogeneïc haematopoïetic stem cell transplantation from a haploïdentical sibling donor, i.e. his younger healthy brother.

Taken as a whole, the patient presented the clinical picture of CID characterized by recurrent respiratory tract infections and EBV-associated Hodgkin`s lymphoma-like lymphoproliferative disease.

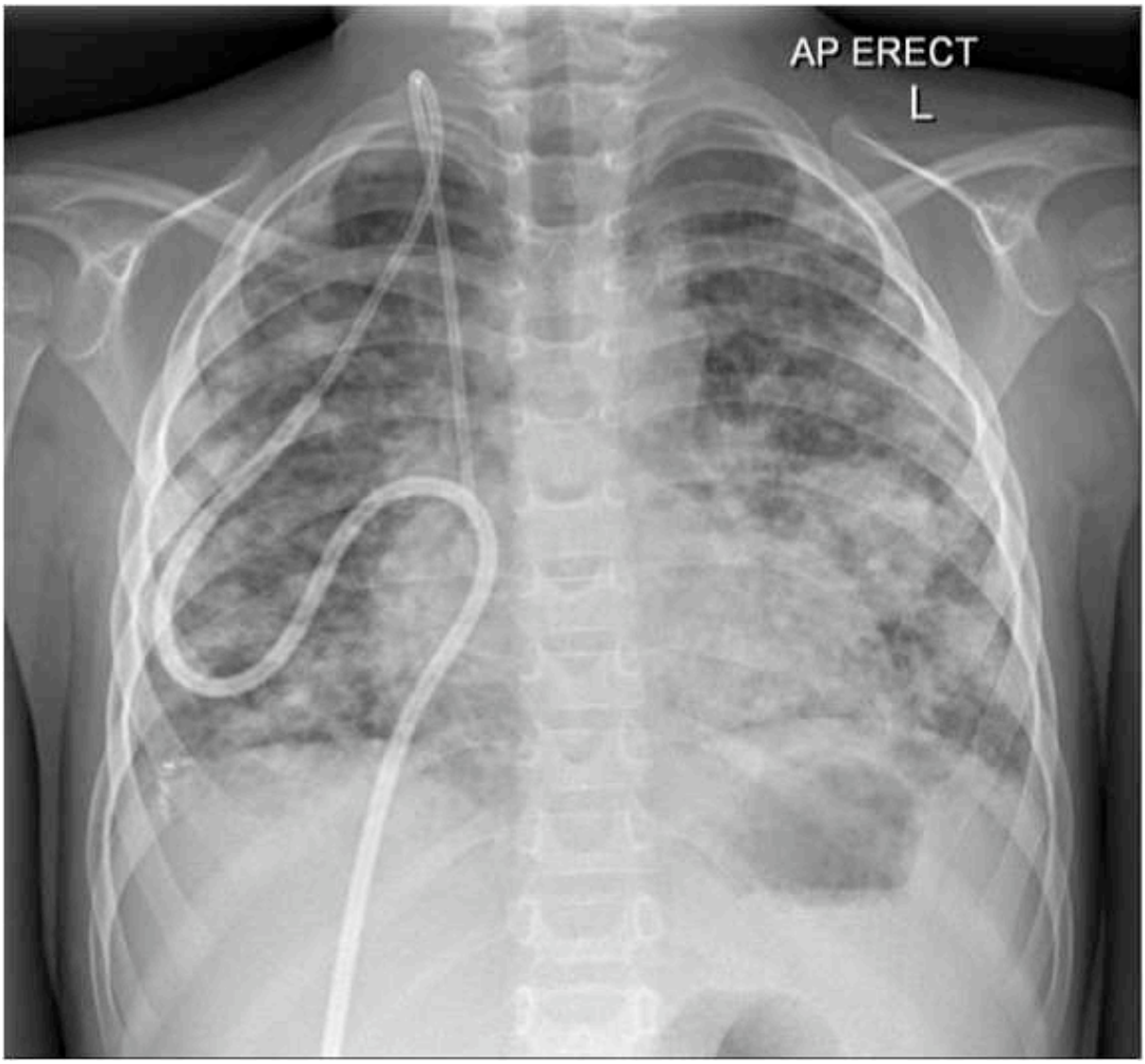

Figure 50. Chest radiography of the miliary infiltrate.

Conventional chest radiography showing a diffuse miliary infiltrate of the entire lung.

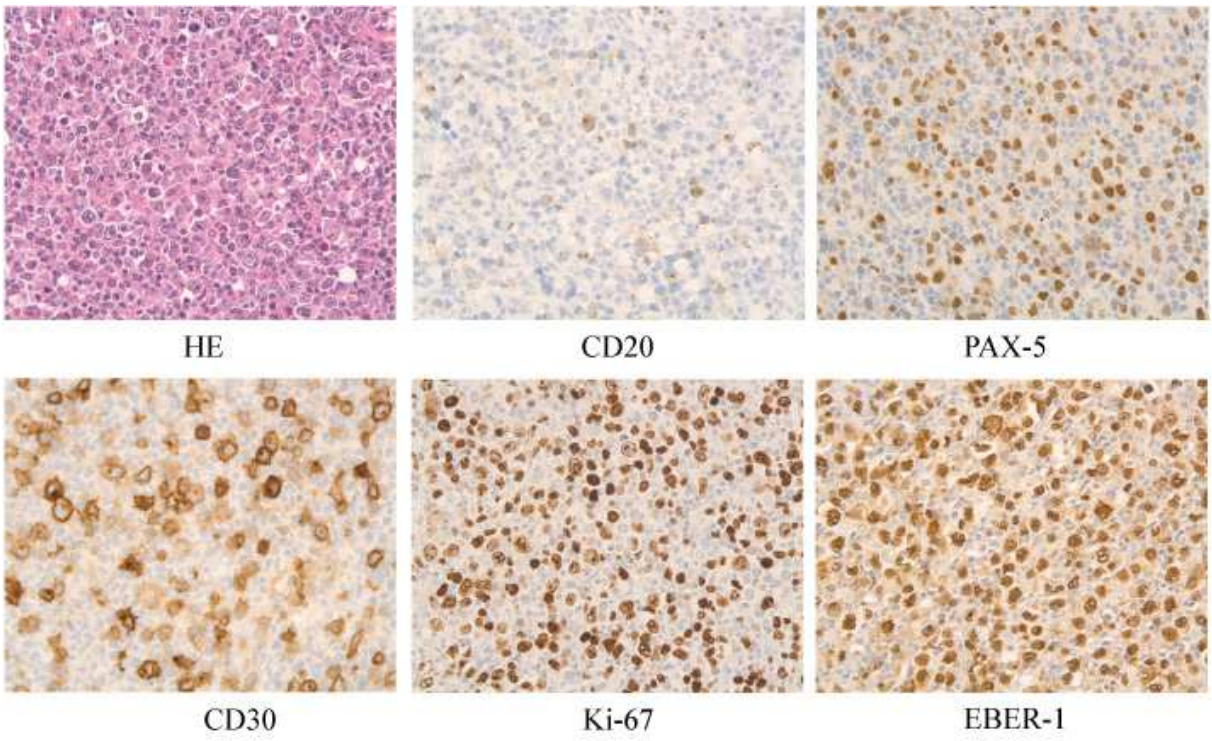

Figure 51. Immunohistochemical work-up of the pulmonary infiltrate.

Representative pulmonary biopsy specimens of the nodular infiltrate show a polymorphic abnormal lymphoïd tissue (haematoxylin and eosin staining, HE) that predominantly is composed of B cells expressing CD20 and PAX-5. Additionally, Hodgkin and Sternber-Reed cells are positive for CD30. The majority of the lymphoïd tissue is highly positive for the proliferation marker Ki-67 and the EBV-encoded small RNA 1 (EBER-1). Thus, the specimens reveal an EBV-associated Hodgkin`s lymphoma-like lymphoproliferative disease.

One year after allogeneïc haematopoïetic stem cell transplantation, a third child was born to the family that performed regular postnatal adaptation and showed no signs of infection or inflammation (Fig. 55A). However, he was diagnosed having an developmental disorder of its colon, that is congenital aganglionic megacolon or Hirschsprungs's disease.[461] The newborn thus underwent abdominal surgery and currently is prepared for curative allogeneïc haematopoïetic stem cell transplantation (see paragraphe 3.2.3). Up to now he has not yet encountered EBV.

3.3.2 Immunological phenotype

PBMCs of a healthy control, the patient and the newborn brother were isolated, stained with fluorochrome-labeled isotype controls or mAbs, analysed by flowcytometry on a FACSCanto II and data was processed with FlowJo software as described in paragraphe 3.1.2. The proliferation capacity of the patient's T cells was analysed as indicated in paragraphe

3.1.1. Immunological investigations of the patient at the age of 46 and 52 months and of the newborn brother two weeks after birth are summarized in Tab. 8.

Table 8. Immunological features of the ITK-deficient patient and the newborn brother.

	Patient		**Newborn**
	46 months	**52 month**	**After birth**
TRECs (Target/Reference 5.69^{-3})	n.d.	n.d.	Target/Reference 2.97^{-3}
Lymphocytes (2,300-5,400/µl) (3,400-7,600/µl)[1]	642	1,300	3,800
T cells (/µl)			
$CD3^+$ (1,400-3,700) (2,500-5,500)	254	871	1,558
$CD4^+$ (700-2,200) (1,600-4,000)	103	195	1,102
$CD8^+$ (490-1,300) (560-1,700)	112	533	266
T cells (%)			
$TCR\alpha\beta^+$ cells (90-100)	80	86.9	89,2
$TCR\gamma\delta^+$ cells (0-10)	20	13.1	10,8
CD4/CD8 ratio (0.9-2.3)	0.92	0.37	4,14
T cell proliferation (cpm)			
No stimulation (656)[2]	85	n.d.	see Fig. 53
PHA (5.0 µg/ml) (207,664)	14,211	n.d.	see Fig. 53
PHA (2.5 µg/ml) (204,047)	5,680	n.d.	see Fig. 53
NK cells (/µl)			
$CD16^+CD56^+$ (130-720) (170-1,100)	84	416	494
B cells (/µl)			
$CD19^+$ (390-1,400) (300-2,000)	298	3[3]	1596
B cells (%)			
$CD19^+CD27^-IgD^+$ naïve B cells (50-77)	97	n.d.	n.d.
$CD19^+CD27^+IgD^+$ memory B cells (5-16)	3	n.d.	n.d.
$CD19^+CD27^+IgD^-$ switched-memory B cells (2-6)	0	n.d.	n.d.
Serum immunoglobulins (g/l)			
IgG (4.9-16.1)	4.3	n.d.	n.d.
IgA (0.40-2.00)	0.4	n.d.	n.d.
IgM (0.50-2.00)	0.45	n.d.	n.d.
Specific antibodies[4]			
Tetanus toxoïd (0.1-10 IU/ml)	2.94	n.d.	n.d.
H. influenzae type b (1.0-20 mg/l)	1.0	n.d.	n.d.

n.d.: not determined. [1]Age-matched normal values are indicated in separated parentheses for the patient and the newborn brother when differing. [2]Results of a healthy control are indicated in parentheses. [3]After having been treated with rituximab. [4]The patient had received four 5-valent vaccines against *Haemophilus influenzae type b*, the toxoïd of *Corynebacterium diphtheriae*, *Bordetella pertussis*, the toxoïd of *Clostridium tetani* and *Poliovirus* type *1, 2, and 3*.

The patient had predominant $CD4^+$ T cell lymphopenia with an inverse CD4/CD8 ratio and an altered proportion of $TCR\alpha\beta^+$ and $TCR\gamma\delta^+$ cells. Only 43.6% of $CD4^+$ T_H had a $CD45RA^+CD27^+$ naïve phenotype, while 48.9% were $CD45RA^-CD27^+$ T_{CM} and 7.4% $CD45RA^-CD27^-$ peripheral effector T cells. Only 7.3% of the $CD8^+$ T_{Cyt} were $CD45RA^+CD27^+$ naïve and 8.6% were $CD45RA^-CD27^+$ T_{CM} while 31.5% were $CD45RA^-CD27^-$ peripheral effector and 52.5% $CD45RA^+CD27^-$ exhausted T_{EMRA}-like cells. The percentage of HLA-DR^+ cells was increased (11.8%) and that of $CD4^+CD25^+CD127^{low}$ T_{Reg} was reduced (2.5%). $CD3^+CD161^+V\alpha7.2^+$ MAIT cells (1.57%) were present but $CD3^+V\alpha24^+V\beta11^+$ iNKT cells were virtually absent. The patient had increased $CD3^+CD25^-CD127^-$ T cells as compared to his healthy brother (Fig. 52A and B). The proliferation capacity of the patient's T cells was reduced in response to PHA as compared to a healthy control (Tab. 8).

The newborn had a normal amount of TRECs but combined $CD4^+$ and $CD8^+$ T cell lymphopenia with a reduced CD4/CD8 ratio and an altered proportion of $TCR\alpha\beta^+$ and $TCR\gamma\delta^+$ cells (Tab. 8). Only 54.6% of $CD4^+$ T_H had a $CD45RA^+CD27^+$ naïve phenotype, while 44.8% were $CD45RA^-CD27^+$ T_{CM}. 82.0% of the $CD8^+$ T_{Cyt} were $CD45RA^+CD27^+$ naïve and 17.9% were $CD45RA^-CD27^+$ T_{CM} while there were no $CD45RA^-CD27^-$ peripheral effector and $CD45RA^+CD27^-$ exhausted T_{EMRA}-like cells detectable. The percentages of HLA-DR^+ cells (0.266%) and of $CD4^+CD25^+CD127^{low}$ T_{Reg} (5.05%) were normal. $CD3^+CD161^+V\alpha7.2^+$ MAIT cells (0.4%) and $CD3^+V\alpha24^+V\beta11^+$ iNKT cells (0.066%) were present. The newborn had an unsuspicious amount of $CD3^+CD25^-CD127^-$ T cells (Fig. 52C). However, T cell blast proliferation of the newborn after stimulation with IL-2, anti-CD3- + anti-CD28-beads or PMA + ionomycin, respectively, was impaired as compared to a healthy control, even though both were able to upregulated CD25 after stimulation in a comparable manner (Fig. 53).

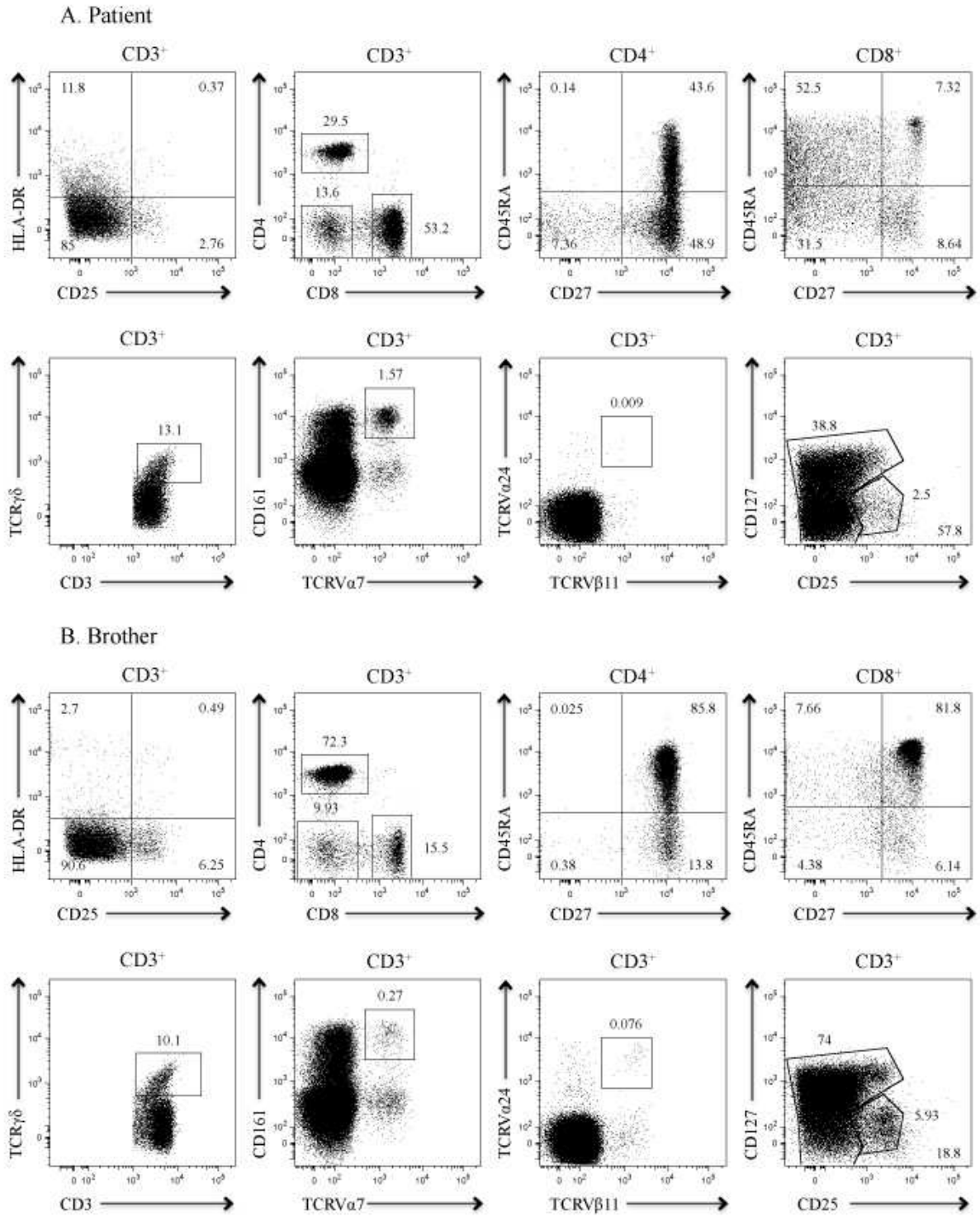
A. Patient
CD3+
11.8
0.37
85
2.76
HLA-DR
CD25
CD3+
29.5
13.6
53.2
CD4
CD8
CD4+
0.14
43.6
7.36
48.9
CD45RA
CD27
CD8+
52.5
7.32
31.5
8.64
CD45RA
CD27
CD3+
13.1
TCRγδ
CD3
CD3+
1.57
CD161
TCRVα7
CD3+
0.009
TCRVα24
TCRVβ11
CD3+
38.8
2.5
57.8
CD127
CD25
B. Brother
CD3+
2.7
0.49
90.6
6.25
HLA-DR
CD25
CD3+
72.3
9.93
15.5
CD4
CD8
CD4+
0.025
85.8
0.38
13.8
CD45RA
CD27
CD8+
7.66
81.8
4.38
6.14
CD45RA
CD27
CD3+
10.1
TCRγδ
CD3
CD3+
0.27
CD161
TCRVα7
CD3+
0.076
TCRVα24
TCRVβ11
CD3+
74
5.93
18.8
CD127
CD25

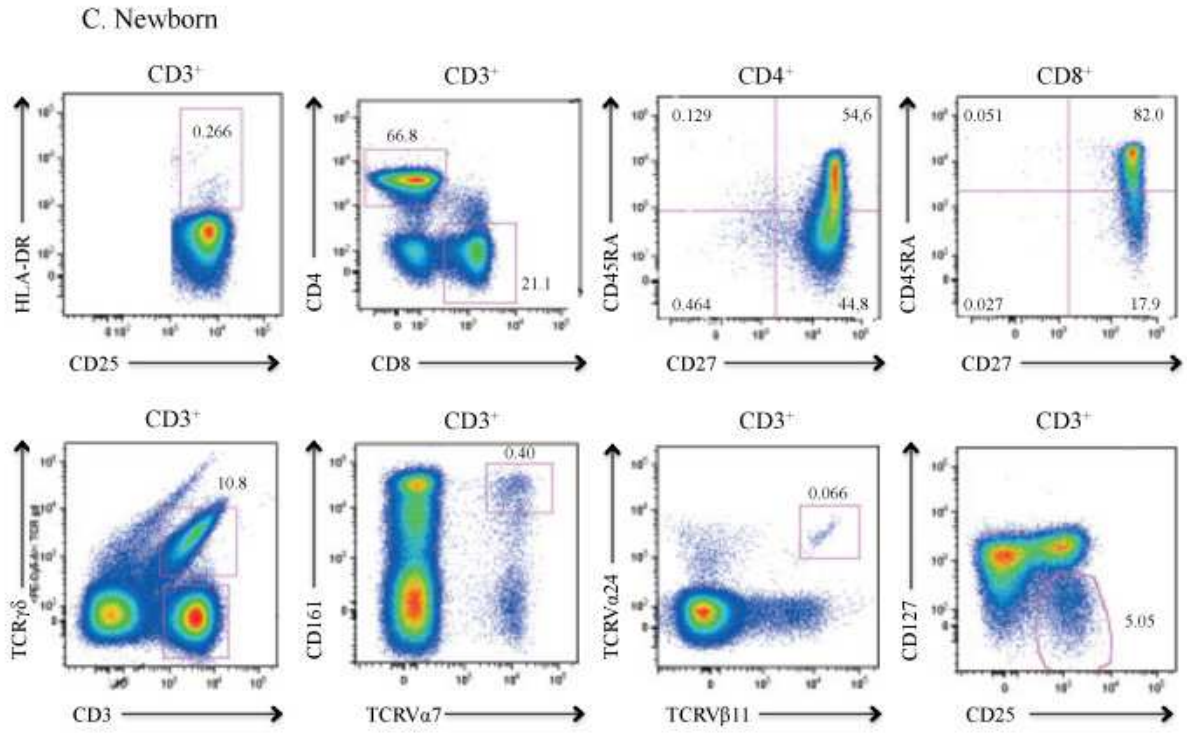

Figure 52. Immunophenotype of ITK-deficient PBMCs.

Flow cytometric analysis of PBMCs of the ITK-deficient patient (A), his healthy brother (B) and the newborn brother (C) for the expression of HLA-DR and CD25, CD4 and CD8, CD45RA and CD27 after gating on total $CD3^+$ T cells and $CD3^+CD4^+$ T_H and $CD3^+CD8^+$ T_{Cyt}, respectively, is shown. Determination of the percentages of $CD3^+TCR\gamma\delta^+$ cells, $CD161^+V\alpha7.2^+$ MAIT, $V\alpha24^+V\beta11^+$ iNKT and $CD25^+CD127^{low}$ T_{Reg} after gating on total $CD3^+$ T cells is given. The corresponding percentages are indicated for each square.

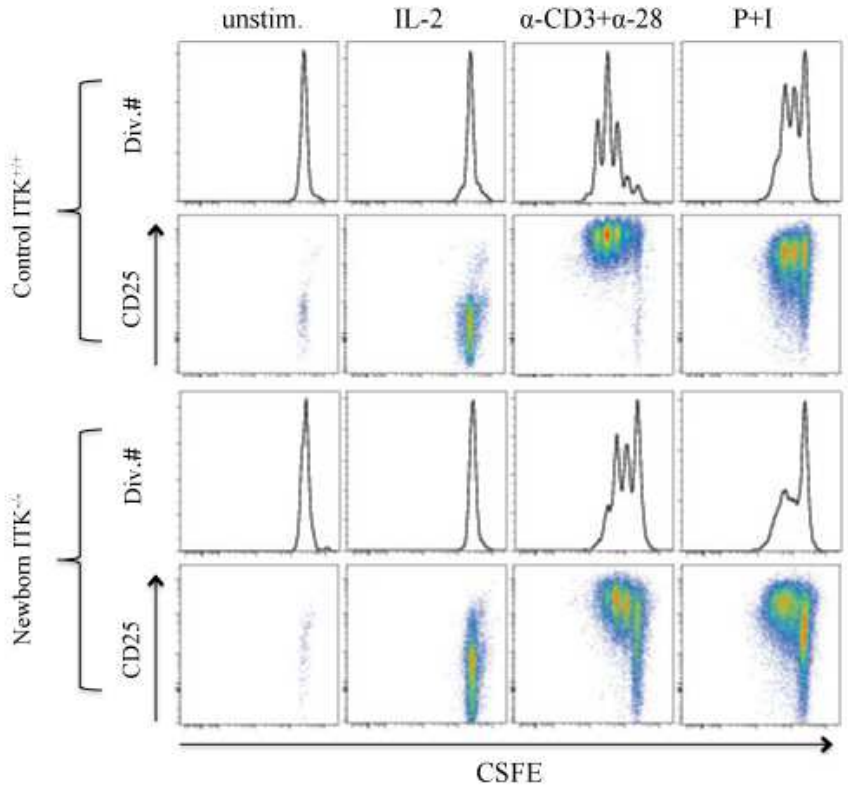

Figure 53. Proliferation of T cell blasts of the newborn ITK-deficient brother.

Flow cytometric analysis of T cell blast proliferation as a function of CSFE-dilution and CD25-upregulation after stimulation with IL-2, anti-CD3- + anti-CD28-beads or PMA + ionomycin are shown for a healthy control and the ITK-deficient newborn brother, respectively.

For the patient ITK-deficient, the TCRVβ repertoire for TCRαβ$^+$CD3$^+$CD4$^+$ and TCRαβ$^+$CD3$^+$CD4$^-$ T cells was analysed by flow cytometry using fluorochrome-labelled mAbs directed against 24 distinct TCRVβ families (IOTest Beta Mark TCR Repertoire Kit, Beckman Coulter). All the analysed TCRVβ families were present in the TCRαβ$^+$CD3$^+$CD4$^+$ and TCRαβ$^+$CD3$^+$CD4$^-$ T cell fractions, thus excluding a major perturbation of thymic repertoire selection (Fig. 54A and B). When comparing the relative expression of the distinct TCRVβ families to age-matched normal values, in TCRαβ$^+$CD3$^+$CD4$^+$ T cells two TCRVβ families were reduced (Vβ11 and Vβ13.1) and two were expanded (Vβ12 and Vβ18) and in TCRαβ$^+$CD3$^+$CD4$^-$ T cells five TCRVβ families were reduced (Vβ1, Vβ4, Vβ5.2, Vβ7.1 and Vβ11) and three were expanded (Vβ13.1, Vβ20 and Vβ23) (Tab. 9).[462] The reduced or expanded TCRVβ families did not correlate in between the TCRαβ$^+$CD3$^+$CD4$^+$ and the TCRαβ$^+$CD3$^+$CD4$^-$ T cell populations. Whether this alterations were due to subtle thymic repertoire selection defects or were a consequence of T cell lymphopenia and chronic viral

infection and malignancy remained unclear, but taking into account the altered T cell phenotypes described above the latter possibility seemed more probable.

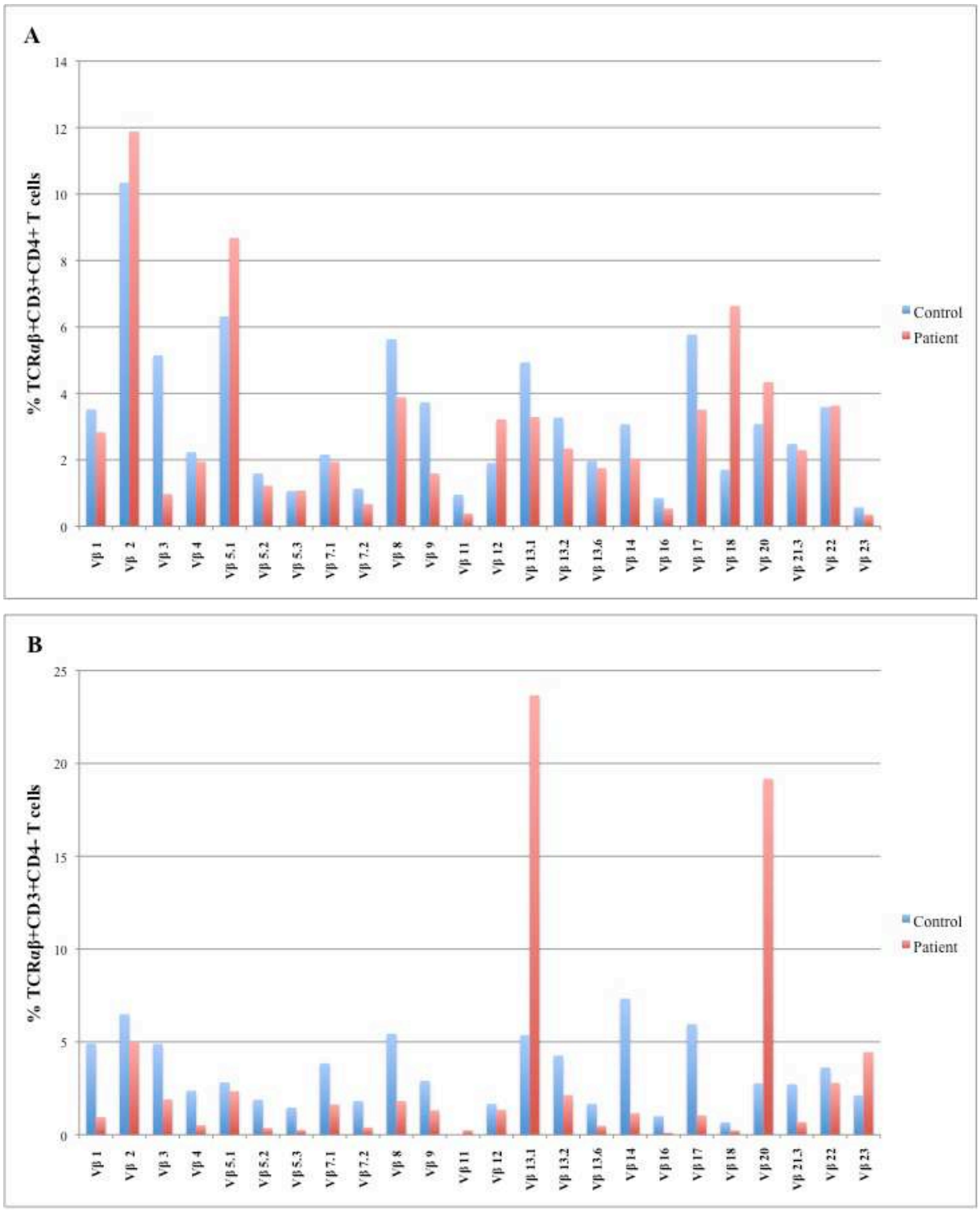

Figure 54. Analysis of the ITK-deficient patient's TCRVβ repertoire by flow cytometry.

PBMCs of the ITK-deficient patient were stained with mAbs against TCRαβ, CD3, CD4 and 24 Vβ families. After gating on (A) $TCR\alpha\beta^{+}CD3^{+}CD4^{+}$ and (B) $TCR\alpha\beta^{+}CD3^{+}CD4^{-}$ T cells the relative usage of the distinct TCRVβ families was determined and compared to age-matched normal values.[462]

Table 9. TCRVβ repertoire of the ITK-deficient patient.

TCR Vβ	$CD4^+$ %	$CD4^-$ %	TCR Vβ	$CD4^+$ %	$CD4^-$ %
Vβ1	2.83 (3.52, 0.77)[1]	0.95 (4.91, 1.23)	Vβ12	3.22 (1.90, 0.33)	1.34 (1.66, 0.68)
Vβ2	11.88 (10.34, 1.62)	5.03 (6.49, 1.75)	Vβ13.1	3.29 (4.93, 0.38)	23.66 (5.37, 1.40)
Vβ3	0.97 (5.14, 3.06)	1.90 (4.89, 2.78)	Vβ13.2	2.34 (3.27, 1.28)	2.14 (4.26, 1.53)
Vβ4	1.94 (2.23, 0.28)	0.51 (2.37, 0.39)	Vβ13.6	1.75 (1.97, 0.36)	0.48 (1.66, 0.66)
Vβ5.1	8.68 (6.32, 1.15)	2.34 (2.82, 0.82)	Vβ14	2.04 (3.07, 0.70)	1.16 (7.33, 2.20)
Vβ5.2	1.22 (1.59, 0.20)	0.36 (1.88, 0.41)	Vβ16	0.53 (0.85, 0.20)	0.11 (1.00, 0.38)
Vβ5.3	1.07 (1.06, 0.14)	0.26 (1.46, 1.11)	Vβ17	3.51 (5.77, 1.13)	1.04 (5.96, 1.88)
Vβ7.1	1.94 (2.16, 0.58)	1.63 (3.85, 0.70)	Vβ18	6.63 (1.70, 0.82)	0.23 (0.67, 0.39)
Vβ7.2	0.67 (1.13, 0.72)	0.39 (1.81, 1.22)	Vβ20	4.34 (3.08, 0.83)	19.17 (2.77, 1.37)
Vβ8	3.88 (5.63, 0.93)	1.82 (5.44, 1.64)	Vβ21.3	2.29 (2.48, 0.32)	0.69 (2.72, 0.74)
Vβ9	1.59 (3.73, 0.51)	1.31 (2.90, 0.61)	Vβ22	3.63 (3.59, 0.34)	2.79 (3.62, 1.27)
Vβ11	0.38[2] (0.95, 0.14)	0.24 (0.91, 0.20)	Vβ23	0.35 (0.57, 0.19)	4.45 (2.12, 0.71)
Total $CD4^+$	71.02 (76.98, 2.23)		**Total $CD4^-$**	74.04 (77.78, 8.78)	

[1]Age matched normal values are indicated in parentheses as the mean and standard deviation.

[2]Outliers are defined as outwith three standard deviations and are indicated in red.[462]

NK and B cell counts were normal in the ITK-deficient patient and the ITK-deficient newborn brother. In the patient, $CD19^+CD27^+IgD^+$ memory B cells were reduced and $CD19^+CD27^+IgD^-$ switched-memory B cells were absent, IgM and IgG were slightly reduced and IgA was found at the lower normal range. Specific antibodies against the tetanus toxoïd and the components of *H. influenzae type b* were present, even thought the latter was at the lower normal range (Tab. 8).

Taken as a whole, the ITK-deficient patient showed normal V(D)J-recombination and qualitative thymic output as judged by the polyclonal αβ TCR repertoire. However later on, he developed progressive loss of naïve $CD4^+$ T_H and naïve $CD8^+$ T_{Cyt} and innate-like NKT cells were virtually absent while MAIT cells were preserved. The ITK-deficient newborn brother had normal TRECs but combined $CD4^+$ T_H and $CD8^+$ T_{Cyt} lymphopenia with the latter being more reduced. However, innate-like MAIT and iNKT cells were present. Both ITK-deficient patient and newborn brother displayed defective T cell proliferation. In combination, these data might argue for a TCR:CD3:ζ-signalling-related disorder slightly affecting thymic lineage commitment and more prominently interfering with peripheral T cell homeostasis. In the patient, the remaining peripheral T cell populations displayed memory-like phenotypes

more pronounced for the $CD8^+$ T_{Cyt} compartment and reduced CD127 expression probably as a consequence of LIP and CIP. In the newborn brother, the proportions of memory-like $CD4^+$ T_H but also of $CD8^+$ T_{Cyt} were increased, but not yet as pronounced as in the older and diseased patient. It is likely that $CD4^+$ T_H were not able to provide adequate help towards B cells as judged by borderline hypogammaglobulinaemia and weak specific antibody responses towards vaccination antigens in the patient. Together, these findings suggest a more subtle TCR:CD3:ζ-signalling defect than that found in LCK- and ZAP-70-deficiency, with a loss of naïve T cells over time as a sign of disturbed peripheral T cell homeostasis.

3.3.3 Gene defect

The clinical and immunological phenotypes of the patient were indicative of a T cell immunodeficiency. Taking into account that $CD4^+$ T cell lymphopenia and EBV-driven pulmonary Hodgkin's-like disease are hallmarks of ITK-deficiency, ITK gene defect was considered.[420, 463] The exons 1-17 including the flanking intronic regions of *ITK* (NG_016276.1) were sequenced (for primer information see Tab. 10) from genomic DNA isolated from PBMCs of the patient, his parents and his two siblings. PBMCs of the patient and his newborn brother were found to carry the homozygous nucleotide transition *ITK* c.626G>A (NM_005546.3) changing codon 209 (TGG) into a premature stop codon (TAG). The patient's parents and the older sibling were found to be heterozygous carriers of the transition (Fig. 55A). At the protein level, the premature stop condon results in a truncated ITK form (p.W209X) which lacks the SH2 and the kinase domains. While the expected molecular weight of wildtype ITK is 71.8 kDa, the molecular weight of the truncated ITK p.W209X is 8.94 kDa (Fig. 54B).

Table 10. Genomic *ITK* sequencing primers.

Primer name	Primer sequence
Forward primer exon 1	5'-GAAAGGATGTGGTTTCGGCCTTTG-3'
Reverse primer exon 1	5'-TTTCCTGTGCTCTATTTTATGCTATG-3'
Forward primer exon 2	5'-GCCAATGGATCTTATCTAGCAGTAG-3'
Reverse primer exon 2	5'-CTGCACCCGGCTGTGACTGAAG-3'
Forward primer exon 3	5'-CACTCTCGGCTCAGTAGGTCTG-3'
Reverse primer exon 3	5'-TCTCACACCACACTCTATTCTATTG-3'
Forward primer exon 4	5'-GGCTCACTCAGCCAGGTCTAATC-3'
Reverse primer exon 4	5'-TGCATTCTGTTCCTGACACCCTC-3'

Forward primer exon 5	5'-CAAGTCAGGTTTCACTGTGTCTTAT-3'
Reverse primer exon 5	5'-GACATGCAAATAGGAACATGCCAAT-3'
Forward primer exon 6	5'-CCAGAGGAAGGCAGACTGTCTC-3'
Reverse primer exon 6	5'-CTGTGGGAGATAGGACAAATCATC-3'
Forward primer exon 7	5'-ATATTCCCCAATCTTTAAATGACTTTTA-3'
Reverse primer exon 7	5'-AGTCAACCAATAATTTATTCCTAACTTA-3'
Forward primer exon 8	5'-ATGACCATATGATTTTCTAGCATTGTC-3'
Reverse primer exon 8	5'-GCCTGCCAAATCGCTGGGATTC-3'
Forward primer exon 9	5'-CCTACAGTATTTCCTCCTTCTGTG-3'
Reverse primer exon 9	5'-CTACCTCTTGCACTGTCTAACTTTG-3'
Forward primer exon 10	5'-GTTATAAGACAAAGATAATAAGAACTTAA-3'
Reverse primer exon 10	5'-AGAAGGCAGAGCTCAGGCAGTAA-3'
Forward primer exon 11	5'-TAGTGATTTAAGTTAGATGGTTGCTAG-3'
Reverse primer exon 11	5'-ATTTGTAGTCTGAGGAACAGGTAG-3'
Forward primer exon 12	5'-GGCTAAAATTCTAGTTAGGGCTTTAT-3'
Reverse primer exon 12	5'-GCATTTCAAGAACACTGAACCGAT-3'
Forward primer exon 13	5'-AGACAAAATGACCATTGGCTATTTTG-3'
Reverse primer exon 13	5'-AGATTATCTGTAATGTATTATTTATTAATG-3'
Forward primer exons 14, 15	5'-TGCAGTAAAGCAAAGGACTGTGATT-3'
Reverse primer exons 14, 15	5'-CAGGGTTCAGTGTGGGTAGGGTT-3'
Forward primer exon 16	5'-AATCCTAATGCAAGGAGTCTGTAATT-3'
Reverse primer exon 16	5'-TGCCTCATCCTTCTGAGAGGGTT-3'
Forward primer exon 17	5'-AATCCACAGGGGATGCTGCTATTA-3'
Reverse primer exon 17	5'-GCACCACATGTGACAAGAGGCTA-3'

To analyse the effect of the p.W209X mutation on ITK expression, T cell blasts of a healthy control, the patient and his family members were expanded as described in paragraphe 3.1.3 with the exception that PMA 10 ng/ml, ionomycin 1 µM and IL-2 100 U/ml were used. Total protein extracts were obtained and analysed by immunoblotting with a mouse anti-ITK mAb directed against the N-terminus (#2380, Cell Signaling Technology) and an anti-actin mAb as a loading control. While control cells expressed ITK, there was no detectable expression in the cells of the patient, thus indicating that p.W209X is an amorphic (null) mutation. The heterozygous family members displayed intermediate ITK expression levels (Fig. 55C). Of note, they are healthy, have already encountered EBV and have not developed clinical signs of immunodeficiency or lymphoproliferation so far.

A

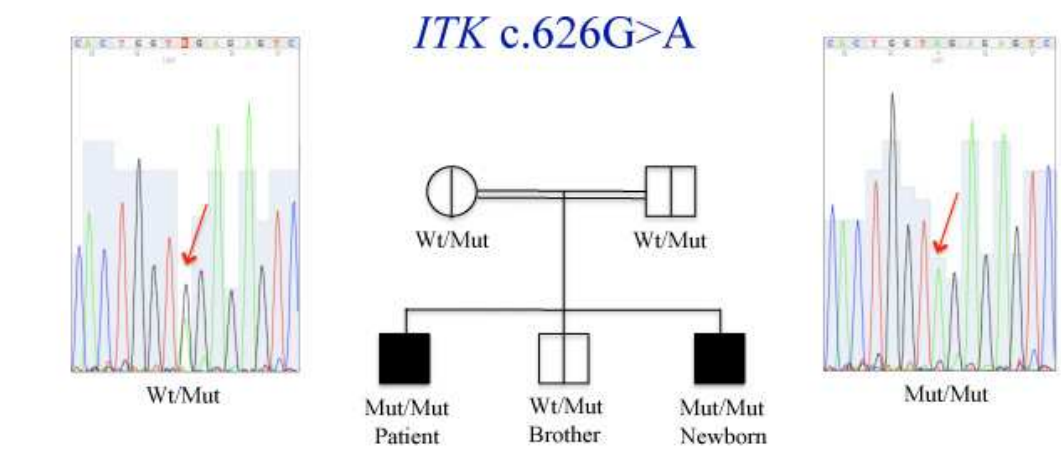
ITK c.626G>A
Wt/Mut
Wt/Mut
Wt/Mut
Mut/Mut
Patient
Wt/Mut
Brother
Mut/Mut
Newborn
Mut/Mut

B

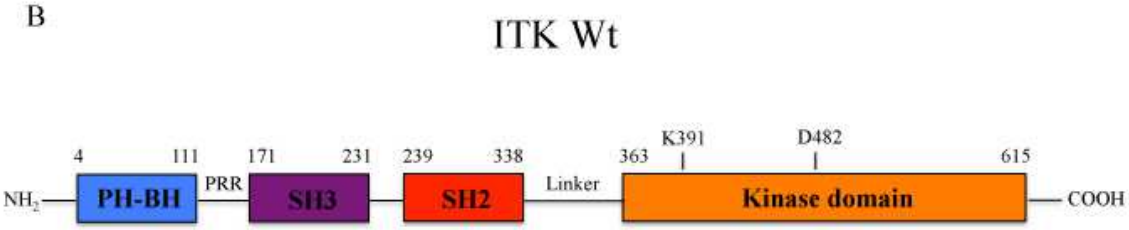
ITK Wt
4
111
171
231
239
338
363
K391
D482
615
NH2
PH-BH
PRR
SH3
SH2
Linker
Kinase domain
COOH

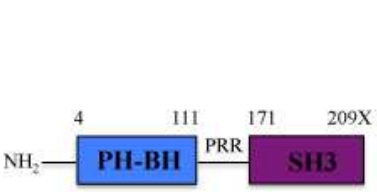
ITK p.W209X
4
111
171
209X
NH2
PH-BH
PRR
SH3

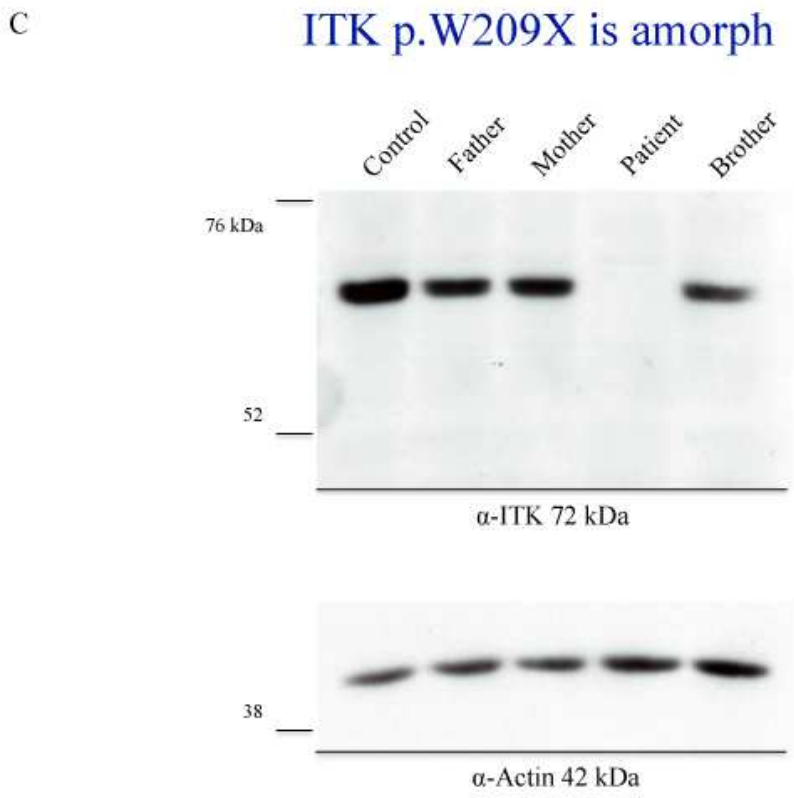

Figure 55. Genetic analysis of the ITK-deficient patient and his family.

(A) The pedigree and the corresponding electropherograms obtained by sequencing the exons including the intronic regions of *ITK* of the index patient and his family are shown The ITK-deficient patient and his newborn brother (black squares) were found homozygous for the nonsense mutation *ITK* c.626G>A (red arrow), while the mother, father and healthy brother (white circle and squares with vertical line, respectively) were heterozygous (red arrow).

(B). The domain structure of wildtype ITK (Wt) and truncated ITK p.W209X are shown. The PH-BH, SH2, SH3 and kinase domains are indicated in blue, purple, red and orange, respectively. The PRR and the SH2-kinase-linker are indicated by black solid lines, and the amino acids numbers corresponding to the domain boundaries as well as the ATP-binding K391 and the proton acceptor D482 are indicated (not drawn to scale). For ITK p.W209X the positioning of the premature stop is given (not drawn to scale).

(C) Total protein extracts of a healthy control, the father, mother, patient and his healthy brother were separated by SDS-PAGE and subjected to immunblotting with mAbs raised against ITK (α-ITK) and actin (α-Actin). Molecular weight markers in kDa are given on the left (black lines) and name and molecular weight of specific bands are indicated on the bottom.

3.3.4 Analysis of TCR:CD3:ζ-signalling in ITK-deficiency

In order to characterize the consequence of the ITK p.W209X mutation on proximal TCR:CD3:ζ-signalling, PMA and ionomycin expanded T cell blasts were stimulated with anti-CD3 antibody for 0, 2, 5, 15 and 30 minutes or with PMA and ionomycin for 30 minutes.

Protein lysates were obtained and analysed by immunoblotting with mAbs directed against phosphorylated tyrosine residues. While TCR:CD3:ζ-stimulation in T cell blasts of a healthy control resulted in strong protein tyrosine phosphorylation, in cells of the ITK-deficient patient the signal was weak. Interestingly, in cells of the brother of, who is a heterozygous carrier of the ITK p.W209X mutation, the signal was intermediate. All bands corresponding to known TCR:CD3:ζ-signalling substrates such as the ζ-chain, LCK, ZAP-70, LAT, SLP-76, PLCγ-1 and CBL were detectable. Protein loading was controlled by immunoblotting for actin and found to be equal for all samples (Fig. 56).

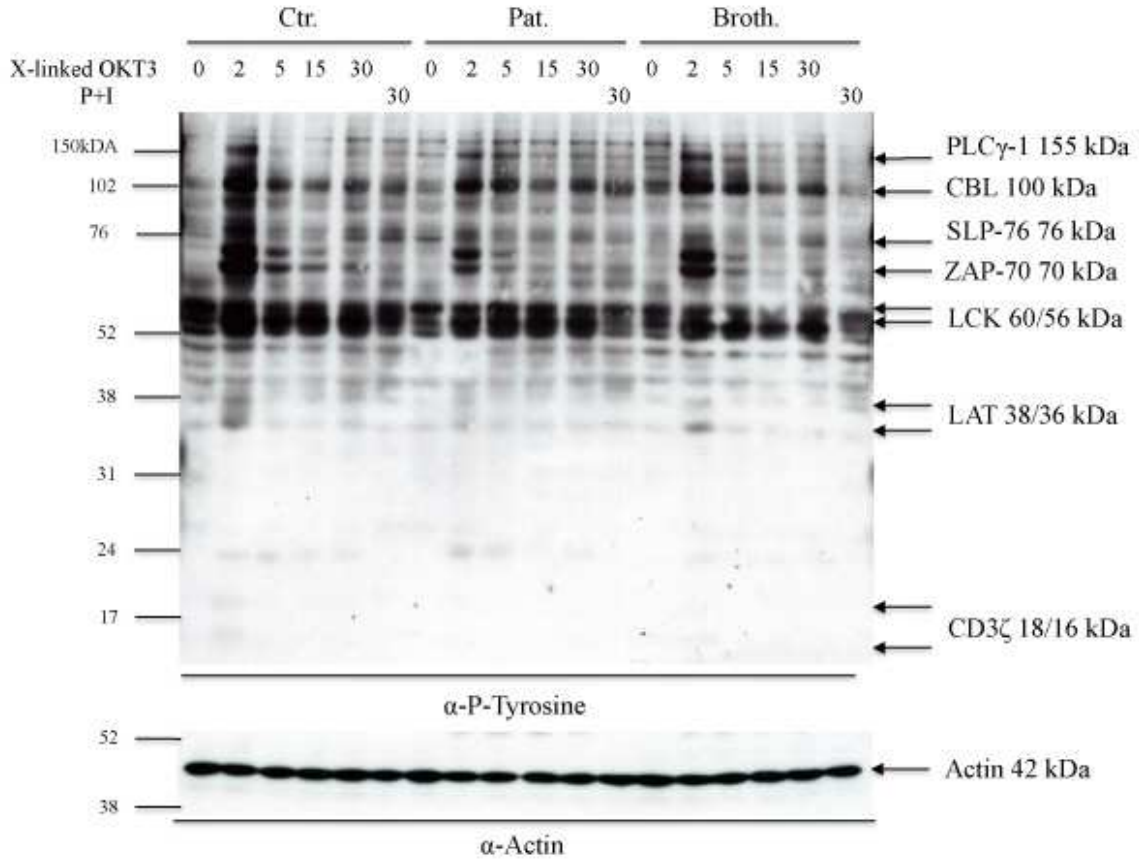

Figure 56. Impaired protein tyrosine phosphorylation in ITK-deficient T cell blasts.

T cell blasts of a healthy control (Ctr.), the ITK-deficient patient (Pat.) and his heterozygous brother (Broth.) were stimulated with OKT3 1 µg/ml cross-linked with polyclonal rabbit anti-mouse Ig 2 µg/ml (x-linked OKT3) for 0, 2, 5, 15 and 30 minutes or with PMA 10 ng/ml and ionomycin 1 µM (P+I) for 30 minutes. Protein extracts were separated by SDS-PAGE and immunblotting with mAbs against phosphorylated tyrosine residues (α-P-Tyrosine) or actin (α-Actin) was performed. Molecular weight markers in kDa are given on the left (black lines) and names and molecular weights of specific bands are indicated on the right (black arrows).

TCR:CD3:ζ-induced activation of the LAT:SLP-76-signalosome intermediates was analysed by immunoblotting with mAbs against phosphorylated PKCθ or actin as a loading control. A strong phosphorylation of PKCθ was detected in response to CD3 stimulation in

control cells, but in the ITK-deficient patient cells PKCθ phosphorylation was markedly weakened, while in cells of his brother heterozygous for the ITK p.W209X mutation the signal was moderately decreased. (Fig. 57).

Therefore, the signalling strenght of TCR:CD3:ζ-induced protein tyrosine phosphorylation and phosphorylation of PKCθ correlated with ITK expression levels in T cell blasts with high signals in control cells with normal ITK expression, intermediate signals in cells with diminished ITK expression heterozygous for the ITK p.W209X mutation and low signals in cells with no ITK expression homozygous for the ITK p.W209X mutation. Even though ITK is classically located downstream of TCR:CD3:ζ-signalling as a molecular participant of the LAT:SLP-76-signalosome and phosphorylates PLCγ−1, the ITK-dose dependent protein tyrosine phosphorylation proposes that it might also play a role in proximal TCR:CD3:ζ-signalling by amplifying initial tyrosine phosphorylation including ITAM- and ZAP-70-phosphorylation.[172, 173]

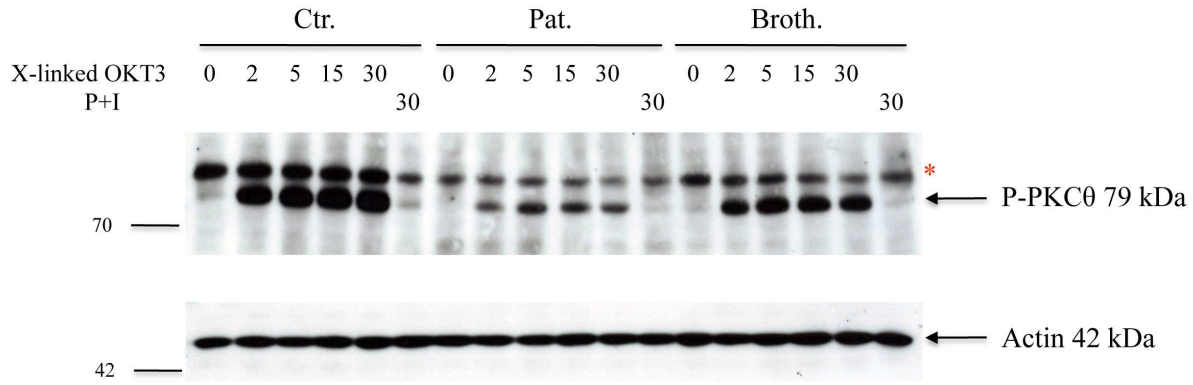

Figure 57. Impaired PKCθ phosphorylation in ITK-deficient T cell blasts.

T cell blasts of a healthy control (Ctr.), the ITK-deficient patient (Pat.) and his heterozygous brother (Broth.) were stimulated with OKT3 1 µg/ml cross-linked with polyclonal rabbit anti-mouse Ig 2 µg/ml (x-linked OKT3) for 0, 2, 5, 15 and 30 minutes or with PMA 10 ng/ml and ionomycin 1 µM (P+I) for 30 minutes. Protein extracts were separated by SDS-PAGE and immunblotting with mAbs to phosphorylated PKCθ (P-PKCθ) and actin (Actin) was performed. Molecular weight markers in kDa are given on the left (black lines) and names and molecular weights of specific bands are indicated on the right (black arrows). Unspecific bands are marked with a red asterisk.

Ca^{2+}-flux was analysed in ITK-deficient T cell blasts in response to TCR:CD3:ζ-stimulation by flow cytometry as described in paragraphe 3.1.4. Cells of the ITK-deficient patient, his heterozygous brother and his newborn brother, who is a homozygous carrier of the ITK p.W209X mutation, were analysed and compared to cells of healthy controls. Cells of the

newborn brother were analysed separately in a later experiment. Stimulation with anti-CD3 induced a clear Ca^{2+}-flux in $CD4^+$ T_H and $CD8^+$ T_{Cyt} of the healthy controls and the heterozygous brother whereas no significant Ca^{2+}-flux was observed in $CD4^+$ T_H and $CD8^+$ T_{Cyt} of the ITK-deficient patient (Fig. 58A and B). In contrast, in cells of the newborn, the Ca^{2+}-flux was not completely abolished and residual Ca^{2+}-flux was detectable (Fig. 58C). Stimulation with ionomycin resulted in strong Ca^{2+}-fluxes in all analysed cell populations (Fig. 58).

Thus, the ITK-dose dependent effects observed for protein tyrosine phosphorylation and phosphorylation of PKCθ were not recapitulated by the Ca^{2+}-flux amplitude, that was completely abrogated in T cell blasts of the patient and normal in those of the heterozygous brother. Maybe full amplitude of PLCγ-1-mediated Ca^{2+}-flux is obtained by suboptimal ITK-signalling strenght as observed in the heterozygous carrier but with different oscillation kinetics, that cannot be monitored by this *in vitro* technique. Importantly, T cell blasts of the newborn displayed residual Ca^{2+}-flux suggesting an ITK-independent PLCγ-1-activation mechanism. The total absence of Ca^{2+}-flux in the ITK-deficient patient might be biased and a consequence of T cell exhaustion as the experiment was done from blood samples at a time when the patient was severely diseased. Also, the experimental conditions in Fig. 58A and B were suboptimal as not enough cells were available and analysed for the patient and his brother, explaining the strong fluctuations of the particular curves. Further experiments will need to clarify this observations.

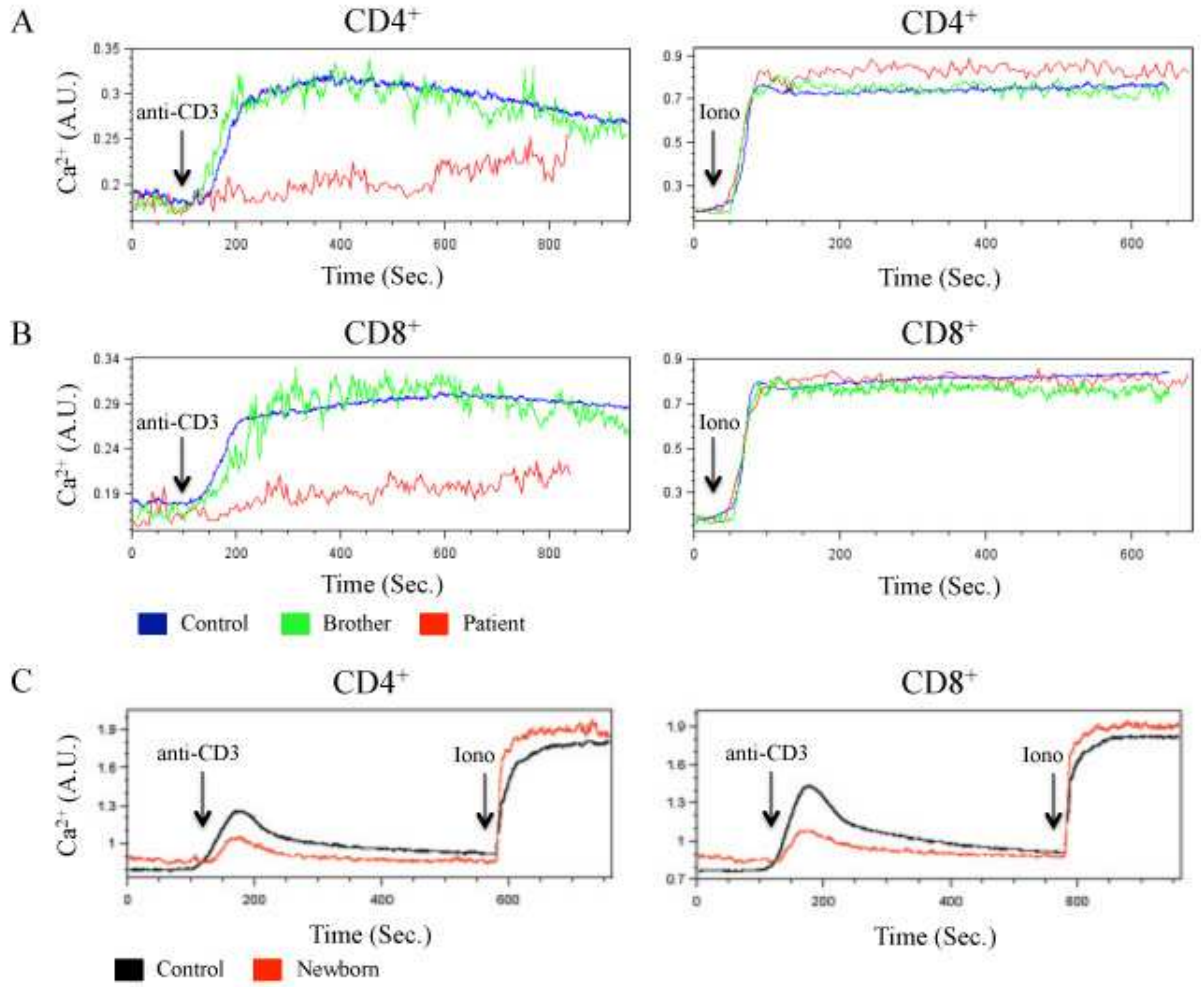

Figure 58. Impaired Ca^{2+}-flux in ITK-deficient T cell blasts.

(A and B) T cell blasts of a healthy control (blue), the ITK-deficient patient (green), the heterozygous brother (red) and (C) the newborn ITK-deficient brother were stained with anti-CD4 and anti-CD8, charged with 5 µM of the Ca^{2+}-sensitive fluorescent dye Indo-1-acetoxymethyl ester and Ca^{2+}-flux of the particular $CD4^+$ and $CD8^+$ populations were analysed with a FACS ARIA II. Aliquots of the T cell blasts were left unstimulated for two minutes, than either stimulated with OKT3 1 µg cross-linked with rabbit-anti-mouse-IgG 10 µg (anti-CD3, vetrtical arrow) or ionomycin 1 µM (Iono, vertical arrow). Ca^{2+}-flux was calculated and expressed in arbitrary units (A.U.) and expressed over time (Sec.).

TCR:CD3:ζ-induced distal signalling was analysed by looking at NFATc2 and ERK-1/2 activation. While control T cell blasts displayed efficient dephosphorylation and rephosphorylation of NFATc2 upon CD3 stimulation, T cell blasts of the ITK-deficient patient exhibited only residual signals and in T cell blasts of the heterozygous brother signals were intermediate. Same profiles were observed for ERK-1/2 phosphorylation that was effective in control cells, residual in ITK-deficient patient cells and intermediate in cells of the heterozygous brother. Stimulation with PMA and ionomycin that bypasses proximal TCR:CD3:ζ-signalling resulted in equally strong dephosphorylation of NFATc2 and

phosphorylation of ERK-1/2 in cells of the control, the ITK-deficient patient and the heterozygous brother (Fig. 59).

Thus, the ITK-dose dependent effects observed for protein tyrosine phosphorylation and phosphorylation of PKCθ were recapitulated by the amplitude of MAPK and NFAT activation, both of which integrate multiple upstream pathways for proper activation.

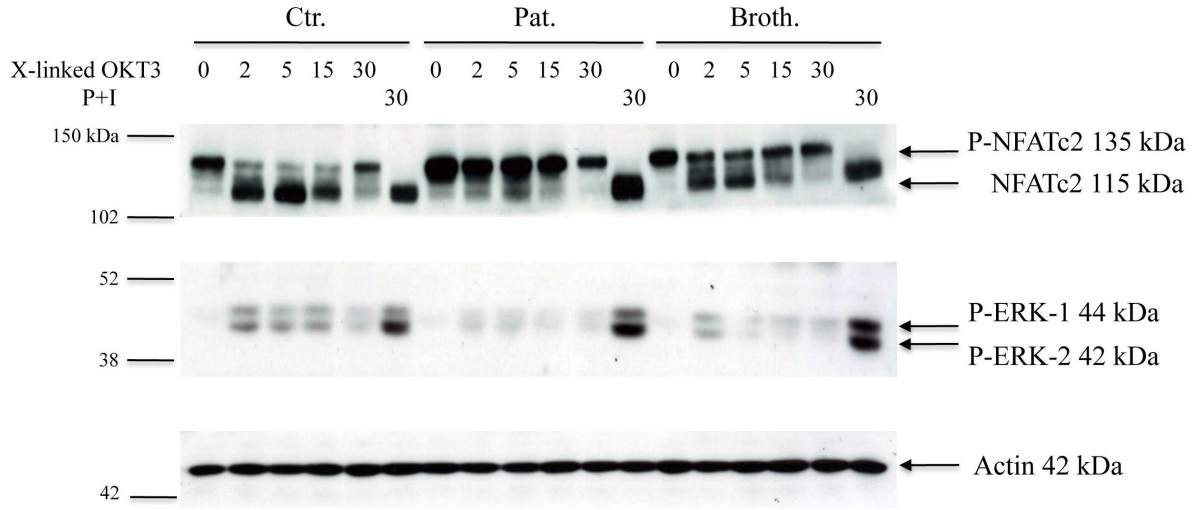

Figure 59. Impaired distal TCR:CD3:ζ-signalling in ITK-deficient T cell blasts.

T cell blasts of a healthy control (Ctr.), the ITK-deficient patient (Pat.) and his heterozygous brother (Broth.) were stimulated with OKT3 1 µg/ml cross-linked with polyclonal rabbit anti-mouse Ig 2 µg/ml (x-linked OKT3) for 0, 2, 5, 15 and 30 minutes or with PMA 10 ng/ml and ionomycin 1 µM (P+I) for 30 minutes. Protein extracts were separated by SDS-PAGE and immunblotting was performed with mAbs against NFATc2 (P-NFATc2 and NFATc2), phosphorylated ERK-1/2 (P-ERK-1 and P-ERK-2) and actin (Actin) as a loading control. Molecular weight markers in kDa are given on the left (black lines) and names and molecular weights of specific bands are indicated on the right (black arrows).

EBV-associated lymphoproliferative disease with a preferential localization to the lungs seems to be a particular feature of human ITK-deficiency.[420, 463, 464] This might reflect a defect in migration of T cells towards the lungs as Itk was shown to be involved in chemokine receptor signalling and T cell migration based on studies in *Itk*$^{-/-}$ mice.[465-468] To test this hypothesis, chemokine-dependent CD4^{+} and CD8^{+} T cell blast migration was analysed for the ITK-deficient patient and compared to that of cells from a healthy control. A Boyden chamber 5 µm transwell system was used and relative migration towards medium alone, stromal cell-derived factor 1 (SDF-1) and chemokine C-C motif ligand 21 (CCL21) was determined. As internal control, SDF-1- and CCL21-dependent migration was blocked by adding the CXC chemokine receptor type 4 (CXCR4) blocking agent AMD3100 (Plerixafor) and the CC chemokine receptor type 7 (CCR7) blocking mAb anti-CCR7, respectively. ITK-deficient

$CD4^+$ and $CD8^+$ T cell blasts showed reduced spontaneous migration towards empty medium and reduced specific migration towards SDF-1 and CCL21 when compared to cells of a healthy control. Specific migration of $CD4^+$ and $CD8^+$ T cell blasts of the ITK-deficient patient was completely abrogated by the CXCR4- and CCR7-blocking agents, while that of a healthy control was only partially reduced (Fig. 60). Therefore, these data show that ITK-deficient T cells display impaired spontaneous migration and specific chemokinesis.

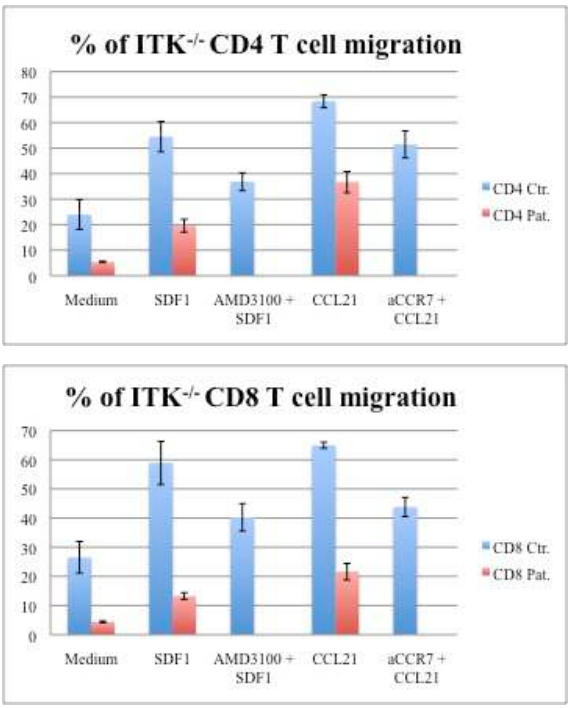

Figure 60. Impaired migration of ITK-deficient T cell blasts.

The percentages of $CD4^+$ and $CD8^+$ T cell blasts migrating in a Boyden chamber 5 µm transwell system towards culture medium alone or medium containing the chemokines SDF-1 600 ng/ml, CCL21 300 ng/ml in the presence or not of the chemokine receptor blockers AMD3100 (Plerixafor) and anti-CCR7, are shown for T cell blasts of a healthy control (Ctr. in blue) and the ITK-deficient patient (Pat. in red). The experiment was performed in triplicates with 0.15 x 10^6 T cell blasts and standard deviation scores are indicated by error bars. Data are representative of two independent experiments.

In conclusion, the amorphic ITK p.W209X mutation leads to reduced TCR:CD3:ζ-signalling strenght in a dose-dependent manner. Ca^{2+}-flux is found completely abrogated in ITK-deficient T cells of the patient, but residual Ca^{2+}-flux is detectable in ITK-deficient T cells of the newborn brother, who is not yet clinically affected. This discrepancy could be explained by the exhausted phenotype of T cells of the patient that might be particularly dependent on ITK to generate Ca^{2+}-flux. Importantly, it is found that ITK-deficient T cells have an impaired capacity to perform chemokinesis. This is a feature not observed in ZAP-

70-deficient cells (data not shown) and probably reflects the involvement of ITK in actin dynamics.[172] This defect might favour the particular lung localization of EBV-associated lymphoproliferative disease in ITK-deficient patient. Globally, these findings suggest a more subtle TCR:CD3:ζ-signalling defect than that associated with LCK- and ZAP-70-deficiency with an additional impairement of chemokinesis.

4 Discussion

4.1 LCK-deficiency

We report the first case of autosomal recessive human LCK-deficiency caused by complete maternal UPD of chromosome 1 harboring the mutated *LCK* c.1022T>C allele at 1p34.3. UPD is defined as the inheritance of a pair of duplicated chromosomes from a single parent and is associated with two principal developmental risks such as the occurrence of imprinting disorders and the inheritance of recessive traits.[469] Four autosomal recessive PIDs due to UPD have been reported to date, including Chediak-Higashi syndrome (*LYST*, 1q42.1-q42.2), IFN-γR1-deficiency (*IFNGR1*, 6q23.3), cartilage hair hypoplasia (*RMRP*, 9p21-p12) and perforin-deficiency (*PRF1*, 10q22) with three of them following the classical phenotype of the autosomal recessive trait and one of them showing additional syndromic features probably related to imprinting disorder.[470-473] Therefore in the LCK-deficient patient, it cannot be ruled out that additionally imprinting imbalances and homozygous polymorphisms or mutations in other genes on chromosome 1 might have contributed to the clinical phenotype (Tab. 11).

Table 11. Known PID-causing genes on chromosome 1.

Gene	Location
RFX5	1q21
HAX1	1q21.3
LAMTOR2	1q22
CD247 (ζ-chain)	1q22-q23
FASLG	1q23
NCF2	1q25
PTPRC (CD45)	1q31-q32
IL10	1q31-q32
CFH	1q32
CD46	1q32
LYST	1q42.1-q42.2
NLRP3	1q44
NRAS	1p13.2
GFI1	1p22

C8A	1p32
C8B	1p32
AK2	1p34
LCK	1p34.3
FCN3	1p36.11
C1QA	1p36.12
C1QB	1p36.12
C1QC	1p36.11
MASP2	1p36.3-p36.2

Genes involved in LCK-signalling, the complement system and inflammation are shown in red, blue and green, respectively.

On the protein level, *in silico* analysis predicted the LCK p.L341P mutation to disturb proper protein folding as the proline substitution introduced a kink that disrupted the three-dimensional secondary structure of its own α-helix and the local hydrogen bond network of the adjacent α-helices, necessary for the correct tertiary structure of LCK. In the patient's PBMCs and T cell blasts and in the transient and retroviral LCK p.L341P overexpression systems only the lower and not yet post-translationally modified 56 kDa band was expressed.[102] The upper 60 kDa band, corresponding to post-translationally modified LCK, was not expressed in the patient and could only be restored partially in the transient overexpression system by inhibiting the proteasomal degradation pathway.[102] As post-translational lipidation and phosphorylation are important for proper membrane localization and conformational changes of LCK, it seems plausible that the instable LCK p.L341P was not located to the membrane and was not susceptible to allosteric regulation.[85, 88] Additionally, LCK p.L341P was found to be polyubiquitinated and devoid of any kinase activity in an *in vitro* kinase-activity assay. In summary, the LCK p.L341P mutation most probable was an instable, dislocalized and kinase-dead loss-of-function mutation.

Lck$^{-/-}$ mice, generated by homologous recombination, show thymic atrophy, a severe block in thymocyte development at the DN to DP transition and residual CD4^{low} and CD8^{low} peripheral SP T cells that can proliferate after mitogenic stimulation but cannot mount effective anti-viral responses.[456, 474] The immunological phenotype of the LCK-deficient patient resembled that of *Lck*$^{-/-}$ mice with reduced CD4 and CD8 cell surface expression, peripheral T cell lymphopenia and impaired biochemical and functional T cell responses. LCK anchoring to the TCR co-receptors CD4 and CD8α has been shown to play a key role in

preTCR- and αβ TCR:CD3:ζ-signalling by virtue of its kinase function and as an adaptor protein.[70, 92, 94] Biochemically, the expression of the instable and kinase-dead LCK p.L341P lead to a profound TCR:CD3:ζ-signalling defect with weak protein tyrosine phosphorylation and absent Ca^{2+}-flux. Whether the $CD4^{low}$ and $CD8^{low}$ phenotype resulted from T cell immaturity or because the stable expression of the co-receptors at the cell surface might depend on LCK is not clear, but we favor the latter possibility as other PIDs characterized by impaired thymopoïesis, e.g. ZAP-70-deficiency, do not present this feature.[7]

Some T cells developed in the LCK-deficient patient, but thymic output as judged by diminished $CD4^+CD45RA^+CD31^+$ recent thymic emigrants was reduced. The proportion of innate-like γδ T cells was augmented and that of conventional αβ T cells was decreased. The majority of γδ T cells was $CD8\alpha^+$ and their γδ TCR repertoire was shifted towards a putatively skin-homing $TCRV\delta1^+V\gamma5^+$ population.[12] The αβ TCR repertoire and the corresponding CDR3 sequences of the $CD4^{low}$ and $CD8^{low}$ SP T cells were oligoclonal. Thus, like in its murine counterpart, human LCK-deficiency is characterized by disturbed V(D)J-recombination and strongly impaired CD4 and CD8 SP thymocyte development.

The development of the residual LCK-deficient T cells might have been driven by preTCR- and TCR:CD3:ζ-dependent or -independent stimuli. In the murine *Lck*$^{-/-}$ model, stimulation with bacterial superantigens induces IL-2 production in T cells bypassing Lck-dependent TCR:CD3:ζ-signalling via the lipid raft enriched heterotrimeric Gα11 protein and PLCβ.[475] The second Src kinase Fyn contributes to thymocyte development in Lck-deficient mice because *Lck*$^{-/-}$*Fyn*$^{-/-}$ double-knockout mice have a more severe phenotype with a complete block of αβ T cell development at the DN stage.[476] Therefore FYN, that is involved in proximal TCR:CD3:ζ-signalling and that was normaly expressed in the LCK-deficient patient, might have partially compensated for the absence of LCK and allowed for residual αβ T cell development.

In Lck-deficient and γδ TCR-transgenic mice, thymic γδ T cell development is impaired, but extrathymic development and maturation of intestinal $CD8\alpha^+$ γδ T cells is preserved.[477] The putatively skin-homing $CD8\alpha^+TCRV\delta1^+V\gamma5^+$ population found in the LCK-deficient patient might as well have developed extrathymically.

Residual MAPK activation was observed in the LCK-deficient patient's T cells, whereas Ca^{2+}-flux and phosphorylation of IκBα were completely abolished. This is paralleling the situation in mice harbouring an inducible *Lck* transgene, where the activation of PLCγ-1 and PKCθ are strictly dependent on Lck, while the MAPK pathway can be

activated both by Lck and Fyn.[478] Thus, like for residual thymocyte development, FYN might have been involved in generating residual MAPK-signalling in the LCK-deficient patient.

Defective thymocyte development as a consequence of severely reduced preTCR- and TCR:CD3:ζ-signalling strenght might have disturbed mayor thymocyte selection processes that depend on the individual TCR affinity for its cognate self-pMHC. LCK-deficient DP thymocytes that displayed high affinity towards self-pMHCs and physiologically might have succumbed to clonal deletion might have passed positive selection and clonal diversion. LCK-deficient DP thymocytes that bound to self-pMHCs with low or borderline high binding affinity might have been eleminated by neglect (Fig. 13). This might have favoured a oligoclonal TCR repertoire responsive towards self-pMHCs instead of foreign pMHCs.

The majority of the peripheral $CD4^{low}$ SP T cells had an activated T_{EM}-like phenotype while the majority of the $CD8^{low}$ SP T cells had a T_{EMRA}-like phenotype. $CD4^+CD25^+$FOX-$P3^+$ *bona fide* T_{Reg} were present in the LCK-deficient patient, but as activated T cells transiently upregulate CD25 and FOX-P3, it remains difficult to discriminate true T_{Reg} from activated T_H without specific functional assays.[479] The homeostatic peripheral expansion of these oligoclonal T cell populations, resembling LIP and CIP described in the murine model system (Fig. 15) might have been driven by below-threshold TCR:CD3:ζ-signalling induced by self-pMHCs and amplified by increased γ_c-cytokine signalling, such as IL-2, IL-7 and IL-15, resulting in a proliferation signal.[328, 329] . Furthermore in mice harbouring an inducible *Lck* transgene, TCR:CD3:ζ-signalling in naïve $CD8^+$ T_{Cyt} strongly depends on Lck, whereas T_{Mem} are able to respond to antigen independently of Lck.[480]

The remaining LCK-deficient T cells were shown to be dysfunctional as illustrated by AICD, a central mechanism of immune contraction and peripheral tolerance.[14] Another important component of peripheral tolerance are T_{Reg}. The role of T_{Reg} for mucosal immunity has recently been highlighted by the immune dysregulation, polyendocrinopathy, enteropathy, X-linked syndrome (IPEX), caused by hemizygous *FOXP3* mutations.[481] The overall number of LCK-deficient *bona fide* T_{Reg} was low and they most probably were dysfunctional. Thus, disturbed AICD and T_{Reg}-deficiency might have infereed with peripheral tolerance and contributed to the inflammatory bowel disease and sterile skin inflammation found in the LCK-deficient patient.

The consequences of LCK-deficiency in the patient reported here were severe and life-limiting. Early-onset infections were associated with protracted gut disease, failure to thrive, skin and mucosal inflammation and systemic autoimmunity. Especially infections, chronic diarrhea and failure to thrive are commonly seen in a broad range of SCIDs and are due to

absent or non-functional T cell immunity.[7] Skin and mucosal inflammation and systemic autoimmunity, refered to as Omenn syndrome in its most severe manifestation, are often associated with the expansion of oligoclonal αβ and γδ T cell populations and the predominant skin-inflammation in the LCK-deficient patient might have been mediated especially by the $CD8\alpha^{+}TCRV\delta1^{+}V\gamma5^{+}$ population.[482] It is possible, that acute and chronic (viral) infections might additionally have contributed to the inflammatory phenotype by further activating the PRR-pathways of the innate immune system.[483]

Taken as a whole, the alterations of preTCR- and TCR:CD3:ζ-signalling and their consequences for V(D)J-recombination, thymocyte development, central and peripheral tolerance, immune homeostatsis and contraction might have favored the development of oligoclonal and self-reactive LCK-deficient T cells, the loss of T_{Reg} with non-functional capacities and the peripheral expansion of dysregulated memory-like T cells. This might have accounted for the severe immunodeficiency and in concert with acute and chronical (viral) infections might have driven the gradual build-up of mucosal and skin inflammation as well as systemic autoimmunity in the LCK-deficient patient.

Three patients with CID characterized by predominant CD4 T cell lymphopenia associated with low levels of LCK protein or LCK kinase activity have been reported before.[457, 459, 484] In two of them, LCK abnormalities were associated with the predominant expression of the *LCK ΔEx7* mRNA splice variant and it was hypothesized that the resulting LCK ΔEx7 protein might be instable.[457, 484] In the patients with the most severe clinical and immunological phenotypes, TCR:CD3:ζ-induced protein tyrosine phosphorylation, Ca^{2+}-flux and activation of MAPKs were found to be intact.[457] No causative genetic mutation of *LCK* was identified in any of these patients. Thus, CID and common variable immunodeficiency (CVID) in these patients could not be attributed to a primary genetic defect in *LCK* but altered expression of LCK and LCK ΔEx7 might have contributed to their clinical phenotypes.

We were able to clone the *LCK ΔEx7* splice variant from PBMCs of a healthy control and to transiently express the LCK ΔEx7 protein in HEK 293T cells. LCK ΔEx7 is lacking the aa 362-387 of the central part of the kinase domain and was described to be unstable (Fig 61).[457] When immunoblotting with a polyclonal rabbit anti-LCK antibody, LCK ΔEx7 was detectable and its band pattern was comparable to that of wildtype LCK suggesting similar post-translational modifications, i.e. lipidation, protein tyrosine and serine phoshporylation (Fig. 30).[102, 485] However and as expected from *in silico* predictions, the LCK ΔEx7 protein was devoid of any kinase function (Fig. 31). Most importantly and as compared to the parental Jurkat cell line, we detected a protein of 52 kDa that could correspond to LCK ΔEx7

in the JCam1.6 cell line, that had been described as lacking any LCK protein (Fig. 37).[47] When stimulating the JCam1.6 cell line with anti-CD3 antibody, we and others noted that upon a strong stimulation with high concentrations of anti-CD3 some LCK-dependent signals could be observed (Fig. 38 and personal communication with U. Kölsch, Division of Immunology, Berlin, Germany), suggesting residual wildtype LCK expression or LCK-independent mechanisms, as discussed above.

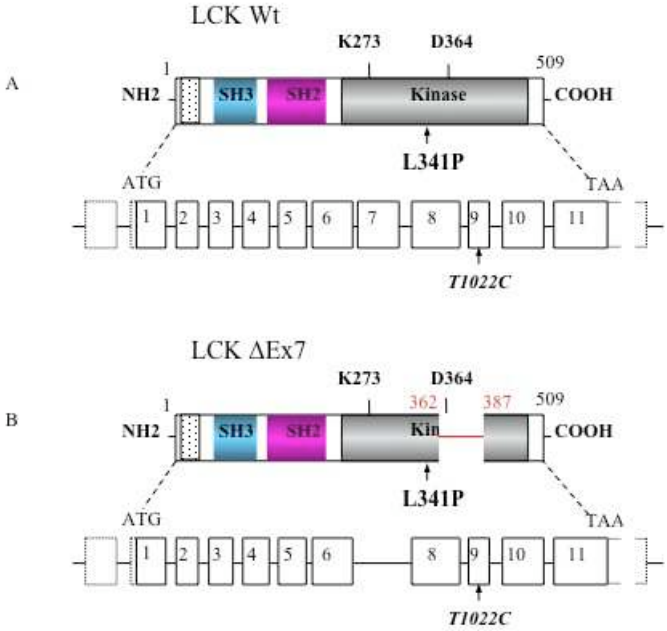

Figure 61. Scheme of wildtype LCK and LCK ΔEx7.

The domain structure of the wildtype LCK (A) and LCK ΔEx7 (B) proteins and the exons spliced to obtain the particular mRNAs are shown. The N-terminal (NH2) spotted box corresponds to the CD4 and CD8 binding regions and the SH2, SH3 and the C-terminal (COOH) kinase domains are indicated by blue, purple or grey boxes, respectively. The ATP-binding K273, the proton acceptor D364 and the p.L341P substitution (upper arrowhead) are indicated (not drawn to scale). The 26 aa deletion from aa 362 to aa 387 in LCK ΔEx7 is shown by a red line and the disruption of the kinase domain is indicated. Protein coding exons (1-11) and non-coding exons are represented by solid or spotted boxes, respectively, and the c.1022T>C transition in coding exon 9 is indicated (lower arrowhead, not drawn to scale).

It was described that in naïve T cells approximately 40% of total LCK was constitutively active and that maintenance of this catalytic LCK pool was dependent on the heat shock protein of 90 kDa (HSP-90):cell division cycle 37 (CDC-37) chaperone complex. After TCR:CD3:ζ-stimulation the overall amount of catalytic LCK remained stable, but still defined the degree of ITAM phosphorylation.[486] The authors concluded that additional regulatory mechanisms that stabilize the active LCK conformation or determine LCK membrane compartmentalization might be operational and it is tempting to speculate that

LCK ΔEx7 might be involved in this fine-tuning network. For example upon TCR:CD3:ζ-stimulation, wildtype LCK could preferentially associate with TCR:CD3:ζ-microclusters and translocate from the pSMAC to the cSMAC while performing ITAM-phopshorylation. On the other hand, LCK ΔEx7 could preferentially associate with unclustered TCR:CD3:ζ-units and stay in the pSMAC or translocate to the dSMAC, thus contributing to TCS architecture by contacting the actin cytoskeleton. Another hypothesis could be that the constitutively active pool of wildtype LCK might not only be balanced by auto- and trans-phosphorylation and by PTP-mediated dephosphorylation, but as well by wildtype LCK:LCK ΔEx7-units following a particular stoichoimetry.

We therefore would like to suggest, that LCK ΔEx7 is a kinase-less protein isoform that might have physiological functions, e.g. that of a negative regulator of TCR:CD3:ζ-signalling, that of an adaptor protein involved in the assembly and disintegration of the LAT:SLP-76-signalosome, or that of a chaperone governing intracellular trafficking and membrane localization of LCK itself. It might also be interesting to analyse intracellular trafficking, membrane localization of LCK and LCK ΔEx7 and TCR:CD3:ζ-signalling properties in particular T cell systems or murine reporter models to further decipher their interactions and particular signalling functions. However, it might be important first to understand under which physiological circumstances LCK ΔEx7 is expressed in T cells and/or in which particular T cell populations.

In line with that is the recent discovery of autosomal dominant uncoordinated 119 (*UNC119*) deficiency that causes CID with predominant $CD4^+$ T cell lymphopenia in one patient.[434] UNC119 is a chaperon that couples LCK to the endosomal pathway and that governs the transport of myristoylated LCK to the cell membrane and induces disruption of intramolecular inhibitory LCK interactions.[487] Hence, UNC119-deficient T cells display abnormal sequestration of LCK to the endosomal compartment and reduced LCK membrane localization.[434] The clinical phenotype of the UNC119-deficient patient is characterized by recurrent repiratory tract infections, recurrent shingles and chronic nail and skin fungal infections. Thus, the clinical course of UNC119 deficiency is less severe than that of LCK-deficiency reported here and more reminiscent of that reported for the above-mentioned immunodeficiencies associated with overexpression of LCK ΔEx7, further arguing for residual LCK function in these molecular settings.[459, 484, 487]

4.2 ZAP-70-deficiency

Few cases of human autosomal recessive ZAP-70-deficiency have been described to date and the predominant immunological features are non-functional $CD4^+$ T_H and a profound $CD8^+$ T_{Cyt} lymphopenia leading to severe combined immunodeficiency (SCID).[435-437] Hardly any detailed TCR:CD3:ζ-signalling studies have been carried out so far in human ZAP-70-deficient T cells and most of our knowledge stems from the *Zap-70*$^{-/-}$ mouse model.[54] Importantly, the phenotype of the Zap-70-deficient mouse, that has been deleted for the entire *Zap-70* gene by homologous recombination, is differing from its human counterpart as it displays an absolute intrathymic block at the DP to SP transition and consequently a combined $CD4^+$ T_H and $CD8^+$ T_{Cyt} lymphopenia.[488]

Table 12. Known human *ZAP-70* mutations.

gDNA mutation	cDNA mutation	Mutant protein expression	Ref.
g.24417G>A/IVS12-11G>A	c.1623-1624ins9	p.K541-K521insLEQ, not detectable	[435, 436]
g.24261C>A	c.1554C>A	p.S518R, not detectable	[436]
g.24217-24229del13	c.1510-1522del13	p.L503fsX35, not detectable	[437, 489]
g.10708C>A g.24518A>T	c.239C>A, c.1714A>T	p.P80Q, not detectable p.M572L, not detectable	[490]
g.24227C>T	c.1520C>T	p.A507V, not detectable	[491, 492]
g.24010G>A	c.1394G>A	p.R465H, not detectable	[493]
g.24009C>T	c.1392C>T	p.R465C, expressed, non-catalytic	[494]
g.21073T>G g.24494T>C	c.1010T>G c.1690T>C	p.L337R, n.d. p.C564R, n.d.	[492]
g.19897G>A/IVS7+121G>A	c.837-838ins78	p.H279ins60X, not detectable, alternative splicing	[495]
g.19896-19897del2	c.836-837del2	p.278TfsX15, n.d.	[496]
g.24247C>T	c.1540C>T	p.R514C, n.d.	[497]
g.24189G>C / IVS11-1G>C	c.1483-1495del13	p.A495fsX75, not detectable, alternative splicing	

n.d.: not determined. The gDNA, cDNA and protein reference sequences NG_007727.1, NM_001079.3 and NP_001070.2 are used, respectively. For cDNA the ATG start codon is denominated position +1. The novel mutation described here is given in red.

We report a novel autosomal recessive amorphic *ZAP-70* mutation in the splice acceptor site in intron 11 (*ZAP-70* g.24189G>C/IVS11-1G>C) that resulted in a 13 bp mRNA deletion (c.1483-1495del13) and abrogated ZAP-70 protein expression by causing a frame shift with a premature stop codon (p.A495fsX75) (Tab. 12). One of the 14 described *ZAP-70* mutations is located to the N-terminal SH2-domain, three to the interdomain B and the remaining 10, including the novel mutation reported here, cluster between aa 465 and 572 in the kinase domain, emphasizing the importance of the kinase domain for protein stability and function (Tab. 12 and Fig. 62). Thus, the amorphic p.A495fsX75 ZAP-70 mutant offered the opportunity to study the consequences of complete ZAP-70-deficiency for human TCR:CD3:ζ-signalling and to compare it to the data obtained for LCK-deficiency.

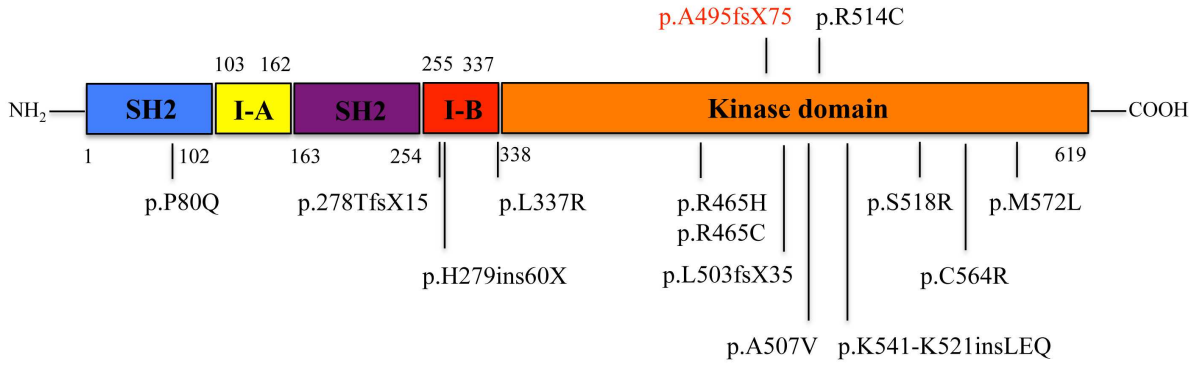

Figure 62. Synopsis of known *ZAP-70* mutations.

ZAP-70 mutations described in the literature and the novel mutation described here are indicated in black and red, respectively. Their relative localization to the ZAP-70 domains is shown (not drawn to scale).

The ZAP-70-deficient patient presented with SCID characterized by early-onset life-threatening systemic VZV-infection, opportunistic bacterial and parasitic infections and could be cured by allogeneïc haematopoïetic stem cell transplantation. Normal total NK, T and B cell counts were found and the ratio of innate-like γδ to conventional αβ T cells was not altered. $CD4^+$ T_H were at the upper normal range and *bona fide* T_{Reg} were present. However, $CD8^+$ T_{Cyt} were profoundly reduced and there were no innate-like MAIT or NKT cells detectable. Analysis of γδ and αβ TCR repertoire by spectratyping showed polyclonality, but thymic output as judged by $CD4^+CD45RA^+CD31^+$ recent thymic emigrants was reduced. Thus, human ZAP-70-deficiency seemed not to interfere with V(D)J-recombination and positive selection, but more selectively disturbed SP T cell lineage commitment as it manifested with reduced global thymic output and virtually abrogated CD8 SP T cell development.

Whether the absence of innate-like MAIT and NKT cells, that develop after so-called agonist-selection and depend on signalling molecules partially different from that necessary for conventional αβ T cell development, was due to impaired positive selection or secondary to increased peripheral apoptosis in the context of inflammation and infection is not clear. However, we favour the first possibility as there was a complete absence of NKT cells comparable to the situation found in human signalling lymphocyte activation molecule-associated protein (SAP)-deficiency and not only a strong reduction as observed in X-linked inhibitor of apoptosis (XIAP)-deficiency.[498-503]

Saini and co-workers recently showed that in Zap-70-deficient mice harboring an inducible *Zap-70*-transgene CD4 SP lineage choice timely preceeds that of CD8 SP lineage choice and is induced by a priming TCR:CD3:ζ-signal that is dependent on Lck and so-called standard amounts of additional signalling components. CD8 SP lineage choice appears thereafter and depends on a prolonged and increasingly strong TCR:CD3:ζ-signal that results from developmentally controlled downregulation of the inhibitory CD5 and upregulation of the TCR and Zap-70.[504, 505]

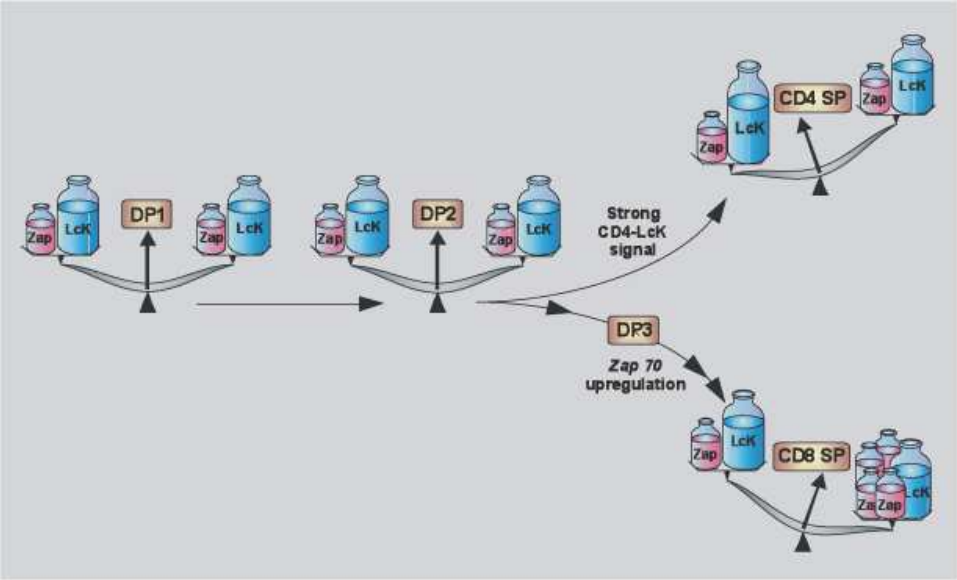

Figure 63. Semiqualitative model of CD4 and CD8 lineage determination.

The developmentally regulated relative abundances of Lck and Zap-70 and their particular contributions to TCR:CD3:ζ-signalling strenght at the DP1-DP3 and the CD4 and CD8 SP stages of murine thymocyte development are symbolized by red and blue balance weights and the resulting balance deflections. An early and strong Lck signal at the DP2-DP3 transition is supposed to lead to CD4 SP lineage commitment while a later and increasingly strong Zap-70 signal starting at the DP3 stage is supposed to induce CD8 SP lineage commitment.

Figure adapted from Alarcon B, van Santen HM, Sci Signal, 2010.[506]

They claim that especially Zap-70 upregulation leads to a temporal separation of CD4 and CD8 SP lineage choice at different signalling thresholds and consequently posit a fusion of the kinetic signalling and the signalling strenght models in SP T cell lineage commitment (Fig. 63).[307, 505, 507]

Our data of human ZAP-70-deficiency pinpoint to a similar mechanisms in men. It might be possible that the same temporal and signalling strenght separation is operational in humans, given that especially CD8 SP lineage choice and agonist-selected innate-like MAIT and NKT cell development are hampered. However, there seem to be different kinetics, signalling strenght requirements or alternative compensatory mechanisms that establish an escape mechanism for CD4 SP T cell development in men. Keeping in mind that murine Lck-deficiency leads to a severe intrathymic block at the DN to DP transition with a profound lack of peripheral CD4 and CD8 SP T cells and human LCK-deficiency only displays oligoclonal $CD4^{low}$ and $CD8^{low}$ SP T cells, it might be possible that the functional separation of LCK and ZAP-70 as master kinases for conventional T cell lineage choice is more pronounced in men than in mice.[456, 506]

Biochemically, proximal TCR:CD3:ζ-signalling in ZAP-70-deficient T cell blasts virtually did not create activating protein tyrosine phosphorylation recapitulating the bottleneck position of ZAP-70.[54] Particular signalling intermediates such as LAT, PLCγ-1 and PKCθ consequently displayed no or only residual and delayed phosphorylation responses, probably due to alternative signalling pathways.[491] TCR:CD3:ζ-signalling in T cell blasts and primary T cells induced no Ca^{2+}-flux in ZAP-70-deficient $CD4^+$ T_H but a residual one in the remaining $CD8^+$ T_{Cyt}. TCR:CD3:ζ-induced distal signalling in T cell blasts, i.e. dephosphorylation of NFATc2 and phosphorylation of ERK-1/2, was severely abrogated. Importantly, the signalling intermediates SYK, i.e. the second SYK-family kinase, LAT, PLCγ-1 and PKCθ were relatively overexpressed in ZAP-70-deficient T cell blasts. A temporal separation of the expression and function of the Syk family kinases during thymopoïesis has been established in mice with Syk and Zap-70 necessary for TCR β-selection and Zap-70 thereafter dynamically replacing Syk for sustained pre- and αβ TCR:CD3:ζ-signalling.[504, 508] Additionally, human ZAP-70-deficient SYK^{high} CD4 T_H have been shown to generate residual MAPK-signalling and to induce class-switch recombination towards IgE in B cells.[491, 493] In our hands however, only ZAP-70-deficient SP CD8 were able to generate an intermediate Ca^{2+}-flux while SP CD4 were not. It might be possible that compensatory SYK expression in concert with upregulated LAT, PLCγ-1 and PKCθ equipped some DP T cells with a TCR:CD3:ζ-signalling capacity strong enough to perform SP CD8

lineage commitment, while the majority of them performed LCK-dominated SP CD4 lineage commitment. This again argues for a more pronounced functional separation of the master kinases LCK and ZAP-70 in human versus murine conventional T cell lineage choice.

No TCR:CD3:ζ-dependent proliferation following stimulation with lectins or antigens and no effector function was found neither in ZAP-70-deficient CD4 T_H nor CD8 T_{Cyt} as documented by absent AICD. B cells that do not express ZAP-70 but strictly depend on SYK were able to produce normal amounts of IgM but only residual amounts of IgG, IgA and specific antibodies were found.[509, 510] This additionally argues for defective T_H cell function towards B cells. Therefore, even though there was residual Ca^{2+}-flux in CD8 T_{Cyt}, the strenght of this signal was not sufficient for effector function maybe as a consequence of ongoing SYK downregulation during SP T cell maturation and after thymic egress.[504]

The majority of the peripheral $CD4^+$ T_H had a T_{CM}- or T_{EM}-like phenotype while the majority of the residual $CD8^+$ T_{Cyt} had a T_{EM}- or T_{EMRA}-like phenotype. It is possible that reduced thymic output was compensated by homeostatic peripheral mechanisms resembling LIP and CIP. As already discussed for LCK-deficiency, this might have been driven by below-threshold TCR:CD3:ζ-signalling induced by self-pMHCs that was amplified by increased γ_c-cytokine signalling, such as IL-2, IL-7 and IL-15.[328, 329] In contrast to LCK-deficiency, where especially oligoclonal $CD8^{low}$ SP were expanded, no obvious peripheral cytokine-driven CD8 SP expansion was found in ZAP-70-deficiency. This might be because ZAP-70-signaling is necessary to reach a cytokine-responsive stage by downregulating SOCS-1 and up-regulating IL-7Rα or because CD4 SP cells that depend more on LCK-signalling might have had an TCR:CD3:ζ-signalling advantage in competing for the rate-limiting IL-7 and therefore occupied the peripheral niche more effectively.[299, 323]

No signs or symptoms of autoinflammation or autoimmunity were found in the ZAP-70-deficient patient reported here and most ZAP-70-deficient patients present with classical SCID. However, one patient with Omenn syndrome and another with pronounced lymphocytic dermatitis due to ZAP-70-deficiency have been reported.[492, 511] Of note, the majority of ZAP-70-deficient individuals succumb to severe infections early in life or a cured by allogeneïc haematopoïetic stem cell transplantation, making it diffiult to exclude the possibility of frequent immunodysregulation later on in life. However, disturbed central tolerance, i.e. reduced expression of autoimmune regulator (AIRE), incomplete terminal differentiation of medullary TEC, reduced intrathymic T_{Reg} cell count and autoimmune mRNA signature of peripheral $CD4^+$ T_H have been described for ZAP-70 deficiency, both theoretically predisposing to immunodysregulation.[512] Additionally, negative selection and

clonal diversion deleting autoreactive clones and giving rise to T_{Reg} might be hampered as a consequence of reduced TCR:CD3:ζ-signalling strenght as discussed above for LCK-deficiency. As activated T cells transiently upregulate CD25 and FOX-P3 it remains difficult to discriminate true T_{Reg} from activated CD4 SP T cells in the ZAP-70-deficient patient without additional functional testing.[479] However, abrogated TCR:CD3:ζ-signalling resulting from ZAP-70-deficiency and developmentally determined downregulation of SYK in maturating SP T cells and $CD4^+$ T_H reinforce the ZAP-70 bottleneck function in TCR:CD3:ζ-signalling. Thus, impaired activation, proliferation and autoimmune effector function of the presumably autoreactive ZAP-70 deficient T cell pool might explain the scarcity of immunodysregulation in ZAP-70-deficiency to some extend. Additionally, early-onset manifestation and SCID severity, that commonly lead to mortality or curative allogeneïc haematopoïetic stem cell transplantation early in life, simply might prevent development of overt immunodysregulation in the majority of ZAP-70-deficient patients.

4.3 ITK-deficiency

Few cases of human autosomal recessive ITK-deficiency have been described so far and the predominant immunological features are progressive T cell lymphopenia, loss of T cell naïvety and hypogammaglobulinaemia leading to CID. Importantly, human ITK-deficiency displays impaired immunity towards EBV leading to lymphoproliferative disease and Hodgkin's-like lymphoma preferably located to the lungs.[420, 463, 464] Hardly any detailed TCR:CD3:ζ-signalling studies have been carried out so far in human ITK-deficient T cells and most of our knowledge stems from the *Itk*$^{-/-}$ mouse model.[86] Moreover, EBV is not infecting mice and therefore a hallmark of human ITK-deficiency is not recapitulated by the murine model.[513]

We report a novel autosomal recessive *ITK* missense mutation (c.626G>A) that on the protein level translates into the amorphic ITK p.W209X (Fig. 55). One of the four *ITK* mutations described so far is located to the N-terminal PH-BH, one to the SH2 and two to the C-terminal kinase domain. The novel *ITK* mutation described here is the first one located to the SH3 domain (Tab. 13 and Fig. 64). Currently, there is no clear clustering of pathogenic *ITK* mutations to the kinase domain, e.g. as found for *ZAP-70* mutations (Fig. 62). This might indicate that not only the ITK kinase function but as well the ITK adaptor protein features are equally important for proper TCR:CD3:ζ-signalling, but the overall number of known *ITK* mutations at present is too low to allow for such generalized conclusions.

Table 13. Known human *ITK* mutations.

gDNA mutation	cDNA mutation	Mutant protein expression	Ref.
g.61124G>A	c.1961G>A	p.R335W, n.d.	[420]
g.68084C>G	c.1746C>G	p.Y588X, not detectable	[463]
g.168G>A	c.86G>A	p.R29H, low or not detectable[1]	[464]
g.64877del1	c.1497del1	p.500TfsX503, n.d.	[464]
g.42097G>A	c.626G>A	p.W209X, not detectable	

n.d.: not determined The gDNA, cDNA and protein reference sequences (NG_016276.1), (NM_005546.3) and (NP_005537) are used, respectively. For cDNA the ATG start codon is denominated position +1. The novel mutation described here is given in red. [1]Cindy Synaeve and Sylvain Latour, unpublished observation.

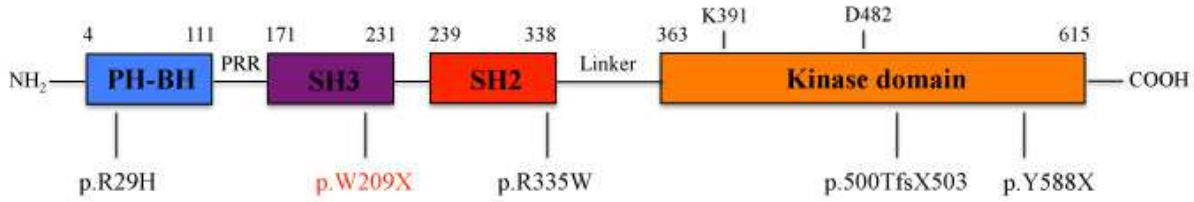

Figure 64. Synopsis of known *ITK* mutations.

ITK mutations described in the literature and the novel mutation described here are indicated in black and red, respectively. Their relative localization to the ITK domains is shown (not drawn to scale).

The ITK-deficient index patient and his newborn brother were found to be homozygous for the ITK p.W209X mutation ($ITK^{-/-}$), while the parents and the second brother were healthy heterozygous mutation carriers ($ITK^{+/-}$, Fig. 55A). As we found abrogated ITK-expression for the $ITK^{-/-}$ patient and intermediate ITK-expression for the $ITK^{+/-}$ family members, this offered the possibility to compare the effects of global ITK-deficiency and presumable ITK-haploinsufficiency on TCR:CD3:ζ-signalling. Furthermore, the newborn $ITK^{-/-}$ brother had not yet encountered EBV and had not yet developed a CID phenotype directly after birth, thus probably allowing for dissecting developmental from acquired phenotypic and functional alterations of the T cell compartment such as progressive T cell lymphopenia, loss of T cell naïvety and altered TCR:CD3:ζ-signalling strenght.

As a consequence of altered TCR:CD3:ζ-signalling strenght, $Itk^{-/-}$ mice have a subtly impaired thymopoïesis with decreased positive selection of conventional αβ T cells.[514] However, they have increased numbers of innate-like αβ T cells that have aquired a memory phenotype during their thymic development and are easily activated in the periphery to produce effector cytokines.[515] In $Itk^{-/-}$ mice TCR:CD3:ζ-induced naïve T cell activation is

impaired and especially $CD4^+$ T_H2 cell differentiation and effector cytokine production are abrogated leading to vulnerability towards parasitic infections.[86] *Itk*$^{-/-}$ $CD8^+$ T_{Cyt} are able to mount virus specific responses even though with delayed kinetics and numbers and whether this is due to an intrinsic T_{Cyt} defect or to impaired T_H cell help has yet to be determined.[86]

In line with the *Itk*$^{-/-}$ mouse model, the ITK-deficient patient showed normal V(D)J-recombination as judged by polyclonal αβ TCR repertoire and in the newborn brother the TREC-screening was not able to detect ITK-deficiency. To which extend during thymopoïesis ITK-deficiency is compensated for by other TEC-family kinases, such as RLK, currently remains unanswered, but data obtained from the murine model suggest complex interactions for thymocyte development and selection.[514, 516]

Already at birth however, the newborn brother displayed reduced global T cell numbers with slightly reduced $CD4^+$ T_H and clearly reduced $CD8^+$ T_{Cyt} while the index patient at the timepoint of clinical manifestation displayed a more severe combined $CD4^+$ T_H and $CD8^+$ T_{Cyt} lymphopenia. Both, the index patient and the newborn brother, had slightly increased proportions of innate-like γδ T cells and reduced proportions of conventional αβ T cells. Importantly, the newborn brother displayed normal amounts of innate-like NKT and MAIT cells, while the index patient, at the timepoint of overt disease, had virtually no innate-like NKT cells, as described for the ITK-deficient patients already published. However, MAIT cells were preserved in the latter. While the newborn brother and the index patient showed a comparable loss-of-naïvety in the $CD4^+$ T_H compartement with equal proportions of naïve and $T_{CM,}$ especially the latter had a profound loss-of-naïvety in the $CD8^+$ T_{Cyt} compartment with T_{EM} and exhausted T_{EMRA}-like cells predominating. In the newborn brother $CD4^+CD25^+CD127^{low}$ T_{Reg} were found in normal numbers, but in the index patient at the timepoint of overt CID, T_{Reg} were reduced and overall CD127 expression was diminished probably as a consequence of LIP and CIP. In the patient $CD4^+$ T_H were not able to provide adequate help towards B cells as judged from borderline hypogammaglobulinaemia and weak specific antibody responses towards vaccination antigens.

Globally, these findings are in line with the ones established in the *Itk*$^{-/-}$ murine model and suggest a more subtle TCR:CD3:ζ-signalling defect than that found in LCK- and ZAP-70-deficiency. ITK-deficiency only slightly affects thymopoïesis and preferably $CD8^+$ T_{Cyt} lineage commitment, while leaving intact agonist-selection of innate-like NKT and MAIT cells. More importantly, ITK-deficiency interferes with peripheral T cell homeostasis and leads to progressive T cell lymphopenia and loss-of-naïvety especially in the $CD8^+$ T_{Cyt}

compartment. Innate-like NKT cells seem to vanish as disease progresses and chronic viral infection, such as EBV, might contribute to that phenomenon.[499]

On the protein level, the ITK p.W209X mutation was amorphic and led to abrogated ITK expression in the homozygous index patient ($ITK^{-/-}$) and reduced expression in the heterozygous family members ($ITK^{+/-}$). Interestingly, the particular protein expression levels were recapitulated by comparable degrees of TCR:CD3:ζ-signalling strenght as illustrated by protein tyrosine phosphorylation, phosphorylation of PKCθ, MAPK- and NFAT-signalling. Especially, the reduced protein tyrosine phosphorylation levels were unexpected, as in classical signalling models ITK is located downstream of ITAM-phosphorylation events where it activates PLCγ-1.[86] However, recently it has been proposed that ITK controls the spatiotemporal organization of TCR:CD3:ζ-signalling and LAT:SLP-76-signalosome-assembly as an adaptor protein and as a central regulator of actin dynamics via RHO:RAC:CDC42 and switch-associated protein 70 (SWAP-70).[172, 173, 517] Our results suggest that ITK once activated might amplify ITAM phosphorylation directly and/or indirectly. It is clear, that more sophisticated approaches on the systems biology level are necessary, to undoubtly address this intriguing issues of ITK-dose-dependent TCR:CD3:ζ-signalling strenght.[518]

Ca^{2+}-flux, that was completely abrogated in $ITK^{-/-}$ T cells of the index patient, was conserved in $ITK^{+/-}$ T cells and therefore not recapitulating the ITK-dose dependent TCR:CD3:ζ-signalling strenght observed before. Maybe full amplitude of PLCγ-1-mediated Ca^{2+}-flux is obtained by suboptimal ITK-signalling strenght in the heterozygous carrier, but with different oscillation kinetics, that cannot be monitored by this *in vitro* technique but that might have been disclosed by the defective NFAT-response.[519] Importantly, Ca^{2+}-flux in $ITK^{-/-}$ T cell blasts of the newborn brother displayed an intermediate response, suggesting an ITK-independent PLCγ-1-activation mechanism, maybe depending on RLK.[514, 516] The total absence of Ca^{2+}-flux in the patient might have been a consequence of T cell exhaustion as the experiment was done from blood samples at a timepoint when the patient was severely diseased. Also, the experimental conditions in Fig. 58A and B were not optimal as not enough cells were available and analysed for the patient and his brother, explaining the strong fluctuations of the particular curves.

In summary, the reduced TCR:CD3:ζ-signalling strenght in ITK-deficiency most probably has caused slightly reduced thymopoïesis, especially of the $CD8^+$ T_{Cyt} compartment, while leaving intact agonist-selected innate-like T cell development. More importantly, ITK-deficient TCR:CD3:ζ-signalling seems insufficient to provide physiological homeostatic

signalling-strenght and causes progressive T cell lymphopenia and loss-of-naïvety.[520] Finally, TCR:CD3:ζ-signalling strenght in ITK-deficiency seems insufficient to control infections with EBV, that has developed sophisticated immune evasion strategies, and thus leads to chronic EBV-infection and T cell exhaustion.[521, 522]

The absence of iNKT cells in diseased ITK-deficient patients might also contribute to the loss of control of EBV-infection. A defect of iNKT cells is a common feature of PIDs associated with susceptibility to EBV-infection including X-linked lymphoproliferative syndrome type 1 and 2 resulting from mutations in *SH2D1A* and *XIAP* and CD27 deficiency.[421, 426, 502, 503] Based on these observations, iNKT cells were proposed to play an important role in the immune response to EBV. In line with that, very recently, evidence was obtained that iNKT cells can directly control EBV-infected cells.[523]

In the murine system it has been shown that chemokine receptor activation results in membrane localization and phosphorylation of Itk and/or Rlk and activation of RHO:RAC:CDC42. Consequently, $Itk^{-/-}Rlk^{-/-}$ double-knockout mice display defective homing to secondary lymphoïd tissues.[466, 467] Furthermore, it has been shown that the T cell specific adaptor protein (TSAD) couples Lck to Itk and that the consecutive phosphorylation of Itk Y511 is necessary to promote CXCL12 induced migration.[468] Interestingly, $Itk^{-/-}$ mice have been found to be less susceptible to allergic airway inflammation and display reduced lymphocyte recruitment to the bronchial system and the lung parenchyma upon antigenic stimulation.[465, 524] The ITK-deficient T cells of the newborn brother also displayed impaired spontaneous migration and specific chemokinesis – a feature not observed in ZAP-70-deficient cells (data not shown) – and as in the murine model this might be related to the involvement of ITK in chemokine receptor signalling and actin dynamics.[172, 173, 517] Tonic TCR:CD3:ζ-signalling and intermittent IL-7-R-signalling that is provided by fibroblastic reticular cells (FRCs) via self-pMHC molecules and membrane bound cytokine IL-7 preferentially in secondary lymphoïd tissues, is central to peripheral T cell homeostasis.[320, 321] Impaired homing to secondary lymphoïd tissues of ITK-deficient T cells in concert with reduced tonic TCR:CD3:ζ-signalling strenght might thus have contributed to the observed progressive T cell lymphopenia and the loss-of-naïvety. It is tempting to speculate, that like in the murine model, ITK-mediated migration is of special importance for immune responses in the respiratory tract and that this might favour the particular lung localization of EBV-associated Hodgkin`s lymphoma-like lymphoproliferative disease. Future analyses are necessary to test this hypothesis.

4.4 Synthesis

We report the first case of autosomal recessive human LCK-deficiency, a novel autosomal recessive mutation leading to human ZAP-70-deficiency and a novel autosomal recessive mutation leading to human ITK-deficiency. We provide detailed clinical, immunological and biochemical analyses especially of TCR:CD3:ζ-signalling and compare our findings to the well-established *Lck*$^{-/-}$, *Zap-70*$^{-/-}$ and *Itk*$^{-/-}$ murine models.

The *LCK* c.1022T>C mutation lead to residual expression of the instable and kinase-dead LCK p.L341P while the *ZAP-70* c.1483-1495del13 and *ITK* c.626G>A mutations abrogated expression of the anticipated ZAP-70 p.A495fsX75 and ITK p.W209X proteins. There was no obvious upregulation of the second SRC family kinase FYN in LCK-deficient T cells, but the second SYK family kinase SYK was found upregulated in ZAP-70-deficient T cells, while the expression level of the TEC family kinases RLK and TEC were not determined in ITK-deficient T cells.

As described for the *Lck*$^{-/-}$ mouse model, in human LCK-deficiency there was disturbed V(D)J-recombination and a profound block at the DP to SP thymocyte transition indicating defective intrathymic pre- and TCR:CD3:ζ-signalling. Consequently, an oligoclonal γδ and αβ TCR repertoire was found, the predominating innate-like γδ T cell population, having a CD8α^{+}TCRVδ1^{+}Vγ5^{+} phenotype, was probably expanded extrathymically and the residual conventional αβ T cells had reduced expression of the TCR co-receptors CD4 and CD8, that physiologically bind to LCK. Peripheral innate-like γδ and conventional αβ T cells were found non-functional.

Differing from the *Zap-70*$^{-/-}$ mouse model, in human ZAP-70-deficiency V(D)J-recombination was intact and a leaky block in SP T cell lineage commitment was observed, thus indicating intact intrathymic preTCR:CD3:ζ-signalling but a more specific TCR:CD3:ζ-signalling defect. Consequently, a polyclonal γδ and αβ TCR repertoire was found, however thymic output was reduced, and conventional CD4^{+} T_H were present while CD8^{+} T_{Cyt} were profoundly reduced and no innate-like MAIT or NKT cells were detectable. Peripheral innate-like γδ and conventional αβ T cells were found non-functional.

Similar to the *Itk*$^{-/-}$ mouse model, in human ITK-deficiency V(D)J-recombination was not affected and thymic output was slightly reduced, especially reducing the CD8^{+} T_{Cyt} compartment, but leaving intact agonist-selected innate-like NKT and MAIT cells. However, probably as a consequence of reduced TCR:CD3:ζ-signalling strenght, impaired chemokinesis and chronic EBV-infection peripheral homeostasis was disturbed and led to a progressive lymphopenia and loss-of-naïvety.

TCR:CD3:ζ-mediated protein tyrosine phosphorylation was weak in LCK-deficient T cell blast, abrogated in ZAP-70-deficient T cell blasts, and reduced – maybe in a dose-dependent-manner – in ITK-deficient T cell blasts. FYN seemed to partially compensate for LCK-deficiency, but ZAP-70 displayed a bottleneck-function in TCR:CD3:ζ-signalling mediated protein tyrosine phosphorylation. ITK-deficiency, even though ITK classically is located downstream of ITAM-phosphorylation where it activates PLCγ-1, still reduced global protein tyrosine phosphorylation, maybe by inferring with LAT:SLP-76-signalosome assembyl and actin dynamics. Ca^{2+}-flux was completely abrogated in LCK-deficient $CD4^+$ T_H and $CD8^+$ T_{Cyt} and, while there was no Ca^{2+}-flux in ZAP-70-deficient $CD4^+$ $T_{H,}$ ZAP-70-deficient $CD8^+$ T_{Cyt} displayed an intermediate one. Following the fusion model of kinetic signalling and signalling strenght in SP T cell lineage commitment proposed by Saini and co-workers, increasing signalling strenght in SP CD8 T cells might be mediated especially by compensatory SYK expression and account for residual peripheral $CD8^+$ T_{Cyt} Ca^{2+}-flux in ZAP-deficiency. Ca^{2+}-flux was found diminished in ITK-deficient newborn T cells, but abrogated in ITK-deficient exhausted T cells, thus reinforcing the role of ITK as a TCR:CD3:ζ-signalling strenght amplifier that might be partially compensated for by RLK in naïve T cells.

There was a prominent peripheral homeostatic proliferation especially in LCK-deficient CD8 T_{Cyt}, maybe driven by TCR:CD3:ζ-independent signalling or by below-threshold TCR:CD3:ζ-signalling induced by self-pMHC that in the context of lymphopenia was amplified by increased γ_c-cytokine singalling. This phenomenom was not observed in ZAP-70-deficient CD8 T_{Cyt} possibly reflecting the bottleneck positioning of ZAP-70 in TCR:CD3:ζ-signalling, differential requirements for LCK- and ZAP-70 in γ_c-cytokine signalling or a more effective competition of the ZAP-70-deficient $CD4^+$ T_H for the rate-limiting IL-7 and the peripheral niche as compared to $CD8^+$ T_{Cyt}. ITK-deficient T cells displayed a progressive lymphopenia and loss-of-naïvety probably as a consequence of reduced TCR:CD3:ζ-signalling strenght and impaired homing to the secondary lymphoïd organs.

In conclusion and even though biological samples are extremely scarce, analysing human PIDs remains an important field of translational research. The results obtained in the abovementioned studies might contribute to our knowledge of CIDs, thus facilitate future diagnosis of further LCK-, ZAP-70 and ITK-deficient patients or related TCR:CD3:ζ-signalling disorders and set the stage for more timely and hopefully life-saving therapeutical interventions. Additionally, the detailed characterization of novel human CIDs might not only

recapitulate the data generated *in vitro* and in the murine model system, but additionally elucidate differences between mice and men not always predictable by mere extrapolation of the murine data and therefore initiate novel fields of basic science.

Acknowledgments

Merci tout d'abord aux membres du jury d'avoir accepté de juger cette thèse.
Merci également à la DFG et la Fondation Imagine pour avoir financé cette thèse.
Merci à Alain Fischer pour m'avoir accepté dans son laboratoire et merci à Sylvain Latour pour son accueil dans son équipe.
Merci à tous les chefs d'équipes, tous les post-docs, tous les étudiants en thèse et tous les techniciens.
Merci à tous les collaborateurs internationaux.
Merci aux patients et leurs familles.
Merci à ma famille et notamment à ma femme Charlène Hauck-Dugoux.

References

1. Murphy K. Janeway's Immunobiology. 8 ed: Garland Science; 2011.
2. van de Pavert SA, Mebius RE. New insights into the development of lymphoid tissues. Nat Rev Immunol 2010; 10:664-74.
3. Medzhitov R. Origin and physiological roles of inflammation. Nature 2008; 454:428-35.
4. Banchereau J, Steinman RM. Dendritic cells and the control of immunity. Nature 1998; 392:245-52.
5. Blom B, Spits H. Development of human lymphoid cells. Annu Rev Immunol 2006; 24:287-320.
6. Janeway CA, Jr., Medzhitov R. Innate immune recognition. Annu Rev Immunol 2002; 20:197-216.
7. Fischer A. Human primary immunodeficiency diseases. Immunity 2007; 27:835-45.
8. Al-Herz W, Bousfiha A, Casanova JL, Chapel H, Conley ME, Cunningham-Rundles C, et al. Primary immunodeficiency diseases: an update on the classification from the international union of immunological societies expert committee for primary immunodeficiency. Front Immunol 2011; 2:54.
9. Hedrick SM, Cohen DI, Nielsen EA, Davis MM. Isolation of cDNA clones encoding T cell-specific membrane-associated proteins. Nature 1984; 308:149-53.
10. Yanagi Y, Yoshikai Y, Leggett K, Clark SP, Aleksander I, Mak TW. A human T cell-specific cDNA clone encodes a protein having extensive homology to immunoglobulin chains. Nature 1984; 308:145-9.
11. Brenner MB, McLean J, Dialynas DP, Strominger JL, Smith JA, Owen FL, et al. Identification of a putative second T-cell receptor. Nature 1986; 322:145-9.
12. Bonneville M, O'Brien RL, Born WK. Gammadelta T cell effector functions: a blend of innate programming and acquired plasticity. Nat Rev Immunol 2010; 10:467-78.
13. Saito T, Weiss A, Miller J, Norcross MA, Germain RN. Specific antigen-Ia activation of transfected human T cells expressing murine Ti alpha beta-human T3 receptor complexes. Nature 1987; 325:125-30.

14. Snow AL, Pandiyan P, Zheng L, Krummey SM, Lenardo MJ. The power and the promise of restimulation-induced cell death in human immune diseases. Immunol Rev 2010; 236:68-82.
15. Grakoui A, Bromley SK, Sumen C, Davis MM, Shaw AS, Allen PM, et al. The immunological synapse: a molecular machine controlling T cell activation. Science 1999; 285:221-7.
16. Dustin ML, Depoil D. New insights into the T cell synapse from single molecule techniques. Nat Rev Immunol 2011; 11:672-84.
17. Dustin ML, Chakraborty AK, Shaw AS. Understanding the structure and function of the immunological synapse. Cold Spring Harb Perspect Biol 2010; 2:a002311.
18. Saito H, Kranz DM, Takagaki Y, Hayday AC, Eisen HN, Tonegawa S. A third rearranged and expressed gene in a clone of cytotoxic T lymphocytes. Nature 1984; 312:36-40.
19. Chien YH, Iwashima M, Kaplan KB, Elliott JF, Davis MM. A new T-cell receptor gene located within the alpha locus and expressed early in T-cell differentiation. Nature 1987; 327:677-82.
20. Groettrup M, Ungewiss K, Azogui O, Palacios R, Owen MJ, Hayday AC, et al. A novel disulfide-linked heterodimer on pre-T cells consists of the T cell receptor beta chain and a 33 kd glycoprotein. Cell 1993; 75:283-94.
21. Borowski C, Li X, Aifantis I, Gounari F, von Boehmer H. Pre-TCRalpha and TCRalpha are not interchangeable partners of TCRbeta during T lymphocyte development. J Exp Med 2004; 199:607-15.
22. Call ME, Wucherpfennig KW. The T cell receptor: critical role of the membrane environment in receptor assembly and function. Annu Rev Immunol 2005; 23:101-25.
23. Saint-Ruf C, Ungewiss K, Groettrup M, Bruno L, Fehling HJ, von Boehmer H. Analysis and expression of a cloned pre-T cell receptor gene. Science 1994; 266:1208-12.
24. Aifantis I, Borowski C, Gounari F, Lacorazza HD, Nikolich-Zugich J, von Boehmer H. A critical role for the cytoplasmic tail of pTalpha in T lymphocyte development. Nat Immunol 2002; 3:483-8.
25. Rudolph MG, Stanfield RL, Wilson IA. How TCRs bind MHCs, peptides, and coreceptors. Annu Rev Immunol 2006; 24:419-66.

26. Garboczi DN, Ghosh P, Utz U, Fan QR, Biddison WE, Wiley DC. Structure of the complex between human T-cell receptor, viral peptide and HLA-A2. Nature 1996; 384:134-41.

27. Malu S, Malshetty V, Francis D, Cortes P. Role of non-homologous end joining in V(D)J recombination. Immunol Res 2012.

28. Wucherpfennig KW, Gagnon E, Call MJ, Huseby ES, Call ME. Structural biology of the T-cell receptor: insights into receptor assembly, ligand recognition, and initiation of signaling. Cold Spring Harb Perspect Biol 2010; 2:a005140.

29. Borg NA, Wun KS, Kjer-Nielsen L, Wilce MC, Pellicci DG, Koh R, et al. CD1d-lipid-antigen recognition by the semi-invariant NKT T-cell receptor. Nature 2007; 448:44-9.

30. Bendelac A, Savage PB, Teyton L. The biology of NKT cells. Annu Rev Immunol 2007; 25:297-336.

31. Porcelli S, Yockey CE, Brenner MB, Balk SP. Analysis of T cell antigen receptor (TCR) expression by human peripheral blood CD4-8- alpha/beta T cells demonstrates preferential use of several V beta genes and an invariant TCR alpha chain. J Exp Med 1993; 178:1-16.

32. Gold MC, Cerri S, Smyk-Pearson S, Cansler ME, Vogt TM, Delepine J, et al. Human mucosal associated invariant T cells detect bacterially infected cells. PLoS Biol 2010; 8:e1000407.

33. Le Bourhis L, Martin E, Peguillet I, Guihot A, Froux N, Core M, et al. Antimicrobial activity of mucosal-associated invariant T cells. Nat Immunol 2010; 11:701-8.

34. Shimamura M, Huang YY, Okamoto N, Suzuki N, Yasuoka J, Morita K, et al. Modulation of Valpha19 NKT cell immune responses by alpha-mannosyl ceramide derivatives consisting of a series of modified sphingosines. Eur J Immunol 2007; 37:1836-44.

35. Shin S, El-Diwany R, Schaffert S, Adams EJ, Garcia KC, Pereira P, et al. Antigen recognition determinants of gammadelta T cell receptors. Science 2005; 308:252-5.

36. Adams EJ, Strop P, Shin S, Chien YH, Garcia KC. An autonomous CDR3delta is sufficient for recognition of the nonclassical MHC class I molecules T10 and T22 by gammadelta T cells. Nat Immunol 2008; 9:777-84.

37. Garcia KC, Adams JJ, Feng D, Ely LK. The molecular basis of TCR germline bias for MHC is surprisingly simple. Nat Immunol 2009; 10:143-7.
38. Huseby ES, White J, Crawford F, Vass T, Becker D, Pinilla C, et al. How the T cell repertoire becomes peptide and MHC specific. Cell 2005; 122:247-60.
39. Manolios N, Letourneur F, Bonifacino JS, Klausner RD. Pairwise, cooperative and inhibitory interactions describe the assembly and probable structure of the T-cell antigen receptor. EMBO J 1991; 10:1643-51.
40. Borst J, Prendiville MA, Terhorst C. Complexity of the human T lymphocyte-specific cell surface antigen T3. J Immunol 1982; 128:1560-5.
41. Call ME, Pyrdol J, Wucherpfennig KW. Stoichiometry of the T-cell receptor-CD3 complex and key intermediates assembled in the endoplasmic reticulum. EMBO J 2004; 23:2348-57.
42. Call ME, Pyrdol J, Wiedmann M, Wucherpfennig KW. The organizing principle in the formation of the T cell receptor-CD3 complex. Cell 2002; 111:967-79.
43. Siegers GM, Swamy M, Fernandez-Malave E, Minguet S, Rathmann S, Guardo AC, et al. Different composition of the human and the mouse gammadelta T cell receptor explains different phenotypes of CD3gamma and CD3delta immunodeficiencies. J Exp Med 2007; 204:2537-44.
44. Hayes SM, Shores EW, Love PE. An architectural perspective on signaling by the pre-, alphabeta and gammadelta T cell receptors. Immunol Rev 2003; 191:28-37.
45. Manolios N, Bonifacino JS, Klausner RD. Transmembrane helical interactions and the assembly of the T cell receptor complex. Science 1990; 249:274-7.
46. Reth M. Antigen receptor tail clue. Nature 1989; 338:383-4.
47. Straus DB, Weiss A. Genetic evidence for the involvement of the lck tyrosine kinase in signal transduction through the T cell antigen receptor. Cell 1992; 70:585-93.
48. Iwashima M, Irving BA, van Oers NS, Chan AC, Weiss A. Sequential interactions of the TCR with two distinct cytoplasmic tyrosine kinases. Science 1994; 263:1136-9.
49. June CH, Fletcher MC, Ledbetter JA, Samelson LE. Increases in tyrosine phosphorylation are detectable before phospholipase C activation after T cell receptor stimulation. J Immunol 1990; 144:1591-9.
50. Aivazian D, Stern LJ. Phosphorylation of T cell receptor zeta is regulated by a lipid dependent folding transition. Nat Struct Biol 2000; 7:1023-6.

51. Xu C, Gagnon E, Call ME, Schnell JR, Schwieters CD, Carman CV, et al. Regulation of T cell receptor activation by dynamic membrane binding of the CD3epsilon cytoplasmic tyrosine-based motif. Cell 2008; 135:702-13.

52. Kim ST, Takeuchi K, Sun ZY, Touma M, Castro CE, Fahmy A, et al. The alphabeta T cell receptor is an anisotropic mechanosensor. J Biol Chem 2009; 284:31028-37.

53. Valitutti S, Muller S, Salio M, Lanzavecchia A. Degradation of T cell receptor (TCR)-CD3-zeta complexes after antigenic stimulation. J Exp Med 1997; 185:1859-64.

54. Wang H, Kadlecek TA, Au-Yeung BB, Goodfellow HE, Hsu LY, Freedman TS, et al. ZAP-70: an essential kinase in T-cell signaling. Cold Spring Harb Perspect Biol 2010; 2:a002279.

55. Feske S, Skolnik EY, Prakriya M. Ion channels and transporters in lymphocyte function and immunity. Nat Rev Immunol 2012; 12:532-47.

56. Balagopalan L, Coussens NP, Sherman E, Samelson LE, Sommers CL. The LAT story: a tale of cooperativity, coordination, and choreography. Cold Spring Harb Perspect Biol 2010; 2:a005512.

57. Monks CR, Freiberg BA, Kupfer H, Sciaky N, Kupfer A. Three-dimensional segregation of supramolecular activation clusters in T cells. Nature 1998; 395:82-6.

58. Varma R, Campi G, Yokosuka T, Saito T, Dustin ML. T cell receptor-proximal signals are sustained in peripheral microclusters and terminated in the central supramolecular activation cluster. Immunity 2006; 25:117-27.

59. Yokosuka T, Kobayashi W, Sakata-Sogawa K, Takamatsu M, Hashimoto-Tane A, Dustin ML, et al. Spatiotemporal regulation of T cell costimulation by TCR-CD28 microclusters and protein kinase C theta translocation. Immunity 2008; 29:589-601.

60. Kaizuka Y, Douglass AD, Varma R, Dustin ML, Vale RD. Mechanisms for segregating T cell receptor and adhesion molecules during immunological synapse formation in Jurkat T cells. Proc Natl Acad Sci U S A 2007; 104:20296-301.

61. Springer TA. Adhesion receptors of the immune system. Nature 1990; 346:425-34.

62. Hartman NC, Nye JA, Groves JT. Cluster size regulates protein sorting in the immunological synapse. Proc Natl Acad Sci U S A 2009; 106:12729-34.
63. Lee KH, Holdorf AD, Dustin ML, Chan AC, Allen PM, Shaw AS. T cell receptor signaling precedes immunological synapse formation. Science 2002; 295:1539-42.
64. Lee KH, Dinner AR, Tu C, Campi G, Raychaudhuri S, Varma R, et al. The immunological synapse balances T cell receptor signaling and degradation. Science 2003; 302:1218-22.
65. Swain SL. T cell subsets and the recognition of MHC class. Immunol Rev 1983; 74:129-42.
66. Brady RL, Lange G, Barclay AN. Structural studies of CD4: crystal structure of domains 3 and 4 and their implication for the overall receptor structure. Biochem Soc Trans 1993; 21:958-63.
67. Gay D, Maddon P, Sekaly R, Talle MA, Godfrey M, Long E, et al. Functional interaction between human T-cell protein CD4 and the major histocompatibility complex HLA-DR antigen. Nature 1987; 328:626-9.
68. Leahy DJ, Axel R, Hendrickson WA. Crystal structure of a soluble form of the human T cell coreceptor CD8 at 2.6 A resolution. Cell 1992; 68:1145-62.
69. Devine L, Sun J, Barr MR, Kavathas PB. Orientation of the Ig domains of CD8 alpha beta relative to MHC class I. J Immunol 1999; 162:846-51.
70. Veillette A, Bookman MA, Horak EM, Bolen JB. The CD4 and CD8 T cell surface antigens are associated with the internal membrane tyrosine-protein kinase p56lck. Cell 1988; 55:301-8.
71. Rhee I, Veillette A. Protein tyrosine phosphatases in lymphocyte activation and autoimmunity. Nat Immunol 2012; 13:439-47.
72. Holmes N. CD45: all is not yet crystal clear. Immunology 2006; 117:145-55.
73. Desai DM, Sap J, Silvennoinen O, Schlessinger J, Weiss A. The catalytic activity of the CD45 membrane-proximal phosphatase domain is required for TCR signaling and regulation. EMBO J 1994; 13:4002-10.
74. Xu Z, Weiss A. Negative regulation of CD45 by differential homodimerization of the alternatively spliced isoforms. Nat Immunol 2002; 3:764-71.
75. Zikherman J, Weiss A. Alternative splicing of CD45: the tip of the iceberg. Immunity 2008; 29:839-41.

76. Choudhuri K, Wiseman D, Brown MH, Gould K, van der Merwe PA. T-cell receptor triggering is critically dependent on the dimensions of its peptide-MHC ligand. Nature 2005; 436:578-82.
77. Ostergaard HL, Shackelford DA, Hurley TR, Johnson P, Hyman R, Sefton BM, et al. Expression of CD45 alters phosphorylation of the lck-encoded tyrosine protein kinase in murine lymphoma T-cell lines. Proc Natl Acad Sci U S A 1989; 86:8959-63.
78. D'Oro U, Ashwell JD. Cutting edge: the CD45 tyrosine phosphatase is an inhibitor of Lck activity in thymocytes. J Immunol 1999; 162:1879-83.
79. Boomer JS, Green JM. An enigmatic tail of CD28 signaling. Cold Spring Harb Perspect Biol 2010; 2:a002436.
80. Veillette A. SLAM-family receptors: immune regulators with or without SAP-family adaptors. Cold Spring Harb Perspect Biol 2010; 2:a002469.
81. Keir ME, Butte MJ, Freeman GJ, Sharpe AH. PD-1 and its ligands in tolerance and immunity. Annu Rev Immunol 2008; 26:677-704.
82. Schwartz RH. T cell clonal anergy. Curr Opin Immunol 1997; 9:351-7.
83. Xing Y, Hogquist KA. T-cell tolerance: central and peripheral. Cold Spring Harb Perspect Biol 2012; 4.
84. Scholer A, Hugues S, Boissonnas A, Fetler L, Amigorena S. Intercellular adhesion molecule-1-dependent stable interactions between T cells and dendritic cells determine CD8+ T cell memory. Immunity 2008; 28:258-70.
85. Salmond RJ, Filby A, Qureshi I, Caserta S, Zamoyska R. T-cell receptor proximal signaling via the Src-family kinases, Lck and Fyn, influences T-cell activation, differentiation, and tolerance. Immunol Rev 2009; 228:9-22.
86. Andreotti AH, Schwartzberg PL, Joseph RE, Berg LJ. T-cell signaling regulated by the Tec family kinase, Itk. Cold Spring Harb Perspect Biol 2010; 2:a002287.
87. Palacios EH, Weiss A. Function of the Src-family kinases, Lck and Fyn, in T-cell development and activation. Oncogene 2004; 23:7990-8000.
88. Kabouridis PS, Magee AI, Ley SC. S-acylation of LCK protein tyrosine kinase is essential for its signalling function in T lymphocytes. EMBO J 1997; 16:4983-98.
89. Turner JM, Brodsky MH, Irving BA, Levin SD, Perlmutter RM, Littman DR. Interaction of the unique N-terminal region of tyrosine kinase p56lck with cytoplasmic domains of CD4 and CD8 is mediated by cysteine motifs. Cell 1990; 60:755-65.

90. Lin RS, Rodriguez C, Veillette A, Lodish HF. Zinc is essential for binding of p56(lck) to CD4 and CD8alpha. J Biol Chem 1998; 273:32878-82.

91. Wiest DL, Yuan L, Jefferson J, Benveniste P, Tsokos M, Klausner RD, et al. Regulation of T cell receptor expression in immature CD4+CD8+ thymocytes by p56lck tyrosine kinase: basis for differential signaling by CD4 and CD8 in immature thymocytes expressing both coreceptor molecules. J Exp Med 1993; 178:1701-12.

92. van Oers NS, Killeen N, Weiss A. Lck regulates the tyrosine phosphorylation of the T cell receptor subunits and ZAP-70 in murine thymocytes. J Exp Med 1996; 183:1053-62.

93. Denny MF, Kaufman HC, Chan AC, Straus DB. The lck SH3 domain is required for activation of the mitogen-activated protein kinase pathway but not the initiation of T-cell antigen receptor signaling. J Biol Chem 1999; 274:5146-52.

94. Rudd ML, Tua-Smith A, Straus DB. Lck SH3 domain function is required for T-cell receptor signals regulating thymocyte development. Mol Cell Biol 2006; 26:7892-900.

95. Bergman M, Mustelin T, Oetken C, Partanen J, Flint NA, Amrein KE, et al. The human p50csk tyrosine kinase phosphorylates p56lck at Tyr-505 and down regulates its catalytic activity. EMBO J 1992; 11:2919-24.

96. Eck MJ, Atwell SK, Shoelson SE, Harrison SC. Structure of the regulatory domains of the Src-family tyrosine kinase Lck. Nature 1994; 368:764-9.

97. Brdicka T, Pavlistova D, Leo A, Bruyns E, Korinek V, Angelisova P, et al. Phosphoprotein associated with glycosphingolipid-enriched microdomains (PAG), a novel ubiquitously expressed transmembrane adaptor protein, binds the protein tyrosine kinase csk and is involved in regulation of T cell activation. J Exp Med 2000; 191:1591-604.

98. Xu W, Harrison SC, Eck MJ. Three-dimensional structure of the tyrosine kinase c-Src. Nature 1997; 385:595-602.

99. Xu W, Doshi A, Lei M, Eck MJ, Harrison SC. Crystal structures of c-Src reveal features of its autoinhibitory mechanism. Mol Cell 1999; 3:629-38.

100. Veillette A, Fournel M. The CD4 associated tyrosine protein kinase p56lck is positively regulated through its site of autophosphorylation. Oncogene 1990; 5:1455-62.

101. Watts JD, Sanghera JS, Pelech SL, Aebersold R. Phosphorylation of serine 59 of p56lck in activated T cells. J Biol Chem 1993; 268:23275-82.
102. Schroder AJ, Quehl P, Muller J, Samstag Y. Conversion of p56(lck) to p60(lck) in human peripheral blood T lymphocytes is dependent on co- stimulation through accessory receptors: involvement of phospholipase C, protein kinase C and MAP-kinases in vivo. Eur J Immunol 2000; 30:635-43.
103. McNeill L, Salmond RJ, Cooper JC, Carret CK, Cassady-Cain RL, Roche-Molina M, et al. The differential regulation of Lck kinase phosphorylation sites by CD45 is critical for T cell receptor signaling responses. Immunity 2007; 27:425-37.
104. Chiang GG, Sefton BM. Specific dephosphorylation of the Lck tyrosine protein kinase at Tyr-394 by the SHP-1 protein-tyrosine phosphatase. J Biol Chem 2001; 276:23173-8.
105. Hasegawa K, Martin F, Huang G, Tumas D, Diehl L, Chan AC. PEST domain-enriched tyrosine phosphatase (PEP) regulation of effector/memory T cells. Science 2004; 303:685-9.
106. Chan AC, Iwashima M, Turck CW, Weiss A. ZAP-70: a 70 kd protein-tyrosine kinase that associates with the TCR zeta chain. Cell 1992; 71:649-62.
107. Sloan-Lancaster J, Presley J, Ellenberg J, Yamazaki T, Lippincott-Schwartz J, Samelson LE. ZAP-70 association with T cell receptor zeta (TCRzeta): fluorescence imaging of dynamic changes upon cellular stimulation. J Cell Biol 1998; 143:613-24.
108. Yokosuka T, Sakata-Sogawa K, Kobayashi W, Hiroshima M, Hashimoto-Tane A, Tokunaga M, et al. Newly generated T cell receptor microclusters initiate and sustain T cell activation by recruitment of Zap70 and SLP-76. Nat Immunol 2005; 6:1253-62.
109. Chan AC, Irving BA, Fraser JD, Weiss A. The zeta chain is associated with a tyrosine kinase and upon T-cell antigen receptor stimulation associates with ZAP-70, a 70-kDa tyrosine phosphoprotein. Proc Natl Acad Sci U S A 1991; 88:9166-70.
110. Hatada MH, Lu X, Laird ER, Green J, Morgenstern JP, Lou M, et al. Molecular basis for interaction of the protein tyrosine kinase ZAP-70 with the T-cell receptor. Nature 1995; 377:32-8.

111. Folmer RH, Geschwindner S, Xue Y. Crystal structure and NMR studies of the apo SH2 domains of ZAP-70: two bikes rather than a tandem. Biochemistry 2002; 41:14176-84.

112. Watts JD, Affolter M, Krebs DL, Wange RL, Samelson LE, Aebersold R. Identification by electrospray ionization mass spectrometry of the sites of tyrosine phosphorylation induced in activated Jurkat T cells on the protein tyrosine kinase ZAP-70. J Biol Chem 1994; 269:29520-9.

113. Chan AC, Dalton M, Johnson R, Kong GH, Wang T, Thoma R, et al. Activation of ZAP-70 kinase activity by phosphorylation of tyrosine 493 is required for lymphocyte antigen receptor function. EMBO J 1995; 14:2499-508.

114. Pelosi M, Di Bartolo V, Mounier V, Mege D, Pascussi JM, Dufour E, et al. Tyrosine 319 in the interdomain B of ZAP-70 is a binding site for the Src homology 2 domain of Lck. J Biol Chem 1999; 274:14229-37.

115. Zhao Q, Weiss A. Enhancement of lymphocyte responsiveness by a gain-of-function mutation of ZAP-70. Mol Cell Biol 1996; 16:6765-74.

116. Brdicka T, Kadlecek TA, Roose JP, Pastuszak AW, Weiss A. Intramolecular regulatory switch in ZAP-70: analogy with receptor tyrosine kinases. Mol Cell Biol 2005; 25:4924-33.

117. Sasahara Y, Rachid R, Byrne MJ, de la Fuente MA, Abraham RT, Ramesh N, et al. Mechanism of recruitment of WASP to the immunological synapse and of its activation following TCR ligation. Mol Cell 2002; 10:1269-81.

118. Rao N, Lupher ML, Jr., Ota S, Reedquist KA, Druker BJ, Band H. The linker phosphorylation site Tyr292 mediates the negative regulatory effect of Cbl on ZAP-70 in T cells. J Immunol 2000; 164:4616-26.

119. Wang HY, Altman Y, Fang D, Elly C, Dai Y, Shao Y, et al. Cbl promotes ubiquitination of the T cell receptor zeta through an adaptor function of Zap-70. J Biol Chem 2001; 276:26004-11.

120. Dong S, Corre B, Foulon E, Dufour E, Veillette A, Acuto O, et al. T cell receptor for antigen induces linker for activation of T cell-dependent activation of a negative signaling complex involving Dok-2, SHIP-1, and Grb-2. J Exp Med 2006; 203:2509-18.

121. Bubeck Wardenburg J, Fu C, Jackman JK, Flotow H, Wilkinson SE, Williams DH, et al. Phosphorylation of SLP-76 by the ZAP-70 protein-tyrosine kinase is required for T-cell receptor function. J Biol Chem 1996; 271:19641-4.

122. Zhang W, Sloan-Lancaster J, Kitchen J, Trible RP, Samelson LE. LAT: the ZAP-70 tyrosine kinase substrate that links T cell receptor to cellular activation. Cell 1998; 92:83-92.

123. Jordan MS, Koretzky GA. Coordination of receptor signaling in multiple hematopoietic cell lineages by the adaptor protein SLP-76. Cold Spring Harb Perspect Biol 2010; 2:a002501.

124. Weber JR, Orstavik S, Torgersen KM, Danbolt NC, Berg SF, Ryan JC, et al. Molecular cloning of the cDNA encoding pp36, a tyrosine-phosphorylated adaptor protein selectively expressed by T cells and natural killer cells. J Exp Med 1998; 187:1157-61.

125. Brown DA. Lipid rafts, detergent-resistant membranes, and raft targeting signals. Physiology (Bethesda) 2006; 21:430-9.

126. Lin J, Weiss A, Finco TS. Localization of LAT in glycolipid-enriched microdomains is required for T cell activation. J Biol Chem 1999; 274:28861-4.

127. Hundt M, Tabata H, Jeon MS, Hayashi K, Tanaka Y, Krishna R, et al. Impaired activation and localization of LAT in anergic T cells as a consequence of a selective palmitoylation defect. Immunity 2006; 24:513-22.

128. Brignatz C, Restouin A, Bonello G, Olive D, Collette Y. Evidences for ubiquitination and intracellular trafficking of LAT, the linker of activated T cells. Biochim Biophys Acta 2005; 1746:108-15.

129. Paz PE, Wang S, Clarke H, Lu X, Stokoe D, Abo A. Mapping the Zap-70 phosphorylation sites on LAT (linker for activation of T cells) required for recruitment and activation of signalling proteins in T cells. Biochem J 2001; 356:461-71.

130. Perez-Villar JJ, Whitney GS, Sitnick MT, Dunn RJ, Venkatesan S, O'Day K, et al. Phosphorylation of the linker for activation of T-cells by Itk promotes recruitment of Vav. Biochemistry 2002; 41:10732-40.

131. Jiang Y, Cheng H. Evidence of LAT as a dual substrate for Lck and Syk in T lymphocytes. Leuk Res 2007; 31:541-5.

132. Singer AL, Bunnell SC, Obstfeld AE, Jordan MS, Wu JN, Myung PS, et al. Roles of the proline-rich domain in SLP-76 subcellular localization and T cell function. J Biol Chem 2004; 279:15481-90.

133. Bunnell SC, Singer AL, Hong DI, Jacque BH, Jordan MS, Seminario MC, et al. Persistence of cooperatively stabilized signaling clusters drives T-cell activation. Mol Cell Biol 2006; 26:7155-66.

134. Baker JE, Majeti R, Tangye SG, Weiss A. Protein tyrosine phosphatase CD148-mediated inhibition of T-cell receptor signal transduction is associated with reduced LAT and phospholipase Cgamma1 phosphorylation. Mol Cell Biol 2001; 21:2393-403.

135. Houtman JC, Higashimoto Y, Dimasi N, Cho S, Yamaguchi H, Bowden B, et al. Binding specificity of multiprotein signaling complexes is determined by both cooperative interactions and affinity preferences. Biochemistry 2004; 43:4170-8.

136. Zhang W, Trible RP, Zhu M, Liu SK, McGlade CJ, Samelson LE. Association of Grb2, Gads, and phospholipase C-gamma 1 with phosphorylated LAT tyrosine residues. Effect of LAT tyrosine mutations on T cell angigen receptor-mediated signaling. J Biol Chem 2000; 275:23355-61.

137. Lin J, Weiss A. Identification of the minimal tyrosine residues required for linker for activation of T cell function. J Biol Chem 2001; 276:29588-95.

138. Yablonski D, Kuhne MR, Kadlecek T, Weiss A. Uncoupling of nonreceptor tyrosine kinases from PLC-gamma1 in an SLP-76-deficient T cell. Science 1998; 281:413-6.

139. Liu SK, Fang N, Koretzky GA, McGlade CJ. The hematopoietic-specific adaptor protein gads functions in T-cell signaling via interactions with the SLP-76 and LAT adaptors. Curr Biol 1999; 9:67-75.

140. Berry DM, Nash P, Liu SK, Pawson T, McGlade CJ. A high-affinity Arg-X-X-Lys SH3 binding motif confers specificity for the interaction between Gads and SLP-76 in T cell signaling. Curr Biol 2002; 12:1336-41.

141. Lock LS, Royal I, Naujokas MA, Park M. Identification of an atypical Grb2 carboxyl-terminal SH3 domain binding site in Gab docking proteins reveals Grb2-dependent and -independent recruitment of Gab1 to receptor tyrosine kinases. J Biol Chem 2000; 275:31536-45.

142. Zhu M, Janssen E, Zhang W. Minimal requirement of tyrosine residues of linker for activation of T cells in TCR signaling and thymocyte development. J Immunol 2003; 170:325-33.

143. Wange RL. LAT, the linker for activation of T cells: a bridge between T cell-specific and general signaling pathways. Sci STKE 2000; 2000:re1.

144. Houtman JC, Yamaguchi H, Barda-Saad M, Braiman A, Bowden B, Appella E, et al. Oligomerization of signaling complexes by the multipoint binding of GRB2 to both LAT and SOS1. Nat Struct Mol Biol 2006; 13:798-805.

145. Fukazawa T, Reedquist KA, Trub T, Soltoff S, Panchamoorthy G, Druker B, et al. The SH3 domain-binding T cell tyrosyl phosphoprotein p120. Demonstration of its identity with the c-cbl protooncogene product and in vivo complexes with Fyn, Grb2, and phosphatidylinositol 3-kinase. J Biol Chem 1995; 270:19141-50.

146. Wunderlich L, Farago A, Downward J, Buday L. Association of Nck with tyrosine-phosphorylated SLP-76 in activated T lymphocytes. Eur J Immunol 1999; 29:1068-75.

147. Rellahan BL, Graham LJ, Tysgankov AY, DeBell KE, Veri MC, Noviello C, et al. A dynamic constitutive and inducible binding of c-Cbl by PLCgamma1 SH3 and SH2 domains (negatively) regulates antigen receptor-induced PLCgamma1 activation in lymphocytes. Exp Cell Res 2003; 289:184-94.

148. Duan L, Reddi AL, Ghosh A, Dimri M, Band H. The Cbl family and other ubiquitin ligases: destructive forces in control of antigen receptor signaling. Immunity 2004; 21:7-17.

149. Jackman JK, Motto DG, Sun Q, Tanemoto M, Turck CW, Peltz GA, et al. Molecular cloning of SLP-76, a 76-kDa tyrosine phosphoprotein associated with Grb2 in T cells. J Biol Chem 1995; 270:7029-32.

150. Wu J, Motto DG, Koretzky GA, Weiss A. Vav and SLP-76 interact and functionally cooperate in IL-2 gene activation. Immunity 1996; 4:593-602.

151. Raab M, da Silva AJ, Findell PR, Rudd CE. Regulation of Vav-SLP-76 binding by ZAP-70 and its relevance to TCR zeta/CD3 induction of interleukin-2. Immunity 1997; 6:155-64.

152. Bunnell SC, Diehn M, Yaffe MB, Findell PR, Cantley LC, Berg LJ. Biochemical interactions integrating Itk with the T cell receptor-initiated signaling cascade. J Biol Chem 2000; 275:2219-30.

153. Asada H, Ishii N, Sasaki Y, Endo K, Kasai H, Tanaka N, et al. Grf40, A novel Grb2 family member, is involved in T cell signaling through interaction with SLP-76 and LAT. J Exp Med 1999; 189:1383-90.

154. Musci MA, Hendricks-Taylor LR, Motto DG, Paskind M, Kamens J, Turck CW, et al. Molecular cloning of SLAP-130, an SLP-76-associated substrate of the T

cell antigen receptor-stimulated protein tyrosine kinases. J Biol Chem 1997; 272:11674-7.

155. Sauer K, Liou J, Singh SB, Yablonski D, Weiss A, Perlmutter RM. Hematopoietic progenitor kinase 1 associates physically and functionally with the adaptor proteins B cell linker protein and SLP-76 in lymphocytes. J Biol Chem 2001; 276:45207-16.

156. Horn J, Wang X, Reichardt P, Stradal TE, Warnecke N, Simeoni L, et al. Src homology 2-domain containing leukocyte-specific phosphoprotein of 76 kDa is mandatory for TCR-mediated inside-out signaling, but dispensable for CXCR4-mediated LFA-1 activation, adhesion, and migration of T cells. J Immunol 2009; 183:5756-67.

157. Kiefer F, Tibbles LA, Anafi M, Janssen A, Zanke BW, Lassam N, et al. HPK1, a hematopoietic protein kinase activating the SAPK/JNK pathway. EMBO J 1996; 15:7013-25.

158. Zeng R, Cannon JL, Abraham RT, Way M, Billadeau DD, Bubeck-Wardenberg J, et al. SLP-76 coordinates Nck-dependent Wiskott-Aldrich syndrome protein recruitment with Vav-1/Cdc42-dependent Wiskott-Aldrich syndrome protein activation at the T cell-APC contact site. J Immunol 2003; 171:1360-8.

159. Rivero-Lezcano OM, Marcilla A, Sameshima JH, Robbins KC. Wiskott-Aldrich syndrome protein physically associates with Nck through Src homology 3 domains. Mol Cell Biol 1995; 15:5725-31.

160. Rohatgi R, Nollau P, Ho HY, Kirschner MW, Mayer BJ. Nck and phosphatidylinositol 4,5-bisphosphate synergistically activate actin polymerization through the N-WASP-Arp2/3 pathway. J Biol Chem 2001; 276:26448-52.

161. Fruman DA, Bismuth G. Fine tuning the immune response with PI3K. Immunol Rev 2009; 228:253-72.

162. Fruman DA, Rameh LE, Cantley LC. Phosphoinositide binding domains: embracing 3-phosphate. Cell 1999; 97:817-20.

163. Siliciano JD, Morrow TA, Desiderio SV. itk, a T-cell-specific tyrosine kinase gene inducible by interleukin 2. Proc Natl Acad Sci U S A 1992; 89:11194-8.

164. Gibson S, Leung B, Squire JA, Hill M, Arima N, Goss P, et al. Identification, cloning, and characterization of a novel human T-cell-specific tyrosine kinase

located at the hematopoietin complex on chromosome 5q. Blood 1993; 82:1561-72.

165. Yamada N, Kawakami Y, Kimura H, Fukamachi H, Baier G, Altman A, et al. Structure and expression of novel protein-tyrosine kinases, Emb and Emt, in hematopoietic cells. Biochem Biophys Res Commun 1993; 192:231-40.

166. August A, Sadra A, Dupont B, Hanafusa H. Src-induced activation of inducible T cell kinase (ITK) requires phosphatidylinositol 3-kinase activity and the Pleckstrin homology domain of inducible T cell kinase. Proc Natl Acad Sci U S A 1997; 94:11227-32.

167. Su YW, Zhang Y, Schweikert J, Koretzky GA, Reth M, Wienands J. Interaction of SLP adaptors with the SH2 domain of Tec family kinases. Eur J Immunol 1999; 29:3702-11.

168. Heyeck SD, Wilcox HM, Bunnell SC, Berg LJ. Lck phosphorylates the activation loop tyrosine of the Itk kinase domain and activates Itk kinase activity. J Biol Chem 1997; 272:25401-8.

169. Wilcox HM, Berg LJ. Itk phosphorylation sites are required for functional activity in primary T cells. J Biol Chem 2003; 278:37112-21.

170. Joseph RE, Min L, Xu R, Musselman ED, Andreotti AH. A remote substrate docking mechanism for the tec family tyrosine kinases. Biochemistry 2007; 46:5595-603.

171. Perez-Villar JJ, Kanner SB. Regulated association between the tyrosine kinase Emt/Itk/Tsk and phospholipase-C gamma 1 in human T lymphocytes. J Immunol 1999; 163:6435-41.

172. Labno CM, Lewis CM, You D, Leung DW, Takesono A, Kamberos N, et al. Itk functions to control actin polymerization at the immune synapse through localized activation of Cdc42 and WASP. Curr Biol 2003; 13:1619-24.

173. Dombroski D, Houghtling RA, Labno CM, Precht P, Takesono A, Caplen NJ, et al. Kinase-independent functions for Itk in TCR-induced regulation of Vav and the actin cytoskeleton. J Immunol 2005; 174:1385-92.

174. LaFevre-Bernt M, Sicheri F, Pico A, Porter M, Kuriyan J, Miller WT. Intramolecular regulatory interactions in the Src family kinase Hck probed by mutagenesis of a conserved tryptophan residue. J Biol Chem 1998; 273:32129-34.

175. Joseph RE, Min L, Andreotti AH. The linker between SH2 and kinase domains positively regulates catalysis of the Tec family kinases. Biochemistry 2007; 46:5455-62.

176. Shan X, Czar MJ, Bunnell SC, Liu P, Liu Y, Schwartzberg PL, et al. Deficiency of PTEN in Jurkat T cells causes constitutive localization of Itk to the plasma membrane and hyperresponsiveness to CD3 stimulation. Mol Cell Biol 2000; 20:6945-57.

177. Andreotti AH, Bunnell SC, Feng S, Berg LJ, Schreiber SL. Regulatory intramolecular association in a tyrosine kinase of the Tec family. Nature 1997; 385:93-7.

178. Brazin KN, Fulton DB, Andreotti AH. A specific intermolecular association between the regulatory domains of a Tec family kinase. J Mol Biol 2000; 302:607-23.

179. Severin A, Joseph RE, Boyken S, Fulton DB, Andreotti AH. Proline isomerization preorganizes the Itk SH2 domain for binding to the Itk SH3 domain. J Mol Biol 2009; 387:726-43.

180. Rhee SG, Bae YS. Regulation of phosphoinositide-specific phospholipase C isozymes. J Biol Chem 1997; 272:15045-8.

181. Li Y, Sedwick CE, Hu J, Altman A. Role for protein kinase Ctheta (PKCtheta) in TCR/CD28-mediated signaling through the canonical but not the non-canonical pathway for NF-kappaB activation. J Biol Chem 2005; 280:1217-23.

182. Smith-Garvin JE, Koretzky GA, Jordan MS. T cell activation. Annu Rev Immunol 2009; 27:591-619.

183. Hayashi K, Altman A. Protein kinase C theta (PKCtheta): a key player in T cell life and death. Pharmacol Res 2007; 55:537-44.

184. Baier G, Telford D, Giampa L, Coggeshall KM, Baier-Bitterlich G, Isakov N, et al. Molecular cloning and characterization of PKC theta, a novel member of the protein kinase C (PKC) gene family expressed predominantly in hematopoietic cells. J Biol Chem 1993; 268:4997-5004.

185. Liu Y, Witte S, Liu YC, Doyle M, Elly C, Altman A. Regulation of protein kinase Ctheta function during T cell activation by Lck-mediated tyrosine phosphorylation. J Biol Chem 2000; 275:3603-9.

186. Kong KF, Yokosuka T, Canonigo-Balancio AJ, Isakov N, Saito T, Altman A. A motif in the V3 domain of the kinase PKC-theta determines its localization in the

immunological synapse and functions in T cells via association with CD28. Nat Immunol 2011; 12:1105-12.

187. Bi K, Tanaka Y, Coudronniere N, Sugie K, Hong S, van Stipdonk MJ, et al. Antigen-induced translocation of PKC-theta to membrane rafts is required for T cell activation. Nat Immunol 2001; 2:556-63.

188. Spitaler M, Emslie E, Wood CD, Cantrell D. Diacylglycerol and protein kinase D localization during T lymphocyte activation. Immunity 2006; 24:535-46.

189. Schechtman D, Mochly-Rosen D. Adaptor proteins in protein kinase C-mediated signal transduction. Oncogene 2001; 20:6339-47.

190. Huang J, Lo PF, Zal T, Gascoigne NR, Smith BA, Levin SD, et al. CD28 plays a critical role in the segregation of PKC theta within the immunologic synapse. Proc Natl Acad Sci U S A 2002; 99:9369-73.

191. Toker A, Newton AC. Cellular signaling: pivoting around PDK-1. Cell 2000; 103:185-8.

192. Liu Y, Graham C, Li A, Fisher RJ, Shaw S. Phosphorylation of the protein kinase C-theta activation loop and hydrophobic motif regulates its kinase activity, but only activation loop phosphorylation is critical to in vivo nuclear-factor-kappaB induction. Biochem J 2002; 361:255-65.

193. Thuille N, Heit I, Fresser F, Krumbock N, Bauer B, Leuthaeusser S, et al. Critical role of novel Thr-219 autophosphorylation for the cellular function of PKCtheta in T lymphocytes. EMBO J 2005; 24:3869-80.

194. Sommer K, Guo B, Pomerantz JL, Bandaranayake AD, Moreno-Garcia ME, Ovechkina YL, et al. Phosphorylation of the CARMA1 linker controls NF-kappaB activation. Immunity 2005; 23:561-74.

195. Matsumoto R, Wang D, Blonska M, Li H, Kobayashi M, Pappu B, et al. Phosphorylation of CARMA1 plays a critical role in T Cell receptor-mediated NF-kappaB activation. Immunity 2005; 23:575-85.

196. Li Y, Hu J, Vita R, Sun B, Tabata H, Altman A. SPAK kinase is a substrate and target of PKCtheta in T-cell receptor-induced AP-1 activation pathway. EMBO J 2004; 23:1112-22.

197. Vallabhapurapu S, Karin M. Regulation and function of NF-kappaB transcription factors in the immune system. Annu Rev Immunol 2009; 27:693-733.

198. Schulze-Luehrmann J, Ghosh S. Antigen-receptor signaling to nuclear factor kappa B. Immunity 2006; 25:701-15.

199. Sun L, Deng L, Ea CK, Xia ZP, Chen ZJ. The TRAF6 ubiquitin ligase and TAK1 kinase mediate IKK activation by BCL10 and MALT1 in T lymphocytes. Mol Cell 2004; 14:289-301.

200. Karin M, Ben-Neriah Y. Phosphorylation meets ubiquitination: the control of NF-[kappa]B activity. Annu Rev Immunol 2000; 18:621-63.

201. Hoffmann A, Levchenko A, Scott ML, Baltimore D. The IkappaB-NF-kappaB signaling module: temporal control and selective gene activation. Science 2002; 298:1241-5.

202. Arenzana-Seisdedos F, Turpin P, Rodriguez M, Thomas D, Hay RT, Virelizier JL, et al. Nuclear localization of I kappa B alpha promotes active transport of NF-kappa B from the nucleus to the cytoplasm. J Cell Sci 1997; 110 (Pt 3):369-78.

203. Macian F. NFAT proteins: key regulators of T-cell development and function. Nat Rev Immunol 2005; 5:472-84.

204. Shaw JP, Utz PJ, Durand DB, Toole JJ, Emmel EA, Crabtree GR. Identification of a putative regulator of early T cell activation genes. Science 1988; 241:202-5.

205. Northrop JP, Ho SN, Chen L, Thomas DJ, Timmerman LA, Nolan GP, et al. NF-AT components define a family of transcription factors targeted in T-cell activation. Nature 1994; 369:497-502.

206. Hoey T, Sun YL, Williamson K, Xu X. Isolation of two new members of the NF-AT gene family and functional characterization of the NF-AT proteins. Immunity 1995; 2:461-72.

207. Lopez-Rodriguez C, Aramburu J, Rakeman AS, Rao A. NFAT5, a constitutively nuclear NFAT protein that does not cooperate with Fos and Jun. Proc Natl Acad Sci U S A 1999; 96:7214-9.

208. Garcia-Cozar FJ, Okamura H, Aramburu JF, Shaw KT, Pelletier L, Showalter R, et al. Two-site interaction of nuclear factor of activated T cells with activated calcineurin. J Biol Chem 1998; 273:23877-83.

209. Okamura H, Aramburu J, Garcia-Rodriguez C, Viola JP, Raghavan A, Tahiliani M, et al. Concerted dephosphorylation of the transcription factor NFAT1 induces a conformational switch that regulates transcriptional activity. Mol Cell 2000; 6:539-50.

210. Hogan PG, Chen L, Nardone J, Rao A. Transcriptional regulation by calcium, calcineurin, and NFAT. Genes Dev 2003; 17:2205-32.

211. Okamura H, Garcia-Rodriguez C, Martinson H, Qin J, Virshup DM, Rao A. A conserved docking motif for CK1 binding controls the nuclear localization of NFAT1. Mol Cell Biol 2004; 24:4184-95.

212. Arron JR, Winslow MM, Polleri A, Chang CP, Wu H, Gao X, et al. NFAT dysregulation by increased dosage of DSCR1 and DYRK1A on chromosome 21. Nature 2006; 441:595-600.

213. Beals CR, Sheridan CM, Turck CW, Gardner P, Crabtree GR. Nuclear export of NF-ATc enhanced by glycogen synthase kinase-3. Science 1997; 275:1930-4.

214. Terui Y, Saad N, Jia S, McKeon F, Yuan J. Dual role of sumoylation in the nuclear localization and transcriptional activation of NFAT1. J Biol Chem 2004; 279:28257-65.

215. Huang GN, Huso DL, Bouyain S, Tu J, McCorkell KA, May MJ, et al. NFAT binding and regulation of T cell activation by the cytoplasmic scaffolding Homer proteins. Science 2008; 319:476-81.

216. Aramburu J, Yaffe MB, Lopez-Rodriguez C, Cantley LC, Hogan PG, Rao A. Affinity-driven peptide selection of an NFAT inhibitor more selective than cyclosporin A. Science 1999; 285:2129-33.

217. Jain J, McCaffrey PG, Valge-Archer VE, Rao A. Nuclear factor of activated T cells contains Fos and Jun. Nature 1992; 356:801-4.

218. Macian F, Lopez-Rodriguez C, Rao A. Partners in transcription: NFAT and AP-1. Oncogene 2001; 20:2476-89.

219. Alberola-Ila J, Forbush KA, Seger R, Krebs EG, Perlmutter RM. Selective requirement for MAP kinase activation in thymocyte differentiation. Nature 1995; 373:620-3.

220. Dong C, Yang DD, Wysk M, Whitmarsh AJ, Davis RJ, Flavell RA. Defective T cell differentiation in the absence of Jnk1. Science 1998; 282:2092-5.

221. Yujiri T, Sather S, Fanger GR, Johnson GL. Role of MEKK1 in cell survival and activation of JNK and ERK pathways defined by targeted gene disruption. Science 1998; 282:1911-4.

222. Li W, Whaley CD, Mondino A, Mueller DL. Blocked signal transduction to the ERK and JNK protein kinases in anergic CD4+ T cells. Science 1996; 271:1272-6.

223. Ashwell JD. The many paths to p38 mitogen-activated protein kinase activation in the immune system. Nat Rev Immunol 2006; 6:532-40.

224. Buday L, Egan SE, Rodriguez Viciana P, Cantrell DA, Downward J. A complex of Grb2 adaptor protein, Sos exchange factor, and a 36-kDa membrane-bound tyrosine phosphoprotein is implicated in ras activation in T cells. J Biol Chem 1994; 269:9019-23.

225. Dower NA, Stang SL, Bottorff DA, Ebinu JO, Dickie P, Ostergaard HL, et al. RasGRP is essential for mouse thymocyte differentiation and TCR signaling. Nat Immunol 2000; 1:317-21.

226. Kaga S, Ragg S, Rogers KA, Ochi A. Activation of p21-CDC42/Rac-activated kinases by CD28 signaling: p21-activated kinase (PAK) and MEK kinase 1 (MEKK1) may mediate the interplay between CD3 and CD28 signals. J Immunol 1998; 160:4182-9.

227. Downward J, Graves JD, Warne PH, Rayter S, Cantrell DA. Stimulation of p21ras upon T-cell activation. Nature 1990; 346:719-23.

228. Crews CM, Alessandrini AA, Erikson RL. Mouse Erk-1 gene product is a serine/threonine protein kinase that has the potential to phosphorylate tyrosine. Proc Natl Acad Sci U S A 1991; 88:8845-9.

229. Canagarajah BJ, Khokhlatchev A, Cobb MH, Goldsmith EJ. Activation mechanism of the MAP kinase ERK2 by dual phosphorylation. Cell 1997; 90:859-69.

230. Bellon S, Fitzgibbon MJ, Fox T, Hsiao HM, Wilson KP. The structure of phosphorylated p38gamma is monomeric and reveals a conserved activation-loop conformation. Structure 1999; 7:1057-65.

231. Mor A, Philips MR. Compartmentalized Ras/MAPK signaling. Annu Rev Immunol 2006; 24:771-800.

232. Gardner P. Patch clamp studies of lymphocyte activation. Annu Rev Immunol 1990; 8:231-52.

233. Haase H, Hebel S, Engelhardt G, Rink L. Flow cytometric measurement of labile zinc in peripheral blood mononuclear cells. Anal Biochem 2006; 352:222-30.

234. Prakriya M. The molecular physiology of CRAC channels. Immunol Rev 2009; 231:88-98.

235. Hogan PG, Lewis RS, Rao A. Molecular basis of calcium signaling in lymphocytes: STIM and ORAI. Annu Rev Immunol 2010; 28:491-533.

236. Zweifach A, Lewis RS. Mitogen-regulated Ca2+ current of T lymphocytes is activated by depletion of intracellular Ca2+ stores. Proc Natl Acad Sci U S A 1993; 90:6295-9.

237. Roos J, DiGregorio PJ, Yeromin AV, Ohlsen K, Lioudyno M, Zhang S, et al. STIM1, an essential and conserved component of store-operated Ca2+ channel function. J Cell Biol 2005; 169:435-45.

238. Stathopulos PB, Li GY, Plevin MJ, Ames JB, Ikura M. Stored Ca2+ depletion-induced oligomerization of stromal interaction molecule 1 (STIM1) via the EF-SAM region: An initiation mechanism for capacitive Ca2+ entry. J Biol Chem 2006; 281:35855-62.

239. Zhang SL, Yu Y, Roos J, Kozak JA, Deerinck TJ, Ellisman MH, et al. STIM1 is a Ca2+ sensor that activates CRAC channels and migrates from the Ca2+ store to the plasma membrane. Nature 2005; 437:902-5.

240. Park CY, Hoover PJ, Mullins FM, Bachhawat P, Covington ED, Raunser S, et al. STIM1 clusters and activates CRAC channels via direct binding of a cytosolic domain to Orai1. Cell 2009; 136:876-90.

241. Stathopulos PB, Zheng L, Ikura M. Stromal interaction molecule (STIM) 1 and STIM2 calcium sensing regions exhibit distinct unfolding and oligomerization kinetics. J Biol Chem 2009; 284:728-32.

242. Feske S, Gwack Y, Prakriya M, Srikanth S, Puppel SH, Tanasa B, et al. A mutation in Orai1 causes immune deficiency by abrogating CRAC channel function. Nature 2006; 441:179-85.

243. McNally BA, Yamashita M, Engh A, Prakriya M. Structural determinants of ion permeation in CRAC channels. Proc Natl Acad Sci U S A 2009; 106:22516-21.

244. Zhou Y, Ramachandran S, Oh-Hora M, Rao A, Hogan PG. Pore architecture of the ORAI1 store-operated calcium channel. Proc Natl Acad Sci U S A 2010; 107:4896-901.

245. Muik M, Frischauf I, Derler I, Fahrner M, Bergsmann J, Eder P, et al. Dynamic coupling of the putative coiled-coil domain of ORAI1 with STIM1 mediates ORAI1 channel activation. J Biol Chem 2008; 283:8014-22.

246. Baughman JM, Perocchi F, Girgis HS, Plovanich M, Belcher-Timme CA, Sancak Y, et al. Integrative genomics identifies MCU as an essential component of the mitochondrial calcium uniporter. Nature 2011; 476:341-5.

247. Li FY, Chaigne-Delalande B, Kanellopoulou C, Davis JC, Matthews HF, Douek DC, et al. Second messenger role for Mg2+ revealed by human T-cell immunodeficiency. Nature 2011; 475:471-6.

248. Goytain A, Quamme GA. Identification and characterization of a novel mammalian Mg2+ transporter with channel-like properties. BMC Genomics 2005; 6:48.

249. Hirano T, Murakami M, Fukada T, Nishida K, Yamasaki S, Suzuki T. Roles of zinc and zinc signaling in immunity: zinc as an intracellular signaling molecule. Adv Immunol 2008; 97:149-76.

250. Kim PW, Sun ZY, Blacklow SC, Wagner G, Eck MJ. A zinc clasp structure tethers Lck to T cell coreceptors CD4 and CD8. Science 2003; 301:1725-8.

251. Yu M, Lee WW, Tomar D, Pryshchep S, Czesnikiewicz-Guzik M, Lamar DL, et al. Regulation of T cell receptor signaling by activation-induced zinc influx. J Exp Med 2011; 208:775-85.

252. Huang J, Zhang D, Xing W, Ma X, Yin Y, Wei Q, et al. An approach to assay calcineurin activity and the inhibitory effect of zinc ion. Anal Biochem 2008; 375:385-7.

253. Beemiller P, Krummel MF. Mediation of T-cell activation by actin meshworks. Cold Spring Harb Perspect Biol 2010; 2:a002444.

254. Miller MJ, Wei SH, Parker I, Cahalan MD. Two-photon imaging of lymphocyte motility and antigen response in intact lymph node. Science 2002; 296:1869-73.

255. Jacobelli J, Bennett FC, Pandurangi P, Tooley AJ, Krummel MF. Myosin-IIA and ICAM-1 regulate the interchange between two distinct modes of T cell migration. J Immunol 2009; 182:2041-50.

256. Nolz JC, Medeiros RB, Mitchell JS, Zhu P, Freedman BD, Shimizu Y, et al. WAVE2 regulates high-affinity integrin binding by recruiting vinculin and talin to the immunological synapse. Mol Cell Biol 2007; 27:5986-6000.

257. Kupfer A, Swain SL, Singer SJ. The specific direct interaction of helper T cells and antigen-presenting B cells. II. Reorientation of the microtubule organizing center and reorganization of the membrane-associated cytoskeleton inside the bound helper T cells. J Exp Med 1987; 165:1565-80.

258. Combs J, Kim SJ, Tan S, Ligon LA, Holzbaur EL, Kuhn J, et al. Recruitment of dynein to the Jurkat immunological synapse. Proc Natl Acad Sci U S A 2006; 103:14883-8.

259. Cannon JL, Burkhardt JK. Differential roles for Wiskott-Aldrich syndrome protein in immune synapse formation and IL-2 production. J Immunol 2004; 173:1658-62.

260. Husson J, Chemin K, Bohineust A, Hivroz C, Henry N. Force generation upon T cell receptor engagement. PLoS One 2011; 6:e19680.

261. Chang JT, Palanivel VR, Kinjyo I, Schambach F, Intlekofer AM, Banerjee A, et al. Asymmetric T lymphocyte division in the initiation of adaptive immune responses. Science 2007; 315:1687-91.

262. Koch U, Radtke F. Mechanisms of T cell development and transformation. Annu Rev Cell Dev Biol 2011; 27:539-62.

263. Plum J, De Smedt M, Leclercq G, Taghon T, Kerre T, Vandekerckhove B. Human intrathymic development: a selective approach. Semin Immunopathol 2008; 30:411-23.

264. Holland AM, Zakrzewski JL, Goldberg GL, Ghosh A, van den Brink MR. Adoptive precursor cell therapy to enhance immune reconstitution after hematopoietic stem cell transplantation in mouse and man. Semin Immunopathol 2008; 30:479-87.

265. Bassing CH, Swat W, Alt FW. The mechanism and regulation of chromosomal V(D)J recombination. Cell 2002; 109 Suppl:S45-55.

266. de Villartay JP, Fischer A, Durandy A. The mechanisms of immune diversification and their disorders. Nat Rev Immunol 2003; 3:962-72.

267. Krangel MS. Mechanics of T cell receptor gene rearrangement. Curr Opin Immunol 2009; 21:133-9.

268. Jenkins MK, Chu HH, McLachlan JB, Moon JJ. On the composition of the preimmune repertoire of T cells specific for Peptide-major histocompatibility complex ligands. Annu Rev Immunol 2010; 28:275-94.

269. Singer A, Adoro S, Park JH. Lineage fate and intense debate: myths, models and mechanisms of CD4- versus CD8-lineage choice. Nat Rev Immunol 2008; 8:788-801.

270. Cheng T, Rodrigues N, Shen H, Yang Y, Dombkowski D, Sykes M, et al. Hematopoietic stem cell quiescence maintained by p21cip1/waf1. Science 2000; 287:1804-8.

271. Zhang J, Niu C, Ye L, Huang H, He X, Tong WG, et al. Identification of the haematopoietic stem cell niche and control of the niche size. Nature 2003; 425:836-41.

272. Yahata T, Muguruma Y, Yumino S, Sheng Y, Uno T, Matsuzawa H, et al. Quiescent human hematopoietic stem cells in the bone marrow niches organize the hierarchical structure of hematopoiesis. Stem Cells 2008; 26:3228-36.

273. Manz MG, Miyamoto T, Akashi K, Weissman IL. Prospective isolation of human clonogenic common myeloid progenitors. Proc Natl Acad Sci U S A 2002; 99:11872-7.

274. Haddad R, Guardiola P, Izac B, Thibault C, Radich J, Delezoide AL, et al. Molecular characterization of early human T/NK and B-lymphoid progenitor cells in umbilical cord blood. Blood 2004; 104:3918-26.

275. Rossi MI, Yokota T, Medina KL, Garrett KP, Comp PC, Schipul AH, Jr., et al. B lymphopoiesis is active throughout human life, but there are developmental age-related changes. Blood 2003; 101:576-84.

276. Ryan DH, Nuccie BL, Ritterman I, Liesveld JL, Abboud CN, Insel RA. Expression of interleukin-7 receptor by lineage-negative human bone marrow progenitors with enhanced lymphoid proliferative potential and B-lineage differentiation capacity. Blood 1997; 89:929-40.

277. Res P, Martinez-Caceres E, Cristina Jaleco A, Staal F, Noteboom E, Weijer K, et al. CD34+CD38dim cells in the human thymus can differentiate into T, natural killer, and dendritic cells but are distinct from pluripotent stem cells. Blood 1996; 87:5196-206.

278. Dik WA, Pike-Overzet K, Weerkamp F, de Ridder D, de Haas EF, Baert MR, et al. New insights on human T cell development by quantitative T cell receptor gene rearrangement studies and gene expression profiling. J Exp Med 2005; 201:1715-23.

279. Lefranc MP. IMGT databases, web resources and tools for immunoglobulin and T cell receptor sequence analysis, http://imgt.cines.fr. Leukemia 2003; 17:260-6.

280. Lefranc MP. IMGT, the international ImMunoGeneTics database. Nucleic Acids Res 2003; 31:307-10.

281. van Dongen JJ, Langerak AW, Bruggemann M, Evans PA, Hummel M, Lavender FL, et al. Design and standardization of PCR primers and protocols for detection of clonal immunoglobulin and T-cell receptor gene recombinations

in suspect lymphoproliferations: report of the BIOMED-2 Concerted Action BMH4-CT98-3936. Leukemia 2003; 17:2257-317.

282. Arden B, Clark SP, Kabelitz D, Mak TW. Human T-cell receptor variable gene segment families. Immunogenetics 1995; 42:455-500.

283. Blom B, Verschuren MC, Heemskerk MH, Bakker AQ, van Gastel-Mol EJ, Wolvers-Tettero IL, et al. TCR gene rearrangements and expression of the pre-T cell receptor complex during human T-cell differentiation. Blood 1999; 93:3033-43.

284. Davis MM, Bjorkman PJ. T-cell antigen receptor genes and T-cell recognition. Nature 1988; 334:395-402.

285. Arstila TP, Casrouge A, Baron V, Even J, Kanellopoulos J, Kourilsky P. A direct estimate of the human alphabeta T cell receptor diversity. Science 1999; 286:958-61.

286. Tonegawa S. Somatic generation of antibody diversity. Nature 1983; 302:575-81.

287. McBlane JF, van Gent DC, Ramsden DA, Romeo C, Cuomo CA, Gellert M, et al. Cleavage at a V(D)J recombination signal requires only RAG1 and RAG2 proteins and occurs in two steps. Cell 1995; 83:387-95.

288. van Gent DC, Mizuuchi K, Gellert M. Similarities between initiation of V(D)J recombination and retroviral integration. Science 1996; 271:1592-4.

289. Agrawal A, Schatz DG. RAG1 and RAG2 form a stable postcleavage synaptic complex with DNA containing signal ends in V(D)J recombination. Cell 1997; 89:43-53.

290. Ma Y, Pannicke U, Schwarz K, Lieber MR. Hairpin opening and overhang processing by an Artemis/DNA-dependent protein kinase complex in nonhomologous end joining and V(D)J recombination. Cell 2002; 108:781-94.

291. Lewis SM. P nucleotide insertions and the resolution of hairpin DNA structures in mammalian cells. Proc Natl Acad Sci U S A 1994; 91:1332-6.

292. Komori T, Okada A, Stewart V, Alt FW. Lack of N regions in antigen receptor variable region genes of TdT-deficient lymphocytes. Science 1993; 261:1171-5.

293. Grawunder U, Zimmer D, Fugmann S, Schwarz K, Lieber MR. DNA ligase IV is essential for V(D)J recombination and DNA double-strand break repair in human precursor lymphocytes. Mol Cell 1998; 2:477-84.

294. Buck D, Malivert L, de Chasseval R, Barraud A, Fondaneche MC, Sanal O, et al. Cernunnos, a novel nonhomologous end-joining factor, is mutated in human immunodeficiency with microcephaly. Cell 2006; 124:287-99.

295. Verschuren MC, Wolvers-Tettero IL, Breit TM, Noordzij J, van Wering ER, van Dongen JJ. Preferential rearrangements of the T cell receptor-delta-deleting elements in human T cells. J Immunol 1997; 158:1208-16.

296. Breit TM, Wolvers-Tettero IL, van Dongen JJ. Unique selection determinant in polyclonal V delta 2-J delta 1 junctional regions of human peripheral gamma delta T lymphocytes. J Immunol 1994; 152:2860-4.

297. Villey I, Caillol D, Selz F, Ferrier P, de Villartay JP. Defect in rearrangement of the most 5' TCR-J alpha following targeted deletion of T early alpha (TEA): implications for TCR alpha locus accessibility. Immunity 1996; 5:331-42.

298. Starr TK, Jameson SC, Hogquist KA. Positive and negative selection of T cells. Annu Rev Immunol 2003; 21:139-76.

299. Chong MM, Cornish AL, Darwiche R, Stanley EG, Purton JF, Godfrey DI, et al. Suppressor of cytokine signaling-1 is a critical regulator of interleukin-7-dependent CD8+ T cell differentiation. Immunity 2003; 18:475-87.

300. Kappler JW, Roehm N, Marrack P. T cell tolerance by clonal elimination in the thymus. Cell 1987; 49:273-80.

301. Bautista JL, Lio CW, Lathrop SK, Forbush K, Liang Y, Luo J, et al. Intraclonal competition limits the fate determination of regulatory T cells in the thymus. Nat Immunol 2009; 10:610-7.

302. Leung MW, Shen S, Lafaille JJ. TCR-dependent differentiation of thymic Foxp3+ cells is limited to small clonal sizes. J Exp Med 2009; 206:2121-30.

303. Ouyang W, Beckett O, Ma Q, Li MO. Transforming growth factor-beta signaling curbs thymic negative selection promoting regulatory T cell development. Immunity 2010; 32:642-53.

304. Teh HS, Kisielow P, Scott B, Kishi H, Uematsu Y, Bluthmann H, et al. Thymic major histocompatibility complex antigens and the alpha beta T-cell receptor determine the CD4/CD8 phenotype of T cells. Nature 1988; 335:229-33.

305. Catlett IM, Hedrick SM. Suppressor of cytokine signaling 1 is required for the differentiation of CD4+ T cells. Nat Immunol 2005; 6:715-21.

306. Erman B, Alag AS, Dahle O, van Laethem F, Sarafova SD, Guinter TI, et al. Coreceptor signal strength regulates positive selection but does not determine

CD4/CD8 lineage choice in a physiologic in vivo model. J Immunol 2006; 177:6613-25.

307. Brugnera E, Bhandoola A, Cibotti R, Yu Q, Guinter TI, Yamashita Y, et al. Coreceptor reversal in the thymus: signaled CD4+8+ thymocytes initially terminate CD8 transcription even when differentiating into CD8+ T cells. Immunity 2000; 13:59-71.

308. Bosselut R, Guinter TI, Sharrow SO, Singer A. Unraveling a revealing paradox: Why major histocompatibility complex I-signaled thymocytes "paradoxically" appear as CD4+8lo transitional cells during positive selection of CD8+ T cells. J Exp Med 2003; 197:1709-19.

309. Park JH, Adoro S, Guinter T, Erman B, Alag AS, Catalfamo M, et al. Signaling by intrathymic cytokines, not T cell antigen receptors, specifies CD8 lineage choice and promotes the differentiation of cytotoxic-lineage T cells. Nat Immunol 2010; 11:257-64.

310. Adoro S, McCaughtry T, Erman B, Alag A, Van Laethem F, Park JH, et al. Coreceptor gene imprinting governs thymocyte lineage fate. EMBO J 2012; 31:366-77.

311. Sawada S, Scarborough JD, Killeen N, Littman DR. A lineage-specific transcriptional silencer regulates CD4 gene expression during T lymphocyte development. Cell 1994; 77:917-29.

312. Ellmeier W, Sunshine MJ, Losos K, Littman DR. Multiple developmental stage-specific enhancers regulate CD8 expression in developing thymocytes and in thymus-independent T cells. Immunity 1998; 9:485-96.

313. He X, Dave VP, Zhang Y, Hua X, Nicolas E, Xu W, et al. The zinc finger transcription factor Th-POK regulates CD4 versus CD8 T-cell lineage commitment. Nature 2005; 433:826-33.

314. Sun G, Liu X, Mercado P, Jenkinson SR, Kypriotou M, Feigenbaum L, et al. The zinc finger protein cKrox directs CD4 lineage differentiation during intrathymic T cell positive selection. Nat Immunol 2005; 6:373-81.

315. Taniuchi I, Osato M, Egawa T, Sunshine MJ, Bae SC, Komori T, et al. Differential requirements for Runx proteins in CD4 repression and epigenetic silencing during T lymphocyte development. Cell 2002; 111:621-33.

316. Jenkinson SR, Intlekofer AM, Sun G, Feigenbaum L, Reiner SL, Bosselut R. Expression of the transcription factor cKrox in peripheral CD8 T cells reveals

substantial postthymic plasticity in CD4-CD8 lineage differentiation. J Exp Med 2007; 204:267-72.

317. He X, Park K, Wang H, Zhang Y, Hua X, Li Y, et al. CD4-CD8 lineage commitment is regulated by a silencer element at the ThPOK transcription-factor locus. Immunity 2008; 28:346-58.

318. Setoguchi R, Tachibana M, Naoe Y, Muroi S, Akiyama K, Tezuka C, et al. Repression of the transcription factor Th-POK by Runx complexes in cytotoxic T cell development. Science 2008; 319:822-5.

319. Sato T, Ohno S, Hayashi T, Sato C, Kohu K, Satake M, et al. Dual functions of Runx proteins for reactivating CD8 and silencing CD4 at the commitment process into CD8 thymocytes. Immunity 2005; 22:317-28.

320. Hataye J, Moon JJ, Khoruts A, Reilly C, Jenkins MK. Naive and memory CD4+ T cell survival controlled by clonal abundance. Science 2006; 312:114-6.

321. Link A, Vogt TK, Favre S, Britschgi MR, Acha-Orbea H, Hinz B, et al. Fibroblastic reticular cells in lymph nodes regulate the homeostasis of naive T cells. Nat Immunol 2007; 8:1255-65.

322. Park JH, Yu Q, Erman B, Appelbaum JS, Montoya-Durango D, Grimes HL, et al. Suppression of IL7Ralpha transcription by IL-7 and other prosurvival cytokines: a novel mechanism for maximizing IL-7-dependent T cell survival. Immunity 2004; 21:289-302.

323. Surh CD, Sprent J. Homeostasis of naive and memory T cells. Immunity 2008; 29:848-62.

324. Marelli-Berg FM, Cannella L, Dazzi F, Mirenda V. The highway code of T cell trafficking. J Pathol 2008; 214:179-89.

325. Mazzucchelli R, Durum SK. Interleukin-7 receptor expression: intelligent design. Nat Rev Immunol 2007; 7:144-54.

326. Khaled AR, Durum SK. Lymphocide: cytokines and the control of lymphoid homeostasis. Nat Rev Immunol 2002; 2:817-30.

327. Min B, McHugh R, Sempowski GD, Mackall C, Foucras G, Paul WE. Neonates support lymphopenia-induced proliferation. Immunity 2003; 18:131-40.

328. Goldrath AW, Bevan MJ. Low-affinity ligands for the TCR drive proliferation of mature CD8+ T cells in lymphopenic hosts. Immunity 1999; 11:183-90.

329. Schluns KS, Kieper WC, Jameson SC, Lefrancois L. Interleukin-7 mediates the homeostasis of naive and memory CD8 T cells in vivo. Nat Immunol 2000; 1:426-32.

330. Sherr CJ, Roberts JM. CDK inhibitors: positive and negative regulators of G1-phase progression. Genes Dev 1999; 13:1501-12.

331. Cho JH, Boyman O, Kim HO, Hahm B, Rubinstein MP, Ramsey C, et al. An intense form of homeostatic proliferation of naive CD8+ cells driven by IL-2. J Exp Med 2007; 204:1787-801.

332. Ramsey C, Rubinstein MP, Kim DM, Cho JH, Sprent J, Surh CD. The lymphopenic environment of CD132 (common gamma-chain)-deficient hosts elicits rapid homeostatic proliferation of naive T cells via IL-15. J Immunol 2008; 180:5320-6.

333. Davey GM, Starr R, Cornish AL, Burghardt JT, Alexander WS, Carbone FR, et al. SOCS-1 regulates IL-15-driven homeostatic proliferation of antigen-naive CD8 T cells, limiting their autoimmune potential. J Exp Med 2005; 202:1099-108.

334. Macagno A, Napolitani G, Lanzavecchia A, Sallusto F. Duration, combination and timing: the signal integration model of dendritic cell activation. Trends Immunol 2007; 28:227-33.

335. Hickman HD, Takeda K, Skon CN, Murray FR, Hensley SE, Loomis J, et al. Direct priming of antiviral CD8+ T cells in the peripheral interfollicular region of lymph nodes. Nat Immunol 2008; 9:155-65.

336. John B, Harris TH, Tait ED, Wilson EH, Gregg B, Ng LG, et al. Dynamic Imaging of CD8(+) T cells and dendritic cells during infection with Toxoplasma gondii. PLoS Pathog 2009; 5:e1000505.

337. Bretscher P, Cohn M. A theory of self-nonself discrimination. Science 1970; 169:1042-9.

338. Bernard A, Lamy, Alberti I. The two-signal model of T-cell activation after 30 years. Transplantation 2002; 73:S31-5.

339. Zhu J, Yamane H, Paul WE. Differentiation of effector CD4 T cell populations (*). Annu Rev Immunol 2010; 28:445-89.

340. Zhang N, Bevan MJ. CD8(+) T cells: foot soldiers of the immune system. Immunity 2011; 35:161-8.

341. Badovinac VP, Haring JS, Harty JT. Initial T cell receptor transgenic cell precursor frequency dictates critical aspects of the CD8(+) T cell response to infection. Immunity 2007; 26:827-41.

342. Michalek RD, Rathmell JC. The metabolic life and times of a T-cell. Immunol Rev 2010; 236:190-202.

343. Hsieh CS, Macatonia SE, Tripp CS, Wolf SF, O'Garra A, Murphy KM. Development of TH1 CD4+ T cells through IL-12 produced by Listeria-induced macrophages. Science 1993; 260:547-9.

344. Mullen AC, High FA, Hutchins AS, Lee HW, Villarino AV, Livingston DM, et al. Role of T-bet in commitment of TH1 cells before IL-12-dependent selection. Science 2001; 292:1907-10.

345. Szabo SJ, Kim ST, Costa GL, Zhang X, Fathman CG, Glimcher LH. A novel transcription factor, T-bet, directs Th1 lineage commitment. Cell 2000; 100:655-69.

346. Usui T, Nishikomori R, Kitani A, Strober W. GATA-3 suppresses Th1 development by downregulation of Stat4 and not through effects on IL-12Rbeta2 chain or T-bet. Immunity 2003; 18:415-28.

347. Swain SL, Weinberg AD, English M, Huston G. IL-4 directs the development of Th2-like helper effectors. J Immunol 1990; 145:3796-806.

348. Zheng W, Flavell RA. The transcription factor GATA-3 is necessary and sufficient for Th2 cytokine gene expression in CD4 T cells. Cell 1997; 89:587-96.

349. Zhu J, Cote-Sierra J, Guo L, Paul WE. Stat5 activation plays a critical role in Th2 differentiation. Immunity 2003; 19:739-48.

350. Aggarwal S, Ghilardi N, Xie MH, de Sauvage FJ, Gurney AL. Interleukin-23 promotes a distinct CD4 T cell activation state characterized by the production of interleukin-17. J Biol Chem 2003; 278:1910-4.

351. Park H, Li Z, Yang XO, Chang SH, Nurieva R, Wang YH, et al. A distinct lineage of CD4 T cells regulates tissue inflammation by producing interleukin 17. Nat Immunol 2005; 6:1133-41.

352. Ivanov, II, McKenzie BS, Zhou L, Tadokoro CE, Lepelley A, Lafaille JJ, et al. The orphan nuclear receptor RORgammat directs the differentiation program of proinflammatory IL-17+ T helper cells. Cell 2006; 126:1121-33.

353. Harris TJ, Grosso JF, Yen HR, Xin H, Kortylewski M, Albesiano E, et al. Cutting edge: An in vivo requirement for STAT3 signaling in TH17 development and TH17-dependent autoimmunity. J Immunol 2007; 179:4313-7.

354. Chen W, Jin W, Hardegen N, Lei KJ, Li L, Marinos N, et al. Conversion of peripheral CD4+CD25- naive T cells to CD4+CD25+ regulatory T cells by TGF-beta induction of transcription factor Foxp3. J Exp Med 2003; 198:1875-86.

355. Zheng SG, Wang JH, Gray JD, Soucier H, Horwitz DA. Natural and induced CD4+CD25+ cells educate CD4+CD25- cells to develop suppressive activity: the role of IL-2, TGF-beta, and IL-10. J Immunol 2004; 172:5213-21.

356. Burchill MA, Yang J, Vogtenhuber C, Blazar BR, Farrar MA. IL-2 receptor beta-dependent STAT5 activation is required for the development of Foxp3+ regulatory T cells. J Immunol 2007; 178:280-90.

357. Breitfeld D, Ohl L, Kremmer E, Ellwart J, Sallusto F, Lipp M, et al. Follicular B helper T cells express CXC chemokine receptor 5, localize to B cell follicles, and support immunoglobulin production. J Exp Med 2000; 192:1545-52.

358. Reinhardt RL, Liang HE, Locksley RM. Cytokine-secreting follicular T cells shape the antibody repertoire. Nat Immunol 2009; 10:385-93.

359. Nurieva RI, Chung Y, Martinez GJ, Yang XO, Tanaka S, Matskevitch TD, et al. Bcl6 mediates the development of T follicular helper cells. Science 2009; 325:1001-5.

360. Joshi NS, Cui W, Chandele A, Lee HK, Urso DR, Hagman J, et al. Inflammation directs memory precursor and short-lived effector CD8(+) T cell fates via the graded expression of T-bet transcription factor. Immunity 2007; 27:281-95.

361. Rutishauser RL, Martins GA, Kalachikov S, Chandele A, Parish IA, Meffre E, et al. Transcriptional repressor Blimp-1 promotes CD8(+) T cell terminal differentiation and represses the acquisition of central memory T cell properties. Immunity 2009; 31:296-308.

362. Takemoto N, Intlekofer AM, Northrup JT, Wherry EJ, Reiner SL. Cutting Edge: IL-12 inversely regulates T-bet and eomesodermin expression during pathogen-induced CD8+ T cell differentiation. J Immunol 2006; 177:7515-9.

363. Pipkin ME, Sacks JA, Cruz-Guilloty F, Lichtenheld MG, Bevan MJ, Rao A. Interleukin-2 and inflammation induce distinct transcriptional programs that promote the differentiation of effector cytolytic T cells. Immunity 2010; 32:79-90.

364. Kalia V, Sarkar S, Subramaniam S, Haining WN, Smith KA, Ahmed R. Prolonged interleukin-2Ralpha expression on virus-specific CD8+ T cells favors terminal-effector differentiation in vivo. Immunity 2010; 32:91-103.

365. Tough DF, Borrow P, Sprent J. Induction of bystander T cell proliferation by viruses and type I interferon in vivo. Science 1996; 272:1947-50.

366. Guo L, Wei G, Zhu J, Liao W, Leonard WJ, Zhao K, et al. IL-1 family members and STAT activators induce cytokine production by Th2, Th17, and Th1 cells. Proc Natl Acad Sci U S A 2009; 106:13463-8.

367. Yang J, Zhu H, Murphy TL, Ouyang W, Murphy KM. IL-18-stimulated GADD45 beta required in cytokine-induced, but not TCR-induced, IFN-gamma production. Nat Immunol 2001; 2:157-64.

368. Palmer EM, Holbrook BC, Arimilli S, Parks GD, Alexander-Miller MA. IFNgamma-producing, virus-specific CD8+ effector cells acquire the ability to produce IL-10 as a result of entry into the infected lung environment. Virology 2010; 404:225-30.

369. Sun J, Dodd H, Moser EK, Sharma R, Braciale TJ. CD4+ T cell help and innate-derived IL-27 induce Blimp-1-dependent IL-10 production by antiviral CTLs. Nat Immunol 2011; 12:327-34.

370. Pepper M, Jenkins MK. Origins of CD4(+) effector and central memory T cells. Nat Immunol 2011; 12:467-71.

371. Ashwell JD, Longo DL, Bridges SH. T-cell tumor elimination as a result of T-cell receptor-mediated activation. Science 1987; 237:61-4.

372. Lenardo MJ. Interleukin-2 programs mouse alpha beta T lymphocytes for apoptosis. Nature 1991; 353:858-61.

373. Ju ST, Panka DJ, Cui H, Ettinger R, el-Khatib M, Sherr DH, et al. Fas(CD95)/FasL interactions required for programmed cell death after T-cell activation. Nature 1995; 373:444-8.

374. Duke RC, Cohen JJ. IL-2 addiction: withdrawal of growth factor activates a suicide program in dependent T cells. Lymphokine Res 1986; 5:289-99.

375. Bouillet P, Metcalf D, Huang DC, Tarlinton DM, Kay TW, Kontgen F, et al. Proapoptotic Bcl-2 relative Bim required for certain apoptotic responses, leukocyte homeostasis, and to preclude autoimmunity. Science 1999; 286:1735-8.

376. Swain SL, Hu H, Huston G. Class II-independent generation of CD4 memory T cells from effectors. Science 1999; 286:1381-3.

377. Zhang X, Sun S, Hwang I, Tough DF, Sprent J. Potent and selective stimulation of memory-phenotype CD8+ T cells in vivo by IL-15. Immunity 1998; 8:591-9.

378. Becker TC, Wherry EJ, Boone D, Murali-Krishna K, Antia R, Ma A, et al. Interleukin 15 is required for proliferative renewal of virus-specific memory CD8 T cells. J Exp Med 2002; 195:1541-8.

379. Carrio R, Rolle CE, Malek TR. Non-redundant role for IL-7R signaling for the survival of CD8+ memory T cells. Eur J Immunol 2007; 37:3078-88.

380. Purton JF, Tan JT, Rubinstein MP, Kim DM, Sprent J, Surh CD. Antiviral CD4+ memory T cells are IL-15 dependent. J Exp Med 2007; 204:951-61.

381. Homann D, Teyton L, Oldstone MB. Differential regulation of antiviral T-cell immunity results in stable CD8+ but declining CD4+ T-cell memory. Nat Med 2001; 7:913-9.

382. Sallusto F, Lenig D, Forster R, Lipp M, Lanzavecchia A. Two subsets of memory T lymphocytes with distinct homing potentials and effector functions. Nature 1999; 401:708-12.

383. Seder RA, Ahmed R. Similarities and differences in CD4+ and CD8+ effector and memory T cell generation. Nat Immunol 2003; 4:835-42.

384. Pepper M, Linehan JL, Pagan AJ, Zell T, Dileepan T, Cleary PP, et al. Different routes of bacterial infection induce long-lived TH1 memory cells and short-lived TH17 cells. Nat Immunol 2010; 11:83-9.

385. Tonegawa S, Berns A, Bonneville M, Farr A, Ishida I, Ito K, et al. Diversity, development, ligands, and probable functions of gamma delta T cells. Cold Spring Harb Symp Quant Biol 1989; 54 Pt 1:31-44.

386. Lefranc MP, Rabbitts TH. A nomenclature to fit the organization of the human T-cell receptor gamma and delta genes. Res Immunol 1990; 141:615-8.

387. Constant P, Davodeau F, Peyrat MA, Poquet Y, Puzo G, Bonneville M, et al. Stimulation of human gamma delta T cells by nonpeptidic mycobacterial ligands. Science 1994; 264:267-70.

388. Tanaka Y, Morita CT, Nieves E, Brenner MB, Bloom BR. Natural and synthetic non-peptide antigens recognized by human gamma delta T cells. Nature 1995; 375:155-8.

389. Chien YH, Konigshofer Y. Antigen recognition by gammadelta T cells. Immunol Rev 2007; 215:46-58.

390. Hayday AC. Gammadelta T cells and the lymphoid stress-surveillance response. Immunity 2009; 31:184-96.

391. Aydintug MK, Roark CL, Chain JL, Born WK, O'Brien RL. Macrophages express multiple ligands for gammadelta TCRs. Mol Immunol 2008; 45:3253-63.

392. Raulet DH, Guerra N. Oncogenic stress sensed by the immune system: role of natural killer cell receptors. Nat Rev Immunol 2009; 9:568-80.

393. Qin G, Mao H, Zheng J, Sia SF, Liu Y, Chan PL, et al. Phosphoantigen-expanded human gammadelta T cells display potent cytotoxicity against monocyte-derived macrophages infected with human and avian influenza viruses. J Infect Dis 2009; 200:858-65.

394. Strid J, Roberts SJ, Filler RB, Lewis JM, Kwong BY, Schpero W, et al. Acute upregulation of an NKG2D ligand promotes rapid reorganization of a local immune compartment with pleiotropic effects on carcinogenesis. Nat Immunol 2008; 9:146-54.

395. Halary F, Pitard V, Dlubek D, Krzysiek R, de la Salle H, Merville P, et al. Shared reactivity of V{delta}2(neg) {gamma}{delta} T cells against cytomegalovirus-infected cells and tumor intestinal epithelial cells. J Exp Med 2005; 201:1567-78.

396. Gapin L, Matsuda JL, Surh CD, Kronenberg M. NKT cells derive from double-positive thymocytes that are positively selected by CD1d. Nat Immunol 2001; 2:971-8.

397. Griewank K, Borowski C, Rietdijk S, Wang N, Julien A, Wei DG, et al. Homotypic interactions mediated by Slamf1 and Slamf6 receptors control NKT cell lineage development. Immunity 2007; 27:751-62.

398. Kovalovsky D, Uche OU, Eladad S, Hobbs RM, Yi W, Alonzo E, et al. The BTB-zinc finger transcriptional regulator PLZF controls the development of invariant natural killer T cell effector functions. Nat Immunol 2008; 9:1055-64.

399. Godfrey DI, Stankovic S, Baxter AG. Raising the NKT cell family. Nat Immunol 2010; 11:197-206.

400. Lee WY, Moriarty TJ, Wong CH, Zhou H, Strieter RM, van Rooijen N, et al. An intravascular immune response to Borrelia burgdorferi involves Kupffer cells and iNKT cells. Nat Immunol 2010; 11:295-302.

401. Wong CH, Jenne CN, Lee WY, Leger C, Kubes P. Functional innervation of hepatic iNKT cells is immunosuppressive following stroke. Science 2011; 334:101-5.

402. Brennan PJ, Brigl M, Brenner MB. Invariant natural killer T cells: an innate activation scheme linked to diverse effector functions. Nat Rev Immunol 2013; 13:101-17.

403. Treiner E, Duban L, Bahram S, Radosavljevic M, Wanner V, Tilloy F, et al. Selection of evolutionarily conserved mucosal-associated invariant T cells by MR1. Nature 2003; 422:164-9.

404. Kjer-Nielsen L, Patel O, Corbett AJ, Le Nours J, Meehan B, Liu L, et al. MR1 presents microbial vitamin B metabolites to MAIT cells. Nature 2012; 491:717-23.

405. Martin E, Treiner E, Duban L, Guerri L, Laude H, Toly C, et al. Stepwise development of MAIT cells in mouse and human. PLoS Biol 2009; 7:e54.

406. Dusseaux M, Martin E, Serriari N, Peguillet I, Premel V, Louis D, et al. Human MAIT cells are xenobiotic-resistant, tissue-targeted, CD161hi IL-17-secreting T cells. Blood 2011; 117:1250-9.

407. van Zelm MC, van der Burg M, Langerak AW, van Dongen JJ. PID comes full circle: applications of V(D)J recombination excision circles in research, diagnostics and newborn screening of primary immunodeficiency disorders. Front Immunol 2011; 2:12.

408. Buckley RH. The long quest for neonatal screening for severe combined immunodeficiency. J Allergy Clin Immunol 2012; 129:597-604; quiz 5-6.

409. Puck JM. Laboratory technology for population-based screening for severe combined immunodeficiency in neonates: the winner is T-cell receptor excision circles. J Allergy Clin Immunol 2012; 129:607-16.

410. Railey MD, Lokhnygina Y, Buckley RH. Long-term clinical outcome of patients with severe combined immunodeficiency who received related donor bone marrow transplants without pretransplant chemotherapy or post-transplant GVHD prophylaxis. J Pediatr 2009; 155:834-40 e1.

411. Hacein-Bey-Abina S, Hauer J, Lim A, Picard C, Wang GP, Berry CC, et al. Efficacy of gene therapy for X-linked severe combined immunodeficiency. N Engl J Med 2010; 363:355-64.

412. Milner JD, Holland SM. The cup runneth over: lessons from the ever-expanding pool of primary immunodeficiency diseases. Nat Rev Immunol 2013; 13:635-48.

413. Notarangelo LD. Functional T cell immunodeficiencies (with T cells present). Annu Rev Immunol 2013; 31:195-225.

414. Durandy A, Kracker S, Fischer A. Primary antibody deficiencies. Nat Rev Immunol 2013; 13:519-33.

415. Picard C, McCarl CA, Papolos A, Khalil S, Luthy K, Hivroz C, et al. STIM1 mutation associated with a syndrome of immunodeficiency and autoimmunity. N Engl J Med 2009; 360:1971-80.

416. Lanzi G, Moratto D, Vairo D, Masneri S, Delmonte O, Paganini T, et al. A novel primary human immunodeficiency due to deficiency in the WASP-interacting protein WIP. J Exp Med 2012; 209:29-34.

417. Thrasher AJ, Burns SO. WASP: a key immunological multitasker. Nat Rev Immunol 2010; 10:182-92.

418. Zhang Q, Davis JC, Lamborn IT, Freeman AF, Jing H, Favreau AJ, et al. Combined immunodeficiency associated with DOCK8 mutations. N Engl J Med 2009; 361:2046-55.

419. Cannons JL, Tangye SG, Schwartzberg PL. SLAM family receptors and SAP adaptors in immunity. Annu Rev Immunol 2011; 29:665-705.

420. Huck K, Feyen O, Niehues T, Ruschendorf F, Hubner N, Laws HJ, et al. Girls homozygous for an IL-2-inducible T cell kinase mutation that leads to protein deficiency develop fatal EBV-associated lymphoproliferation. J Clin Invest 2009; 119:1350-8.

421. Latour S. Natural killer T cells and X-linked lymphoproliferative syndrome. Curr Opin Allergy Clin Immunol 2007; 7:510-4.

422. Latour S, Gish G, Helgason CD, Humphries RK, Pawson T, Veillette A. Regulation of SLAM-mediated signal transduction by SAP, the X-linked lymphoproliferative gene product. Nat Immunol 2001; 2:681-90.

423. Moshous D, Martin E, Carpentier W, Lim A, Callebaut I, Canioni D, et al. Whole-exome sequencing identifies Coronin-1A deficiency in 3 siblings with immunodeficiency and EBV-associated B-cell lymphoproliferation. J Allergy Clin Immunol 2013; 131:1594-603.

424. Salzer E, Daschkey S, Choo S, Gombert M, Santos-Valente E, Ginzel S, et al. Combined immunodeficiency with life-threatening EBV-associated lymphoproliferative disorder in patients lacking functional CD27. Haematologica 2013; 98:473-8.

425. Shiow LR, Roadcap DW, Paris K, Watson SR, Grigorova IL, Lebet T, et al. The actin regulator coronin 1A is mutant in a thymic egress-deficient mouse strain

and in a patient with severe combined immunodeficiency. Nat Immunol 2008; 9:1307-15.

426. van Montfrans JM, Hoepelman AI, Otto S, van Gijn M, van de Corput L, de Weger RA, et al. CD27 deficiency is associated with combined immunodeficiency and persistent symptomatic EBV viremia. J Allergy Clin Immunol 2012; 129:787-93 e6.

427. Veillette A, Pérez-Quintero L-A, Latour S. X-linked lymphoproliferative syndromes and related autosomal recessive disorders. Curr Opin Allergy Clin Immunol 2013; In press.

428. Morgan NV, Goddard S, Cardno TS, McDonald D, Rahman F, Barge D, et al. Mutation in the TCRalpha subunit constant gene (TRAC) leads to a human immunodeficiency disorder characterized by a lack of TCRalphabeta+ T cells. J Clin Invest 2011; 121:695-702.

429. Arnaiz-Villena A, Timon M, Corell A, Perez-Aciego P, Martin-Villa JM, Regueiro JR. Brief report: primary immunodeficiency caused by mutations in the gene encoding the CD3-gamma subunit of the T-lymphocyte receptor. N Engl J Med 1992; 327:529-33.

430. Dadi HK, Simon AJ, Roifman CM. Effect of CD3delta deficiency on maturation of alpha/beta and gamma/delta T-cell lineages in severe combined immunodeficiency. N Engl J Med 2003; 349:1821-8.

431. de Saint Basile G, Geissmann F, Flori E, Uring-Lambert B, Soudais C, Cavazzana-Calvo M, et al. Severe combined immunodeficiency caused by deficiency in either the delta or the epsilon subunit of CD3. J Clin Invest 2004; 114:1512-7.

432. Rieux-Laucat F, Hivroz C, Lim A, Mateo V, Pellier I, Selz F, et al. Inherited and somatic CD3zeta mutations in a patient with T-cell deficiency. N Engl J Med 2006; 354:1913-21.

433. Hauck F, Randriamampita C, Martin E, Gerart S, Lambert N, Lim A, et al. Primary T-cell immunodeficiency with immunodysregulation caused by autosomal recessive LCK deficiency. J Allergy Clin Immunol 2012; 130:1144-52 e11.

434. Gorska MM, Alam R. A mutation in the human Uncoordinated 119 gene impairs TCR signaling and is associated with CD4 lymphopenia. Blood 2012; 119:1399-406.

435. Arpaia E, Shahar M, Dadi H, Cohen A, Roifman CM. Defective T cell receptor signaling and CD8+ thymic selection in humans lacking zap-70 kinase. Cell 1994; 76:947-58.

436. Chan AC, Kadlecek TA, Elder ME, Filipovich AH, Kuo WL, Iwashima M, et al. ZAP-70 deficiency in an autosomal recessive form of severe combined immunodeficiency. Science 1994; 264:1599-601.

437. Elder ME, Lin D, Clever J, Chan AC, Hope TJ, Weiss A, et al. Human severe combined immunodeficiency due to a defect in ZAP-70, a T cell tyrosine kinase. Science 1994; 264:1596-9.

438. Crequer A, Troeger A, Patin E, Ma CS, Picard C, Pedergnana V, et al. Human RHOH deficiency causes T cell defects and susceptibility to EV-HPV infections. J Clin Invest 2012; 122:3239-47.

439. Nehme NT, Pachlopnik Schmid J, Debeurme F, Andre-Schmutz I, Lim A, Nitschke P, et al. MST1 mutations in autosomal recessive primary immunodeficiency characterized by defective naive T-cell survival. Blood 2012; 119:3458-68.

440. Abdollahpour H, Appaswamy G, Kotlarz D, Diestelhorst J, Beier R, Schaffer AA, et al. The phenotype of human STK4 deficiency. Blood 2012; 119:3450-7.

441. Chaigne-Delalande B, Li FY, O'Connor GM, Lukacs MJ, Jiang P, Zheng L, et al. Mg2+ regulates cytotoxic functions of NK and CD8 T cells in chronic EBV infection through NKG2D. Science 2013; 341:186-91.

442. Stepensky P, Keller B, Buchta M, Kienzler AK, Elpeleg O, Somech R, et al. Deficiency of caspase recruitment domain family, member 11 (CARD11), causes profound combined immunodeficiency in human subjects. J Allergy Clin Immunol 2013; 131:477-85 e1.

443. Greil J, Rausch T, Giese T, Bandapalli OR, Daniel V, Bekeredjian-Ding I, et al. Whole-exome sequencing links caspase recruitment domain 11 (CARD11) inactivation to severe combined immunodeficiency. J Allergy Clin Immunol 2013; 131:1376-83 e3.

444. Jabara HH, Ohsumi T, Chou J, Massaad MJ, Benson H, Megarbane A, et al. A homozygous mucosa-associated lymphoid tissue 1 (MALT1) mutation in a family with combined immunodeficiency. J Allergy Clin Immunol 2013; 132:151-8.

445. Schimke LF, Rieber N, Rylaarsdam S, Cabral-Marques O, Hubbard N, Puel A, et al. A novel gain-of-function IKBA mutation underlies ectodermal dysplasia

with immunodeficiency and polyendocrinopathy. J Clin Immunol 2013; 33:1088-99.

446. Kotlarz D, Zietara N, Uzel G, Weidemann T, Braun CJ, Diestelhorst J, et al. Loss-of-function mutations in the IL-21 receptor gene cause a primary immunodeficiency syndrome. J Exp Med 2013; 210:433-43.

447. Byun M, Ma CS, Akcay A, Pedergnana V, Palendira U, Myoung J, et al. Inherited human OX40 deficiency underlying classic Kaposi sarcoma of childhood. J Exp Med 2013; 210:1743-59.

448. Samuels ME, Majewski J, Alirezaie N, Fernandez I, Casals F, Patey N, et al. Exome sequencing identifies mutations in the gene TTC7A in French-Canadian cases with hereditary multiple intestinal atresia. J Med Genet 2013; 50:324-9.

449. Chen R, Giliani S, Lanzi G, Mias GI, Lonardi S, Dobbs K, et al. Whole-exome sequencing identifies tetratricopeptide repeat domain 7A (TTC7A) mutations for combined immunodeficiency with intestinal atresias. J Allergy Clin Immunol 2013; 132:656-64 e17.

450. Pachlopnik Schmid J, Lemoine R, Nehme N, Cormier-Daire V, Revy P, Debeurme F, et al. Polymerase epsilon1 mutation in a human syndrome with facial dysmorphism, immunodeficiency, livedo, and short stature ("FILS syndrome"). J Exp Med 2012; 209:2323-30.

451. Junge S, Kloeckener-Gruissem B, Zufferey R, Keisker A, Salgo B, Fauchere JC, et al. Correlation between recent thymic emigrants and CD31+ (PECAM-1) CD4+ T cells in normal individuals during aging and in lymphopenic children. Eur J Immunol 2007; 37:3270-80.

452. Willinger T, Freeman T, Hasegawa H, McMichael AJ, Callan MF. Molecular signatures distinguish human central memory from effector memory CD8 T cell subsets. J Immunol 2005; 175:5895-903.

453. Pannetier C LA, Even J, Kourilsky P. The immunoscope approach for the analysis of T cell repertoires. Landes Bioscience, Chapman & Hall. 1997.

454. Lim A, Baron V, Ferradini L, Bonneville M, Kourilsky P, Pannetier C. Combination of MHC-peptide multimer-based T cell sorting with the Immunoscope permits sensitive ex vivo quantitation and follow-up of human CD8+ T cell immune responses. J Immunol Methods 2002; 261:177-94.

455. Brochet X, Lefranc MP, Giudicelli V. IMGT/V-QUEST: the highly customized and integrated system for IG and TR standardized V-J and V-D-J sequence analysis. Nucleic Acids Res 2008; 36:W503-8.

456. Molina TJ, Kishihara K, Siderovski DP, van Ewijk W, Narendran A, Timms E, et al. Profound block in thymocyte development in mice lacking p56lck. Nature 1992; 357:161-4.

457. Goldman FD, Ballas ZK, Schutte BC, Kemp J, Hollenback C, Noraz N, et al. Defective expression of p56lck in an infant with severe combined immunodeficiency. J Clin Invest 1998; 102:421-9.

458. Clappier E, Cuccuini W, Kalota A, Crinquette A, Cayuela JM, Dik WA, et al. The C-MYB locus is involved in chromosomal translocation and genomic duplications in human T-cell acute leukemia (T-ALL), the translocation defining a new T-ALL subtype in very young children. Blood 2007; 110:1251-61.

459. Sawabe T, Horiuchi T, Nakamura M, Tsukamoto H, Nakahara K, Harashima SI, et al. Defect of lck in a patient with common variable immunodeficiency. Int J Mol Med 2001; 7:609-14.

460. Latour S, Chow LM, Veillette A. Differential intrinsic enzymatic activity of Syk and Zap-70 protein-tyrosine kinases. J Biol Chem 1996; 271:22782-90.

461. Takahashi Y, Sipp D, Enomoto H. Tissue interactions in neural crest cell development and disease. Science 2013; 341:860-3.

462. McLean-Tooke A, Barge D, Spickett GP, Gennery AR. T cell receptor Vbeta repertoire of T lymphocytes and T regulatory cells by flow cytometric analysis in healthy children. Clin Exp Immunol 2008; 151:190-8.

463. Stepensky P, Weintraub M, Yanir A, Revel-Vilk S, Krux F, Huck K, et al. IL-2-inducible T-cell kinase deficiency: clinical presentation and therapeutic approach. Haematologica 2011; 96:472-6.

464. Linka RM, Risse SL, Bienemann K, Werner M, Linka Y, Krux F, et al. Loss-of-function mutations within the IL-2 inducible kinase ITK in patients with EBV-associated lymphoproliferative diseases. Leukemia 2012; 26:963-71.

465. Mueller C, August A. Attenuation of immunological symptoms of allergic asthma in mice lacking the tyrosine kinase ITK. J Immunol 2003; 170:5056-63.

466. Fischer AM, Mercer JC, Iyer A, Ragin MJ, August A. Regulation of CXC chemokine receptor 4-mediated migration by the Tec family tyrosine kinase ITK. J Biol Chem 2004; 279:29816-20.

467. Takesono A, Horai R, Mandai M, Dombroski D, Schwartzberg PL. Requirement for Tec kinases in chemokine-induced migration and activation of Cdc42 and Rac. Curr Biol 2004; 14:917-22.

468. Berge T, Sundvold-Gjerstad V, Granum S, Andersen TC, Holthe GB, Claesson-Welsh L, et al. T cell specific adapter protein (TSAd) interacts with Tec kinase ITK to promote CXCL12 induced migration of human and murine T cells. PLoS One 2010; 5:e9761.

469. Kotzot D. Complex and segmental uniparental disomy (UPD): review and lessons from rare chromosomal complements. J Med Genet 2001; 38:497-507.

470. Dufourcq-Lagelouse R, Lambert N, Duval M, Viot G, Vilmer E, Fischer A, et al. Chediak-Higashi syndrome associated with maternal uniparental isodisomy of chromosome 1. Eur J Hum Genet 1999; 7:633-7.

471. Prando C, Boisson-Dupuis S, Grant AV, Kong XF, Bustamante J, Feinberg J, et al. Paternal uniparental isodisomy of chromosome 6 causing a complex syndrome including complete IFN-gamma receptor 1 deficiency. Am J Med Genet A 2010; 152A:622-9.

472. Sulisalo T, Makitie O, Sistonen P, Ridanpaa M, el-Rifai W, Ruuskanen O, et al. Uniparental disomy in cartilage-hair hypoplasia. Eur J Hum Genet 1997; 5:35-42.

473. Al-Jasmi F, Abdelhaleem M, Stockley T, Lee KS, Clarke JT. Novel mutation of the perforin gene and maternal uniparental disomy 10 in a patient with familial hemophagocytic lymphohistiocytosis. J Pediatr Hematol Oncol 2008; 30:621-4.

474. Molina TJ, Bachmann MF, Kundig TM, Zinkernagel RM, Mak TW. Peripheral T cells in mice lacking p56lck do not express significant antiviral effector functions. J Immunol 1993; 151:699-706.

475. Bueno C, Lemke CD, Criado G, Baroja ML, Ferguson SS, Rahman AK, et al. Bacterial superantigens bypass Lck-dependent T cell receptor signaling by activating a Galpha11-dependent, PLC-beta-mediated pathway. Immunity 2006; 25:67-78.

476. van Oers NS, Lowin-Kropf B, Finlay D, Connolly K, Weiss A. alpha beta T cell development is abolished in mice lacking both Lck and Fyn protein tyrosine kinases. Immunity 1996; 5:429-36.

477. Penninger J, Kishihara K, Molina T, Wallace VA, Timms E, Hedrick SM, et al. Requirement for tyrosine kinase p56lck for thymic development of transgenic gamma delta T cells. Science 1993; 260:358-61.

478. Lovatt M, Filby A, Parravicini V, Werlen G, Palmer E, Zamoyska R. Lck regulates the threshold of activation in primary T cells, while both Lck and Fyn contribute to the magnitude of the extracellular signal-related kinase response. Mol Cell Biol 2006; 26:8655-65.

479. Gavin MA, Torgerson TR, Houston E, DeRoos P, Ho WY, Stray-Pedersen A, et al. Single-cell analysis of normal and FOXP3-mutant human T cells: FOXP3 expression without regulatory T cell development. Proc Natl Acad Sci U S A 2006; 103:6659-64.

480. Tewari K, Walent J, Svaren J, Zamoyska R, Suresh M. Differential requirement for Lck during primary and memory CD8+ T cell responses. Proc Natl Acad Sci U S A 2006; 103:16388-93.

481. Barzaghi F, Passerini L, Bacchetta R. Immune dysregulation, polyendocrinopathy, enteropathy, x-linked syndrome: a paradigm of immunodeficiency with autoimmunity. Front Immunol 2012; 3:211.

482. Villa A, Notarangelo LD, Roifman CM. Omenn syndrome: inflammation in leaky severe combined immunodeficiency. J Allergy Clin Immunol 2008; 122:1082-6.

483. de Villartay JP, Lim A, Al-Mousa H, Dupont S, Dechanet-Merville J, Coumau-Gatbois E, et al. A novel immunodeficiency associated with hypomorphic RAG1 mutations and CMV infection. J Clin Invest 2005; 115:3291-9.

484. Hubert P, Bergeron F, Ferreira V, Seligmann M, Oksenhendler E, Debre P, et al. Defective p56Lck activity in T cells from an adult patient with idiopathic CD4+ lymphocytopenia. Int Immunol 2000; 12:449-57.

485. Veillette A, Horak ID, Horak EM, Bookman MA, Bolen JB. Alterations of the lymphocyte-specific protein tyrosine kinase (p56lck) during T-cell activation. Mol Cell Biol 1988; 8:4353-61.

486. Nika K, Soldani C, Salek M, Paster W, Gray A, Etzensperger R, et al. Constitutively active Lck kinase in T cells drives antigen receptor signal transduction. Immunity 2010; 32:766-77.

487. Gorska MM, Liang Q, Karim Z, Alam R. Uncoordinated 119 protein controls trafficking of Lck via the Rab11 endosome and is critical for immunological synapse formation. J Immunol 2009; 183:1675-84.

488. Negishi I, Motoyama N, Nakayama K, Senju S, Hatakeyama S, Zhang Q, et al. Essential role for ZAP-70 in both positive and negative selection of thymocytes. Nature 1995; 376:435-8.

489. Meinl E, Lengenfelder D, Blank N, Pirzer R, Barata L, Hivroz C. Differential requirement of ZAP-70 for CD2-mediated activation pathways of mature human T cells. J Immunol 2000; 165:3578-83.

490. Matsuda S, Suzuki-Fujimoto T, Minowa A, Ueno H, Katamura K, Koyasu S. Temperature-sensitive ZAP70 mutants degrading through a proteasome-independent pathway. Restoration of a kinase domain mutant by Cdc37. J Biol Chem 1999; 274:34515-8.

491. Noraz N, Schwarz K, Steinberg M, Dardalhon V, Rebouissou C, Hipskind R, et al. Alternative antigen receptor (TCR) signaling in T cells derived from ZAP-70-deficient patients expressing high levels of Syk. J Biol Chem 2000; 275:15832-8.

492. Turul T, Tezcan I, Artac H, de Bruin-Versteeg S, Barendregt BH, Reisli I, et al. Clinical heterogeneity can hamper the diagnosis of patients with ZAP70 deficiency. Eur J Pediatr 2009; 168:87-93.

493. Toyabe S, Watanabe A, Harada W, Karasawa T, Uchiyama M. Specific immunoglobulin E responses in ZAP-70-deficient patients are mediated by Syk-dependent T-cell receptor signalling. Immunology 2001; 103:164-71.

494. Elder ME, Skoda-Smith S, Kadlecek TA, Wang F, Wu J, Weiss A. Distinct T cell developmental consequences in humans and mice expressing identical mutations in the DLAARN motif of ZAP-70. J Immunol 2001; 166:656-61.

495. Picard C, Dogniaux S, Chemin K, Maciorowski Z, Lim A, Mazerolles F, et al. Hypomorphic mutation of ZAP70 in human results in a late onset immunodeficiency and no autoimmunity. Eur J Immunol 2009; 39:1966-76.

496. Newell A, Dadi H, Goldberg R, Ngan BY, Grunebaum E, Roifman CM. Diffuse large B-cell lymphoma as presenting feature of Zap-70 deficiency. J Allergy Clin Immunol 2011; 127:517-20.

497. Karaca E, Karakoc-Aydiner E, Bayrak OF, Keles S, Sevli S, Barlan IB, et al. Identification of a novel mutation in ZAP70 and prenatal diagnosis in a Turkish family with severe combined immunodeficiency disorder. Gene 2013; 512:189-93.

498. Medoff BD, Sandall BP, Landry A, Nagahama K, Mizoguchi A, Luster AD, et al. Differential requirement for CARMA1 in agonist-selected T-cell development. Eur J Immunol 2009; 39:78-84.

499. Gerart S, Siberil S, Martin E, Lenoir C, Aguilar C, Picard C, et al. Human iNKT and MAIT cells exhibit a PLZF-dependent proapoptotic propensity that is counterbalanced by XIAP. Blood 2013; 121:614-23.

500. Nichols KE, Hom J, Gong SY, Ganguly A, Ma CS, Cannons JL, et al. Regulation of NKT cell development by SAP, the protein defective in XLP. Nat Med 2005; 11:340-5.

501. Oda H, Tamehiro N, Patrick MS, Hayakawa K, Suzuki H. Differential requirement for RhoH in development of TCRalphabeta CD8alphaalpha IELs and other types of T cells. Immunol Lett 2013; 151:1-9.

502. Pasquier B, Yin L, Fondaneche MC, Relouzat F, Bloch-Queyrat C, Lambert N, et al. Defective NKT cell development in mice and humans lacking the adapter SAP, the X-linked lymphoproliferative syndrome gene product. J Exp Med 2005; 201:695-701.

503. Rigaud S, Fondaneche MC, Lambert N, Pasquier B, Mateo V, Soulas P, et al. XIAP deficiency in humans causes an X-linked lymphoproliferative syndrome. Nature 2006; 444:110-4.

504. Palacios EH, Weiss A. Distinct roles for Syk and ZAP-70 during early thymocyte development. J Exp Med 2007; 204:1703-15.

505. Saini M, Sinclair C, Marshall D, Tolaini M, Sakaguchi S, Seddon B. Regulation of Zap70 expression during thymocyte development enables temporal separation of CD4 and CD8 repertoire selection at different signaling thresholds. Sci Signal 2010; 3:ra23.

506. Alarcon B, van Santen HM. Two receptors, two kinases, and T cell lineage determination. Sci Signal 2010; 3:pe11.

507. Matechak EO, Killeen N, Hedrick SM, Fowlkes BJ. MHC class II-specific T cells can develop in the CD8 lineage when CD4 is absent. Immunity 1996; 4:337-47.

508. Cheng AM, Negishi I, Anderson SJ, Chan AC, Bolen J, Loh DY, et al. The Syk and ZAP-70 SH2-containing tyrosine kinases are implicated in pre-T cell receptor signaling. Proc Natl Acad Sci U S A 1997; 94:9797-801.

509. Turner M, Mee PJ, Costello PS, Williams O, Price AA, Duddy LP, et al. Perinatal lethality and blocked B-cell development in mice lacking the tyrosine kinase Syk. Nature 1995; 378:298-302.

510. Cheng AM, Rowley B, Pao W, Hayday A, Bolen JB, Pawson T. Syk tyrosine kinase required for mouse viability and B-cell development. Nature 1995; 378:303-6.

511. van der Burg M, Gennery AR. Educational paper. The expanding clinical and immunological spectrum of severe combined immunodeficiency. Eur J Pediatr 2011; 170:561-71.

512. Poliani PL, Fontana E, Roifman CM, Notarangelo LD. zeta Chain-associated protein of 70 kDa (ZAP70) deficiency in human subjects is associated with abnormalities of thymic stromal cells: Implications for T-cell tolerance. J Allergy Clin Immunol 2013; 131:597-600 e1-2.

513. Pachlopnik Schmid J, Ho CH, Chretien F, Lefebvre JM, Pivert G, Kosco-Vilbois M, et al. Neutralization of IFNgamma defeats haemophagocytosis in LCMV-infected perforin- and Rab27a-deficient mice. EMBO Mol Med 2009; 1:112-24.

514. Schaeffer EM, Broussard C, Debnath J, Anderson S, McVicar DW, Schwartzberg PL. Tec family kinases modulate thresholds for thymocyte development and selection. J Exp Med 2000; 192:987-1000.

515. Berg LJ. Signalling through TEC kinases regulates conventional versus innate CD8(+) T-cell development. Nat Rev Immunol 2007; 7:479-85.

516. Schaeffer EM, Debnath J, Yap G, McVicar D, Liao XC, Littman DR, et al. Requirement for Tec kinases Rlk and Itk in T cell receptor signaling and immunity. Science 1999; 284:638-41.

517. Singleton KL, Gosh M, Dandekar RD, Au-Yeung BB, Ksionda O, Tybulewicz VL, et al. Itk controls the spatiotemporal organization of T cell activation. Sci Signal 2011; 4:ra66.

518. Salek M, Acuto O. Quantitative dynamics of phosphoproteome: the devil is in the details. Anal Chem 2012; 84:8431-6.

519. Tomida T, Hirose K, Takizawa A, Shibasaki F, Iino M. NFAT functions as a working memory of Ca2+ signals in decoding Ca2+ oscillation. EMBO J 2003; 22:3825-32.

520. Sprent J, Surh CD. Normal T cell homeostasis: the conversion of naive cells into memory-phenotype cells. Nat Immunol 2011; 12:478-84.

521. Wherry EJ. T cell exhaustion. Nat Immunol 2011; 12:492-9.

522. Hislop AD, Taylor GS, Sauce D, Rickinson AB. Cellular responses to viral infection in humans: lessons from Epstein-Barr virus. Annu Rev Immunol 2007; 25:587-617.

523. Chung BK, Tsai K, Allan LL, Zheng DJ, Nie JC, Biggs CM, et al. Innate immune control of EBV-infected B cells by invariant natural killer T cells. Blood 2013.

524. Ferrara TJ, Mueller C, Sahu N, Ben-Jebria A, August A. Reduced airway hyperresponsiveness and tracheal responses during allergic asthma in mice lacking tyrosine kinase inducible T-cell kinase. J Allergy Clin Immunol 2006; 117:780-6.